The role of Fc receptor-like 6 in innate and adaptive immunity

Yash Patel

University College London

and

The Francis Crick Institute

PhD Supervisor: Dr George Kassiotis

A thesis submitted for the degree of

Doctor of Philosophy

University College London

September 2019

Declaration

I Yash Patel, confirm that the work presented in this thesis is my own. Where information has been derived from other sources, I confirm that this has been indicated in the thesis.

Abstract

Fc receptor-like 6 (FCRL6) is an immunoreceptor tyrosine-based inhibitory motif-bearing transmembrane receptor upregulated on human cytotoxic T and NK cells during chronic immune activation. It has been suggested to act as an inhibitory receptor by possibly interacting with human leukocyte antigen-DR (HLA-DR), but its function remains largely unknown. We initially investigated the role of FCRL6 in T cells using its murine counterpart. However, *Fcrl6* expression was absent in developing, mature or activated mouse T cells. Therefore, we generated a human FCRL6 (hFCRL6) expressing transgenic mouse to investigate the function of this receptor. The expression of HLA-DR on antigen presenting cells resulted in reduced *in vitro* proliferation of hFCRL6^{+} CD4^{+} T cells. However, we were unable to recapitulate this inhibitory effect of the hFCRL6:HLA-DR axis in an *in vivo* environment. Further characterisation of mouse immune populations revealed *Fcrl6* expression in natural killer (NK) and developing B cells. Analysis of *Fcrl6*$^{-/-}$ mice showed that the development of these cells as well as T cells and the splenic proportion of most major immune populations remained unaffected by FCRL6 deletion. We observed a reduction in the proportion of splenic macrophages and NK cells in *Fcrl6*$^{-/-}$ and NK conditional *Fcrl6*$^{-/-}$ mice, respectively. However, NK cell responses in a chronic retroviral infection model as well as a tumour model remained unaffected by FCRL6 deletion. Similarly, B cell antibody production in response to retroviral infection was also unaffected by FCRL6 deletion. Overall, data obtained here suggested that the mouse ortholog of FCRL6 might not possess the potential immunoregulatory capacity of its human counterpart and thus may have evolved to mediate non-immunoregulatory functions. Further studies will be required to define the role of mouse FCRL6 in NK cells and macrophages in addition to hFCRL6 in NK cells and T cells.

Impact Statement

The findings from my thesis suggested that mouse and human FCRL6 may mediate distinct functions in their respective species. Consequently, this should be considered when attributing possible functions of mouse FCRL6 to its human counterpart. The data in my thesis also suggested that human FCRL6 might possess inhibitory functionality as evidenced by reduced *in vitro* proliferation of human FCRL6 expressing mouse $CD4^+$ T cells. However, further studies will be required to confirm this finding, elucidate the underlying mechanism and precisely define the circumstances where this receptor might play a potential inhibitory role in the human immune system. An increased understanding of the function of human FCRL6 may allow for the development of novel therapeutics that could improve our immunotherapy-based arsenal against infectious disease, cancer and autoimmunity.

Acknowledgement

Firstly, I would like to express my deepest gratitude to my supervisor, Professor George Kassiotis, for his continuous support, patience and immense knowledge. I appreciate his contribution of time and ideas to make my PhD experience both productive and stimulating.

The past and present members of the Kassiotis group have contributed greatly to my scientific development and for this I cannot thank them enough. I am especially grateful to Dr Luca Danelli for his willingness to discuss my research and for providing me with valuable feedback. I would also like to thank Dr Jan Attig and Nikhil Faulkner for their continuous support in the lab but mostly for the Waitrose walks!

Lastly, I am grateful to my family who have always pushed me to fulfil my potential and so I would like to dedicate this work to my loving parents, Prakash and Dina Patel, and my sister, Shachi Patel for their words of encouragement and unrelenting support.

Table of Contents

Table of figures

List of tables

Abbreviations

AICD	Activation-induced cell death
AID	Activation-induced cytidine deaminase
APC	Antigen presenting cell
BCR	B cell receptor
BLIMP1	B lymphocyte-induced maturation protein-1
BM	Bone marrow
BXMAS	B-cell cross-linked by anti-IgM activation sequence
CD	Cluster of differentiation
cDNA	Complimentary DNA
CLP	Common lymphoid progenitor
CLR	C-type lectin receptor
CSR	Class switch recombination
cTEC	Cortical thymic epithelial cell
CTLA-4	Cytotoxic T-lymphocyte-associated protein 4
DAMP	Damage-associated molecular pattern
DC	Dendritic cells
DN	Double negative
DP	Double positive
EBF1	Early B-Cell factor 1
Env	Envelope
ERK	Extracellular signal-regulated kinase
F-MLV	Friend murine leukaemia virus
FACS	Flow activated cell sorting
FcR	Fc receptor
FCRL	Fc receptor-like protein
FDC	Follicular dendritic cell
FOB	Follicular B cell
Foxp3	Forkhead box P3
FV	Friend virus
GC	Germinal centre
GM-CSF	Granulocyte-macrophage colony-stimulating factor
HBV	Hepatitis B virus
HCV	Hepatitis C virus
HIV	Human immunodeficiency virus
HSC	Haematopoietic stem cell

HVEM	Herpesvirus entry mediator
IFN	Interferon
Ig	Immunoglobulin
IKK	IκB kinase
IL	Interleukin
IRAK	IL-1R-associated kinases
ITAM	Immunoreceptor tyrosine-based activation motif
ITIM	Immunoreceptor tyrosine-based inhibitory motif
ITSM	Immunoreceptor tyrosine-based switch motif
IκB	IkappaB
JAK	Janus kinase
KLRG1	Killer-cell lectin like receptor G1
LAG-3	Lymphocyte-activation gene 3
LAIR-1	Leukocyte-associated immunoglobulin-like receptor 1
LCMV	Lymphocytic choriomeningitis virus
LRR	Leucine-rich repeat
MAP	Mitogen-activated protein
MHC	Major histocompatibility complex
MIP	Macrophage inflammatory protein
mTEC	Medullary thymic epithelial cell
MZB	Marginal zone B cell
MZM	Marginal zone macrophage
NFκB	Nuclear factor kappa-light-chain-enhancer of activated B cells
NK	Natural killer
NKT	Natural killer T
NLR	Nucleotide-binding oligomerization domain-like receptors
PAMP	Pathogen-associated molecular patterns
PD-1	Programmed cell death protein 1
PIR-B	Paired Ig-like receptor B
PRR	Pattern recognition receptor
PU.1	Purine box factor 1
R	Receptor
RAG	Recombination-activating gene
RLR	RIG-1 like receptors
RNA	Ribonucleic acid
RT	Room temperature
RUNX3	Runt-related transcription factor 3
SFFV	Spleen focus forming virus
SH2	Src homology 2

Ship	Src homology 2-containing inositol 5-phosphatase
SHM	Somatic hypermutation
Shp	Src homology 2-containing tyrosine phosphatase
SMAC	Supramolecular activation complex
SOCS1	Suppressor of cytokine signaling 1
SP	Single positive
STAT	Signal transducer and activator of transcription
Syk	Spleen tyrosine kinase
TCR	T cell receptor
TdT	Terminal deoxynucleotidyl transferase
T_{FH}	T follicular helper cell
Tg	Transgenic
TGF	Transforming growth factor
T_H	T helper cell
TIM-3	T-cell immunoglobulin and mucin-domain containing-3
TLR	Toll like receptor
TNF	Tumour necrosis factor
TRAF	TNF receptor-associated factor
T_{reg}	Regulatory T cell
Zap70	Zeta-chain-associated protein kinase 70

Chapter 1. Introduction

1.1 The immune system

Humans and others mammals exist in an environment rife with microbes as well as a range of allergenic and toxic substances that threaten homeostasis. The mammalian immune system has evolved to not only react against these harmful stimuli, but also be tolerant to self-tissues and commensal microbes that complement normal host function. It is composed of an elaborate network of cytokines, humoral factors, cells and lymphoid organs that cooperate to effectively recognise self from non-self. Such distinction is primarily achieved by recognition of structural features of the pathogen, allergen or toxic substance that are distinct from that of the host. The mechanisms that permit this recognition are broadly divided into two categories: i) germline encoded responses that recognise molecular patterns shared by multiple microbes and toxins; and ii) responses that involve somatic recombination of germlines genes to generate antigen-binding molecules that recognise a specific foreign structure. These responses termed innate and adaptive immunity, respectively differ both temporally and qualitatively, with each offering its own set of distinct benefits. Intimate crosstalk and synergy are required between these two arms of the immune system for effective host protection.

1.1.1 Innate immunity

The innate immune system is comprised of all components of the host's defence mechanisms that are encoded by germline cells, including chemical and physical barriers in addition to cellular immunity. The positioning of these components at crucial interfaces with the external environment ensures that the innate immune system is poised to react rapidly against invading pathogens. Non-cellular components of innate immunity include epithelial cell layers with tight cell to cell contacts, mucus layers and cilia that overlay the respiratory, gastrointestinal and genitourinary epithelial surfaces as well as soluble proteins and bioactive small molecules such as complement cascade proteins and defensins that are constitutively present in body fluids. These alongside

other non-cellular components of innate immunity act to prevent the free entry of pathogens into the body. However, under certain circumstances, pathogens are able to penetrate the peripheral shield formed by these barriers. These pathogens are immediately recognised by cells of the innate immune system which become activated and initiate the early immune response. These cells include macrophages, neutrophils, eosinophils, mast cells, basophils, natural killer (NK) cells and dendritic cells (DCs). The recruitment and activation of these cells except NK cells is mediated through sensors known as pattern recognition receptors (PRRs) (Chaplin 2010). The development and activation of NK cells is discussed in sections 5.1.1 and 5.1.2 of this thesis.

PRRs are able to detect invariant molecular patterns shared by a class of microorganisms known as pathogen-associated molecular patterns (PAMPs) (Iwasaki & Medzhitov 2010). These sensors are also able to detect indicators of cellular damage known as danger-associated molecular patterns (DAMPs) on endogenous molecules released from damaged cells (Amarante-Mendes *et al.* 2018). PRRs are usually found associated to subcellular compartments such as the cellular and endosomal/lysosomal membranes and cytoplasm of macrophages, neutrophils and DCs. They can also be detected on other immune and non-immune cells as well as extracellularly in the blood and interstitial fluid. PRRs are subdivided into four main families: transmembrane Toll-like receptors (TLRs) and C-type lectin like receptors (CLRs), and cytoplasmic Nucleotide-binding oligomerization domain-like receptors (NLRs) and RIG-1 like receptors (RLRs) (Takeuchi & Akira 2010).

TLRs are an indispensable component of innate immunity highlighted by their evolutionary conservation across both invertebrate and vertebrate lineages. Till date, the TLR family remains one of the best-characterised family of PRRs in humans. The ten members of this family are categorised depending on their subcellular location and pathogen specificity which includes bacteria, fungi, parasites, protozoa, self and viruses. Broadly, TLR1, TLR2, TLR4 and TLR6 are located on the cell membrane whilst TLR3, TLR8 and TLR9 are found on endosomal/lysosomal membranes where they detect lipids and nucleic acids, respectively from both self and microbial sources via leucine-rich repeat (LRR) sequences in their ectodomains. The other transmembrane

PRRs belong to the CLR family which are found on the cell membrane where they primarily detect carbohydrates from microbial sources. Cytoplasmic PRRs include NLRs and RLRs which detect nucleic acids from foreign microbial sources (Bell *et al.* 2003; Hoving *et al.* 2014; Kawai & Akira 2009). In addition to these differences in localisation and pathogen specificities, PRRs have a diverse range of functions which likely stem from their association with various downstream signalling pathways thereby allowing activation of multiple and diversified target genes (Lee & Kim 2007). Thus, PRRs allow the innate immune system to initiate different responses according to the nature of the invading pathogen.

A central feature of the cellular innate immune response is the early recruitment of neutrophils. During the initial stages of an infection, activated macrophages release cytokines such as granulocyte and granulocyte-macrophage colony stimulating factors to stimulate bone marrow (BM) division of myeloid precursors. This causes the release of millions of cells into the circulation resulting in the characteristic neutrophil leucocytosis associated with acute infection or inflammation. Neutrophils are then recruited via a multistep process involving proinflammatory mediators, adhesion molecules, chemoattractants, and chemokines. Once at the site of infection, these cells alongside macrophages use their PRRs to detect PAMPs and become activated (Parkin & Cohen 2001). Neutrophils have been described to form clusters that isolate the site of infection as well as the pathogen in a manner that resembles the swarming behaviour of some insects (Kienle & Lämmermann 2016). Monocytes are also recruited to the infected tissue where they differentiate into inflammatory macrophages or DCs (León *et al.* 2007; Yang *et al.* 2014). Following activation, macrophages and neutrophils share similar mechanisms for pathogen killing such as cytokine production or direct killing via phagocytosis, release of reactive oxygen species or lytic granules (Flannagan *et al.* 2015; Segal 2005). Neutrophils have also been identified to release web-like chromatin structures known as neutrophil extracellular traps in order to neutralise larger pathogens (Papayannopoulos 2018). Cytokine production by activated macrophages, neutrophils and DCs restricts pathogen spread and assists in the recruitment of adaptive immune cells to the site of infection. The activation of DCs also serves to mature these cells into highly capable antigen presenting cells (APCs) that travel to the lymph nodes and prime T lymphocytes

(Sallusto & Lanzavecchia 2002). Thus, the function of DCs lies at the interface between innate and adaptive immunity. The innate immune response has evolved over millennia into its current form where it effectively, but non-specifically provides protection against a range of invading pathogens. Its reliance on germline encoded recognition receptors that detect conserved sequences on pathogens restricts the ability of innate immune cells to respond to rapidly evolving pathogens thereby, limiting the ultimate usefulness of innate immunity.

1.1.2 Adaptive immunity

In addition to innate immunity, vertebrates have developed adaptive immunity which is characterised by a comparatively slower but more tailored response to an invading pathogen. It also possesses a memory component that allows for a more efficient immune response following reinvasion by the same pathogen. Evolution has led to the emergence of two divergent adaptive immune systems; jawless vertebrates possess a system based around variable lymphocyte receptors that use LRR sequences for antigen binding whilst jawed vertebrates use an immunoglobulin (Ig) domain-based system to produce antigen-binding B and T cell receptors (BCRs and TCRs) expressed on B and T cells, respectively (Hirano *et al.* 2011). As observed following pathogen recognition by PRRs on innate immune cells, the BCR and TCR deliver activation signals to B and T cells following the binding of an antigen. However, unlike germline encoded PRRs, the BCR and TCR are generated as a result of somatic recombination events during the development of B and T cells (Bonilla & Oettgen 2010). This recombination allows the adaptive immune system to construct highly diverse and antigen specific receptors to not only detect invading but also future pathogens. Mature B and T cells are derived from the hematopoietic stem cells (HSCs) residing in the BM. However, their later development occurs in separate locations with B cells continuing their development in the BM whilst common lymphoid progenitors (CLPs) destined for the T-lineage leave the BM to complete their development in the thymus (Kondo *et al.* 1997). The development and activation of B and T cells is discussed in further detail in chapters 4 and 6 of this thesis, respectively.

1.2 Regulation of the immune response

An ideal immune response is one that is rapid, proportionate and effective but also finite. Disproportionate or temporally extended immune responses can be deleterious to the host as observed following chronic unregulated inflammation during autoimmune conditions. Thus, multiple mechanisms exist and act at different levels to regulate and ultimately terminate immune responses. Some of those that function at the cellular level include downregulation of activating receptor expression, induction of apoptosis or induction of anergy. Sub-cellularly, pathways induced by activating receptors can be inhibited by recruitment of tyrosine phosphatases or through de novo generation of counter regulatory molecules such as IkappaB (IκB) which is synthesised to terminate TLR4-mediated responses. Negative immune regulation may also occur via generation of inhibitory cytokines such as transforming growth factor (TGF) β and interleukin (IL)-10, osmotic lysis, or physiological signalling switch-off processes. Additionally, receptor-mediated negative immune regulation also plays a crucial role and includes inhibitory receptors that share ligands with activating receptors as well as those that are stimulated by negative feedback loops from activating receptors (Kane *et al.* 2014; Kawasaki & Kawai 2014). The existence of such mechanisms is central to the functioning of a healthy immune system. Some of the mechanisms employed to regulate immune response are briefly discussed below.

1.2.1 Regulation by competitive antagonism

Competitive antagonism of membrane bound receptors by extracellular soluble counterparts represents one of the most effective and common strategies to regulate cellular immune responses. These molecules function by either acting as decoy proteins and binding their membrane bound counterparts or by competitively binding the ligands of their membrane bound counterparts. Production of these soluble molecules occurs via different pathways; some may be splice variants of their membrane bound counterparts (Rose-John *et al.* 2006), some have been shown to be cleaved products of surface receptors (Levine 2004) and some are encoded by distinct genes to their membrane bound counterparts (Sims & Smith 2010). An example of soluble

molecule based competitive antagonism in context of the immune system is IL-1 and its receptor. The signalling cascade induced following binding of IL-1α and IL-1β to the IL-1 receptor (IL-1R1) is counter regulated through production of a soluble IL-1R antagonist that competitively binds IL-1R1 to prevent further ligand binding (Greenfeder *et al.* 1995). Importantly, the expression of this antagonist is upregulated by various inflammatory stimuli including IL-1 thus forming a negative feedback loop (Sims & Smith 2010). Alternatively, competitive antagonism by soluble molecules may also result in an augmented immune response. The discovery of soluble programmed cell death protein 1 (sPD-1) shows that competitive antagonism may increase the effector function of immune cells as sPD1 can compete with the inhibitory receptor PD-1 to bind its ligand, PD-L1 thereby, reducing its interaction with PD-1 expressed on T cells and improving their responses (He *et al.* 2005; Zhu & Lang 2017).

1.2.2 Regulation by ubiquitin

Ubiquitin is a highly conserved 8.5 kilodalton peptide that mediates regulation of immune responses by binding and targeting key signalling proteins for proteasomal degradation (Malynn & Ma 2010). Ubiquitination and deubiquitination are critical during the innate immune response. Activation of PRRs such as TLRs, NLRs and RLRs leads to a nuclear-factor κB (NFκB) dependent increase in the transcription of proinflammatory genes. This is associated with a concomitant induction of ubiquitin ligases which polyubiquitinate several intracellular regulatory molecules such as TNF receptor-associated factor (TRAF)2, TRAF3, TRAF6 and TRIM25. These function as both adaptor proteins and ubiquitin ligases that catalyse ubiquitination of other molecules (Sun 2008). For example, TL4 signalling induces TRAF6 that ubiquitinates and degrades the regulatory subunit of the enzyme IκB kinase (IKK) thereby causing phosphorylation, ubiquitination and degradation of IκB, which negatively regulates NFκB signalling thereby, forming a positive feedback loop following TLR4 activation. This is counter-regulated by increased expression of the deubiquitinating enzymes A20 and CYLD which prevent polyubiquitin chain formation on IκB by TRAF6 and IKK and thus, negatively regulate NFκB signalling (Bhoj & Chen 2009). Ubiquitin ligases are also crucial during various aspects of the adaptive immune response such as following

TCR stimulation where they function to degrade IκB and allow NFκB activation (Zhang 2004). Thus, ubiquitination represents a fundamental mechanism that regulates immune responses as well as other biological processes through ubiquitinating enzymes and deubiquitinating enzymes.

1.2.3 Regulation by intracellular negative regulators

Auto-inhibition describes a process by which a stimulus not only initiates an appropriate positive response but also a mechanism that prevents further response to that particular stimulus. This can be witnessed in the context of the immune system following TLR signalling. Generally, TLRs signal via two major pathways; MyD88-dependent and MyD88-independent (Kawai & Akira 2006). MyD88-dependent TLR4 signalling induces auto-inhibition by intracellular negative regulators. Briefly, MyD88 recruitment following TLR4 stimulation results in activation of IL-1R-associated kinases (IRAKs) thereby, allowing further downstream signalling through mitogen-activated protein (MAP) kinase and/or NFκB activation pathways (O'Neill *et al.* 2013). Monocytes and macrophages respond by upregulating the expression of intracellular negative regulators such as MyD88s, IRAK-M, SOCS1, NOD2, phosphatidylinositol 3-kinase (PI3K), Toll-interacting protein amongst others that function by different mechanisms to counteract the TLR4 mediated activation (Liew *et al.* 2005). For example, MyD88s is a truncated, alternatively spliced protein that competes with MyD88 and prevents IRAK-mediated activation whilst IRAK-M, an IRAK family member without kinase activity competitively inhibits the IRAK-mediated activation cascade (Janssens *et al.* 2002; Kobayashi *et al.* 2002).

1.2.4 Regulation by receptor downregulation

Physical removal of a receptor from the cell membrane is another effective route of regulating activating signals. A classic example of this is the downregulation of the TCR following its activation due to binding of its cognate antigen (José *et al.* 2000). In resting T cells, the TCR is continually endocytosed and re-expressed on the cell surface. However, following activation, TCR downregulation is achieved by a combination of increased internalisation, reduced recycling and

increased degradation (Alcover & Alarcón 2000). The internalisation of the TCR occurs via both clathrin-dependent endocytosis and clathrin-independent mechanisms (Dietrich *et al.* 1994; Monjas *et al.* 2004). TCR downregulation contributes to the termination of TCR-mediated signalling as it reduces cellular sensitivity to further stimulation (Cai *et al.* 1997; Schönrich *et al.* 1991; Valitutti *et al.* 1996; Zanders *et al.* 1983). Other examples of receptors that are downregulated following ligand binding are the G-protein-coupled receptors of chemokines, prostaglandins, bradykinins and platelet-activating factors (Sun & Ye 2012). Briefly, ligand binding induces signal transduction following which the ligand-receptor complex is internalised and undergoes degradation in endosomes. Alternatively, the receptor may also be recycled back to the cell membrane following removal and endosomal degradation of the bound ligand (Ferguson 2001; Magalhaes *et al.* 2012; SPÄT & HUNYADY 2004). Thus, receptor downregulation following activation functions to reduce the number of activating receptors present on the cell surface to transduce further activating signals.

1.2.5 Regulation by immunoreceptor tyrosine-based motifs

Activating and inhibitory receptors expressing immunoreceptor tyrosine-based motifs represent one of the most crucial mechanisms of regulating immune responses. Some examples of these receptors are discussed below.

Immunoreceptor tyrosine-based activating motifs

Activating receptors are characterised by their expression of a cytoplasmic immunoreceptor tyrosine-based activating motif (ITAM) which has a consensus 14-18 amino acid sequence of YxxI/Lx(6-12)YxxI/L where x represents any amino acid. Ligand engagement of ITAM bearing receptors leads to receptor aggregation and subsequent phosphorylation of both tyrosine residues within the ITAM by Src family protein tyrosine kinases. Next, the dually phosphorylated ITAM acts as a binding site for the two SH2 domains of Syk family non-receptor protein tyrosine kinases such as Zap70 and Syk which in turn cause activation of further downstream signalling. There are numerous examples of activating receptors including the BCR and TCR that rely on

ITAM-induced signalling following binding of their ligand (Humphrey *et al.* 2005; Latour & Veillette 2001). For example, BCR associated Igα and Igβ subunits each contain an ITAM and drive an ITAM-mediated signalosome that generates potent activating signals following binding of a cognate antigen to the BCR (Li *et al.* 2002). Similarly, the TCR complex relies on ITAM bearing CD3ε, δ, γ and ζ chain subunits in order to transduce activating signals following antigen binding (Love & Hayes 2010).

Immunoreceptor tyrosine-based inhibitory motifs

Multiple inhibitory receptor systems have been identified on lymphoid cells. The importance of such systems has been established through studies in which targeted disruption of inhibitory receptors in mice leads to unrestrained inflammatory responses and potentially fatal autoreactivity (Bolland & Ravetch 2000; Clynes *et al.* 1999; O'Keefe *et al.* 1999). Inhibitory receptors are characterised by a cytoplasmic immunoreceptor tyrosine-based inhibitory motif which consists of a consensus 6 amino acid sequence of S/I/V/LxYxxI/V/L where x represents any amino acid. These motifs are able to transduce signals following activation and clustering of inhibitory receptors due to phosphorylation of their tyrosine residue by Src tyrosine kinases. This leads to the subsequent recruitment of SH2-domain-containing tyrosine phosphatases such as Shp-1 or Shp-2, or the inositol phosphatases Ship-1 or Ship-2. These phosphatases dephosphorylate up- and downstream signalling molecules in order to terminate cellular activation (Tourdot *et al.* 2013).

Immunoreceptor tyrosine-based activating inhibitory and inhibitory activating motifs

Emerging evidence has suggested that ITAMs and ITIMs may also additionally mediate inhibition and activation, respectively. ITAMs possessing such activity have been termed ITAM inhibitory whilst ITIMs with such functionality are known as ITIM activating. The mechanisms underlying the ability of these motifs to mediate both activation and inhibition remain to be fully elucidated. However, some studies have suggested that the nature of the binding ligand and its affinity for the expressing receptor could determine the outcome. For example, binding of FcαRI by monomeric IgA elicits anti-inflammatory effects due to partial ITAM phosphorylation that

simultaneously recruits Syk and Shp-1 resulting in net inhibition, whilst IgA oligomers induce pro-inflammatory effects due to greater ITAM phosphorylation causing enhanced recruitment of Syk family kinases compared to Shp-1 leading to net activation (Pasquier *et al.* 2005; van Egmond *et al.* 2001).

Immunoreceptor tyrosine-based switch motifs

Additionally, the discovery of immunoreceptor tyrosine-based switch motifs (ITSMs) has further complicated the paradigm of immune modulation by ITAM and ITIM bearing receptors. The ITSM consists of a consensus 6 amino acid sequence of TxYxxI/V where x represents any amino acid (Shlapatska *et al.* 2001). A number of receptors expressing cytosolic ITSMs have been identified and include inhibitory killer-cell immunoglobulin-like receptors (Yusa *et al.* 2004), CD150 (Shlapatska *et al.* 2001), sialic acid-binding Ig-like lectins (Avril *et al.* 2004) and PD-1 (Chemnitz *et al.* 2004). The exact role of ITSMs is less well understood compared to ITAMs and ITIMs, but it is believed that these motifs moderate ITAM/ITIM effects due to sequence similarity and proximity to these motifs. Thus, it is probable that ITSMs could mediate their effect by sharing their tyrosine residue with that of an ITAM or ITIM (Kane *et al.* 2014). This is supported by a study which demonstrated that phosphorylation of closely located ITIMs and ITSMs in the orexin receptor was required to provide the two SH2 domains necessary for Shp-2 binding (El Firar *et al.* 2009).

1.2.6 Inhibitory receptors expressed by lymphocytes

Detailed analysis of inhibitory receptor systems has led to the emergence of a central paradigm in which activation must be paired with inhibition in order to effectively terminate immune responses. Thus, a crucial distinguishing feature of inhibitory receptors is an ability to attenuate activation signals delivered by ITAM bearing receptors. Receptors encoding cytosolic ITIMs and ITSMs as well as those that do not possess classical tyrosine-based motifs mediate this function. In certain circumstances, inhibitory receptors recognise distinct ligands to activating receptors and the net outcome on cellular activation is determined by the relative strength of the opposing

signal whilst in other cases, activating and inhibitory receptors bind identical ligands and the relative affinity of these receptors for a particular ligand, and their level of expression determines the state of cellular activation (Ravetch & Lanier 2000). Some of the inhibitory receptors expressed by lymphocytes are discussed below. Likewise, NK cells rely on multiple inhibitory receptors to maintain tolerance to self and prevent induction of auto-immunity. This is discussed in section 5.1.2 of the thesis.

1.2.6.1 B cell expressed inhibitory receptors

An important inhibitory receptor expressed by B cells is the IgG binding FcγRIIB. Studies on this receptor were pivotal in defining the physiological role of inhibitory receptors in context of the immune system. IgG immune complexes had long been identified as potent inhibitory ligands (Chan & Sinclair 1971). The molecular mechanism underlying their inhibitory effect was later discovered to be reliant on their binding to FcγRIIB. The extracellular domains of FcγRIIB are linked to ITIM bearing cytoplasmic domains that use three distinct inhibitory mechanisms to reduce BCR-induced calcium mobilisation and cell proliferation (Ravetch & Lanier 2000). A vital role of this receptor in maintaining peripheral tolerance has been exemplified by the autoimmune phenotype of FcγRIIB deficient mice (Li *et al.* 2014b). In addition to FcγRIIB, B cells express other ITIM-containing inhibitory receptors such as CD5, CD22, CD66a, CD72, PD-1, PIR-B, ILT and LAIR-1 in order to regulate the amplitude of the BCR response (Ravetch & Lanier 2000). For example, CD22 binds sialic acid-bearing ligands which in turn causes phosphorylation of its ITIM associated tyrosine, and leads to recruitment of Shp-1 and Ship-1 that induce inhibitory signals to prevent B cell hyperstimulation. Interestingly, CD22 is omitted from the activating signalosome following BCR ligation by a foreign antigen, but included within the signalosome with additional inhibitory receptors following binding of the BCR with self-antigen to provide a strong inhibitory signal to maintain tolerance (Poe & Tedder 2012). Consequently, CD22 deficient mice display B cell hyperresponsiveness and auto-antibody production (O'Keefe *et al.* 1996). Thus, inhibitory receptors expressed by B cells are crucial for preventing hyperresponsiveness to BCR stimulation and autoimmunity.

1.2.6.2 T cell expressed inhibitory receptors

The immune response must be terminated following clearance of a pathogen to reduce tissue damage and avoid chronic inflammation. Coinhibitory receptors capable of modulating TCR signalling such as cytotoxic T-lymphocyte antigen-4 (CTLA-4), PD-1, CD272 (Chen 2004), CD244 (Boles *et al.* 2001), T-cell immunoglobulin mucin-3 (TIM-3) (Zhu *et al.* 2010), CD160 (Kaye 2008), lymphocyte-activation gene 3 (LAG-3) (Huard *et al.* 1994) amongst others mediate termination of the T cell response and consequently, also contribute to regulation of spontaneous autoimmunity (Bour-Jordan *et al.* 2011; Fife & Pauken 2011; Nurieva *et al.* 2011).

Two primary mechanisms exist to induce contraction of the effector phase of the T cell immune response; inhibition of T cell proliferation via coinhibitory molecules such as CTLA-4 and PD-1 (Chambers *et al.* 2001) or induction of apoptosis in activated T cells through a process known as activation-induced cell death (AICD) regulated by molecules such as CD95 and CD95 ligand (Arnold *et al.* 2006; Chen *et al.* 2007; Hildeman *et al.* 2002). A crucial immunoregulatory role of coinhibitory molecules is highlighted by the observation of severe autoimmune and lymphoproliferative diseases due to a lack or abnormal expression of these receptors (Mueller 2010).

One of the most well characterised inhibitory receptor systems involves interactions of the coinhibitory molecule CTLA-4 and the costimulatory molecule CD28 with CD80 or CD86 expressed on APCs such as DCs. Engagement of CD28 on T cells by CD80 or CD86 synergises with TCR signalling to stimulate cell activation. CTLA-4 expression is upregulated on activated $CD4^+$ and $CD8^+$ T cells and it has also been identified to have a higher affinity for CD80 and CD86 compared to CD28 (Chambers *et al.* 2001; Collins *et al.* 2002). Thus, CTLA-4 is able to directly compete with and reduce access of CD28 to CD80 and CD86 in order to terminate the second signal necessary to sustain TCR-mediated T cell activation. The cytoplasmic region of CTLA-4 has also been shown to antagonise CD28 mediated activation as mice expressing an intracellular deficient variant of CTLA-4 display a lymphoproliferative phenotype (Carreno *et al.* 2000; Masteller *et al.* 2000). However, the cytoplasmic region of CTLA-4 does not contain a bona fide

ITIM and also lacks intrinsic enzymatic activity but it does contain numerous protein–protein interacting motifs. Thus, it has been suggested that that intracellular region of CTLA-4 does not induce inhibitory signals but functions to control the turnover and consequently, surface expression of the receptor thereby allowing it to mediate its primary function of regulating the access of CD28 to CD80 and CD86 (Choi *et al.* 2008; Walker & Sansom 2015). Moreover, cell extrinsic mechanisms also exist to explain the inhibitory function of CTLA-4. In addition to conventional T cells, regulatory T cells (T_{reg}) also express CTLA-4 and can bind to DCs expressing CD80 and CD86 thereby reducing access of CD28 expressed on conventional T cells to its ligands. Furthermore, the interaction of T_{reg} cells with CD80 or CD86 on DCs may also remove these molecules from the surface of these cells via a process known as transendocytosis. Transendocytosis of CD80 and CD86 may also be mediated by CTLA-4 expressed on conventional T cells (Qureshi *et al.* 2011; Walker & Sansom 2015).

PD-1 is another critical coinhibitory receptor expressed by activated $CD4^+$ and $CD8^+$ T cells. Its expression is induced on T cells as a result of TCR mediated signalling (Greenwald *et al.* 2005; Nakae *et al.* 2006). The ligands of PD1, PD-L1 and PD-L2, differ in terms of their expression with PD-L1 being found on a wide range of cells including vascular endothelial cells, epithelial cells, myocytes, hepatocytes amongst others whilst PD-L2 is expressed by hematopoietic cells such as DCs, macrophages and mast cells (Ishida *et al.* 2002; Latchman *et al.* 2001). PD-1 and its ligands regulate the activating and inhibitory signals required for an effective immune response against pathogens (Freeman *et al.* 2000; Okazaki & Honjo 2006). Engagement of PD-1 with its ligands leads to phosphorylation of tyrosine residues within its cytoplasmic ITIM and ITSM by Src family kinases. This in turn leads to Shp-2 recruitment to the membrane distal phospho-tyrosine and ultimately results in decreased phosphorylation of several molecules associated with T cell activation including CD3ζ, ZAP70, Vav, Akt, and ERK (Chemnitz *et al.* 2004; Okazaki *et al.* 2001; Patsoukis *et al.* 2013; Yokosuka *et al.* 2012). Interactions of PD-1 with its ligands cause inhibition of CD28-induced costimulation and consequently, TCR induced proliferation and cytokine secretion. The expression of PD-1 ligands as well as CD80 and CD86 by APCs determines the

extent of T cell activation (Sugiura *et al.* 2019) whilst PD-L1 expression on nonlymphoid cells regulates the effector response at sites of inflammation (Freeman *et al.* 2000).

Other coinhibitory molecules expressed by T cells include LAG-3 which has been suggested to function by selectively binding stable complexes of peptide and MHC class II and subsequently, inducing inhibitory signals via its intracellular region (Maruhashi *et al.* 2018). CD272 is also expressed by T cells and has been demonstrated to recruit phosphatases to reduce TCR signalling (Sedy *et al.* 2005) via engagement of the herpesvirus entry mediator (HVEM) expressed on naïve B and T cells. HVEM-CD272 signalling has been demonstrated to reduce *in vivo* T-cell activity and also negatively regulate $CD4^+$ and $CD8^+$ T cell homeostatic expansion (Krieg *et al.* 2007). Additionally, HVEM may also bind CD160 to induce inhibitory signalling that reduces T-cell activation (Kaye 2008). Thus, several inhibitory receptor systems are expressed by T cells and upregulated following their activation in order to terminate immune responses and maintain tolerance.

1.2.7 Functional exhaustion of T cells

During a chronic viral infection or within the tumour microenvironment, multiple inhibitory receptors are up-regulated on antigen-specific effector T cells. This expression is associated with a dysfunctional state known as exhaustion. Exhaustion results in a progressive loss of T cell effector functions and ultimately results in deletion of exhausted cells. The loss of T cell functionality has been demonstrated to occur in a sequential manner with ability of IL-2 production and T-cell proliferation being lost first followed by loss of TNFα production and cytotoxic capacity and finally, loss of IFNγ production following which, these cells are deleted via induction of apoptosis (Wherry *et al.* 2003). The current understanding suggests that exhaustion occurs as a result of persistent antigen stimulation which causes the immune system to upregulate expression of inhibitory receptors to limit effector T cell responses and avoid autoimmunity. However, this mechanism also compromises the ability of the effector T cell response to provide immunity against persistent antigens in the form of chronic infection or tumours (Sharpe *et al.* 2007).

T cell exhaustion was first identified in mice during chronic lymphocytic choriomeningitis virus (LCMV) infection following detection of virus-specific $CD8^+$ T cells that lacked cytotoxic potential during the chronic infection phase (Zajac *et al.* 1998). Exhausted $CD8^+$ T cells have also been observed following simian immunodeficiency virus (Velu *et al.* 2009), human immunodeficiency virus (HIV) (Day *et al.* 2006), hepatitis B virus (HBV) (Das *et al.* 2008), hepatitis C virus (HCV) (Urbani *et al.* 2006) and human T-lymphotropic virus 1 infection (Kozako *et al.* 2009) as well as in patients with persistent tumours (Lee *et al.* 1999).

PD-1 was the first inhibitory receptor to be associated with exhaustion as LCMV antigen-specific $CD8^+$ T cells were discovered to have very high levels of PD-1 expression (Barber *et al.* 2006; Ishida *et al.* 1992). Subsequently, other studies have confirmed the involvement of PD-1 in the phenotype of exhausted cells and increased susceptibility of these cells to apoptosis following infection of human viruses such as HIV (Day *et al.* 2006), HBV (Das *et al.* 2008), HCV (Urbani *et al.* 2006) as well as in tumour microenvironments (Ahmadzadeh *et al.* 2009).

Global gene expression profile analysis of exhausted virus-specific $CD8^+$ T cells following LCMV infection has revealed multiple other inhibitory receptors that also contribute to their dysfunctional state (Blackburn *et al.* 2009; Wherry *et al.* 2007). Amongst these are TIM-3, LAG-3, CD244, CTLA-4, CD160, CD272, KLRG1, CD305, and CD200R which have been further investigated and found to also be involved in generation of exhausted T cells following human viral infections and establishment of tumours (Viganò *et al.* 2012). Particularly, co-expression of TIM-3 and PD-1 has been identified to represent one of the most exhausted populations of $CD8^+$ T cells following infection of patients with HIV (Jones *et al.* 2008) and HCV (Golden-Mason *et al.* 2009) and also in several mouse models of cancer and in patients with advanced melanoma (Fourcade *et al.* 2010; Sakuishi *et al.* 2010).

The expression of inhibitory receptors also occurs in the steady state and is linked to T cell activation and differentiation. For example, expression of the inhibitory receptors CD244, CD160

and KLRG1 correlates with T cell differentiation whilst CD272 is expressed at a high level on naïve cells but decreases following differentiation (Fuertes Marraco *et al.* 2015). Similarly, PD-1 up-regulation is a normal feature of early T-cell activation where its inhibitory functionality allows it to act as a rheostat regulating TCR signalling in a cell-intrinsic manner. This is essential as excessive TCR stimulation can result in more pronounced terminal differentiation and reduced cell survival of antigen-specific T cells. Thus, expression of PD-1 on early activated T cells allows the immune system to optimise effector T cell and memory responses (Ahn *et al.* 2018). Consequently, it is crucial to keep in consideration that inhibitory receptor expression is linked to the differentiation status of T cells, and that this relationship is evident in healthy individuals, where expression of these receptors does not cause the exhaustion that is associated with chronic antigen stimulation.

1.2.8 Therapeutic potential of inhibitory receptor blockade

In vitro and *in vivo* blockade of PD-1 signalling results in an increased ability of exhausted virus-specific $CD8^+$ T cells to survive and proliferate as well as produce cytokines and cytotoxic molecules following encounter of cognate antigen (Barber *et al.* 2006; Trautmann *et al.* 2006). Additionally, blockade of TIM-3 in conjunction with PD-1 on exhausted antigen-specific $CD8^+$ T cells restores the proliferative and cytotoxic ability of these cells in addition to inhibiting tumour growth (McMahan *et al.* 2010; Sakuishi *et al.* 2010). Similarly, *in vivo* LAG-3 blockade in combination with PD-1 synergistically improves T cell responses and results in lower viral loads following LCMV infection (Blackburn *et al.* 2009). Thus, the well-established immunosuppressive functions of these receptors as well the potential to revert exhausted T cell responses following their blockade has made these molecules exciting therapeutic targets to treat patients with persistent viral infections or cancer.

In particular, the development of checkpoint inhibitors which are antibodies that target inhibitory receptors, has revolutionised the field of immuno-oncology. Tumour cells are able to evade immune surveillance through multiple mechanisms including activation of inhibitory pathways

such as PD-1 to suppress the anti-tumour response (Alsaab *et al.* 2017). Checkpoint inhibitors are able to block some of these pathways in order to promote immune mediated deletion of tumour cells. Ipilimumab, which blocks CTLA-4 was the first approved checkpoint inhibitor for patients with advanced melanoma (Cameron *et al.* 2011). Following this approval, antibodies targeting other immune checkpoints have also been investigated and currently there are multiple checkpoint inhibitors that are being investigated in phase I, II, III and IV clinical trials for their efficacy as monotherapy or in combination for the treatment of various cancers (Darvin *et al.* 2018). However, accumulating evidence has suggested that only a small percentage of cancer patients benefit from checkpoint inhibitor therapy. Additionally, severe immune-related adverse events are also observed in some patients treated with checkpoint inhibitors (Feng *et al.* 2013). These events refer to local and systemic autoimmune responses that occur as a result of the blockade of normal physiological mechanisms that prevent autoimmunity.

Thus, it is imperative that we continue investigating immunoregulatory networks to discover novel therapeutic molecules that could be targeted to enhance anti-tumour or anti-viral immune responses in states of chronic immune activation without significantly increasing the risk of autoimmunity.

1.3 Fc receptor-like proteins

Despite our best efforts to identify key molecules and pathways involved in the regulation of the immune system, the function of several immune receptors remains unknown. During the early 2000's, a novel family of proteins structurally similar but functionally distinct from classical Fc receptors (FcRs) was identified in the human genome (Chikaev *et al.* 2005; Davis *et al.* 2001, 2002c; Facchetti *et al.* 2002; Guselnikov *et al.* 2002; Hatzivassiliou *et al.* 2001a; Masuda *et al.* 2010; Mechetina *et al.* 2002; Miller *et al.* 2002; Nakayama *et al.* 2001; Wilson & Colonna 2005; Xu *et al.* 2001). Several names existed for these proteins due to their discovery by multiple independent groups and consequently, a unified nomenclature for this family was established in 2006 with members being termed Fc receptor-like (FCRL) proteins (Maltais *et al.* 2006). Till date, a total of eight: six transmembrane (FCRL1-6) and two intracellular proteins (FCRLA and FCRLB) belonging to the FCRL protein family have been identified in humans whilst a total of six: one soluble chimeric (FCRLS) protein, three transmembrane (FCRL1, 5 and 6) and two intracellular (FCRLA and FCRLB) proteins have been identified to belong to the FCRL protein family in mice.

1.3.1 Discovery

The first FCRL protein to be discovered was the rat ortholog of FCRL6, a glycosylphosphatidylinositol-anchored membrane protein known as gp42. Its expression was first detected on rat lymphokine-activated killer cells of NK cell origin following interleukin-2 stimulation (Imboden *et al.* 1989). Human FCRL proteins were discovered later in 2001 as part of a study investigating chromosomal translocation breakpoints in multiple myeloma cells. A novel fusion protein comprised of the signal peptide of FCRL4 and the Ig alpha-1 chain C region of the IgA Fc domain was identified during this study. Subsequently, this led to the discovery of *FCRL4* and its designation as Ig superfamily receptor translocation associated gene (IRTA) 1 (Hatzivassiliou *et al.* 2001a). The same group identified a further four FCRL genes and termed them IRTA2-5 (Table 1 for updated nomenclature) (Hatzivassiliou *et al.* 2001a; Miller *et al.* 2002).

In addition, an independent bioinformatic approach identified the same genes by examining the genome for a consensus motif shared by the extracellular regions of Fcγ receptor (FcγR) I, FcγII, FcγRIII and the polymeric Ig receptor. Accordingly, FCRL genes were designated by this group as Fc receptor homologs (FcRH) (Table 1 for updated nomenclature) (Davis *et al.* 2001). A further gene belonging to the FCRL family was also discovered by this group and termed FcRH6, which under the classification system established in 2006 is now recognised as FCRL6 (Davis *et al.* 2002b). Similarly, an expressed sequence tag database search utilising a consensus sequence derived from the extracellular domain of FcγR1 also identified members of the FCRL family. The resulting genes were named IFGP1-6 (Table 1 for updated nomenclature) owing to their homology to the Ig superfamily (IgSF), gp42 and FcRs (Guselnikov *et al.* 2002). An additional two homologs without transmembrane sequences were also discovered by this group and named FCRL and FCRL2. However, these intracellular members of the FCRL family are now referred to as FCRLA and FCRLB, respectively. These proteins were also simultaneously identified by two other groups who termed them Fc receptor expressed in B-cells (FREB) and FREB2, and Fc related proteins X and Y (Table 1 for updated nomenclature) (Facchetti *et al.* 2002; Hatzivassiliou *et al.* 2001b; Masuda *et al.* 2010; Wilson & Colonna 2005).

An alternative *in silico* approach involving searching for molecules with similar characteristics to the IgSF, Fc receptors and gp42 discovered the proteins corresponding to *FCRL2* and *FCRL3*. They were named Src homology-2 domain containing phosphatase anchoring proteins (SPAP) 1 and 2, respectively (Xu *et al.* 2001). Concurrently, subtractive hybridisation methods employed by another group resulted in the discovery of four FCRL family genes, which they titled B-cell cross-linked by anti-IgM activation sequence (BXMAS) genes (Table 1 for updated nomenclature) (Nakayama *et al.* 2001).

The aforementioned nomenclature identifies each member of this family based upon their domain structure and is now utilised when referring to these proteins. Thus, the designation FCRL6 is now adopted for the protein previously recognised as FcRH6 and IFGP6 (Maltais *et al.* 2006).

Table 1. A summary of the existing and updated nomenclature of the human FCRL protein family along with their accession numbers.

Current Designation	Previous Designations	Accession Number
FCRL1	IRTA5, FcRH1, IFGP1, BXMAS1	Q96LA6
FCRL2	IRTA4, FcRH2, IFGP4, SPAP1, BXMAS2	Q96LA5e
FCRL3	IRTA3, FcRH3, IFGP3, SPAP2, BXMAS3	Q96P31
FCRL4	IRTA1, FcRH4, IFGP2	Q96PJ5
FCRL5	IRTA2, FcRH5, IFGP5, BXMAS	Q96RD9
FCRL6	FcRH6, IFGP6	Q6DN72
FCRLA	FCRL, FREB, FcRX	Q7L513
FCRLB	FCRL2, FREB2, FcRY	Q6BAA4

1.3.2 Genomic location in humans and mice

Genes encoding FCRL proteins are in close chromosomal proximity to those of classical FcRs. They are found interspersed within the Fc receptor cluster which spans over 15 megabases in the human chromosome 1q21-23 region. The loci for *FCRL1-5* extend over a 240 kilobase region within 1q23.1 where *FCRL1* is flanked at its telomeric end by *CD5L*, a member of the cysteine rich scavenger receptor family. *FCRL6* is present further telomeric at 1q23.2 between the classical FcR gene, *FcεRIα* and the FcR gamma-chain gene, *FcRγ*. *FCRLA* and *B* reside telomeric from the *FCRL6* locus at 1q23.3 where they map within 25 kilobase of the low affinity FcR gene, *FcγRIIB* (Figure 1) (Davis *et al.* 2002b).

Figure 1: Genomic location of the human FCRL protein family.

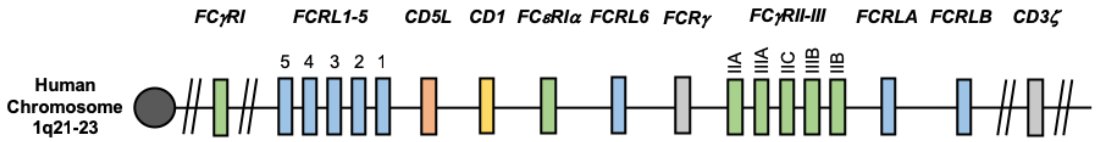

FCRL genes are located within the Fc receptor cluster which spans the q21-q23 region on chromosome 1. FCRL1-5 extend over a 240 kilobase region of in 1q23.1 whilst genes for other FCRL proteins are found at separate telomeric locations. Gene positions have been approximated using data from Ensembl and are not scaled. Adapted from (Davis *et al.* 2002b)

Characterisation of the mouse FCRL family has been limited but has indicated a significant divergence from human FCRL proteins. The mouse FCRL family differs not only in the number of proteins, but in the order as well as in the chromosomal organisation of the encoding genes. *Fcrl* genes are located on two different chromosomes in mice. *Fcrls, Fcrl1* and *Fcrl5* are found in tandem at a syntenic location on chromosome 3 whilst *Fcrl6, Fcrla and Fcrlb* are present at separate loci on chromosome 1 (Figure 2) (Davis *et al.* 2002b).

Figure 2: Genomic location of the mouse FCRL protein family.

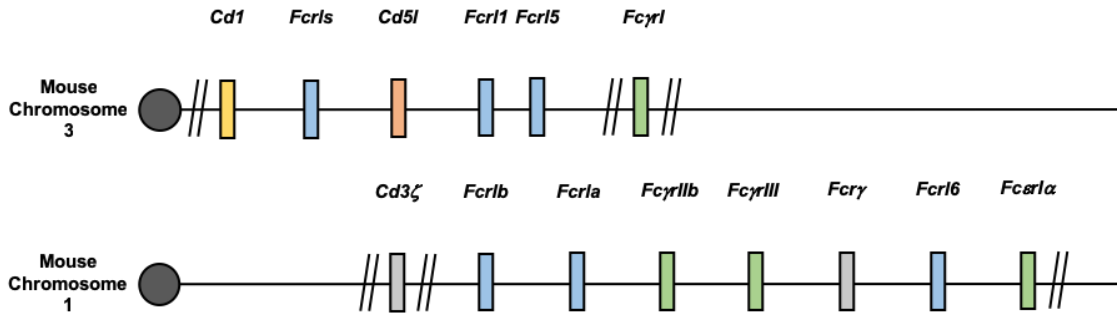

Fcrl genes are located on two different chromosomes in mice. *Fcrls, Fcrl1* and *Fcrl5* are found in tandem at a syntenic location on chromosome 3 whilst *Fcrl6, Fcrla and Fcrlb* are present at separate loci on chromosome 1. Gene positions have been approximated using data from Ensembl and are not scaled. Adapted from (Davis *et al.* 2002b)

1.3.3 Relation to classical Fc receptors

In addition to a shared genomic location, other factors, such as extracellular domain composition, indicate that FCRL proteins share a common ancestry with classical FcRs. Pairwise alignment of the extracellular amino acid sequences of FCRL proteins and classical FcRs suggests that members of these families arose following duplication of exons encoding five different Ig domain subtypes (Davis *et al.* 2001, 2002a, 2002b). Thus, extracellular regions of both classical FcRs and FCRL proteins are comprised of combinations of five different Ig-like C2 type domains. Extracellular regions of classical FcRs primarily consist of two or three Ig-like C2 type domains (subtypes D1, D2 and D3) whilst FCRL proteins possess much larger extracellular domains consisting of three to nine Ig-like C2 type domains (subtypes D1, D2, D3, D4 and D5). Thus, Ig-like C2 type domains 4 and 5 are restricted to the FCRL family of proteins and are not observed in classical FcRs (Figure 3) (Davis *et al.* 2005). A further shared feature of FCRL proteins and classical FcRs is a split signal peptide that is encoded by two separate exons, with the second exon being 21 base pairs (bp) (Davis *et al.* 2001; Pang *et al.* 1993; Qiu *et al.* 1990; van de Winkel *et al.* 1991; van de Winkel & Capel 1993). Despite similarities of FCRL proteins with classical Fc receptors, only human FCRL4, FCRL5 and FCRLA have been shown to be capable of binding Ig thereby, suggesting these proteins have evolved to recognise distinct ligands to classical Fc receptors in both humans and mice (Wilson *et al.* 2012; Wilson & Colonna 2005).

1.3.4 Conservation across different species

Despite differences in the number and chromosomal organisation of FCRL proteins between humans and mice, the close linkage of *Cd5l* with *Fcrl* genes on mouse chromosome 3 and the reversed, but conserved, positioning of *Fcrl* and other homologous genes on mouse chromosome 1 implies that the mouse FCRL family shares a common ancestry with human FCRL proteins. Additionally, mouse FCRL proteins alike members of the human FCRL family, also possess a split signal peptide thereby, further suggesting conservation of this family across the two species (Davis *et al.* 2002b).

In addition to mice, the biological importance of FCRL proteins is highlighted due to their conservation in a range of other vertebrates including bony fish, amphibians and birds. A range of *FCRL*-like genes, termed *XFL*, have been identified in the lymphoid tissues of *Xenopus*. These genes encode transmembrane and secreted proteins with characteristic features of the FCRL family such as Ig-like domains and a tyrosine-dependent signalling potential (Guselnikov *et al.* 2008). This suggests that *FCRL* genes have existed for at least 350 million years as mammals and amphibians share a common ancestor (Hedges & Kumar 1998). Thus, evidence supporting orthology of FCRL genes between species includes sequence similarity, syntenic genomic location, conserved genomic features such as the split signal peptide (21 bp second exon) and intracellular signalling motifs.

1.3.5 Structure of the human and mouse FCRL protein family

FCRL1-6 encode a group of type 1 transmembrane proteins with three to nine extracellular Ig-like C2 type domains and an intracellular region containing ITAMs and/or ITIMs. *FCRL6* encodes a transmembrane protein with three extracellular Ig-like C2 type domains (subtypes D2, D3 and D5), a transmembrane region and an ITIM bearing cytoplasmic tail. Contrastingly, *FCRLA* and *B* produce intracellular proteins with distinctive C-terminal mucin-like regions abundant in proline, leucine and serine/threonine residues. These proteins lack the aforementioned tyrosine-dependent signalling motifs present in transmembrane members of the FCRL protein family (Figure 3) (Li *et al.* 2014a).

Figure 3: Comparison of the structure of human FCRL proteins and classical Fc receptors.

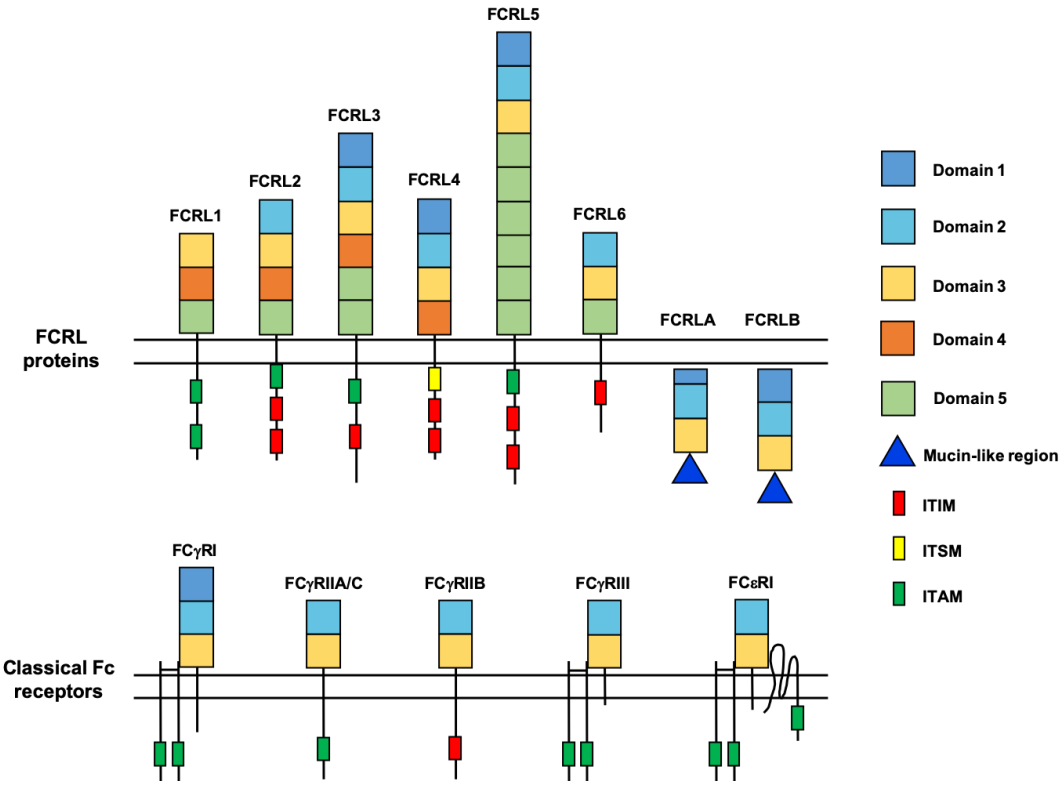

FCRL6 is a type 1 transmembrane protein composed of three extracellular Ig-like domains and contains a consensus ITIM sequence in its cytoplasmic region. Colours indicate structural similarities between the Ig-like domains of FCRL proteins and Fc receptors. Key intracellular motifs are highlighted by coloured boxes. Triangles denote mucin-like regions of the two intracellular FCRL proteins. FCγRI, FCγRIII and FCεRI are displayed in complex with the FCRγ adaptor subunit whilst FCεRI also associates with FcεR1β. Adapted from (Capone *et al.* 2016; Davis 2007)

Mouse FCRL proteins differ significantly in structure compared to their human counterparts. However, some structural similarities persist between the two species. *Fcrl1* and *Fcrl5* encode type 1 transmembrane proteins with relatively comparable features to their human counterparts. However, mouse FCRL5 shares a greater structural similarity with human FCRL2 and FCRL3 rather than its human orthologue. FCRL6 also displays interspecies differences as mouse FCRL6 is composed of two Ig-like C2 type extracellular domains (subtypes D3 and D5) and thus lacks an extracellular domain of the D2 subtype, and also possesses a shorter cytoplasmic region

devoid of a consensus ITIM sequence compared to human FCRL6 (Figure 4) (Li *et al.* 2014a). Thus, ligands and function of human and mouse FCRL6 may have evolved in a species-specific manner.

Figure 4: Structure of the mouse FCRL protein family.

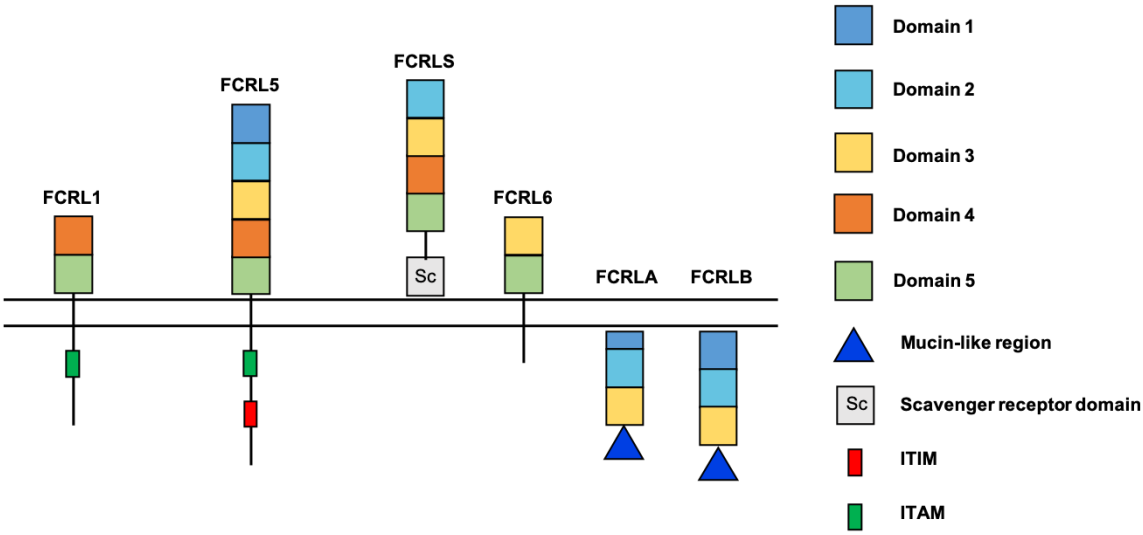

Mouse FCRL6 is composed of two extracellular Ig-like domains and lacks a consensus ITIM sequence in its cytoplasmic region. Colours indicate structural similarities between Ig-like domains of mouse and human FCRL proteins shown in Figure 3. Key intracellular motifs are highlighted by coloured boxes. Triangles denote mucin-rich regions of the two intracellular FCRL proteins. Adapted from (Capone *et al.* 2016; Li *et al.* 2014a)

1.4 Fc receptor-like 6

1.4.1 Isoforms

Potential alternative splicing of FCRL transcripts may generate multiple isoforms of these proteins. Four alternative transcripts of human FCRL6 encoding proteins with differing extracellular and/or intracellular regions (v1 to v4) have been identified (Kulemzin *et al.* 2011a). The majority of the published literature regarding FCRL6 corresponds to FCRL6_v1 which has also been identified as the longest of the four isoforms (Kulemzin *et al.* 2011a; Schreeder *et al.* 2008; Wilson *et al.*

2007a). FCRL6_v1 is translated by a 1943 bp mRNA molecule encompassing 10 exons which produces a 434 amino acid protein. The signal peptide is encoded by the first two exons whilst exons three to five singly encode for each of the three extracellular domains. The transmembrane region is encoded by the sixth exon. The ITIM containing cytoplasmic region is unique amongst transmembrane FCRL proteins as it encoded by four (exons seven to ten) rather than five exons (Davis *et al.* 2002b). FCRL6_v2 has been deduced to possess a single Ig-like C2 type extracellular domain of the fifth subtype along with an identical intracellular region as FCRL6_v1. The extracellular region of FCRL6_v3 contains two Ig-like C2 type extracellular domains of the third and fifth subtype whilst its intracellular region is shortened due to an alteration at the C-terminal which produces a reading frame shift in the tenth exon. FCRL6_v4 is identical in its structure to FCRL6_v1 apart from a shortened intracellular region due to an excision of the ninth exon from the cDNA (Figure 5). The expression of these isoforms has also been characterised with FCRL6_v1 and FCRL6_v4 being expressed at significantly higher levels compared to FCRL6_v2 or FCRL6_v3 (Kulemzin *et al.* 2011a).

Figure 5: Alternative splicing generates four isoforms of human FCRL6.

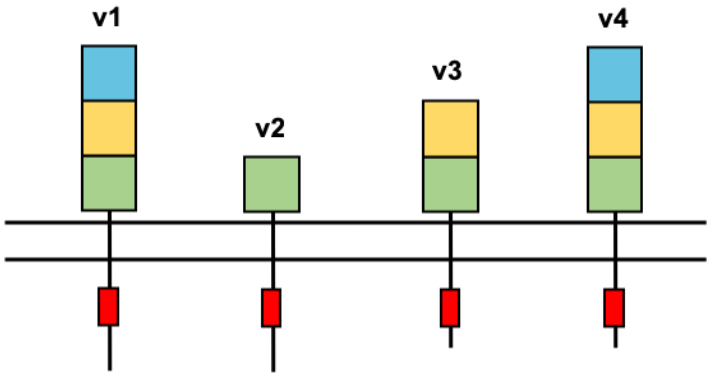

Four alternative transcripts of human FCRL6 encoding proteins with differing extracellular and/or intracellular regions have been identified. FCRL6_v1 and FCRL6_v4 are expressed at significantly higher levels compared to FCRL6_v2 or FCRL6_v3. FCRL6_v4 possesses a shorter cytoplasmic region compared to FCRL6_v1 but both possess identical extracellular regions. Adapted from (Capone *et al.* 2016; Kulemzin *et al.* 2011a)

Till data, the genomic organisation of mouse FCRL6 has not been investigated in similar detail as human FCRL6. However, two isoforms of mouse FCRL6 have been annotated; the canonical isoform is encoded by a 1913 bp mRNA molecule encompassing 7 exons which is translated into a 268 amino acid protein. The signal peptide is encoded by the first two exons. The second exon alongside the third, fourth and fifth exons also encode for the two Ig-like C2 type extracellular domains. The transmembrane region is encoded by the fifth exon which similarly to the second exon also encodes the cytoplasmic region along with the sixth and seventh exons. The amino acid sequence of the second isoform of mouse FCRL6 lacks 24 amino acids near its C-terminal end compared to the canonical isoform. This indicates that it does not encode a significant proportion of the cytoplasmic region (own analysis).

1.4.2 Intracellular signalling

Human FCRL6 contains two tandem tyrosine residues (Y356 and Y371) in its cytoplasmic region. The amino acid sequence surrounding the second tyrosine residue (Y371) fits a consensus ITIM sequence. However, a combination of the amino acid sequence surrounding this and the other tyrosine residue may also comprise a non-canonical ITAM (Kulemzin *et al.* 2011b; Schreeder *et al.* 2008). Thus, this receptor might possess an ability to activate multiple signalling pathways via association with SH2-containing molecules such as phosphatases and kinases.

Phosphorylation of tyrosine residues within the ITIM (Y371) and outside of the motif (Y356) has been shown to result in association of human FCRL6 with tyrosine (Shp-1 and Shp-2) and inositol phosphatases (Ship-1 and Ship-2). Y371 was found to be critical for the binding of Shp-1 and 2 phosphatases. However, effective binding of these phosphatases has been demonstrated to require both tyrosine residues. Accordingly, it has been suggested that Y371 acts as a docking site for the N-terminal SH2-domain of these phosphatases, whilst Y356 serves as the docking site for the C-terminal SH2-domain. Contrastingly, Y356 was found to be crucial for Ship-1 binding whilst Ship-2 association with human FCRL6 was shown to require both tyrosine residues. Despite a potential non-canonical ITAM, human FCRL6 has not been found to associate with

kinases such as Syk, Zap-70 and protein kinase D2 (Kulemzin *et al.* 2011a; Schreeder *et al.* 2008; Wilson *et al.* 2007b). Thus, this alongside its association with the aforementioned phosphatases suggests that human FCRL6 may possess ITIM-dependent inhibitory functionality.

The signalling potential of mouse FCRL6 has not been formally investigated. As previously indicated, the intracellular region of mouse FCRL6 does not contain a canonical ITIM. However, analysis of the amino acid sequence coding for this region reveals a single amino acid difference in a stretch of amino acids that constitute a consensus ITIM sequence. There is a phenylalanine residue at the -2 position from the tyrosine residue instead of a serine, isoleucine, valine or leucine residue (own analysis). Despite the absence of a consensus ITIM sequence, tyrosine phosphorylation and consequently, downstream signalling may still occur as predicted using a phosphorylation site predictor program (NetPhos 2.0) (Blom *et al.* 1999).

1.4.3 Expression

Members of the FCRL protein family are preferentially expressed by B-lineage cells in humans and mice with the exception of human FCRL3, which is additionally detected on NK and regulatory T cells, and human FCRL6 (Figure 6) (Nagata *et al.* 2009; Polson *et al.* 2006; Schreeder *et al.* 2008; Wilson *et al.* 2007a, 2012). Human FCRL6 expression has so far been reported on a range of mature cytotoxic cells including terminally differentiated $CD56^{low}$ NK cells, cytotoxic $CD4^+$ T cells, effector and effector memory $CD8^+$ T cells (Schreeder *et al.* 2008; Wilson *et al.* 2007a). Consequently, it is probable that FCRL6 expression correlates with terminal differentiation of these cytotoxic subsets in humans.

An increased percentage of $FCRL6^+$ NK cells and $CD4^+$ and $CD8^+$ T cells have been observed in patients with B cell chronic lymphocytic leukaemia (B-CLL), and following HIV-1 infection. Further analysis of FCRL6 expression on $CD8^+$ T cell subsets revealed increased expression of FCRL6 on effector and effector memory $CD8^+$ T cells in patients with B-CLL compared to healthy controls. Moreover, an increased number of FCRL6 expressing cells are observed in patients with B-CLL,

and following HIV-1 infection (Schreeder *et al.* 2008; Wilson *et al.* 2007a). It has to be noted though, that this increase in FCRL6 expressing cells is partly due to an expansion of the aforementioned cytotoxic populations during these conditions. Additionally, *FCRL6* expression in peripheral blood mononuclear cells (PBMCs) and $CD3^+$ cells from patients with autoimmune conditions such as rheumatoid arthritis, systemic lupus erythematosus and idiopathic thrombocytopenia purpura has been detected to have decreased compared to healthy controls (Kulemzin *et al.* 2011a). Furthermore, *In vitro* activation of human NK and $CD8^+$ T cells with IL-12 and IL-15, and an anti-CD3 antibody, respectively has been shown to decrease FCRL6 expression on these cells (Wilson *et al.* 2007b). Similarly, mitogen stimulation of PBMCs and $CD3^+$ cells also leads to a downregulation of *FCRL6* expression (Kulemzin *et al.* 2011a). Thus, expression of human FCRL6 appears to be affected following initial stimulation of cells and in states of chronic immune activation. There is an absence of conclusive data in the literature relating to the expression of FCRL6 in mice.

Figure 6: Expression of FCRL proteins in humans and mice.

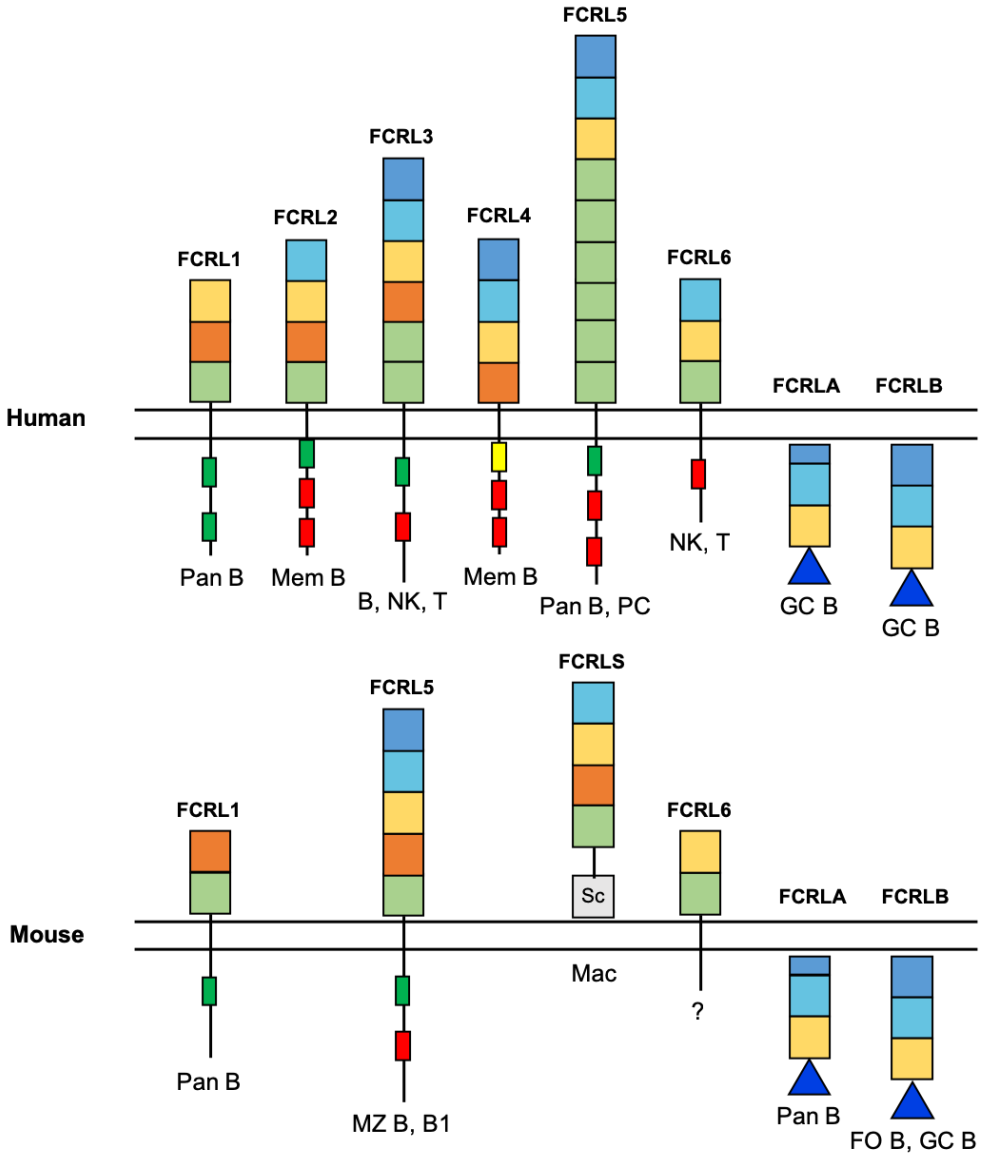

In contrast to the preferential B cell expression observed for the other FCRL protein family members, human FCRL6 is expressed by a range of cytotoxic lymphocytes including terminally differentiated NK cells, cytotoxic $CD4^+$ T cells, effector and effector memory $CD8^+$ T cells. Mouse FCRL6 expression remains to be definitively characterised. Colours indicate structural similarities between Ig-like domains of mouse and human FCRL proteins. Key intracellular motifs are highlighted by coloured boxes – ITIM (red) and ITAM (green). Triangles denote mucin-rich regions of intracellular FCRL proteins. GC B, germinal centre B cells; FO B, follicular B cells; Mac, macrophages; MZ B, marginal zone B cells; NK, natural killer cells; T, cytotoxic $CD4^+$ and $CD8^+$ T cells. Adapted from (Capone *et al.* 2016; Li *et al.* 2014a)

1.4.4 Ligands

Till date, a single study has identified potential ligands of human FCRL6. Human leukocyte antigen (HLA)-DR was found to bind to human FCRL6 with differing affinities dependent on the β chain composition of the HLA-DR molecule. HLA-DRα+β1, HLA-DRα+β4, and HLA-DRα+β5 molecules were found to have a higher affinity for human FCRL6 compared to HLADRα+β3 molecules (Schreeder *et al.* 2010). There are no studies published in the literature which have investigated the potential ligands of mouse FCRL6.

1.4.5 Function

Given the signalling ability and distribution of FCRL proteins amongst lymphocytes, it can be assumed that modulation of their activity may influence cellular activation. Accordingly, several studies have demonstrated that activation of these receptors impact cell behaviour. For example, antibody-mediated ligation of the ITAM-containing FCRL1 has been shown to stimulate B cell proliferation and enhance BCR activation (Leu *et al.* 2005). Conversely, ligation of FCRL2-5 has been shown to have an inhibitory effect on BCR signalling via recruitment of the Src homology region 2 domain-containing phosphatase (SHP)-1 following ITIM associated tyrosine phosphorylation (Ehrhardt *et al.* 2003; Haga *et al.* 2007; Jackson *et al.* 2010; Kochi *et al.* 2009).

There is very limited literature regarding human FCRL6 with only a few studies directly aiming to elucidate the function of this receptor. In earlier studies, antibody crosslinking of human FCRL6 was not found to significantly affect *in vitro* cytotoxicity, cytokine production, apoptosis, or proliferation of primary NK and $CD8^+$ T cells, and human FCRL6 transduced cell lines (Schreeder *et al.* 2008; Wilson *et al.* 2007b). However, a recent study has identified an inhibitory effect of human FCRL6 on the *in vitro* NK cell cytotoxicity in the presence of its ligand, HLA-DR. Expression of HLA-DRα+β1 on the NK sensitive target cell line K562 provided protection from NK92 cells transduced with human FCRL6. The authors also identified a minor inhibitory effect of human FCRL6 expression on IFNγ and TNFα production during *in vitro* expansion of primary

$CD8^+$ T cells with MHCI restricted peptides (Johnson *et al.* 2018a). There are no studies published in the literature which investigated the function of mouse FCRL6.

1.5 Friend virus

1.5.1 The Friend Virus Model

Friend virus (FV) was discovered by Charlotte Friend in 1957. It was initially described as a disease-causing agent that was capable of cell-free transmission and causing leukaemia in Swiss mice (Friend 1957). FV was subsequently identified as a complex of two viruses: replication defective spleen focus forming virus (SFFV) and replication competent Friend-murine leukaemia virus (F-MLV). FV causes a protracted infection which induces a potent innate and adaptive immune response that eventually clears the infection in C57BL/6 mice (Dittmer *et al.* 2019). Thus, this model allows us to investigate factors affecting innate and adaptive immune pathways regulating immunity to retroviral pathogens.

1.5.2 Immune response to Friend virus

Effective clearance of FV infection in resistant host mice is dependent upon the functional activity of B cells, $CD4^+$ T cells, $CD8^+$ T cells and NK cells (Dittmer *et al.* 1999; Littwitz *et al.* 2013; Messer *et al.* 2004).

1.5.2.1 T cell mediated responses

The MHCII haplotype of the host plays an important role in the $CD4^+$ T cell response following FV infection. $CD4^+$ T cells are able to detect FV through two distinct epitopes derived from the envelope glycoprotein 70 (gp70) of FV. One of these epitopes is located within the N terminus of gp70 at amino acids 122 to 141, and is presented on H-2A MHCII alleles whilst the other epitope is located closer to the C terminus of gp70 at amino acids 462 to 479, and is presented on H2-E MHCII alleles (Iwashiro *et al.* 1993). Due to a natural mutation within the H2-E allele of C57BL/6 mice, $CD4^+$ T cells from C57BL/6 mice are restricted to recognising a single epitope ($env_{122-141}$) presented in the context of H-2A MHCII alleles following FV infection. However, it has been demonstrated in mice with functional forms of both H-2A and H2-E MHCII alleles that presentation

through H-2A MHCII alleles is better associated with recovery from infection (Hasenkrug & Chesebro 1997). Thus, the H-2A MHCII allele is vital for the resistance of C57BL/6 mice to FV infection.

$CD4^+$ T cells with cytotoxic potential ($CD4^+$ CTLs) in addition to conventional $CD4^+$ T cells may also play an important role in mediating protection following FV infection (Manzke *et al.* 2013). B cells represent a major reservoir of virus during FV infection. Thus, killing of these cells by MHCII restricted $CD4^+$ CTLs may represent a vital mechanism for reducing viral spread and limiting infection (Hasenkrug *et al.* 1998). However, the primary cells responsible for mediating cytotoxic responses in a competent immune system are $CD8^+$ T cells. These cells are responsible for the direct killing of infected cells via recognition of antigen derived peptides presented in the context of MHCI alleles. $CD8^+$ T cells are essential for mediating immunity against FV as their absence leads to a significantly higher viral load (Joedicke *et al.* 2014).

As mentioned before, C57BL/6 mice are resistant to FV-induced leukaemia but the clearance of the virus is not complete, resulting in a persistent chronic infection. During chronic viral infection, continuous exposure of $CD8^+$ T cells to viral antigens can lead to the expression of inhibitory receptors, causing a dysfunctional state (McLane *et al.* 2019). Nonetheless, FV infection results in the generation of terminally exhausted virus-specific $CD8^+$ T cells that express a range of inhibitory receptors including PD1, Tim-3, LAG-3 and CTLA-4. Acute FV infection is characterised by a rapid expansion of virus-infected erythroblasts. A majority of these erythroblasts expresses PD-L1 and MHCI thereby generating highly tolerogenic environment in which virus-specific $CD8^+$ T cells progressively become non-responsive to further stimulation following expression of inhibitory receptors such as PD-1 (Takamura *et al.* 2010). Expression of PD-1, Tim-3, LAG-3, CTLA-4 and CD244 also increases on activated $CD4^+$ T cells following FV infection. This expression appeared to affect their effector function as CTLA-4 or LAG-3 blockade during FV infection increased the production of IFNγ and TNFα by bone marrow $CD4^+$ T cells following *ex vivo* restimulation with anti-CD3/CD28 antibodies (Teigler *et al.* 2017). Thus, expression of inhibitory receptors and resulting exhaustion of $CD4^+$ and $CD8^+$ T cells following FV infection

allows us to use this model to test the inhibitory potential of novel receptors.

1.5.2.2 NK cell mediated responses

NK cells are vital for the rapid suppression of viral replication. Their importance in mediating retroviral immunity is emphasised by increased viral loads in HIV patients with viral escape from NK cell responses or polymorphisms in their activating NK cell receptors. Similarly, a crucial role of NK cells has been identified during the early stage of FV infection as depletion of NK cells up to four days following infection resulted in an increased viral load (Littwitz *et al.* 2013). NK cells may mediate this protective effect via direct cytotoxicity or through indirect mechanisms such as IFNγ production. NK cell depletion at later stages of FV infection was not shown to significantly affect viral load as a result of a fully developed $CD8^+$ T cell response (Littwitz *et al.* 2013). Thus, NK cells have distinct anti-retroviral effects during the early FV infection as T cell responses have not yet developed thereby allowing us to use this model to investigate factors affecting NK cell function.

1.5.2.3 B cell mediated responses

B cells have been shown to be crucial for mediating immunity against FV. Their primary role involves production of virus-specific neutralising antibodies that control the infection level. This was highlighted by control of FV infection in B cell deficient mice following transfer of virus-specific neutralising antibodies (Messer *et al.* 2004). Additionally, B cells also function as APCs that are able to prime T cells and influence their responses. Following activation, B cells have been shown to endocytose antigen 1000-fold more efficiently than non-specific cells. This is due to their expression of antigen specific BCRs and a reorganisation of their cytoskeleton that not only increases internalisation of antigen bound BCRs but also processing and loading of these complexes onto MHCII molecules thereby, allowing B cells to act as proficient APCs for the *in vivo* priming of $CD4^+$ T cells (Chen & Jensen 2008). Thus, B cells may also affect the quality of the $CD4^+$ T cell response following FV infection in addition to their role of producing virus-specific

neutralising antibodies (Schultz *et al.* 1990). Consequently, we are also able to use the FV model to investigate proteins expressed by B that could affect the antibody response.

1.6 B16 melanoma

The B16 melanoma is a mouse tumour cell line that is used as a model for human skin cancers. A majority of the tumour cells form colonies in the lungs of host mice following intravenous injection. Although the term pulmonary metastasis is used to describe this model, each pulmonary colony is an independent primary tumour rather than true metastasis (Overwijk & Restifo 2001). Immunity to B16 melanoma cells could involve responses by $CD4^+$ and $CD8^+$ T cells as well NK cells (Steinman *et al.* 2003; Takeda *et al.* 2011). The NK cell response following B16 melanoma cell inoculation is discussed below.

1.6.1 NK mediated immune response to B16 melanoma cells

NK cells are critical components of the innate immune system and mediate host defence against viral infection and neoplasms. In anticancer immunity, NK cells are recognised for their role in reducing or preventing tumour metastases (Takeda *et al.* 2011; Vivier *et al.* 2008). This has been shown in multiple studies where depletion of NK cells has resulted in an increase in tumour burden (Gorelik *et al.* 1982; Hanna 1982; Wiltrout *et al.* 1985). Expectedly, NK cells are also involved in the anti-tumour immune response against B16 melanoma cells. This has been highlighted via NK depletion experiments which resulted in an increased number of pulmonary colonies following intravenous injection of B16 melanoma cells into host mice (Grundy *et al.* 2007; Takeda *et al.* 2011). Several cytotoxic molecules, such as perforin, granzymes, TRAIL, and Fas ligand have been identified as the major effectors used by NK cells to suppress metastases (Takeda *et al.* 2001; van den Broek *et al.* 1995; Voskoboinik *et al.* 2006). However, it has been suggested that IFNγ production by NK cells rather than cytotoxicity plays a more important role in inhibiting B16 lung metastases. This was demonstrated in experiments involving deletion of one or more of the aforementioned key NK cytotoxic molecules which failed to affect lung pulmonary burden compared to IFNγ deletion which significantly augmented pulmonary colonies. Accordingly, lung NK cells have been shown to constitutively secrete, and increase their production of IFNγ following B16 tumour cell inoculation. Moreover, adoptive transfer of NK cells from perforin

knockout but not IFNγ knockout mice into IFNγ knockout host mice prevented B16 lung metastasis. Thus, IFNγ production by lung NK cells plays an important role in mediating natural resistance to B16 lung metastasis. One of the mechanisms by which IFNγ could be facilitating this resistance is through an increased activity of phagocytes as NK cell transfer into Rag common γ chain knockout mice inhibits B16 lung metastasis thereby suggesting that the IFNγ responding cells are not lymphocytes. (Takeda *et al.* 2011). The crucial role of NK cells in the B16 melanoma model allows us to use this model to investigate the function of novel proteins expressed by NK cells. Enforced expression or deletion of these proteins may cause changes in NK cell function that could translate into an evident difference in the lung pulmonary load.

1.7 Aims and hypothesis

Conflicting data exists in the literature regarding the functional capacity of human FCRL6. Its ability to potentially recruit tyrosine and inositol phosphatases along with limited expression in healthy individuals but upregulation on cytotoxic lymphocytes cells in states of chronic immune activation suggests that this receptor may possess an immunoregulatory function. The late stages of chronic viral infections and malignancies are frequently accompanied with functional exhaustion of virus and tumour-specific effector T cells (Hashimoto *et al.* 2018; Kahan *et al.* 2015). Reductions in their proliferative capacity and cytotoxicity are often driven by the expression of inhibitory receptors such as PD1, CD244, and CD160 (Agresta *et al.* 2018; Chibueze *et al.* 2014; Jiang *et al.* 2015). The expression profile and signalling potential of human FCRL6 suggests that it may also play a role in this exhaustion. Additionally, human FCRL6 may also act as an inhibitory receptor for NK cells by binding self-ligands to maintain tolerance and prevent autoimmunity.

Till date, the function of human and mouse FCRL6 has not been investigated in an *in vivo* environment. Moreover, the expression profile of mouse FCRL6 also remains to be elucidated. Thus, we aimed to first characterise the expression of FCRL6 in major immune populations of the mouse and subsequently, to analyse the effect of its complete and conditional deletion on the development as well as on the function of these cells in mouse models of retroviral infection and melanoma. Due to the structural differences between human and mouse FCRL6, we also generated a transgenic (Tg) mouse strain expressing human FCRL6 in order to further investigate the function of this receptor in an *in vivo* setting.

Chapter 2. Materials & Methods

2.1 Mice

All mouse strains used in this thesis are listed in Table 2. All animal experiments were approved by the ethical committee of the Francis Crick institute, and conducted according to local guidelines and UK Home Office regulations under the Animals Scientific Procedures Act 1986 (ASPA). Male and female mice were used in separate experiments and were age and gender-matched accordingly. Mice were used at 8–12 weeks of age.

Table 2. A brief description of mice utilised in this thesis

Strain	Description	Reference/Source
C57BL/6 WT	Wild type mice	Jackson laboratory
C57BL/6 *Fcrl6*$^{-/-}$	Mice with germline deletion of the gene encoding Fc receptor-like 6	Unpublished
C57BL/6 B cell conditional *Fcrl6*$^{-/-}$	Mice with B cell specific deletion of the gene encoding Fc receptor-like 6 from the pro-B cell stage of B cell development	Unpublished
C57BL/6 NK cell conditional *Fcrl6*$^{-/-}$	Mice with NK cell specific deletion of the gene encoding Fc receptor-like 6 from the immature NK cell stage of NK cell development	Unpublished
C57BL/6 human FCRL6 transgenic	Transgenic mice expressing human FCRL6 under control of the human CD2 promoter to allow expression in T cells	Unpublished
C57BL/6 EF4.1 TCRβ transgenic	TCRβ transgenic mice with an enriched frequency of FV envelope-specific CD4^{+} T cells	(Antunes *et al.* 2008)
C57BL/6 human FCRL6 EF4.1 TCRβ double transgenic	TCRβ transgenic mice with an enriched frequency of human FCRL6 expressing FV envelope-specific CD4^{+} T cells	Unpublished
C57BL/6 CD45.1 WT	Wild type mice that express the CD45.1 allele which is atypical on the C57BL/6 background to allow identification of transferred cells	Jackson laboratory
C57BL/6 CD45.1/2 WT	Wild type mice that express both the CD45.1 and CD45.2 alleles to serve as recipients for cell transfer experiments	Jackson laboratory

C57BL/6 CD45.1/2 human FCRL6 transgenic	Transgenic mice that express both the CD45.1 and CD45.2 alleles in addition to human FCRL6 to serve as recipients for cell transfer experiments involving human FCRL6 expressing cells	Jackson laboratory
C57BL/6 *Rag1*$^{-/-}$	Mice that are deficient in recombination-activating gene 1 and are consequently deficient in T and B lymphocytes	Jackson laboratory
C57BL/6 *Rag2*$^{-/-}$	Mice that are deficient in recombination-activating gene 2 and are consequently deficient in T and B lymphocytes	Jackson laboratory
129 Sv/Ev *Rag2*$^{-/-}$	Mice that are deficient in recombination-activating gene 2 and are consequently deficient in T and B lymphocytes	Jackson laboratory

2.1.1 Generation of *Fcrl6*$^{-/-}$ mice

The generation of *Fcrl6*$^{-/-}$ mice is detailed in section 3.2.5 whilst generation of B cell conditional *Fcrl6*$^{-/-}$ and NK cell conditional *Fcrl6*$^{-/-}$ mice is described in section 4.3.2.4 and 5.3.2, respectively.

2.1.2 Generation of transgenic mice

2.1.2.1 EF4.1 mice

The EF4.1 mouse is a TCRβ transgenic strain which has been previously generated in the lab (Antunes *et al.* 2008). The fixed TCRβ chain of the EF4.1 mouse is derived from the SB14-31 CD4^{+} T cell clone which recognises the N-terminal region of the envelope glycoprotein of FV (Iwashiro *et al.* 1993)

2.1.2.2 Human FCRL6 transgenic mice

The generation of human FCRL6 expressing Tg mice is discussed in section 6.3.2.

2.2 Tissue and cell preparation

2.2.1 Media and culture conditions

Room temperature (RT) cell incubation, antibody staining, cell sorting and tissue collection was accomplished with Air-Buffered Iscove's-Modified-Dulbecco's-Medium (AB-IMDM) containing 25mM HEPES buffer and L-glutamine, and supplemented with 0.21% NaCl, 60 μg/ml penicillin, and 100 μg/ml streptomycin (Invitrogen). Lysis of erythrocytes was accomplished with Ammonium-Chloride-Potassium (ACK) buffer (0.15 M NH4Cl, 1 mM KHCO3, 0.1 mM EDTA, pH 7.2-7.4). Cells were cultured with complete Iscove's-Modified-Dulbecco's-Medium (IMDM) (Sigma-Aldrich) which was supplemented with 5% heat inactivated foetal calf serum (FCS) (BioSera, Ringmer, UK), 2mM L-glutamine, 100μg/ml penicillin, 100μg/ml streptomycin, and 10^{-5} M mercaptoethanol (Invitrogen). All flow cytometric straining was performed in fluorescence-activated cell (FACS) sorting buffer (PBS, 2% FCS, 0.1% azide). Primary cells and cell lines were cultured at 95% humidity, 5% CO2 and 37°C.

2.2.2 Single cell suspensions

Single cell suspensions were prepared from the spleens and thymi of mice via mechanical disruption through 40μm or 70μm cell-strainers (Falcon, Becton Dickinson Labware) using a 5ml syringe plunger. Spleen suspensions were treated with ACK for a short period of time before being resuspended in AB-IMDM. Bone marrow cell suspensions were prepared by flushing the bone cavities of the femur and tibiae of donor mice with AB-IMDM. This was followed by treatment with ACK lysis buffer. Live cells were subsequently quantified using a Neubauer haemocytometer (Marienfield). Single cell suspensions from lung tissues were prepared by enzymatic digestion in 20 μg/mL Liberase (Sigma-Aldrich) and 50 μg/mL DNase I (STEMCELL Technologies) for 30 min at 37°C followed by homogenization with a GentleMax dissociator (Miltenyi Biotec).

2.2.3 Cell enrichment

Enrichment of primary cells prior to cell sorting was performed using a PE immunomagnetic selection kit (StemCell). Single cell suspensions were prepared to a concentration of $1x10^8$ ml in AB-IMDM and then incubated with required PE-conjugated antibodies for 30 minutes in the dark at RT. Cells were subsequently washed once in AB-IMDM to remove excess antibody and then resuspended in the starting volume of AB-IMDM. This was followed by addition of the EasySep Selection cocktail (25 μl/ml of cells) and incubation of the cell suspension at RT for 15-20 mins. EasySep Magnetic Nanoparticle beads were then added (25 μl/ml of cells) and the suspensions was gently resuspended to ensure uniform distribution of the beads. After 20 minutes, the suspension was further diluted in AB-IMDM according to the manufacturer's instructions and transferred into 14ml round bottom polystyrene tubes (StemCell) before being placed into a separating magnet (StemCell). The magnet generates a high-gradient magnetic field around the polystyrene tube, allowing for the separation of cells labelled with the EasySep Magnetic Nanoparticles. For positive selection: non-labelled cells in the supernatant were poured off after 5 minutes of incubation at RT by inverting the magnet and tube. This was repeated a further two times to increase purity. For negative selection of cells: the supernatant containing desired cells was collected after 5 minutes of incubation whilst unwanted cells captured by the magnet were discarded. Purity was then ascertained using flow cytometry and was typically over 95%.

2.2.4 $CD4^+$ T cell isolation

Isolation of primary $CD4^+$ T cells was achieved using a negative immunomagnetic selection kit (StemCell). Unwanted cells were targeted for removal via biotinylated antibodies directed against non-$CD4^+$ T cells and streptavidin-coated magnetic particles known as RapidSpheres™. Single cell suspensions were prepared at a concentration of $1x10^8$ ml in AB-IMDM and incubated at RT with the isolation antibody cocktail (50μl/ml of cells) and rat serum (50μl/ml of cells) to avoid unspecific binding for 10 minutes in the dark. This was followed by the addition of RapidSpheres™ (75μl/ml of cells) and gentle mixing of the cell suspensions to ensure uniform distribution of the

magnetic particles. After an incubation of 2.5 minutes at RT, the cell suspensions were further diluted with AB-IMDM according to the manufacturer's instructions and transferred into 14ml round bottom polystyrene tubes (StemCell) before being placed into a separating magnet (StemCell). The magnet generates a high-gradient magnetic field around the polystyrene tube, allowing for the separation of non $CD4^+$ T cells labelled with streptavidin-coated magnetic RapidSpheres™. After 2.5 minutes of incubation at RT, the supernatant containing $CD4^+$ T cells was collected whilst non-$CD4^+$ T cells captured by the magnet were discarded. Purity was then ascertained using flow cytometry and was typically over 95%.

2.3 In vitro

2.3.1 In vitro T cell activation

Single cell suspensions were prepared from the spleens of donor mice and resuspended in AB-IMDM and plated at a concentration of $1x10^6$ cells/100μl in 96-well plates (Sigma Aldrich). Cells were then stimulated with the indicated amount of the $env_{122-141}$ epitope (DEPLTSLTPRCNTAWNRLKL) or with anti-CD3/CD28 T cell-activating Dyna Beads according to the manufacturer's instructions (Thermo-Fisher).

Alternatively, for the activation of isolated antigen-specific populations of $CD4^+$ T cells, T cells were cocultured at a concentration of $2x10^5$ cells/100μl with irradiated B3 cells (20Gy) (see section 2.3.3 of the thesis for generation of B3 cells) in 96-well plates at a ratio of 1:5 with respect to T cells and subsequently stimulated with the indicated amount of the $env_{122-141}$ epitope or by H2-Ab covalently linked with F-MLV-$env_{123-139}$ (EPLTSLTPRCNTAWNRL).

T cell activation was assessed 18 hours following stimulation by FACS detection of early markers of activation or 3 and 6 days later by the detection of CellTrace Violet dilution by FACS analysis.

2.3.2 CellTrace Violet labelling

$CD4^+$ T cells were suspended at a concentration of $1x10^6$ cells/ml in phosphate buffered saline (PBS) (Gibco) following which CellTrace Violet (CTV) was added at a dilution of 1:1000. After 20 minutes of incubation at 37°C, cell culture medium at five times the original volume of PBS was added to the cell suspension to remove free dye remaining in the solution. After 5 minutes of incubation at RT, $CD4^+$ T cells were resuspended in fresh pre-warmed cell culture medium and rested for 10 minutes prior to activation as detailed in section 2.3.1. Dividing cells were identified by CTV dilution via FACS analysis following activation.

2.3.3 Generation of B3 cell lines expressing human HLA-DR and mouse MHCII

Plasmids containing the cDNA sequences of human *HLA-DRα*01:02* and *HLA-DRβ1*15:01*, mouse *H2-Aa* and *H2-Ab1* alone or covalently linked with the F-MLV-$env_{123-139}$ (EPLTSLTPRCNTAWNRL) in the pRV retroviral vector were synthesised and sequenced by GENEWIZ (South Plainfield, NJ, USA). Retroviral particles were produced by transfection of pRV plasmids encoding human HLA-DR, mouse MHC II chains alone or covalently linked with the F-MLV-$env_{123-139}$ into the Platinum-E (Plat-E) retroviral packaging cell line, using the GeneJuice transfection reagent (Novagen). Plat-E culture supernatants containing viral stocks were harvested two days after the initial transfection and used for transduction of B3 cells. B3 cells are a mouse pro-B cell leukaemia cell line originally established from IL-7 transgenic mice (Fisher *et al.* 1995). B3 cells were mixed with supernatants containing viral stocks in the presence of 4 μg/ml polybrene (Sigma-Aldrich) and spun at ~315×g for 45 min, before resuspended in IMDM for further culture. Sublines homogenously expressing the transduced gene products were established by cell sorting for HLA-DR and/or mouse MHCII.

2.3.4 Neutralising antibody assay

Mus dunni cells (Lander & Chattopadhyay 1984) were transduced with the XG7 replication-defective retroviral vector which expresses GFP from a human cytomegalovirus promoter (Bock *et al.* 2000). *M. dunni*-XG7 cells were then infected with B-tropic helper murine leukaemia virus following which the culture supernatant containing the pseudotyped XG7 vector was harvested. Serial dilutions of serum from infected mice was mixed with ~1,500 iu/ml of the pseudotyped XG7 vector and incubated for 30 min at 37°C in cell culture medium. Mixtures were subsequently added to untransduced *M. dunni* cells and incubated for 3 days. The percentage of GFP^+ *M. dunni* cells at the end of the incubation period was assessed by FACS analysis, and the dilution of serum which resulted in 75% neutralization (i.e. 75% reduction in the percentage of GFP^+ *M. dunni* cells) was used as the neutralising titre.

2.3.5 F-MLV infected cell binding assay

Serum samples were diluted 1:100 in FACS buffer and incubated with F-MLV-infected *Mus dunni* cells for a period of 30 minutes at RT. The cells were then washed and resuspended for a further 30 minutes at RT in FACS buffer containing fluorescently labelled anti-mouse IgG1, anti-mouse IgG2a/c, anti-mouse IgG2b and anti-mouse IgM antibodies following which, the median fluorescence intensity of the fluorescently labelled antibodies was determined by FACS analysis.

2.3.6 ELISA for serum immunoglobulin

96-well MaxiSorp plates (Nunc) were coated with 0.25 μg/well of the correct coating antibody (Goat anti-mouse IgG, goat anti-mouse IgM and goat-anti mouse IgA – all Southern Biotech) in coating buffer (borate buffered saline) and incubated overnight at 4 °C. The coating antibody was then removed and plates were blocked with 200μl/well of blocking buffer (PBS with 1% bovine serum albumin, 0.3% Tween20 and 0.05% NaN_3) for 2 hours at 37°C. Plates were then washed 4 times with wash buffer (PBS with 0.01% Tween20) following which serial dilutions of serum and

purified immunoglobulin in blocking buffer were added and incubated for 2 hours at RT. The plates were washed 4 times with wash buffer and 50 µl/well of secondary alkaline phosphatase (AP)-conjugated detecting antibodies (Goat anti-mouse IgG (H+L)-AP, goat anti-mouse IgM-AP and goat anti-mouse IgA-AP – all Southern Biotech) diluted 1/1000 were added and incubated for 1 hour at RT. The plates were then washed 4 times with wash buffer and 50 µl/well of 1 mg/ml 4-Nitrophenyl phosphate disodium salt hexahydrate (Sigma) in diethanolamine buffer solution (pH 9.8) was added following which the plates were incubated in the dark until the colour reaction was complete. The optical density was then quantified using a 405 nm measurement wavelength on a Tecan Sapphire.

2.4 In vivo

2.4.1 Adoptive transfers

Single-cell suspensions were prepared from the spleens of donor mice as described in section 2.2.2 and $CD4^+$ T cells were isolated using a negative immunomagnetic selection kit as described in section 2.2.4. A total of $1x10^6$ CD4 T cells were intravenously injected into recipient mice. B3 $MHCII^{env123-139}$ cells were established as described in section 2.3.3. A total of $1.5x10^6$ B3 $MHCII^{env123-139}$ cells were intravenously injected into recipient mice.

2.4.2 Generation of mixed bone-marrow chimeras

Bone marrow cell suspensions were prepared from CD45.1 wild type and *Fcrl6*$^{-/-}$ donor mice as described in section 2.2.2 of the thesis. Cell suspensions were then mixed at the desired ratio and injected into $CD45.1^+/CD45.2^+$ recipient mice myeloablated with Busulfan (20mg/kg). Each recipient mouse received a mixed suspension of $1x10^7$ bone marrow cells following which mice were culled 8-10 weeks post bone marrow transfer for assessment of reconstitution.

2.4.3 FV infection

The FV used in this study is a retroviral complex of a replication-competent B-tropic F-MLV and a replication-defective SFFV. Stocks were propagated *in vivo* and prepared from the spleens of susceptible infected mice. A pool of LDV-free BALB/c mice was infected with FV following which their spleens were isolated 12 days later and homogenized (10% w/v) in PBS. Aliquots of spleen homogenates were frozen and used for infection. Wild type of *Fcrl6*$^{-/-}$ mice received an inoculum of ~1,000 spleen focus-forming units of FV by intravenous injection following which the infection was analysed 7 or 35 days later. FV stocks were free of Sendai virus, Murine hepatitis virus, Parvoviruses 1 and 2, Reovirus 3, Theiler's murine encephalomyelitis virus, Murine rotavirus, Ectromelia virus, Murine cytomegalovirus, K virus, Polyomavirus, Hantaan virus, Murine norovirus, Lymphocytic choriomeningitis virus, Murine adenoviruses FL and K87, Mycoplasma sp. and LDV

2.4.4 DNP-OVA challenge

Wild type or *Fcrl6*$^{-/-}$ mice received 100µg of dinitrophenylated ovalbumin (DNP-OVA) by intraperitoneal injection in a suspension of PBS and the adjuvant, monophosphoryl lipid A. The DNP-specific antibody response as well as germinal centre formation was analysed 14 days later.

2.4.5 B16 melanoma cell inoculation

Wild type or *Fcrl6*$^{-/-}$ mice were intravenously injected with 5×10^5 C56BL/6-derived B16-F0 melanoma cells (CRL-6322) which were maintained as described in section 2.2.1. For counting of lung metastasis, lungs were harvested and fixed in Bouin's solution following which visible nodules were enumerated in a blinded manner.

2.5 Flow cytometric analysis

2.5.1 List of antibodies

Table 3. List of antibodies

Antigen	Description	Clone	Source	Dilution
CD2	PE/Cy7 anti-mouse CD2	RM2-5	BioLegend	1/200
CD4	PE-Cy7 anti-mouse CD4	GK1.5	Insight Biotech (eBiosciences)	1/200
CD4	eFluor450 anti-mouse CD4	RM4-5	eBioscience	1/200
CD4	Brilliant Violet 785 anti-mouse CD4	GK1.5	BioLegend	1/200
CD4	BUV395 anti-mouse CD4	RM4-5	BD Biosciences	1/200
CD8α	APC anti-mouse CD8α	53-6.7	Insight Biotech (eBiosciences)	1/200
CD8α	PE-Cy7 anti-mouse CD8α	53-6.7	Insight Biotech (eBiosciences)	1/200
CD8α	PETxR anti-mouse CD8α	5H10	Invitrogen	1/200
CD8α	PerCP/Cy5.5 anti-mouse CD8α	53-6.7	BioLegend	1/200
CD11b	PE-Cy7 anti-mouse CD11b	M1/70	BioLegend	1/300
CD11c	APC-Alexa Fluor 750 anti-mouse CD11c	N418	Insight Biotech (eBiosciences)	1/200
CD19	FITC anti-mouse CD19	MB19-1	Insight Biotech (eBiosciences)	1/200
CD19	APC anti-mouse CD19	6D5	BioLegend	1/200
CD23	PE anti-mouse CD23	B3B4	BioLegend	1/200
CD25	PE anti-mouse CD25	PC61.5	Insight Biotech	1/300
CD27	APC anti-mouse, human, rat CD27	LG.7F9	Insight Biotech (eBiosciences)	1/200
CD38	APC anti-mouse CD38	90	Insight Biotech (eBiosciences)	1/200
CD43	PE anti-mouse CD43 activation-	1B11	BioLegend	1/200

	associated glycoform			
CD44	Pacific Blue anti-mouse/human CD44	IM7	BioLegend	1/200
CD44	APC anti-mouse/human CD44	IM7	Insight Biotech (eBiosciences)	1/200
CD44	V500 anti-mouse/human CD44	IM7	BD Biosceinces	1/200
CD45.1	eFluor450 anti-mouse CD45.1	A20	eBioscience	1/200
CD45.1	APC-eFluor® 780 anti-mouse CD45.1	A20	eBioscience	1/200
CD45.1	Brilliant Violet 785™ anti-mouse CD45.1	A20	BioLegend UK	1/200
CD45.2	PE anti-mouse CD45.2	104	BioLegend	1/200
CD45.2	APC anti-Mouse CD45.2	104	BioLegend	1/200
CD45.2	Brilliant Violet 711 anti-mouse CD45.2	104	BioLegend	1/200
B220	Pacific Orange anti-Mouse CD45R	RA3-6B2	Invitrogen Limited	1/200
B220	FITC anti-Mouse CD45R	RA3-6B2	Invitrogen Limited	1/200
CD49b	PE anti-mouse CD49b	HMa2	BD Biosciences	1/200
CD49b	PE/Cy7 anti-mouse CD49b	DX5	eBioscience	1/200
CD69	FITC anti-mouse CD69	H1.2F3	Insight Biotech	1/200
CD69	Pacific Blue anti-mouse CD69	H1.2F3	BioLegend	1/200
CD69	Brilliant Violet 785 anti-mouse CD69	H1.2F3	BioLegend	1/200
CD86	Pacific Blue anti-mouse CD86	GL-1	BioLegend	1/200
CD93	APC anti-Mouse CD93	AA4.1	eBioscience	1/200

CD93	PE-Cyanine7 anti-Mouse CD93	AA4.1	eBioscience	1/200
CD95	PE-CF594 anti-mouse CD95	Jo2	BD Biosciences	1/200
CD122	PE anti-mouse CD122 (IL-2 R beta)	5H4	Insight Biotech (eBiosciences)	1/200
CD122	Super Bright 436 anti-mouse CD122 (IL-2 R beta)	TM-b1	ThermoFisher Scientific	1/200
CD184	PerCPeFluor710 anti-mouse CD184 (CXCR4)	2B11	eBioscience	1/200
CD223	PE anti-mouse CD223 (Lag-3)	C9B7W	eBioscience	1/200
CD279	PECy7 anti-mouse CD279 (PD-1)	29F.1A12	BioLegend	1/200
CD335	Brilliant Violet 421 anti-mouse CD335 (NKp46)	29A1.4	BioLegend	1/200
FoxP3	APC anti-mouse/rat FoxP3	FJK-16s	Invitrogen	1/200
GL7	eFluor450 anti-human/mouse GL7	GL-7	BioLegend	1/200
Glyo-gag	Unconjugated 34	N/A	The Francis Crick Institute	1/500
Granzyme B	Pacific Blue anti-human/mouse Granzyme B	GB11	BioLegend	1/50
HLA-DR	PE anti-human HLA-DR	L243	BioLegend	1/200
Human FCRL6	Unconjugated anti-human FCRL6	7B7/FcRL6	BioLegend	1/200
IFNg	PE-Cy7 anti-mouse IFN-gamma, cloneXMG1.2	XMG1.2	eBioscience	1/200
IgD	Brilliant Violet 711 anti-mouse IgD	11-26c.2a	BioLegend	1/200

IgD	Brilliant Violet 421 anti-mouse IgD	11-26c.2a	BioLegend	1/200
IgG1	FITC anti-mouse IgG1	A85-1	BD Biosciences	1/200
IgG1	APC anti-mouse IgG1	X56	BD	1/500
IgG2a	FITC anti-mouse IgG2a	R19-15	BD Biosciences	1/200
IgG2b	FITC anti-mouse IgG2b	R12-3	BD Biosciences	1/200
IL2	PE anti-mouse IL-2	JES6-5H4	Insight Biotech (eBiosciences)	1/200
IgM(b)	FITC mouse anti-mouse IgM(b)	AF6-78	BioLegend	1/200
IgM	PE/Cy7 anti-mouse IgM Antibody	RMM-1	BioLegend	1/200
IgM	PE anti-mouse IgM	R6-60.2	BD Biosciences	1/200
Ly-6C	Pacific Blue anti-mouse Ly-6C	HK1.4	BioLegend	1/200
Ly-6G	FITC anti-mouse Ly-6G	1A8	BioLegend	1/200
MHCII	PerCP/Cyanine 5.5 anti-mouse I-A/I-E	M5/114.15.2	BioLegend	1/200
NK1.1	PE anti-mouse NK-1.1	PK136	BioLegend	1/200
NK1.1	APC anti-mouse NK-1.1	PK136	BioLegend	1/200
NK1.1	Brilliant Violet 785 anti-mouse NK-1.1	PK136	BioLegend	1/200
NK1.1	FITC anti-mouse NK1.1	PK136	eBiosciences	1/200
Ter119	PE anti-mouse TER-119	TER-119	Insight Biotech	1/200
Ter119	APC anti-mouse TER-119	TER-119	Insight Biotech	1/200
Ter119	FITC anti-mouse TER-119	TER-119	BioLegend	1/200
TCRβ	FITC anti-mouse TCRβ	H57-597	BioLegend	1/200
TCRβ	APC anti-mouse TCRβ	H57-597	BioLegend	1/200

TCRβ	PE-Cy7 anti-mouse TCRβ	H57-597	BioLegend	1/200
TCRβ	PerCP/Cy5.5 anti-mouse TCRβ	H57-597	BioLegend	1/200
TNFa	APC anti-Mouse TNFa	MP6-XT22	Insight Biotech (eBiosciences)	1/200
Vα2	FITC anti-Mouse TCR Vα2	B20.1	BD Biosciences	1/200
Vα2	PE anti-Mouse TCR Vα2	B20.1	BD Biosciences	1/200
Vα2	APC anti-Mouse TCR Vα2	B20.1	Insight Biotech (eBiosciences)	1/200

2.5.2 Calculations and absolute numbers

Single-cell suspensions were diluted in AB-IMDM and live cells were counted using a Neubauer haemocytometer (Marienfield).

2.5.3 Cell surface staining

Single cell suspensions were stained with directly conjugated antibodies to cell surface markers obtained from eBiosciences (San Diego, CA, USA), Invitrogen/BD Biosciences (San Jose, CA, USA) or BioLegend (San Diego, CA, USA) and an anti-FcR monoclonal antibody (2.4G2) which was used to block non-specific binding. All staining was performed in FACS buffer at RT for 30 minutes in the dark.

2.5.4 Intracellular cytokine staining

For the intracellular detection of cytokines, cells were stimulated with phorbol 12,13-dibutyrate and ionomycin (both at 0.5 μg/ml) at 37°C in AB-IMDM. After 1 hour, cells were treated with monensin (at 1μg/ml) for a further three hours, to allow for the accumulation of cytokines within the activated cells. Cells were subsequently washed and stained with a live cell/dead cell marker

(see section 2.5.5) followed by surface antibody staining in FACS buffer. The cells were then washed and resuspended in fixation buffer (eBioscience) for 20 minutes following which the cells were then washed again before being resuspended in permeabilization buffer (eBioscience) containing antibodies for cytokine staining for one hour at RT. The cells were then washed a further two times before finally being re-suspended in FACS buffer for analysis.

2.5.5 Live cell/Dead cell discrimination

Live cells were identified using the Zombie UV™ Fixable Viability Kit (Biolegend). Briefly, cell suspensions were suspended in PBS containing the amine reactive Zombie UV™ fluorescent dye at a dilution of 1:800. Cells were then incubated for 20 minutes at RT following which they were washed and resuspend in FACS buffer for further staining or analysis.

2.5.6 Acquisition and cell sorting

Data were collected on BD LSRFortessa (BD Biosciences), BD FACSFortessaX20 (BD Biosciences) and BD FACSFortessaX30 (BD Biosciences) flow cytometers. Cells were sorted on BD FACSAriaII (BD Biosciences), BD Influx (BD Biosciences) or MoFlo XDP cell sorters (Beckman Coulter) at a purity>95%. Data was processed and analysed using BD FACSDiva software (BD biosciences) and FlowJo v10 (TreeStar) analysis software.

2.6 RNA preparation and gene expression analysis

Total RNA from single cell suspensions was extracted with the RNEasy Mini and Micro Plus kits (Qiagen) according to the manufacturer's instructions or isolated using the QIAcube (QIAGEN, Crawley, UK). RNA concentrations were quantified using a Nanodrop 1000 (ThermoScientific). Synthesis of cDNA was carried out with the High Capacity Reverse Transcription kit (Applied Biosystems, Carlsbad, US) with an RNase-inhibitor (Promega Biosciences, Madison, US) according to the manufacturer's instructions. A final clean-up was achieved with the QIAquick

PCR purification kit (Qiagen). Purified cDNA was subsequently used as template for the amplification of target genes using the Fast SYBR™ Green Master Mix (Qiagen) and the primers shown below. All data were normalised to *Hprt* and analysed using the comparative CT method.

Fcrl6

Forward - 5′- TCCCTCCTCGCCTCAGTAAAG-3′

Reverse - 5′- TGCTCTTGATCCAGGCAGTA-3′

GzmB

Forward - 5′- ATGAAGATCCTCCTGCTACTGC-3′

Reverse - 5′- AGTCCGACGACTAGGAACTAGC-3′

Hprt

Forward - 5′- TTGTATACCTAATCATTATGCCGAG-3′

Reverse - 5′- CATCTCGAGCAAGTCTTTCA-3′

2.7 Genomic DNA preparation

2.7.1 Extraction from cells

Cell suspensions were washed in PBS to remove FCS contaminants. Pelleted cells were resuspended in 500μl of Tail buffer (1% SDS, 0.1M NaCl, 0.1M EDTA, 0.05M Tris, 315ml sterile distilled H2O) and digested with 10μl of protease k (20mg/ml) added. This was subsequently left at 56°C for 2 hours on a heat block following which 0.7 volumes of isopropanol was added and vigorously mixed. The material was pelleted, supernatant aspirated, and the material resuspended in 100% ethanol. The material was once again pelleted, supernatant aspirated and the pellet air dried before being resuspended is distilled H_2O at the desired concentration.

2.7.2 F-MLV copy number analysis

DNA copy numbers of F-MLV were determined by real-time quantitative PCR (qRT-PCR) of DNA samples isolated from the spleen cell suspensions of infected mice using primers specific to F-MLV *env* DNA (125 bp product):

Forward - 5′-AAGTCTCCCCCCGCCTCTA-3′

Reverse - 5′-AGTGCCTGGTAAGCTCCCTGT-3′

Signals were normalized for the amount of DNA used in the reactions based on amplification of the single-copy *Ifnar1* gene (150 bp product) with primers:

Forward - 5′-AAGATGTGCTGTTCCCTTCCTCTGCTCTGA-3′

Reverse - 5′-ATTATTAAAAGAAAAGACGAGGCGAAGTGG-3′

Copy numbers were calculated using the comparative CT method and are expressed as copies per $1x10^7$ cells.

2.8 Statistical analysis

Data analysis was performed using GraphPad Prism 8 (GraphPad Software, La Jolla, CA, USA). Parametric comparisons of normally distributed values that satisfied the variance criteria were accomplished with unpaired Student's *t* tests. Differences with $p<0.05$ were considered significant.

Chapter 3. Expression of FCRL6 in the mouse immune system and generation of a *Fcrl6*-deficient mouse strain

3.1 Aims

The expression profile of mouse FCRL6 has not yet been formally investigated in the literature. Thus, in order to use mice as model organisms to determine the function of FCRL6 in context of the immune system, we first needed to characterise its expression in the major immune populations of mice. We measured the expression of FCRL6 via qRT-PCR in selected innate and adaptive immune cells with the aim of building on sparse publicly available expression data and highlighting developmental and activation stages where the receptor may play an important role. We also generated a *Fcrl6*-deficient mouse strain to analyse the effect of its deletion on the development and function of FCRL6 expressing cells.

3.2 Results

3.2.1 Expression in major immune populations

Due to the lack of a commercially available anti-mouse FCRL6 antibody, we relied on quantitative real-time-PCR (qRT-PCR) analysis of sorted immune populations for studying mouse FCRL6 expression. First, we sorted monocytes, macrophages, neutrophils, dendritic cells, NK cells, NKT cells, $\gamma\delta$ T cells, $CD4^+$ T cells, $CD8^+$ T cells, regulatory T cells and B cells from the spleen of wild type (WT) C57Bl/6 mice under steady state conditions and analysed them via qRT-PCR for the expression of *Fcrl6*. Consistent with publicly available expression data (ImmGen consortium), we detected *Fcrl6* in NK cells, but not in the other investigated cell populations (Figure 7a).

3.2.2 Expression in NK cells

To further ascertain the expression profile of *Fcrl6* in NK-lineage cells, we sorted developing and mature NK cells from the bone marrow (NK cell precursors, immature and mature NK cells) of WT mice under steady state conditions and analysed them via qRT-PCR for the expression of *Fcrl6*. We were unable to assess the expression of *Fcrl6* during NK cell development due to the low proportion of NK cell precursors and immature NK cells in the bone marrow of WT mice under steady state conditions. However, we were able to sort sufficient numbers of mature NK cells from the bone marrow and detected the expression of *Fcrl6* in these cells, similar to their splenic counterpart (Figure 7b). Mouse NK can be divided into four stages of maturation depending on the expression of CD11b and CD27 with $CD11b^+$ $CD27^-$ NK cells representing the most cytotoxic and differentiated NK cell subset (Chiossone *et al.* 2009b). In order to establish the expression of *Fcrl6* during this process, we sorted mature NK cells ($CD11b^-$ $CD27^-$, $CD11b^-$ $CD27^+$, $CD11b^+$ $CD27^+$ and $CD11b^+$ $CD27^-$ NK cells) from the spleen of WT mice under steady state conditions and analysed them via qRT-PCR for the expression of *Fcrl6*. We identified that the expression of *Fcrl6* in mouse NK cells positively correlates with maturation as the highest expression was detected in $CD11b^+$ $CD27^-$ NK cells (Figure 7b).

3.2.3 Expression in B cells

FCRL protein family members are preferentially expressed by B-lineage cells at different stages during their development in humans and mice (Li *et al.* 2014a). Consequently, we were interested in identifying the expression profile of *Fcrl6* in B cells. Due to an absence of *Fcrl6* expression in the total B cell population from the spleen, we sought to identify if *Fcrl6* is expressed by developing or mature B cell subsets in mice. We sorted developing B cells from the bone marrow (pro-B, pre-B and immature B cells) and spleen (T1 B, T2 B and T3 B cells) in addition to mature B cells from the bone marrow (recirculating mature B cells) and spleen (follicular B and marginal zone B cells) of WT mice under steady state conditions and analysed them via qRT-PCR for the expression of *Fcrl6*. We also sorted antigen experienced B cells from the spleen (germinal centre B cells) of WT mice at day 35 following infection with FV. We identified *Fcrl6* expression during early B cell

development in pro-B and pre-B cells from the bone marrow but not in other developing, mature or antigen experienced B cell populations from the bone marrow and spleen (Figure 7c).

3.2.4 Expression in T cells

3.2.4.1 Expression in steady state conditions

FCRL6 expression in humans has been reported on cytotoxic $CD4^+$ and effector and effector memory $CD8^+$ T cells (Schreeder *et al.* 2008; Wilson *et al.* 2007b). We aimed to investigate if the expression of *Fcrl6* in T-lineage cells is similar to that of its human ortholog. We did not detect the expression of *Fcrl6* in total $CD4^+$ and $CD8^+$ T cells from the spleen of WT mice under steady state conditions (Figure 7a). We next sorted naïve and memory $CD4^+$ and $CD8^+$ T cells from the spleen of WT mice under steady state conditions and analysed them via qRT-PCR for the expression of *Fcrl6*. Predictably, we did not detect the expression of *Fcrl6* in naïve or memory $CD4^+$ and $CD8^+$ T cells (Figure 7d). Subsequently, we attempted to identify if the expression of *Fcrl6* occurred during T cell development. We sorted thymocytes (double negative, double positive, CD4 single positive and CD8 single positive cells) from the thymus of WT mice under steady state conditions and analysed them via qRT-PCR for the expression of *Fcrl6*. As observed in mature $CD4^+$ and $CD8^+$ T cells, we did not detect the expression of *Fcrl6* in maturing T cells (Figure 7d).

3.2.4.2 Expression following activation of T cells

Next, we aimed to determine if the expression of *Fcrl6* in mouse T cells is regulated by activation as observed for human FCRL6 expression on $CD8^+$ T cells (Schreeder *et al.* 2008; Wilson *et al.* 2007b). We isolated and stimulated $CD8^+$ T cells *in vitro* with anti-CD3/CD28 beads over a 5-day period and analysed the expression of *Fcrl6* via qRT-PCR. We did not detect the expression of *Fcrl6* in $CD8^+$ T cells during the analysed time period (Figure 8a). Additionally, we activated $CD8^+$ T cells *in vivo* by transfer into minor histocompatibility antigen mismatched B and T cell deficient recipient mice and analysed them at day 14 following transfer for the expression of *Fcrl6* via qRT-

PCR. Similar to our *in vitro* result, we did not detect the expression of *Fcrl6* in $CD8^+$ T cells following activation due to a minor alloantigen mismatch (Figure 8b). We also did not detect expression of *Fcrl6* via qRT-PCR in memory $CD4^+$ T cells at day 7 following FV infection (Figure 9).

Figure 7: *Fcrl6* is expressed by developing B cells and mature NK cells.

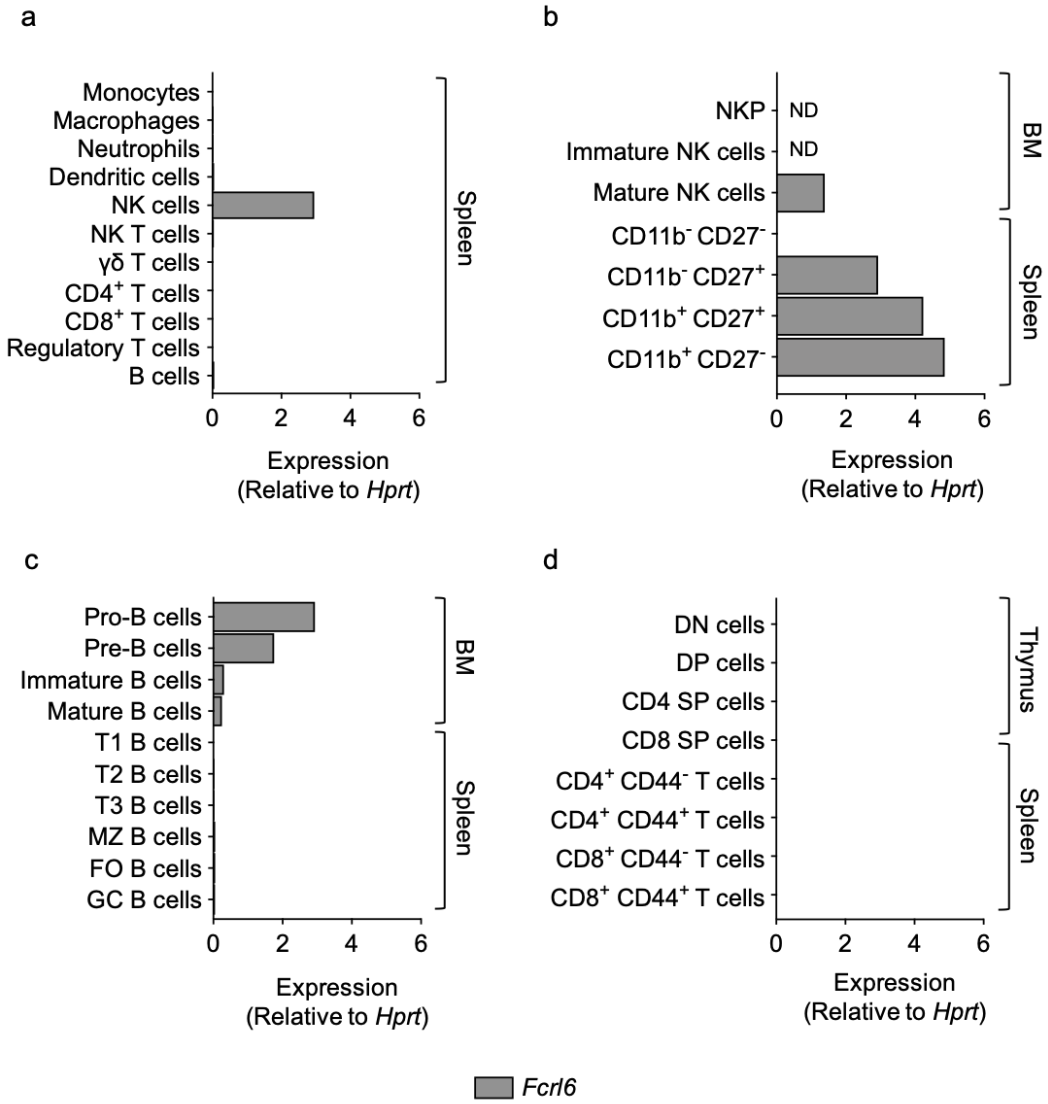

(a) mRNA expression of *Fcrl6* by quantitative real-time-PCR (qRT-PCR) analysis of select innate and adaptive immune cell populations. (b, c and d) mRNA expression of *Fcrl6* by qRT-PCR analysis of NK, B and T cell developmental populations, respectively. All populations except Germinal centre (GC) GC B cells were obtained from wild type (WT) mice under steady state conditions. GC B cells were isolated from Friend virus infected WT mice at 35 days post-infection. All populations were gated and sorted via flow cytometry as depicted in Figures 13, 16, 24 and 30. All data are pooled from 3 or more biological repeats per population and sorting purity was generally greater than 95% for all populations. DN, double negative; DP, double positive; FO, follicular; MZ, marginal zone; ND, not determined; NK, natural killer; NKP, natural killer precursor; SP, single positive; T1, transitional type 1; T2, transitional type 2; T3, transitional type 3.

Figure 8: *Fcrl6* is not expressed following *in vitro* or *in vivo* CD8⁺ T cell activation.

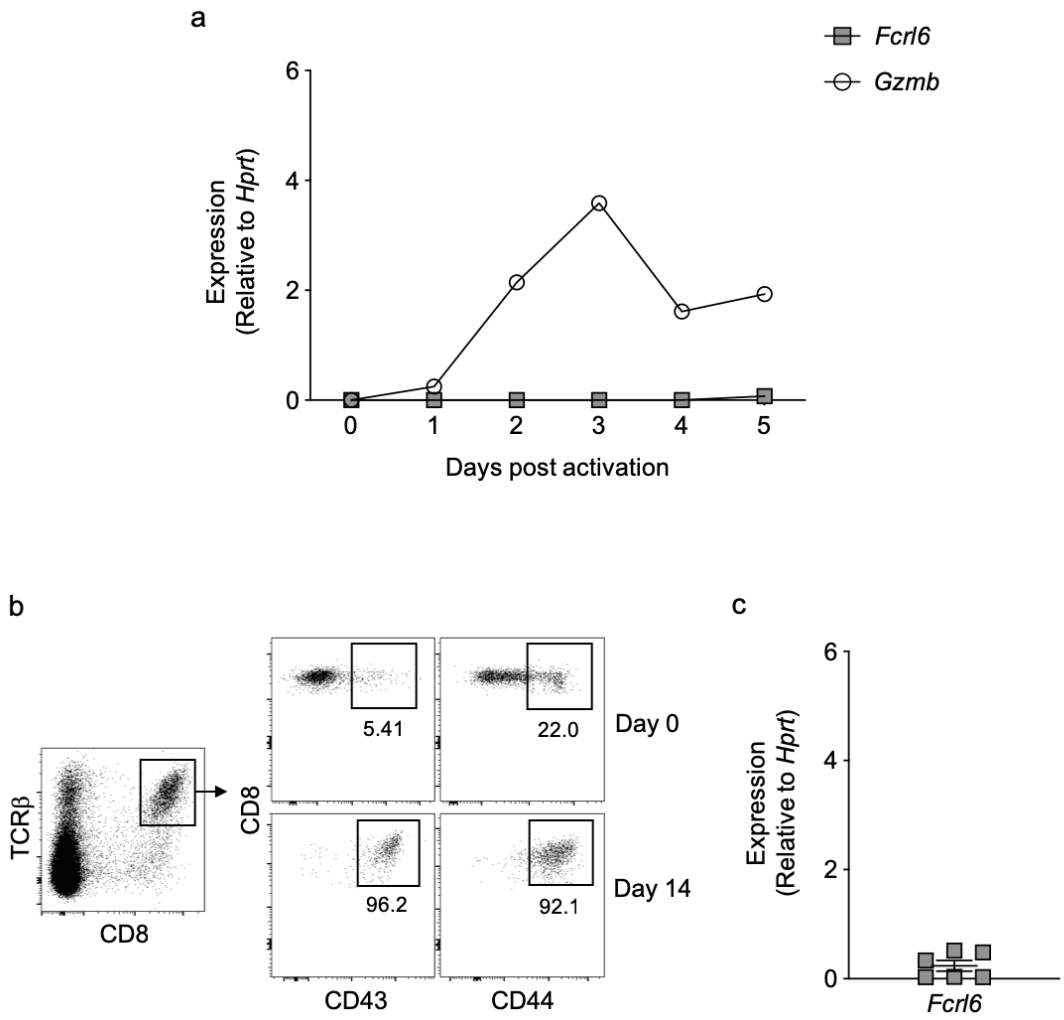

(a) mRNA expression of *Fcrl6* and *Gzmb* by qRT-PCR analysis of CD8+ T cells activated in vitro with anti-CD3/CD28 beads. *Fcrl6* expression is shown as mean ± SEM of 3 biological repeats from 3 independent experiments. *Gzmb* expression is a representative example of all biological repeats. (b) CD43 and CD44 expression indicating CD8+ T cell activation prior to and at day 14 following transfer. (c) mRNA expression of *Fcrl6* by qRT-PCR analysis of CD8⁺ T cells at day 14 following transfer into B and T cell-deficient minor histocompatibility antigen mismatched recipient mice. *Fcrl6* expression is shown as mean ± SEM of 6 biological repeats from 2 independent experiments. CD8⁺ T cells were gated and sorted via flow cytometry at day 14 as TCRβ⁺ CD8⁺ and sorting purity was generally greater than 95%. CD8⁺ T cells for in vitro and in vivo activation were isolated from WT mice under steady state conditions as described in section 2.2.3 of materials and methods.

Figure 9: *Fcrl6* is not expressed by memory CD4⁺ T cells following Friend virus infection.

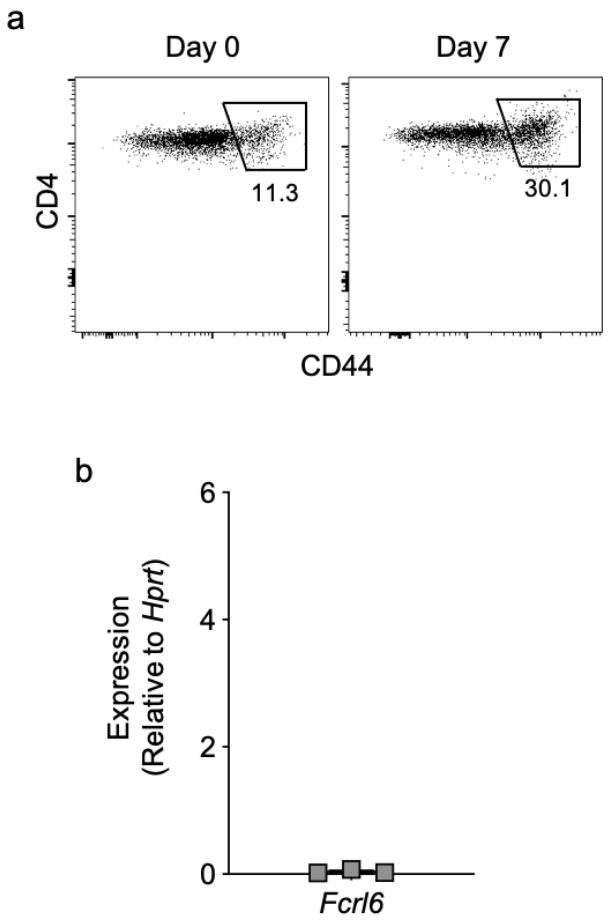

(a) CD44 expression indicating CD4⁺ T cell activation prior to and at day 7 following Friend virus (FV) infection. (b) mRNA expression of *Fcrl6* by qRT-PCR analysis of CD4⁺ T cells at day 7 following FV infection. *Fcrl6* expression is shown as mean ± SEM of 3 biological repeats. WT mice were infected with 1000 spleen focus-forming units of FV by intravenous injection. CD4⁺ T cells were gated and sorted via flow cytometry at day 7 as TCRβ⁺ CD4⁺ CD44⁺ and sorting purity was generally greater than 95%.

3.2.5 Generation of a *Fcrl6*-deficient mouse strain

We aimed to generate a *Fcrl6*-deficient mouse strain in order to analyse the impact of its deletion on the development of the aforementioned immune populations and the immune response. To the best of our knowledge, this was the first attempt at generating a *Fcrl6*-deficient strain since it has never been described before in the literature.

We generated the *Fcrl6*$^{tm1a(KOMP)Wtsi}$ strain on a C57BL/6 background with embryonic stem cells obtained from the Wellcome Sanger Institute's Knockout Mouse Project (KOMP) repository. *Fcrl6*$^{tm1a(KOMP)Wtsi}$ mice contain a construct within the *Fcrl6* gene which targets exons 3-5 for deletion. Exons 3-5 are flanked by locus of X-over P1 (loxP) sites for recombination with a Cre recombinase. 5' of exon 3 is a promoterless reporter cassette containing a neomycin resistance gene for selection and a β-galactosidase reporter gene for assessment of endogenous *Fcrl6* promoter activity. An EN2 splice acceptor site is used to induce splicing into the reporter cassette thereby leading to transcription of both genes from the endogenous *Fcrl6* promoter. The reporter cassette is flanked by flippase (FLP) recombinase targets (FRT) for recombination and deletion via FLP recombinase. The *Fcrl6*$^{tm1a(KOMP)Wtsi}$ is described by KOMP as a 'knockout-first' allele, yet we decided to generate a complete *Fcrl6* null allele. We first crossed *Fcrl6*$^{tm1a(KOMP)Wtsi}$ mice with C57BL/6-*(nogene)*$^{Tg(CAG-flpo)1Afst}$ mice which have FLP under control of the hybrid cytomegalovirus enhancer fused to the chicken beta-actin (CAG) promoter. This cross generates the *Fcrl6*$^{tm1c(KOMP)Wtsi}$ strain which lacks the reporter cassette but still contains exons 3-5 and thus, a functional FCRL6 protein. Consequently, we crossed *Fcrl6*$^{tm1c(KOMP)Wtsi}$ mice with C57BL/6-*Hprt*$^{tm1(CAG-cre)Mnn}$ mice in which the Cre expression cassette driven by the CAG promoter is inserted into the X-linked hypoxanthine-guanine phosphoribosyltransferase locus. This cross efficiently removes exons 3-5 from fertilisation through all developmental stages leaving behind an FRT and loxP site between exon 2 and 6, and generates the *Fcrl6*$^{tm1d(KOMP)Wtsi}$ strain henceforth referred to as the *Fcrl6*$^{-/-}$ strain (Figure 10).

Deletion of exons 3-5 results in loss of a substantial portion of FCRL6 as these exons encode majority of the extracellular and transmembrane regions as well as part of the cytoplasmic region

of the protein. Deletion of *Fcrl6* in *Fcrl6*$^{-/-}$ mice was confirmed via qRT-PCR analysis of NK cells from *Fcrl6*$^{-/-}$ and WT C57BL/6 mice with a primer pair spanning exon 4 and 5 (Figure 11a and 11b). *Fcrl6*$^{-/-}$ mice were used for all of the experimental work described in this study. Experimental mice were bred by mating heterozygous (*Fcrl6*$^{+/-}$) parents to ensure birth of knockout (*Fcrl6*$^{-/-}$) and WT littermate control (*Fcrl6*$^{+/+}$) animals. *Fcrl6*$^{-/-}$ mice were viable, bred normally and produced at expected Mendelian ratios from *Fcrl6*$^{+/-}$ parents. We used WT littermate controls in addition to age and sex-matched WT C57BL/6 mice for analysis of *Fcrl6* phenotypes.

Figure 10: *Fcrl6* KOMP gene targeting strategy and generation of *Fcrl6*-deficient mice.

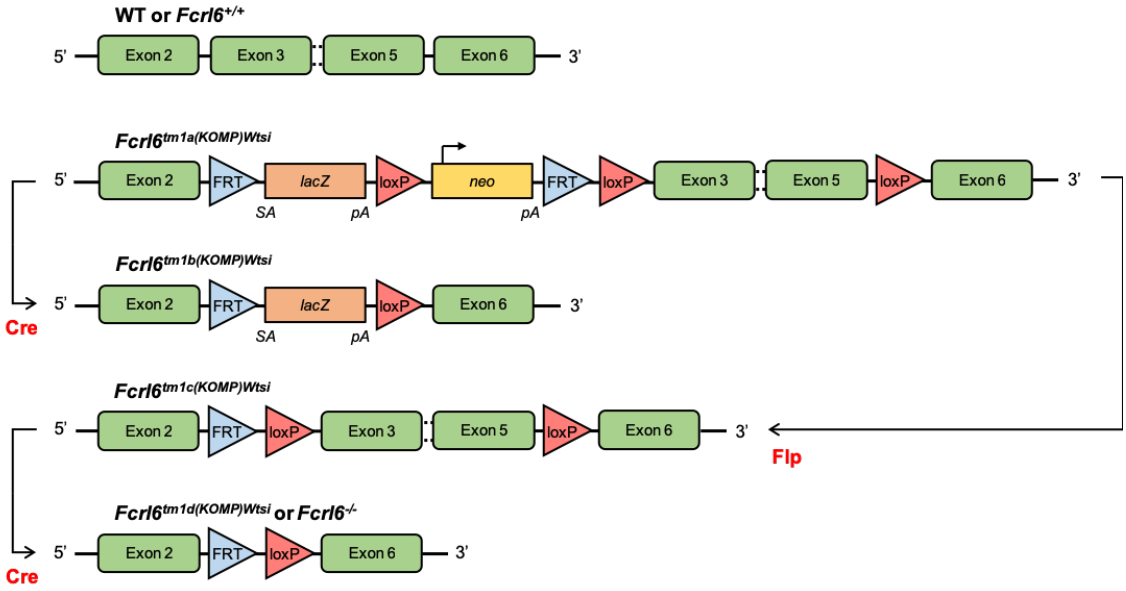

Naturally occurring *Fcrl6*$^{+/+}$ (WT) allele is displayed at the top followed by the Knockout Mouse Project (KOMP) repository-derived, promoter less *Fcrl6*$^{tm1a(KOMP)Wtsi}$ allele. The *Fcrl6*$^{tm1a(KOMP)Wtsi}$ allele contains the coding sequence of the β-galactosidase reporter gene (*lacZ),* flippase (FLP) recombinase targets (FRT) and locus of X-over P1 (loxP) sites. This setup allows deletion of exons 3-5 and permits assessment of *Fcrl6* expression via measurement of β-galactosidase activity as *lacZ* is under control of the endogenous *Fcrl6* promoter. The *Fcrl6*$^{tm1a(KOMP)Wtsi}$ allele can be crossed with Cre or FLP deleter mice to generate *Fcrl6*$^{tm1b(KOMP)Wtsi}$ or *Fcrl6*$^{tm1c(KOMP)Wtsi}$ alleles, respectively. The *Fcrl6*$^{tm1c(KOMP)Wtsi}$ allele can subsequently be crossed with Cre deleter mice to produce the *Fcrl6*$^{tm1d(KOMP)Wtsi}$ or *Fcrl6*$^{-/-}$ allele.

Figure 11: Exons 3-5 of *Fcrl6* are not expressed in *Fcrl6*-deficient mice.

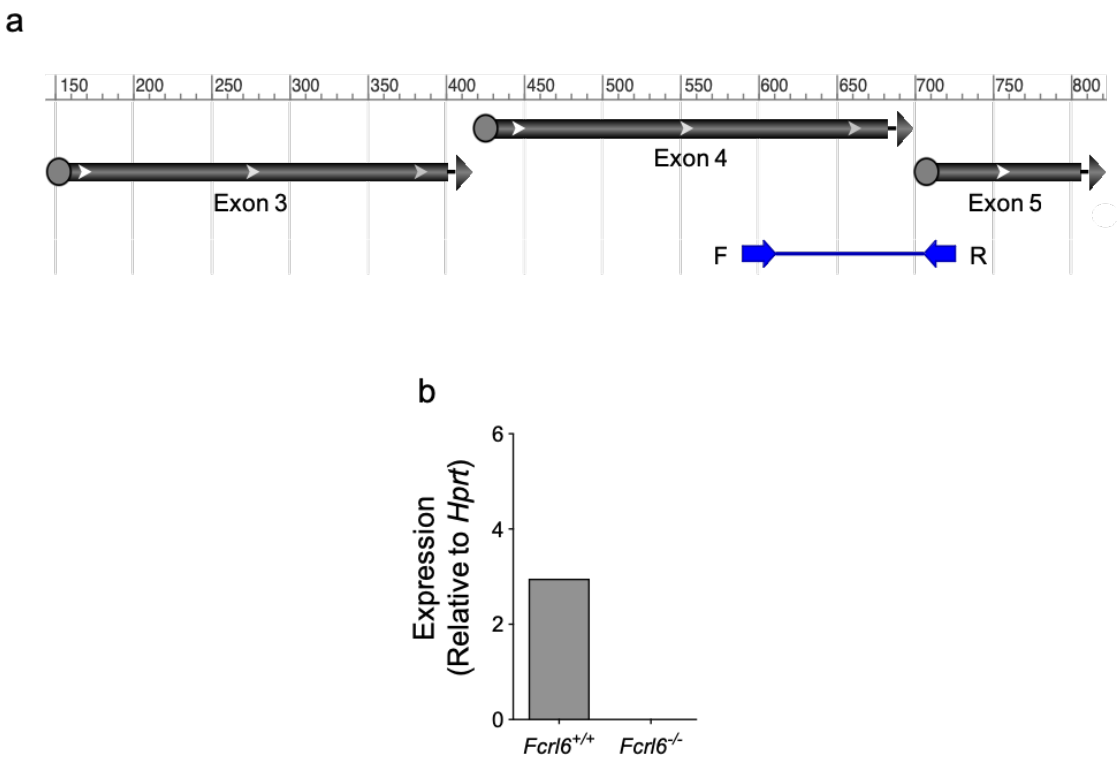

(a) Exons 3-5 of the naturally occurring *Fcrl6*$^{+/+}$ (WT) allele are displayed alongside the binding sites of the forward and reverse primers used to detect the expression of *Fcrl6*. (b) mRNA expression of *Fcrl6* by qRT-PCR analysis of NK cells sorted from the spleen of *Fcrl6*$^{-/-}$ and WT mice under steady state conditions. *Fcrl6* expression in NK cells from both genotypes is pooled from 3 biological repeats. NK cells were gated and sorted via flow cytometry as NK1.1^{+} CD49b^{+} and sorting purity was generally than 95%.

3.2.5.1 Analysis of major myeloid immune populations in Fcrl6$^{-/-}$ mice

Prior to analysis of the development and function of lymphocytes in the absence of *Fcrl6*, we focused on identifying if the composition of the spleen with respect to major myeloid immune populations appears normal following deletion of *Fcrl6*. We accomplished this via a combination of mixed bone marrow chimeras and comparison of *Fcrl6*$^{-/-}$ and WT mice. CD45.2^{+} *Fcrl6*$^{-/-}$ or WT bone marrow cells were mixed with CD45.1^{+} WT bone marrow cells and injected into myeloablated CD45.1/2^{+} WT recipient mice to detect developmental abnormalities arising due to the absence of *Fcrl6*. The mixed bone marrow chimeras were created at a ratio of 55:45% with respect to CD45.2^{+} and CD45.1^{+} cells. *Fcrl6*-deficient bone marrow performed similarly to WT bone marrow at reconstituting dendritic cells, monocytes and neutrophils in the spleen. A slight advantage was observed in favour of *Fcrl6*-deficient bone marrow at reconstituting macrophages in the spleen (Figure 12a). Comparison of complete *Fcrl6*$^{-/-}$ and WT mice revealed a comparable result with a higher percentage of macrophages being observed in the spleen of *Fcrl6*$^{-/-}$ mice compared to WT mice. A trend towards an increased number of splenic macrophages was also detected in *Fcrl6*$^{-/-}$ mice compared to WT mice. In agreement with data from mixed bone marrow chimeras, we did not find differences in the number and percentage of dendritic cells, monocytes and neutrophils between *Fcrl6*$^{-/-}$ mice and WT mice (Figure 12b). We concluded that the development of dendritic cells, monocytes and neutrophils likely remains unaffected by the deletion of *Fcrl6*, whilst the proportion of macrophages in the spleen appears to be slightly affected (Figure 13). Further investigation is required to confirm this finding and address the underlying mechanism.

Figure 12: There are no major differences in the number and percentage of major myeloid immune populations in the spleen of *Fcrl6*$^{-/-}$ mice.

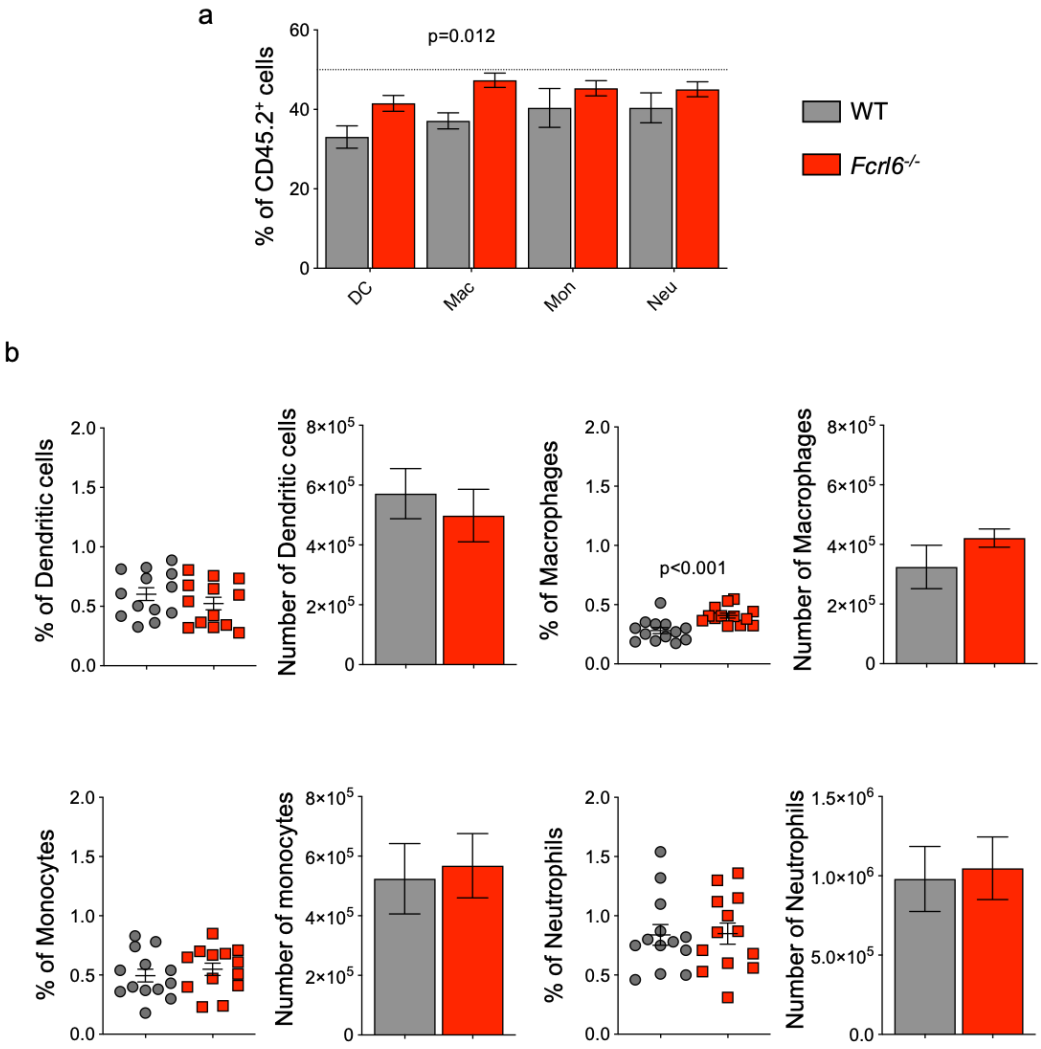

(a) Relative proportions of *Fcrl6*$^{-/-}$ and WT derived dendritic cells, macrophages, monocytes and neutrophils from mixed bone marrow chimeras. Bone marrow from CD45.2^{+} *Fcrl6*$^{-/-}$ and WT mice was mixed with bone marrow from CD45.1^{+} WT mice (55% CD45.2^{+} cells) and injected intravenously into myeloablated CD45.1/2^{+} WT recipient mice. Reconstitution was analysed 8 weeks later via flow cytometry of splenocytes. Bars represent mean ± SEM of 4 (WT) and 14 (*Fcrl6*$^{-/-}$) biological replicates. Cell populations were gated as depicted in Figure 13 with additional gating for CD45.1 and CD45.2. Dotted line indicates injected percentage of CD45.2^{+} cells. (b) Number and percentage of dendritic cells, macrophages, monocytes and neutrophils in the spleens of unchallenged *Fcrl6*$^{-/-}$ and WT mice analysed via flow cytometry. Cell populations were

gated as depicted in Figure 13. Bars and symbols represent mean ± SEM of 13 biological repeats per genotype from 3 independent experiments. DC, dendritic cells; Mac, macrophages; Mon, monocytes; Neu, neutrophils.

Figure 13: There are no major differences in the splenic composition of major myeloid immune populations in *Fcrl6*$^{-/-}$ mice.

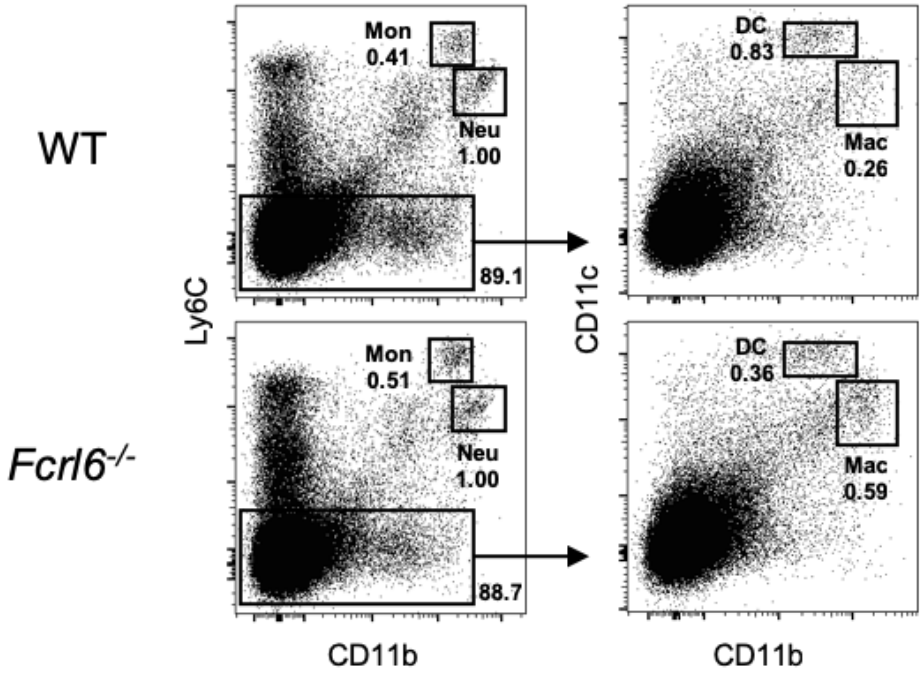

Flow cytometric gating strategy used for analysis and sorting of dendritic cell, macrophage, monocyte and neutrophil populations in Figures 7 and 12. Names are indicated by text next to the gates whilst numbers represent population percentage within that plot. Gating strategies were as follows: Mon, monocytes (B220^{-} TCRβ^{-} NK1.1^{-} Ly6C^{hi} CD11b^{int}); Neu, neutrophils (B220^{-} TCRβ^{-} NK1.1^{-} Ly6C^{int} CD11b^{hi}); DC, dendritic cells (B220^{-} TCRβ^{-} NK1.1^{-} Ly6C^{-} CD11b^{int} CD11c^{hi}) and Mac, macrophages (B220^{-} TCRβ^{-} NK1.1^{-} Ly6C^{-} CD11b^{hi} CD11c^{int}).

3.3 Discussion

Data from previous studies involving analysis of the expression and signalling potential of human FCRL6 suggests that it may function as an immunoregulatory receptor (Kulemzin *et al.* 2011b; Schreeder *et al.* 2008; Wilson *et al.* 2007a). Despite differences in the number and chromosomal organisation of FCRL proteins between humans and mice, close linkage of *Fcrl* genes with homologous genes and similar extracellular domain composition indicates that the mouse FCRL family shares common ancestry and possibly functionality with human FCRL proteins. There are no studies published in the literature relating to the expression or function of mouse FCRL6. To this end, we first measured the expression of mouse FCRL6 via qRT-PCR analysis of developing and mature subsets of major immune populations. Our results agreed with publicly available expression data on ImmGen as we did not identify the expression of *Fcrl6* in a vast majority of the analysed immune populations other than developing B cells and mature NK cells in the bone marrow, and mature NK cells in the spleen. The primers used for the detection of *Fcrl6* amplify a region between exons 4 and 5 which encodes for significant proportions of the canonical and the other isoform of mouse FCRL6. Thus, the reported expression of *Fcrl6* in this thesis is indicative of both reported isoforms of the protein.

3.3.1 Expression in B cells

The expression of human FCRL6 has not been fully characterised in B-lineage cells. FCRL protein family members are preferentially expressed by B cells at different stages during their development in humans and mice (Li *et al.* 2014a). Thus, we were interested in identifying the expression profile of *Fcrl6* in mouse B cells. We did not detect the expression of *Fcrl6* in a majority of the B-lineage cells except pro-B and pre-B cells in the bone marrow. A slightly higher expression of *Fcrl6* was observed in pro-B cells compared to pre-B cells. Additionally, we also did not detect the expression of *Fcrl6* in germinal centre B cells at day 35 following FV infection. The absence of *Fcrl6* expression in mature and antigen experienced B cells indicates that the receptor may function during early B cell development. *Fcrl6* expression could also precede the earliest B-lineage committed precursor analysed in this thesis, thereby suggesting that the receptor may be

involved in B-lineage commitment via signalling that regulates the multitude of transcription factors that control this process. We aimed to investigate the function of mouse FCRL6 during the development of B cells by analysing developing B cell populations in *Fcrl6*$^{-/-}$ mice. Despite an absence of *Fcrl6* expression in mature B cell populations as well as germinal centre B cells, the B cell response to antigen could be affected due to absence of FCRL6 during development. Thus, we also investigated the classical B cell response to T-dependent type 1 antigens in *Fcrl6*$^{-/-}$ mice. The impact of FCRL6 deletion on this and B cell development is discussed in chapter 4 of the thesis.

3.3.2 Expression in NK cells

FCRL6 expression on human NK cells is confined to CD16^{+} CD56^{dim} NK cells, which represent the most cytotoxic and differentiated NK cell subset in humans (Cooper *et al.* 2001; Schreeder *et al.* 2008). Unlike the finely tuned BCR and TCR expressed by B and T cells, NK cells do not possess antigen specific activating receptors. They express multiple activating and inhibitory receptors that regulate their activation by binding self-ligands that arise following pathogen invasion and MHC class I, respectively. In addition to MHC class I binding inhibitory receptors, NK cells from humans and mice also express non-MHC class I binding inhibitory receptors to regulate their activation (He & Tian 2017). The inhibitory potential of human FCRL6 and its ability to bind HLA-DR as well as other potentially unknown ligands could allow this receptor act as a non-MHC class I binding inhibitory receptor for NK cells. Thus, we were interested in analysing the expression of mouse FCRL6 to investigate if it could also act in a comparable manner. We were unable to determine the expression of *Fcrl6* during NK cell development due to the low proportion of NK cell precursors and immature NK cells in the bone marrow under steady state conditions. However, we were able to sort sufficient numbers of mature NK cells from the bone marrow for analysis of *Fcrl6* expression and detected expression of the receptor in these cells. Additionally, we also detected the expression of *Fcrl6* in peripheral mature NK cells from the spleen. The surface expression of CD11b and CD27 can be used to divide peripheral NK cell maturation into four stages with NK cells progressing from the CD11b^{-} CD27^{-} to the CD11b^{+} CD27^{-}

stage by first upregulating the expression of CD27 ($CD11b^{-}$ $CD27^{+}$) followed by CD11b ($CD11b^{+}$ $CD27^{+}$) and finally downregulating the expression of CD27 ($CD11b^{+}$ $CD27^{-}$). This maturation program is associated with increased cytotoxic capacity and decreased proliferative potential. Consequently, $CD11b^{+}$ $CD27^{-}$ NK cells in the periphery represent the most cytotoxic and differentiated NK cell subset in mice (Chiossone *et al.* 2009b). We identified that the expression of *Fcrl6* in peripheral mature NK cells correlates with differentiation as highest expression amongst these subsets was detected in $CD11b^{+}$ $CD27^{-}$ NK cells. Thus, *Fcrl6* is expressed in peripheral mature mouse NK cells and its expression appears to mirror that of its human counterpart, thereby indicating that it may possess similar functionality to its human counterpart at least in NK cells. To address the potential role of FCRL6 in NK cells, we analysed outcome to FV infection and B16 melanoma cell inoculation in *Fcrl6*$^{-/-}$ mice as NK cell-mediated immunity has been demonstrated to play an important role in these models. Despite being unable to analyse the expression of *Fcrl6* in developing NK cells in the bone marrow, we also aimed to investigate the impact of FCRL6 deletion on the development of NK cells by analysing the proportions of developing and mature NK cells in *Fcrl6*$^{-/-}$ mice. The impact of FCRL6 deletion on this and the NK cell response is discussed in chapter 5 of the thesis.

3.3.3 Expression in T cells

Human FCRL6 expression is detected on cytotoxic $CD4^{+}$ T cells as well as effector and effector memory $CD8^{+}$ T cells. Increased expression of human FCRL6 has been reported on these cells following HIV-1 infection and in patients with B-CLL (Schreeder *et al.* 2008; Wilson *et al.* 2007a). This expression pattern alongside the inhibitory potential of human FCRL6 suggests that the receptor may also act as an inhibitory receptor for T cells as well as NK cells in a similar manner to PD-1, TIM-3, LAG-3 and others. Contrary to the expression profile of human FCRL6, we did not detect the expression of mouse FCRL6 in mature T cell populations including naïve and memory $CD4^{+}$ and $CD8^{+}$ T cells as well as regulatory T cells. Analysis of thymocytes also revealed an absence of *Fcrl6* expression during T cell development in the thymus. Human FCRL6 expression has been shown to be downregulated following *in vitro* activation of $CD8^{+}$ T cells

(Wilson *et al.* 2007b). Accordingly, we hypothesised that *Fcrl6* expression may also be regulated by the activation of mouse T cells. We did not detect *Fcrl6* expression following *in vitro* activation of $CD8^+$ T cells with anti-CD3/CD28 beads. Subsequently, we activated mouse $CD8^+$ T cells *in vivo* by transfer into minor histocompatibility antigen mismatched B and T cell deficient recipient mice to simulate chronic activation. However, we still did not detect the expression of *Fcrl6* in $CD8^+$ T cells. Similarly, memory $CD4^+$ T cells sorted from FV infected mice at day 7 following infection also did not display *Fcrl6* expression. Collectively, our results indicated an absence of *Fcrl6* expression in developing and mature mouse T cell populations in the steady state as well as following activation at least in the tested conditions. However, it is possible that the degree of stimulation delivered through the aforementioned activation methods was insufficient to induce the expression of FCRL6 if it does indeed possess immunoregulatory potential in mice. Thus, it would be of interest to evaluate the expression of FCRL6 in $CD8^+$ T cells following challenge of mice in models of chronic infection such as the LCMV model which has been extensively used to characterise inhibitory receptors. Despite an absence of FCRL6 expression in thymocytes, T cell development could be affected by the receptor due to its expression in mTECs (ImmGen consortium) or even T cell committed precursors in the bone marrow that were not analysed in this thesis. Thus, we examined the impact of FCRL6 deletion on T cell development by analysing the relative proportions of thymocytes and mature T cells in *Fcrl6*$^{-/-}$ mice. This is discussed in chapter 6 of the thesis.

3.3.4 *Fcrl6*$^{-/-}$ mice

To address the function of mouse FCRL6, we generated *Fcrl6*$^{-/-}$ mice by using a construct that targeted exons 3-5 of the *Fcrl6* gene for deletion via Cre-Lox mediated recombination. qRT-PCR analysis of NK cells sorted from the spleen of these mice confirmed the deletion of *Fcrl6*. We were unable to confirm absence of cell surface expression of the canonical or the other isoform of mouse FCRL6 via immunoblotting or flow cytometry due to lack of a commercially available monoclonal anti-mouse FCRL6 antibody. However, it is very unlikely that the canonical, the other isoform or even a truncated version of mouse FCRL6 could be expressed in *Fcrl6*$^{-/-}$ mice as we

confirmed deletion of exons 4 and 5 which encode for a vast majority of the canonical and the other isoform of mouse FCRL6 including the extracellular, transmembrane and cytoplasmic regions. Nonetheless, confirmation of the absence of cell surface expressed FCRL6 should be achieved in future studies to validate that *Fcrl6* is non-functional in *Fcrl6*$^{-/-}$ mice.

We first analysed the immune composition of major myeloid cells to identify obvious defects in these populations due to the deletion of *Fcrl6*. We examined the relative proportions of splenic *Fcrl6*$^{-/-}$ bone marrow derived dendritic cells, macrophages, monocytes and neutrophils in mixed bone marrow chimeras, and also compared the number and percentage of these populations in the spleen of *Fcrl6*$^{-/-}$ and WT mice. We did not detect differences in the relative proportion of *Fcrl6*$^{-/-}$ bone marrow derived dendritic cells, monocytes and neutrophils compared to their WT bone marrow derived counterparts, and also did not find differences in the number and percentage of these cells between *Fcrl6*$^{-/-}$ and WT mice. This is unsurprising as we did not detect the expression of *Fcrl6* in these cells in our investigation and also did not identify significant expression of *Fcrl6* in these cells using public available expression data on ImmGen. Thus, we concluded that deletion of FCRL6 does not appear to alter the development of dendritic cells, monocytes and neutrophils.

We detected an increased percentage of macrophages and a trend towards an increase in their number in the spleen of *Fcrl6*$^{-/-}$ mice compared to WT mice. Macrophages with two distinct origins exist in the tissues of mice; a majority are tissue-resident macrophages which self-renew independently of haematopoietic input following establishment during embryonic stages whilst others are derived from tissue-infiltrating monocytes in adulthood (Varol *et al.* 2015). Thus, the macrophage population that we identified in the spleen is heterogenous and comprised of both monocyte-derived and tissue-resident macrophages. It is probable that the observed difference is due to an increase in monocyte-derived macrophages as we detected an increased proportion of *Fcrl6*$^{-/-}$ macrophages in mixed bone marrow chimeras which could only arise from injected haematopoietic stem cells in this setting as tissue-resident macrophages are established during the embryonic stages of life. Multiple factors such as increased infiltration of *Fcrl6*$^{-/-}$ monocytes or

increased proliferation of monocyte-derived macrophages due to the absence of FCRL6 could account for the difference that we observed in both *Fcrl6*$^{-/-}$ mice and mixed bone marrow chimeras. We did not detect the expression of FCRL6 in macrophages from the spleen which suggests that if the observed effect is due to cell intrinsic expression of the receptor then its expression and role must be evident during the developmental stages of monocytes. Additionally, properties of tissue-resident macrophages such as homeostatic renewal may also be affected by FCRL6 due to possible expression of the receptor in precursor cells of this population and the germline nature of *Fcrl6* deletion in *Fcrl6*$^{-/-}$ mice.

3.3.5 Future work

Overall, our results from qRT-PCR analysis indicated that the expression of FCRL6 is observed in developing B cells and mature NK cells in the bone marrow in addition to mature NK cells in the spleen. However, it is important to keep in consideration that expression of *Fcrl6* may not directly correlate with expression of the receptor at the protein level. Thus, future work should involve confirming *Fcrl6* expression in these cells by analysing FCRL6 protein expression levels using a monoclonal anti-mouse FCRL6 antibody. Additionally, it would be of interest to examine the expression of FCRL6 in lymphoid lineage progenitor cells to investigate if the receptor is involved in lymphocyte lineage commitment.

The proportion of macrophages in other tissues of *Fcrl6*$^{-/-}$ mice should be further examined to identify if an increased percentage of these cells is also evident in tissues other than the spleen. Detailed examination of tissue *Fcrl6*$^{-/-}$ macrophages with respect to surface marker expression needs to be undertaken in future studies to identify the origin of the macrophages responsible for the increased percentage observed in the spleen of *Fcrl6*$^{-/-}$ mice. If the increase is found to be driven by monocyte-derived macrophages, the expression of FCRL6 should be investigated in monocyte precursor cells to identify if the difference is due to monocytic lineage intrinsic or extrinsic expression of the receptor. Additionally, as tissue-resident macrophages might also be affected by *Fcrl6* deletion, both *Fcrl6*$^{-/-}$ monocyte-derived and tissue-resident macrophages could

be sequenced in future studies to identify differentially regulated genes and potential pathways that could account for the increased percentage of these cells in the spleen and possibly other tissues. Conditional deletion of *Fcrl6* can be used in conjunction with this analysis to further understand the mechanism and role of FCRL6 in macrophages. The expression of FCRL6 should also be investigated in human macrophages to identify if the expression and a possible role of the receptor in context of macrophages is conserved across the two species.

Chapter 4. Role of FCRL6 in the development and function of B cells

4.1 Introduction

4.1.1 B cell development

Mammalian B cell development occurs in the BM following which, B cells traffic to peripheral lymphoid organs, such as the spleen and lymph nodes, to integrate into the naïve, mature B cell pool. Here, they survey their environment for antigens using their BCR and upon binding of their cognate antigen, they become activated and differentiate into germinal centre (GC) B cells, plasma cells or memory B cells.

4.1.1.1 B cell development in the bone marrow

Development of B-lineage progenitors

CLPs express the FMS-like tyrosine kinase 3 receptor as well as the IL-7 receptor (IL-7R) both of which have been shown to be important for B cell development at this stage (Sitnicka *et al.* 2003). The IL-7R controls the commitment of CLPs to the B-lineage via regulation of the transcription factor, early B cell factor 1 (EBF1) (Dias *et al.* 2005; Zandi *et al.* 2008). Next, CLPs develop into $B220^+$ $CD19^-$ pre-pro B cells that display very strong commitment to the B-lineage (Mansson *et al.* 2008). Transcription factors E2A, EBF1 alongside purine box factor 1 (PU.1) regulate the expression of the transcription factor, paired box gene 5 (PAX5) (O'Riordan & Grosschedl 1999). PAX5 has been highlighted as a vital transcription factor for B-lineage commitment at the $B220^+$ $CD19^-$ pre-pro B stage as well as in mature B cells (Cobaleda *et al.* 2007a; Nutt *et al.* 1999). PAX5 expression is not detected in any progenitor populations prior to B-lineage commitment and hence is known as the guardian of B cell identity (Cobaleda *et al.* 2007b; Fuxa & Busslinger 2007).

$CD19^-$ pre-pro B cells then form $CD19^+$ pro-B cells which definitively marks full commitment of these cells to the B-lineage (Rumfelt *et al.* 2006).

Development of B-lineage cells

The development of B cells has been extensively investigated using flow cytometry resulting in the establishment of nomenclatures based on surface marker expression. The Philadelphia nomenclature is one of the most commonly used nomenclatures and is used in this thesis. B cell development in this nomenclature is divided into stages ranging from pre-pro B cells to mature B cells or fractions A to F (Hardy *et al.* 1991; Hardy & Hayakawa 2001; Li *et al.* 1996).

At the pro-B cell stage, developing B cells start to rearrange the variable (V), diversity (D) and joining (J) gene segments of the IgH locus with D_H-J_H rearrangement occurring prior to V_H to DJ_H rearrangement (Chowdhury & Sen 2001). This process is reliant on multiple factors including IL-7, the transcription factors PAX5 and Yin Yang 1 as well as RAG1 and RAG2 expression (Liu *et al.* 2007; Oettinger *et al.* 1990; Xu *et al.* 2008). Additional BCR diversity is generated by the action of the enzyme terminal deoxynucleotidyl transferase (TdT) which adds random nucleotides to VDJ junctions (Gilfillan *et al.* 1993). Successful rearrangement of the VDJ_H locus leads to surface expression of the pre-BCR which is composed of the rearranged μ heavy chain (μHC) in addition to two surrogate light chains, the Vpre-B and λ5. Cells expressing the pre-BCR are termed pre-B cells and undergo proliferation to form large pre-B cells via the PI3K and extracellular signal-regulated kinase (ERK) pathways due to signalling by the pre-BCR and the IL-7R (Fleming & Paige 2001). Recombination of the second IgH allele is stopped at this stage of B cell development by the action of the pre-BCR and downstream signalling molecules such as spleen tyrosine kinase and zeta-chain associated protein kinase 70 (Schweighoffer *et al.* 2003; ten Boekel *et al.* 1998). Following proliferation induced by the pre-BCR and the IL-7R, pre-B cells once again upregulate RAG1 and RAG2 expression to induce recombination of the V_L and J_L gene segments of the IgL chain in order to form the complete BCR. There are two light chain loci in both humans and mice, Igκ and Igλ. There is a preference for light chain recombination at the

κ locus in mice with 20 times more κ light chains being found in mice compared to λ chains. However, this preference of the κ locus is not observed in humans and the mechanism responsible for this interspecies difference is not known (Kurosaki *et al.* 2010; McGuire & Vitetta 1981). Allelic exclusion of other IgL alleles at this stage in B cell development is accomplished via differential methylation and a regulatory region between V_H and D genes known as the intergenic control region 1 which contains CTCF looping/insulator factor-binding elements (Guo *et al.* 2011; Mostoslavsky *et al.* 1998). Following successful recombination of the light chain, the complete BCR composed of two μHC, two light chains and the functional subunits Igα (CD79A) and Igβ (CD79B) is expressed on the surface of developing B cells which are now termed immature B cells. These cells then undergo positive and negative selection to determine the functional capacity of the newly formed BCR (Kurosaki *et al.* 2010). Immature B cells that possess a weakly self-reactive BCR are ignored during negative selection as tolerance is maintained in the periphery by inhibitory BCR signalling through molecules such as CD22 that increase the activation threshold of these cells. Immature B cells that react strongly to self-antigen during negative selection undergo receptor editing, anergy, or activation-induced cell death. Receptor editing is the most common pathway of dysfunctional immature B cells and involves further VDJ recombination in order to avoid self-reactivity. Failure of receptor editing to produce a non-self-reactive BCR results in the generation of anergic B cells that can travel to the periphery but are not able to respond to antigenic stimulation. Immature B cells with a functional and non-self-reactive BCR deliver satisfactory signals during positive and negative selection, and travel to the periphery to continue normal development (O'Keefe *et al.* 1999; Pelanda & Torres 2012). Approximately $2x10^7$ immature B cells are produced daily in the murine BM of which only 10% exit to the periphery thereby highlighting the critical role of selection in maintaining a functional and non-self-reactive pool of mature B cells.

4.1.1.2 B cell development in the periphery

Immature B cells undergo apoptosis in response to antigenic stimulation. Thus, these cells must undergo further maturation in the periphery (Norvell *et al.* 1995). Once in the spleen, immature B

cells are termed transitional B cells and are divided into three stages; transitional stage (T) 1, 2 and 3. Transitional B cells are differentiated from mature B cells by CD93 expression which can be used alongside IgM and CD23 to delineate the aforementioned transitional B cell populations (IgM^+ $CD23^-$ T1, IgM^+ $CD23^+$ T2 and IgM^- $CD23^-$ T3).

T1 B cells progress onto the T2 stage where these cells start to become reliant on B-cell activating factor (BAFF) and upregulate IgD expression. The transition to the T3 stage has been shown to partially require signalling through Bruton's tyrosine kinase (Btk), a component of the BCR signalling pathway (Allman *et al.* 2001). Of the $2x10^6$ daily émigrés from the BM, around a third progress into the mature B cell pool. This suggests that transitional B cells retain certain properties of their BM counterparts such as susceptibility to selection. Thus, negative selection of B cells appears to be taking place at the T1/T2 and T2/T3 stages.

The T3 B cell population is composed of a large amount of anergic B cells and it is believed that this stage is not a part of conventional B cell development (Chung *et al.* 2003) (Merrell *et al.* 2006; Teague *et al.* 2007). Consequently, progression of transitional B cells into the mature B cell pool is assumed to occur from the T2 stage in the spleen. Additionally, IgD and CD23 expressing, BAFF dependent B cells have also been detected in the murine BM thereby suggesting that B cell maturation may also be occurring concurrently in the BM with cells leaving to enter the periphery in either an immature or semi mature state (Lindsley *et al.* 2007).

The spleen is a major site of peripheral B cell maturation with T2 B cells contributing to either the follicular B cell (FOB) or the marginal zone B cell (MZB) pool with FOBs forming the vast majority of the B cell population in the spleen. Development of T2 B cells into either of these lineages is thought to depend upon signalling in individual cells through pathways such as the BCR. Stronger BCR signalling favours the development of FOBs compared to MZBs. Other factors such as BAFF receptor and NF-κB signalling, NOTCH signalling as well as signals involved in MZB migration and anatomical retention have also been discovered to affect this lineage fate decision (Pillai & Cariappa 2009).

4.1.2 B cell activation

The spleen is an encapsulated organ that is functionally divided into the red and white pulp. The red pulp is involved in filtration of blood, removal of ageing erythrocytes and iron recycling whilst the white pulp is populated by cells of the adaptive immune response. The splenic afferent artery branches into central arterioles that are surrounded by white pulp areas composed of distinct T lymphocyte zones and B cell follicles that contain FOBs as well as follicular dendritic cells (FDCs). The white pulp is enclosed by an area known as the marginal zone which contains MZBs and a discrete subset of macrophages (MZM) (Mebius & Kraal 2005).

B cells become activated following binding of a cognate antigen. Cross linking of the BCR by cognate antigen causes the BCR to change from its resting state to an activated state that allows downstream signalling via kinases. Following initial signalling, the BCR along with the antigen is internalised and processed for presentation to $CD4^+$ T cells via MHCII molecules thereby allowing activated B cells to function as APCs. However, the primary effector mechanism of activated B cells is their differentiation into antibody producing plasma cells and memory B cells. B cells also perform other effector functions in addition to antibody production and antigen presentation through cytokine production such as T follicular helper (T_{FH}) cell support during the germinal centre (GC) reaction and regulation of immune homeostasis in certain autoimmune conditions. Some of the cytokines produced by B cells to perform these functions include IL-1, IL-2, IL-4, IL-6, IL-10, IL-12, IL- 13, IL-16 and IFNγ amongst others (Lund 2008; Mauri & Bosma 2012).

BCR activating ligands are broadly divided into thymus (or T)-independent or T-dependent antigens depending upon analysis of the antibody response in athymic mice. T-independent antigens primarily induce extrafollicular antibody responses that are often initiated by activated MZBs that directly detect pathogens in the circulation and form IgM-producing plasma cells (Zandvoort & Timens 2002).

T-dependent antibody responses are further divided into T-dependent type 1 and type 2 responses that differ in the type of antigen and the type of cell providing the help. The T-

dependent type 1 response is the classical B cell response involving a protein antigen that activates B cells which, then interact with T_{FH} cells to generate GC B cells that differentiate into short- and long-lived plasma cells as well as memory B cells. T-dependent type 2 responses normally involve synthetic, microbial or self-non-protein glycolipid antigens and interactions with natural killer T cells (NKT) to generate the antibody response (Vinuesa & Chang 2013). Only the T-dependent type 1 response is discussed further in this thesis as it has been used to investigate the function of *Fcrl6* during the classic B cell response.

4.1.2.1 T-dependent type 1 response

The initiation of the GC reaction involves multiple cell types that function in a coordinated manner to drive antigen engaged B cells into the GC reaction. The first step of GC formation is the activation of naïve B cells within B cell follicles by FDCs presenting exogenous antigen. FDCs may gain access to exogenous antigen by MZBs that bind immune complexes containing antigen and complement fragments using complement receptors. These MZBs then migrate to the follicular region where FDCs, expressing high amounts of complement receptors, compete with MZBs for antigen binding. Thus, FDCs may gain access to exogenous antigen via MZBs that shuttle between the follicular region and the marginal zone. MZM have been identified to control this process by regulating antigen capture by FDCs.

Concurrently, T cells present in adjacent zones to B cell follicles become activated by DCs and move to the interfollicular region. Antigen engaged B cells also migrate to this region following which they proliferate and form long lived interactions with antigen specific T cells to become fully activated. A subset of these activated B cells moves to the medullary chords within lymph nodes and differentiates into short-lived plasmablasts that secrete antibodies with low affinity for the invading pathogen. Only activated B cells with the highest affinity BCRs gain access to the GC reaction due to interclonal competition for T cell signals.

A majority of the activated T cells acquire a T_{FH} phenotype by day 2 of the GC reaction following which, they migrate from the interfollicular region to within the follicle by day 3 of the GC reaction. GC precursor B cells then move towards the centre of the follicle by day 4 of the GC reaction. Thus, GC commitment appears to occur in T cells prior to that observed in B cells. GC precursor B cells then differentiate into B cell blasts that divide and populate the centre of the follicle. This process displaces naïve B cells from within the follicle and results in formation of the mantle zone that surrounds the GC. The GC continues to increase in size until day 7 following its initiation at which point the full GC is established and divided into two microenvironments known as the dark zone and the light zone.

The dark zone is named as a result of its histological appearance and is composed of densely packed proliferating blasts whilst the light zone contains fewer B cells and is characterised by the presence of other cell types, including T_{FH} cells, FDCs and macrophages. GC B cells cycle between the light zone and dark zone. GC B cells in the dark zone undergo proliferation and upregulation of activation-induced cytidine deaminase (AID) to perform somatic hypermutation (SHM) and class switch recombination (CSR). SHM similar to somatic recombination during B cell development functions to increase the diversity of variable antibody regions by introducing mutations into the V(D)J regions of IgL and IgH loci. CSR is the mechanism by which the constant (C) region of the heavy antibody chain is switched to that of a different isotype to increase the effector capacity of antibodies. Thus, the $C\mu$ of the IgH chain can be exchanged for a $C\gamma$, $C\alpha$ or $C\varepsilon$ region to change the isotype from IgM to IgG, IgA or IgE, respectively depending upon the nature of the stimulus.

After approximately two divisions in the dark zone, GC B cells return to the light zone to test the affinity of their mutated BCR. These GC B cells then interact with FDCs to collect antigen from their surface; the higher the affinity of the mutated BCR, the more antigen that is endocytosed by a particular B cell clone and displayed as peptide MHC (pMHC). Next, these GC B cells compete for help by T_{FH} cells. The more antigen a particular clone presents via pMHC to a cognate T_{FH} cell, the more likely it is that the clone will receive help from T_{FH} cells for survival, primarily in the form

of CD40L, IL-4 and IL-21. Macrophages present within the light zone can take up apoptotic bodies of B cells that fail selection during this process. Successful clones initiate the synthesis phase of the cell cycle in the light zone and migrate to the dark zone where they once again proliferate to start another round of selection. Thus, with repeated exposures to the same antigen presented on FDCs, antibodies with successively greater affinities are produced, a process known as affinity maturation.

Signals that cause exit from the GC reaction and differentiation into plasma cells and memory B cells are still not completely understood. It has recently been identified that expression of E3 ubiquitin ligases Cbl and Cbl-b in light zone GC B cells may control plasma cell differentiation in response to BCR and CD40 stimulation by regulating degradation of IRF4, a transcription factor that facilitates plasma cell fate choice. Memory B cell formation appears to be regulated in response to IL-9 production by T_{FH} cells as deletion of IL-9 in these cells led to an impaired memory B cell response. It has also been suggested that memory B cells exit the GC reaction earlier with fewer mutations than long lived plasma cells that are produced later in the response (Batista & Harwood 2009; Crotty 2014; De Silva & Klein 2015; Li *et al.* 2018; Prokopec *et al.* 2016; Wang *et al.* 2017; Weisel *et al.* 2016).

4.2 Aims

Following qRT-PCR analysis of B-lineage cells, we have identified the expression of FCRL6 in pro-B and pre-B cells. This suggests that FCRL6 could be involved in processes regulating early B cell development in the bone marrow. Thus, we aimed to investigate the consequence of FCRL6 deletion on B cell development by analysing developing and mature B cell populations in *Fcrl6*$^{-/-}$ mice. Additionally, we also examined reconstitution of B-lineage cells derived from *Fcrl6*-deficient bone marrow in competitive mixed bone marrow chimeras to identify the impact of cell intrinsic FCRL6 deletion on B cell development. FCRL6 expression was not detected in mature B cell populations and germinal centre B cells. However, we could not exclude defects with respect to timing, strength or robustness of the B cell response to antigen due to the absence of FCRL6

during development. Accordingly, we investigated the classical B cell response to T-dependent type 1 antigens in *Fcrl6*$^{-/-}$ and B cell conditional *Fcrl6*$^{-/-}$ mice in order to reveal potential cell extrinsic or intrinsic FCRL6-mediated mechanisms that could affect the B cell humoral response.

4.3 Results

4.3.1 Analysis of B cell development in the absence of *Fcrl6* using competitive mixed bone marrow chimeras and in *Fcrl6*$^{-/-}$ mice

4.3.1.1 Analysis of B cell development in the bone marrow

The expression profile of *Fcrl6* suggests a possible role of this protein during early B cell development. Thus, we decided to investigate the effect of *Fcrl6* deletion on B cell development via a combination of mixed bone marrow chimeras and comparison of complete *Fcrl6*$^{-/-}$ and WT mice. CD45.2^{+} *Fcrl6*$^{-/-}$ or WT bone marrow cells were mixed with CD45.1^{+} WT bone marrow cells and injected into myeloablated CD45.1/2^{+} WT recipient mice to detect developmental abnormalities arising due to the absence of *Fcrl6*. The mixed bone marrow chimeras were created at a ratio of 55:45% with respect to CD45.2^{+} and CD45.1^{+} cells. *Fcrl6*-deficient bone marrow performed similarly to WT bone marrow at reconstituting pro-B, pre-B and immature B cells in the bone marrow. A slight advantage was observed in favour of *Fcrl6*-deficient bone marrow in reconstituting recirculating mature B cells in the bone marrow (Figure 14a). However, subsequent analysis of complete *Fcrl6*$^{-/-}$ and WT mice failed to detect an identical difference in this population in the bone marrow under steady state conditions (Figure 14b). Similarly, we did not detect differences in pro-B, pre-B and immature B cells in the bone marrow of complete *Fcrl6*$^{-/-}$ and WT mice under steady state conditions (Figure 14b).

4.3.1.2 Analysis of B cell development in the periphery

Next, we focused on identifying differences in developing B cells in the spleen. *Fcrl6*-deficient bone marrow performed similarly to WT bone marrow at reconstituting transitional type 1, type 2

and type 3 B cell populations in the spleen (Figure 15a). Comparison of transitional B cells in complete *Fcrl6*$^{-/-}$ and WT mice supported this result as we did not find a difference in these populations in terms of percentage or number under steady state conditions (Figure 15b). Thereafter, we focused on analysing mature B cell populations in the spleen. *Fcrl6*-deficient bone marrow performed similarly to WT bone marrow at reconstituting total mature B cells in the spleen (Figure 15a). Analysis of total mature B cells in complete *Fcrl6*$^{-/-}$ and WT mice revealed a comparable result with no difference being detected in the percentage and number of these cells in the spleen of complete *Fcrl6*$^{-/-}$ and WT mice (Figure 15b). Further analysis of mature B cell subsets in mixed bone marrow chimeras showed *Fcrl6*-deficient bone marrow performed similarly to WT bone marrow at reconstituting follicular and marginal zone B cells in the spleen (Figure 15a). Analysis of follicular and marginal zone B cells in complete *Fcrl6*$^{-/-}$ and WT mice also did not reveal differences in terms of percentage or number under steady state conditions (Figure 15b). We were able to conclude following evaluation of cell surface markers in mixed bone marrow chimeras and complete *Fcrl6*$^{-/-}$ mice that development of B cells from pro-B cells to mature follicular and marginal zone B cells remains unperturbed in the absence of *Fcrl6* (Figure 16).

Figure 14: There are no differences during B cell development in the bone marrow in the absence of *Fcrl6*.

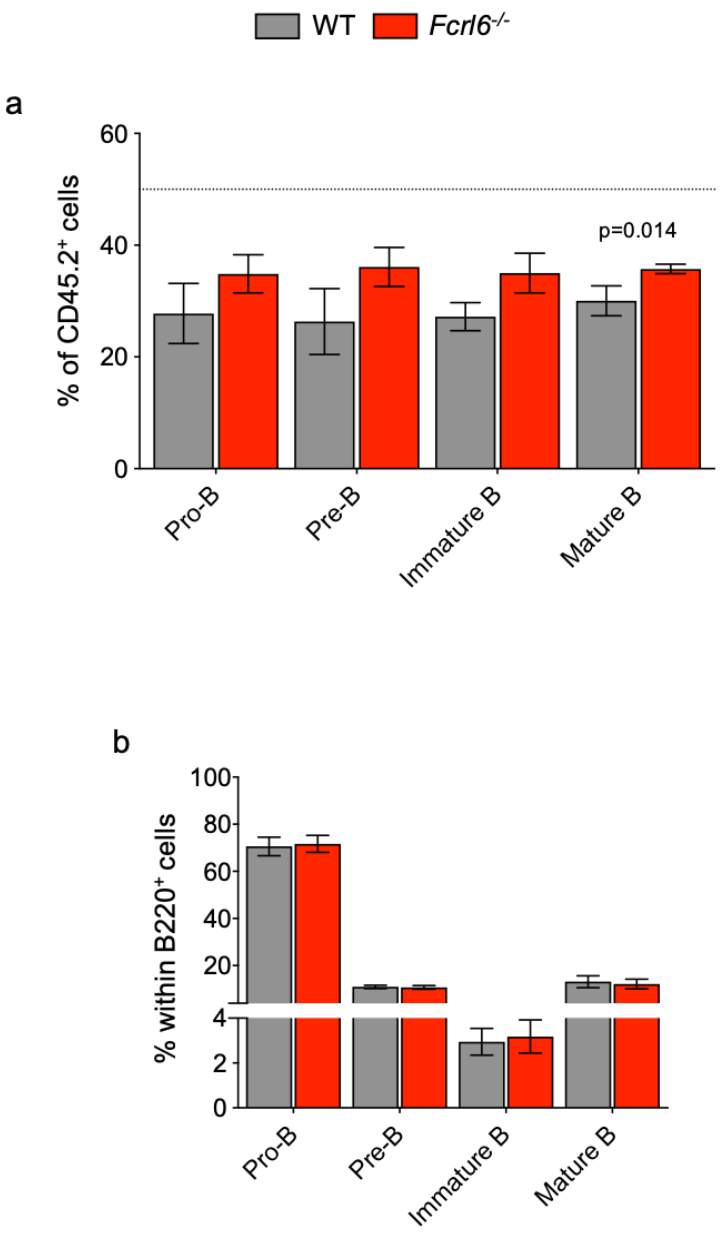

(a) Relative proportions of *Fcrl6*$^{-/-}$ and WT derived developing B cells from mixed bone marrow chimeras. Bone marrow from CD45.2^{+} *Fcrl6*$^{-/-}$ and WT mice was mixed with bone marrow from CD45.1^{+} WT mice (55% CD45.2^{+} cells) and injected intravenously into myeloablated CD45.1/2^{+} WT recipient mice. Reconstitution was analysed 8 weeks later via flow cytometry. Bars represent mean ± SEM of 4 (WT) and 14 (*Fcrl6*$^{-/-}$) biological replicates. Cell populations were gated as depicted in Figure 16 with additional gating for CD45.1 and CD45.2. Dotted line indicates injected percentage of CD45.2^{+} cells. (b) Number and percentage of developing B cells in unchallenged

Fcrl6$^{-/-}$ and WT mice analysed via flow cytometry. Cell populations were gated as depicted in Figure 16. Bars represent mean ± SEM of 13 biological repeats per genotype from 3 independent experiments.

Figure 15: There are no differences in developing and mature B cells in the spleen in the absence of *Fcrl6*.

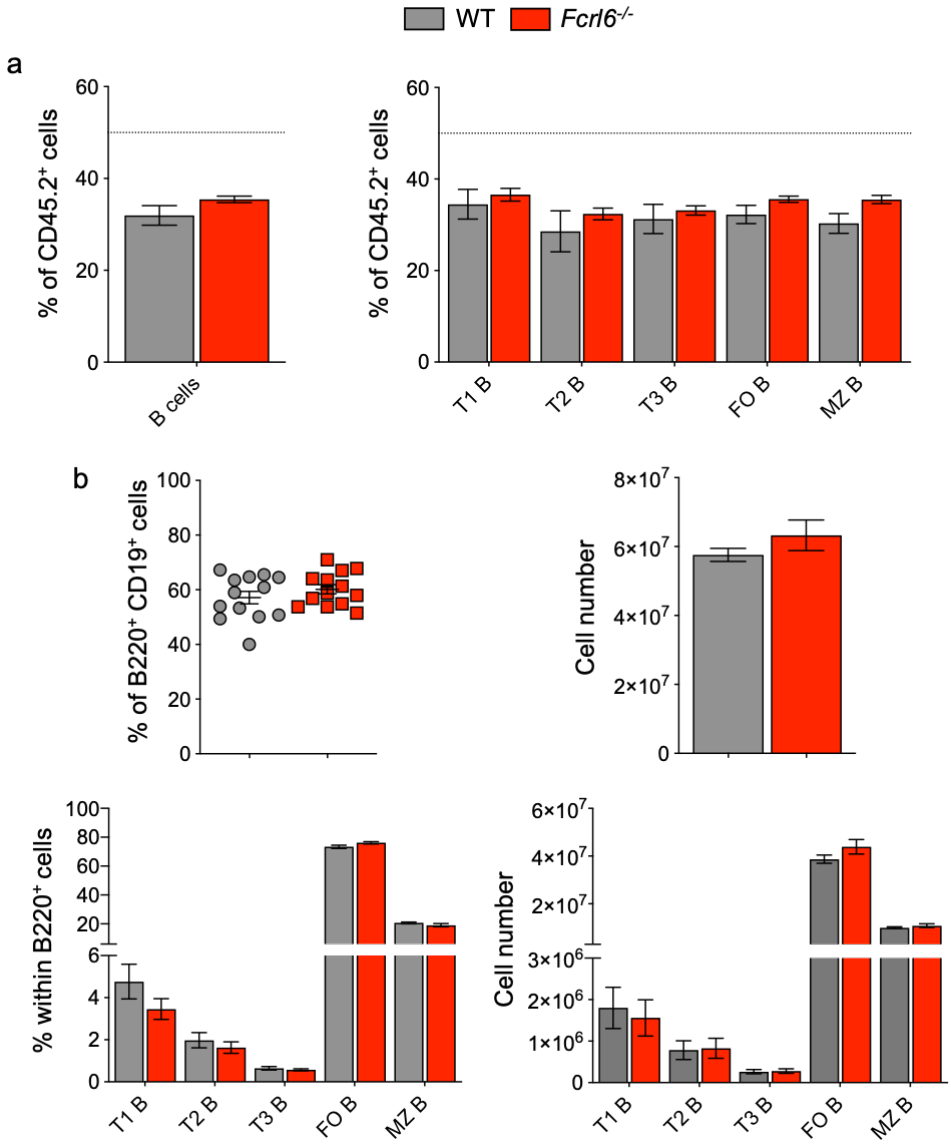

(a) Relative proportions of *Fcrl6*$^{-/-}$ and WT derived developing and mature B cells from mixed bone marrow chimeras. Bone marrow from CD45.2^{+} *Fcrl6*$^{-/-}$ and WT mice was mixed with bone marrow from CD45.1^{+} WT mice (55% CD45.2^{+} cells) and injected intravenously into myeloablated CD45.1/2^{+} WT recipient mice. Reconstitution was analysed 8 weeks later via flow cytometry. Bars represent mean ± SEM of 4 (WT) and 14 (*Fcrl6*$^{-/-}$) biological replicates. Cell populations were gated as depicted in Figure 16 with additional gating for CD45.1 and CD45.2. Dotted line indicates injected percentage of CD45.2^{+} cells. (b) Number and percentage of developing and mature B cells in unchallenged *Fcrl6*$^{-/-}$ and WT mice analysed via flow cytometry. Cell populations were

gated as depicted in Figure 16. Bars and symbols represent mean ± SEM of 13 biological repeats per genotype from 3 independent experiments. FO, follicular; MZ, marginal zone; T1, transitional type 1; T2, transitional type 2; T3, transitional type 3.

Figure 16: *Fcrl6*$^{-/-}$ mice show normal B cell development.

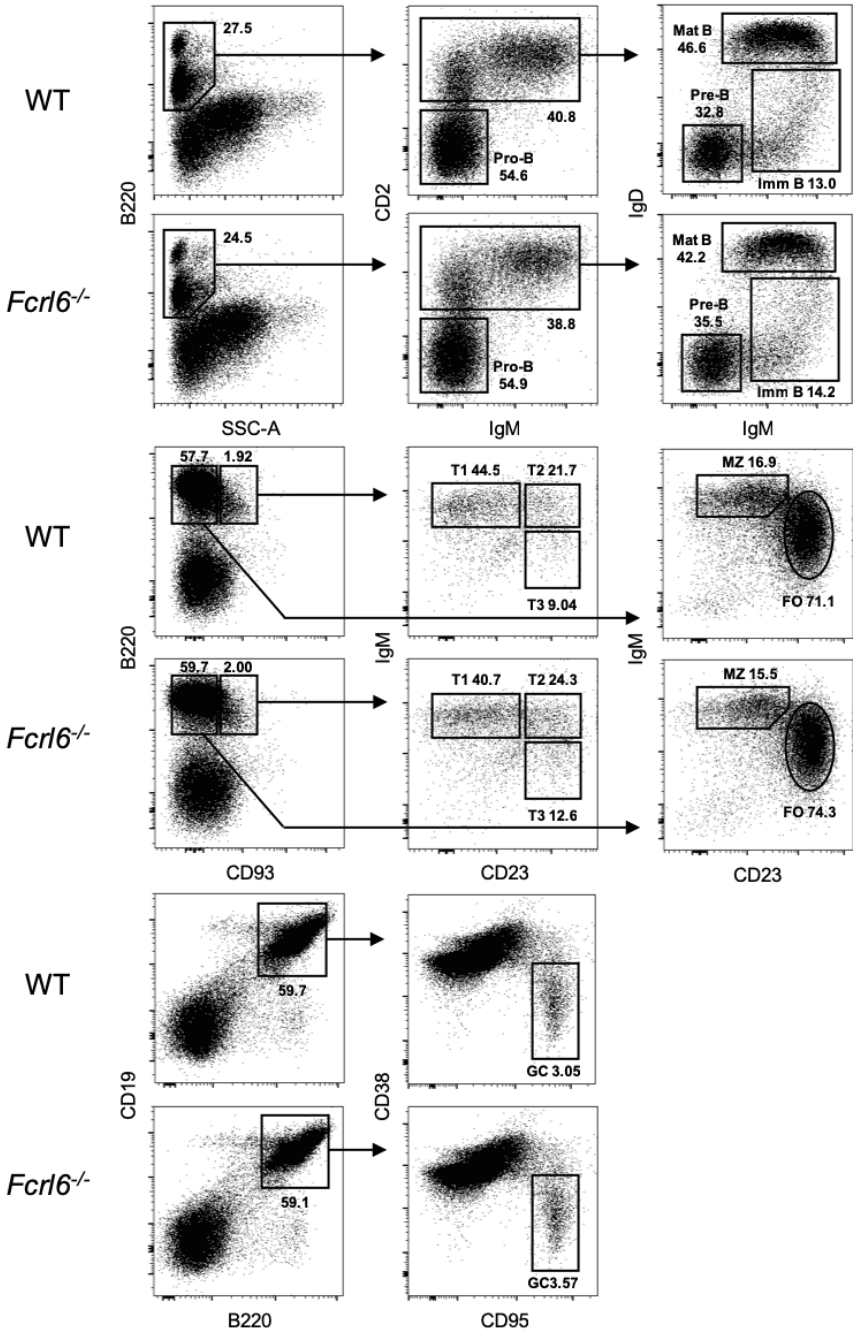

Flow cytometric gating strategy used for analysis and sorting of developing, mature and antigen experienced B cell populations in Figures 7, 14, 15, 19 and 20. Names are indicated by text next to the gates whilst numbers represent population percentage within that plot. Gating strategies were as follows: bone marrow – Imm B, immature B ($B220^+$ $CD2^+$ IgD^- IgM^+); Mat B, mature B ($B220^+$ $CD2^+$ IgD^+ IgM^+); Pre-B ($B220^+$ $CD2^+$ IgD^- IgM^+) and Pro B ($B220^+$ $CD2^-$); spleen – GC, germinal centre B ($B220^+$ $CD19^+$ $CD38^-$ $CD95^+$); FO, follicular B ($B220^+$ $CD93^-$ IgM^{int} $CD23^+$); MZ,

marginal zone B ($B220^+$ $CD93^-$ IgM^{hi} $CD23^-$); T1, transitional type 1 ($B220^+$ $CD93^+$ IgM^+ $CD23^-$); T2, transitional type 2 ($B220^+$ $CD93^+$ IgM^+ $CD23^+$) and T3, transitional type 3 ($B220^+$ $CD93^+$ IgM^- $CD23^+$).

4.3.2 Analysis of the antibody response in the absence of *Fcrl6*

4.3.2.1 Analysis of immunoglobulin levels in Fcrl6$^{-/-}$ mice under steady state conditions

Since B cell development appeared unaffected by the absence of *Fcrl6*, we proceeded to analyse *in vivo* antibody responses in *Fcrl6*$^{-/-}$ mice. Although we did not detect *Fcrl6* expression in GC B cells and the percentage and number of these cells remained unchanged in *Fcrl6*$^{-/-}$ mice compared to WT mice in steady state conditions (data not shown), we could not exclude differences with respect to the timing and or quality of the humoral response due to the absence of *Fcrl6* during development. We first analysed serum antibody levels in unimmunised *Fcrl6*$^{-/-}$ and WT mice. Serum levels of IgA, IgM and IgG did not differ between *Fcrl6*$^{-/-}$ and WT mice co-housed under specific-pathogen free conditions (Figure 17). Subsequently, we started to investigate the antibody response in *Fcrl6*$^{-/-}$ mice to antigen.

4.3.2.2 Analysis of the antibody response to DNP-OVA in Fcrl6$^{-/-}$ mice

First, we analysed the antibody response in *Fcrl6*$^{-/-}$ mice to the T-dependent antigen DNP-OVA (Buchanan *et al.* 1998). Immunisation of *Fcrl6*$^{-/-}$ and WT mice with DNP-OVA resulted in germinal centre formation in both genotypes. However, there were no differences in the number and percentage of germinal centre B cells in *Fcrl6*$^{-/-}$ and WT mice (Figure 18a and 18b). The immunisation also induced a DNP-specific IgG and IgM response in the serum. Comparison of serum DNP-specific IgG and IgM also did not reveal differences between *Fcrl6*$^{-/-}$ and WT mice (Figure 18c). We concluded that the antibody response to DNP-OVA is not affected by the absence of *Fcrl6*.

Figure 17: *Fcrl6*$^{-/-}$ mice have normal serum immunoglobulin levels of IgA, IgM and IgG.

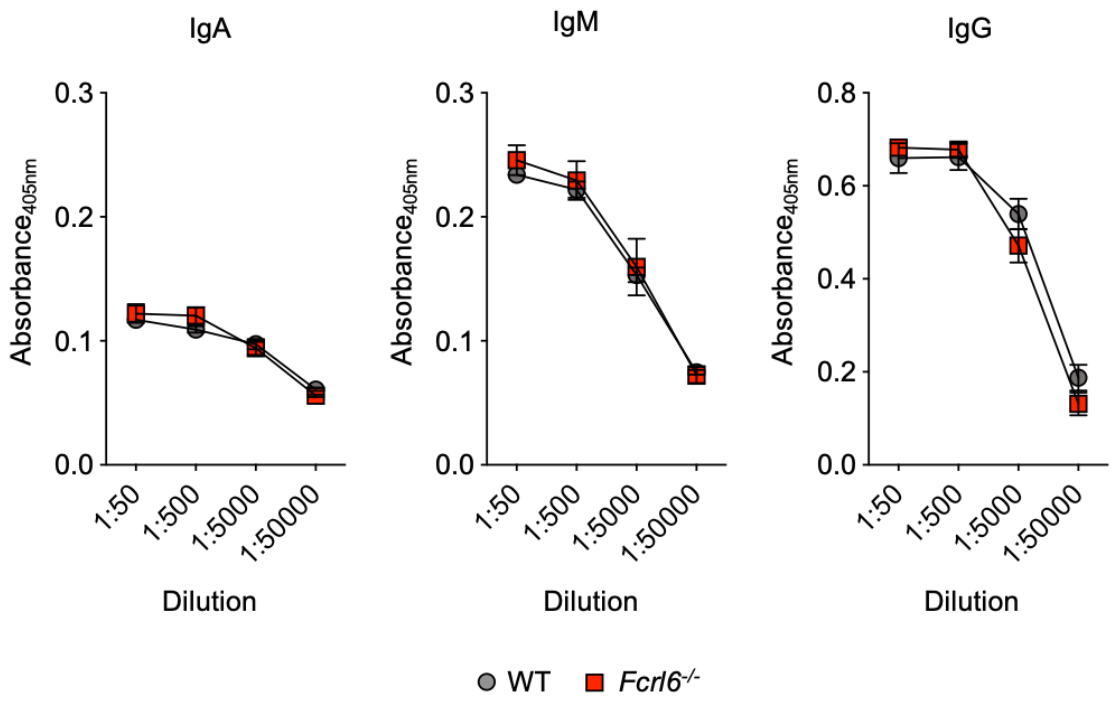

Levels of IgA, IgM and IgG in the serum of unchallenged *Fcrl6*$^{-/-}$ or WT mice. Immunoglobulin levels were measured by ELISA. Symbols indicate mean ± SEM of 5 biological replicates from 3 independent experiments.

Figure 18: *Fcrl6*$^{-/-}$ mice respond normally to the T-dependent antigen, DNP-OVA.

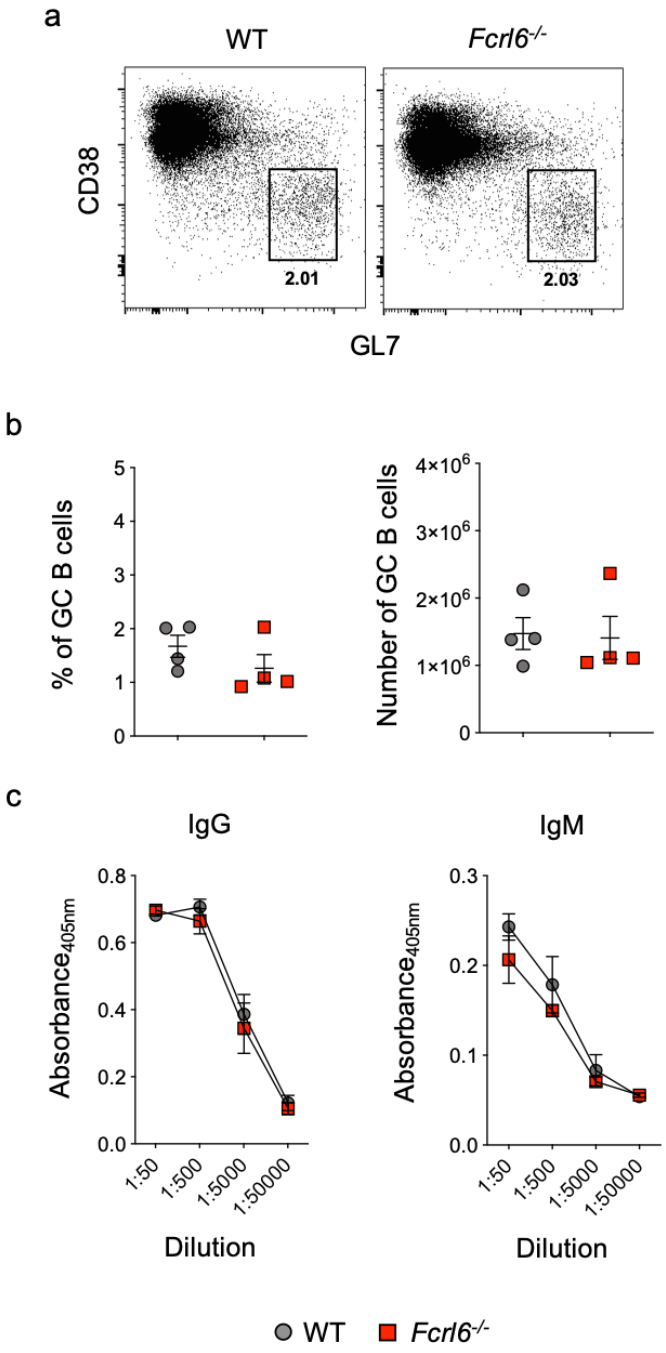

(a) GC formation at day 14 in *Fcrl6*$^{-/-}$ and WT mice following DNP-OVA challenge (b) GC percentage and number at day 14 following DNP-OVA challenge. (c) DNP specific IgG and IgM at day 14 following DNP-OVA challenge. Immunoglobulin levels were detected via ELISA. *Fcrl6*$^{-/-}$ or WT mice were injected intraperitoneally with 100mg of DNP-OVA following which GC and immunoglobulin formation was analysed 14 days later. Symbols and bars show mean ± SEM of 4 biological replicates per genotype. GC B cells were gated as B220^{+} IgD^{low} CD38^{-} GL7^{+}.

4.3.2.3 Analysis of the antibody response to FV in Fcrl6$^{-/-}$ mice

Next, we analysed the antibody response in *Fcrl6*$^{-/-}$ mice to FV infection. FV induces a robust adaptive immune response resulting in the peak of germinal centre formation and antibody response at day 35 following infection (Young *et al.* 2012). Since we could not exclude that Fcrl6 inactivation would affect viral clearance thereby affecting overall antigen load and GC formation, we first determined the extent of FV replication by measuring the percentage of infected Ter119^{+} cells in the spleen of *Fcrl6*$^{-/-}$ and WT mice. Our results suggested that FCRL6 deficiency does not affect virus replication after 35 days following FV infection (Figure 19a). Thus, we analysed germinal centre formation, serum FV-specific neutralising antibody level and serum F-MLV infected cell-binding IgG and IgM levels in *Fcrl6*$^{-/-}$ and WT mice at day 35 following FV infection. We observed a similar response in term of number and percentage of germinal centre B cells in the spleen of complete *Fcrl6*$^{-/-}$ and WT mice at this time point following FV infection. Furthermore, the ratio of dark zone to light zone germinal centre B cells was also comparable (Figure 19b and 19c). Similarly, we did not find a difference in the levels of FV specific neutralising antibodies at the analysed time points in complete *Fcrl6*$^{-/-}$ and WT mice. The levels of FV specific neutralising antibodies are very low during the early phase of FV infection. In order to obtain an accurate readout relating to the antibody response, we measured the serum titres of F-MLV infected cell-binding IgG and IgM. Similar to the neutralising antibody result, we did not find a difference in the serum levels of F-MLV infected-cell binding IgG and IgM at the analysed time points in *Fcrl6*$^{-/-}$ and WT mice (Figure 19d). We concluded that the antibody response to FV infection remains is not affected by global FCRL6 deficiency.

Figure 19: *Fcrl6*$^{-/-}$ mice show a normal antibody response to Friend virus infection.

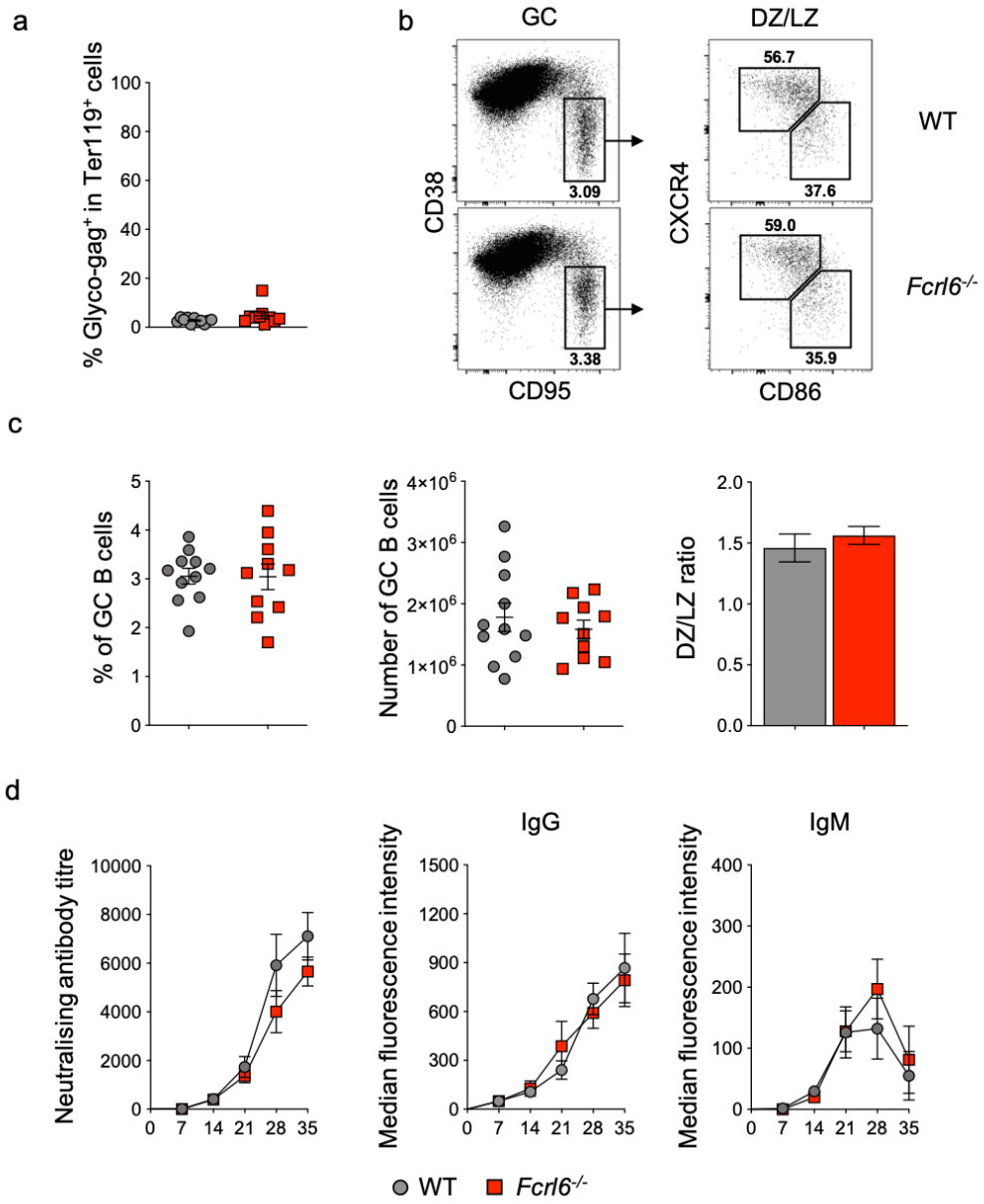

(a) Percentage of infected Ter119^{+} cells in the spleen at day 35 following FV infection. (b) GC formation at day 35 in *Fcrl6*$^{-/-}$ and WT mice following FV infection (c) GC percentage, number and dark zone/light zone ratio at day 35 following FV infection. (d) Kinetics of FV specific neutralising antibodies and F-MLV infected cell-binding IgG and IgM following FV infection. Neutralising antibody and immunoglobulin levels were detected via flow cytometry. *Fcrl6*$^{-/-}$ or WT mice were infected with 1000 spleen focus-forming units of FV by intravenous injection. Symbols and bars show mean ± SEM of 11 biological replicates per genotype from 2 independent experiments.

Numbers on the X axis indicate days post FV infection. GC B cells were gated as depicted in Figure 16. Dark zone (DZ) and light zone (LZ) GC B cells were gated as $B220^{+}$ $CD19^{+}$ $CD38^{-}$ $GL7^{+}$ $CXCR4^{+}$ $CD86^{-}$ and $B220^{+}$ $CD19^{+}$ $CD38^{-}$ $GL7^{+}$ $CXCR4^{-}$ $CD86^{+}$, respectively.

4.3.2.4 Analysis of the antibody response to FV in B cell conditional Fcrl6$^{-/-}$ mice

We created B cell conditional *Fcrl6*$^{-/-}$ mice to confirm the that intrinsic deletion of *Fcrl6* in B-lineage cells during development does not affect the classical B cell *in vivo* antibody response. We generated the B conditional *Fcrl6*$^{-/-}$ strain by crossing *Fcrl6*$^{tm1c(KOMP)Wtsi}$ mice with C57BL/6-*Cd79a*$^{tm1(cre)Reth}$ mice. *Cd79a* encodes the immunoglobulin-α signalling subunit of the B cell receptor and is expressed exclusively in B-lineage cells from the pro-B cell stage (Hobeika *et al.* 2006). Thus, *Fcrl6* should be deleted in B cell conditional *Fcrl6*$^{-/-}$ mice at the pro-B cell stage in the bone marrow. We infected B cell conditional *Fcrl6*$^{-/-}$ and littermate WT controls with FV and analysed germinal centre formation and antibody response. As observed in *Fcrl6*$^{-/-}$ mice, mice with conditional B cell-specific Fcrl6 deficiency cleared FV infection at day 35 similar to their WT counterpart (Figure 20a). We did not detect differences in the number and percentage of germinal centre B cells, as well as in the dark zone to light zone GC ratio, in B cell-conditional *Fcrl6*$^{-/-}$ and littermate WT mice at this time point following FV infection (Figure 20b and 20c). In accordance with cellular data, we did not detect a difference in the serum FV-specific neutralising antibody level between B cell conditional *Fcrl6*$^{-/-}$ and littermate WT mice at all analysed time points except day 21 following infection. However, analysis of F-MLV infected cell-binding IgG and IgM levels did not show differences between infected B cell conditional *Fcrl6*$^{-/-}$ and littermate WT mice (Figure 20d). We concluded that the antibody response to FV remains broadly unaffected by a cell intrinsic absence of *Fcrl6* in the B-lineage cells during development.

Figure 20: B cell conditional *Fcrl6*$^{-/-}$ mice show a normal antibody response to Friend virus infection.

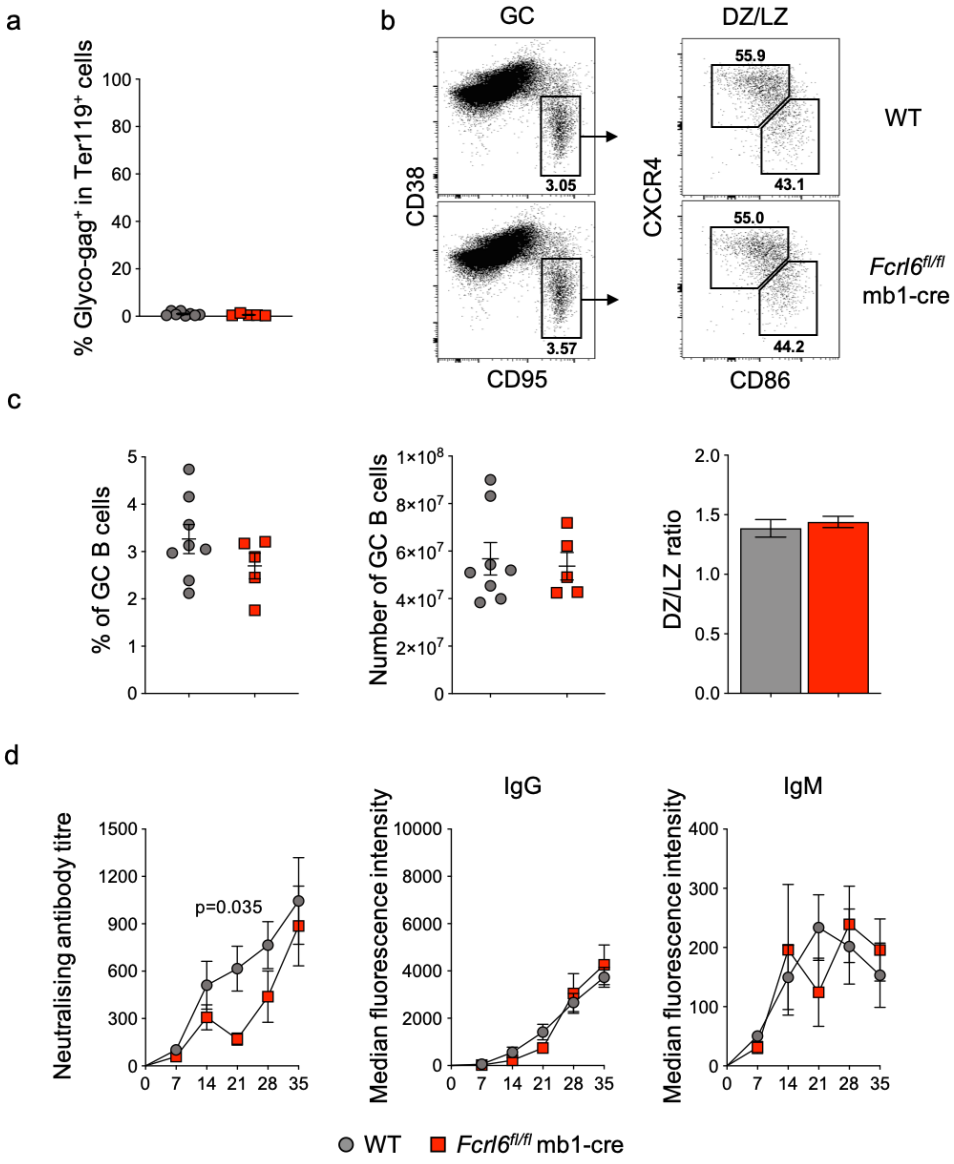

(a) Percentage of infected Ter119^{+} cells in the spleen at day 35 following FV infection. (b) GC formation at day 35 in *Fcrl6*$^{fl/fl}$ mb1-cre and WT mice following FV infection (c) Germinal centre percentage, number and dark zone/light zone ratio at day 35 following FV infection. (d) Kinetics of FV specific neutralising antibodies and F-MLV infected cell-binding IgG and IgM following FV infection. Neutralising antibody and immunoglobulin levels were detected via flow cytometry. *Fcrl6*$^{-/-}$ or WT mice were infected with 1000 spleen focus-forming units of FV by intravenous injection. Symbols and bars show mean ± SEM of 7 (WT) and 5 (*Fcrl6*$^{fl/fl}$ mb1-cre) biological

replicates. Numbers on the X axis indicate days post FV infection. GC B cells were gated as depicted in Figure 16. Dark zone (DZ) and light zone (LZ) GC B cells were gated as $B220^{+}$ $CD19^{+}$ $CD38^{-}$ $GL7^{+}$ $CXCR4^{+}$ $CD86^{-}$ and $B220^{+}$ $CD19^{+}$ $CD38^{-}$ $GL7^{+}$ $CXCR4^{-}$ $CD86^{+}$, respectively.

4.4 Discussion

Members of the FCRL protein family are preferentially expressed by B-lineage cells in both humans and mice. Specifically, in mice, FCRL protein family members are primarily expressed by mature B cell subsets (Li *et al.* 2014a). However, we did not detect expression of *Fcrl6* in mature B cells but found it restricted to early B cell developmental stages in the bone marrow. Thus, we aimed to investigate if this expression of FCRL6 was essential for B cell development or affected the classical response of mature B cells to T-dependent type 1 antigens.

4.4.1 FCRL6 and B cell development

We did not find differences in B cell development in *Fcrl6*$^{-/-}$ mice as the number and percentage of developing and mature B cell populations remained unaffected by the absence of *Fcrl6* in these mice. Additionally, we also did not detect differences in the development of B cells from *Fcrl6*-deficient bone marrow under competition with WT cells in mixed bone marrow chimeras. Interestingly, CD45.2^{+} WT and *Fcrl6*$^{-/-}$ derived developing and mature B cells were outperformed by their CD45.1^{+} WT derived counterparts in the bone marrow and spleen. This difference appears to be driven by the allelic variants of CD45 which are essential for the identification of congenic populations. CD45 is a phosphatase that plays an important role in regulating signalling thresholds (Hermiston *et al.* 2003). Although CD45.1 and CD45.2 are suggested to be functionally equivalent, subtle differences in their function can result in skewed development of a particular congenic population (Basu *et al.* 2013; Chisolm *et al.* 2019). For this reason, mice injected with CD45.1^{+} WT and CD45.2^{+} WT bone marrow as an internal control within our experimental cohort were used to validate our data. Overall, our results from mixed bone marrow chimeras and the analysis of B cell development in *Fcrl6*$^{-/-}$ mice indicated that FCRL6 is dispensable for B cell development despite its expression in B cell progenitors. It is unlikely that mechanisms compensating for the germline deletion of FCRL6 exist in *Fcrl6*$^{-/-}$ mice and allow normal B cell development as we did not detect B cell developmental differences in B cell conditional *Fcrl6*$^{-/-}$ mice where FCRL6 is deleted at the pro-B cell stage in B-lineage cells (data not shown).

4.4.2 FCRL6 and the B cell response to T-dependent type 1 antigens

Prior to testing if the expression of *Fcrl6* during B cell development influenced their functionality with respect to generation of *in vivo* humoral responses, we first measured if *Fcrl6*$^{-/-}$ mice had equivalent antibody levels to WT mice prior to antigen exposure. We found that serum levels of IgA, IgG and IgM were present at equal levels in the absence of *Fcrl6* in these mice compared to WT mice. Next, we analysed the antibody response in *Fcrl6*$^{-/-}$ mice to the T-dependent antigen DNP-OVA. We did not find a difference in the number and percentage of GC B cells in the spleen as well as serum DNP-specific IgG and IgM antibody levels of *Fcrl6*$^{-/-}$ mice compared to WT mice. Thereafter, we evaluated the B cell response to FV infection in *Fcrl6*$^{-/-}$ mice. We did not observe a difference in viral load as measured by the percentage of infected splenic Ter119^{+} cells or GC formation including relative proportions of dark and light zone GC B cells in *Fcrl6*$^{-/-}$ mice compared to WT mice. In agreement with cellular data, the levels of virus-specific neutralising antibodies in the serum of *Fcrl6*$^{-/-}$ mice did not differ compared to WT mice. However, the level of virus-specific neutralising antibodies is very low during the early phase of FV infection to be accurately measured by neutralising antibody assays. Thus, in order to obtain an accurate readout relating to the virus-specific humoral response at early time points following FV infection, we measured serum levels of virus-specific antibodies through assessment of F-MLV (FV) infected cell-binding IgG and IgM levels. Similar to the neutralising antibody result, we did not find a difference in the serum levels of F-MLV infected-cell binding IgG and IgM at all analysed time points in *Fcrl6*$^{-/-}$ mice compared to WT mice. It could be argued that deletion of FCRL6 in other cell types such as NK cells which perform a vital role during early FV infection could mask effects of its deletion on the B cell response. In order to circumvent such issues, we investigated the B cell response following FV infection in B cell conditional *Fcrl6*$^{-/-}$ mice where FCRL6 is specifically deleted in B-lineage cells from the pro-B cell stage. Viral load, GC formation including proportions of dark and light zone GC B cells as well as F-MLV infected-cell binding IgG and IgM antibody levels did not show differences between B cell conditional *Fcrl6*$^{-/-}$ mice and litter mate WT control mice at day 35 following infection. There was a decrease in the virus-specific neutralising antibody level at day

21 following infection in B cell conditional *Fcrl6*$^{-/-}$ mice. However, this reduction in serum virus-specific neutralising antibody titre was not sustained as B cell conditional *Fcrl6*$^{-/-}$ mice did not show similar differences at subsequent time points. This suggests that it was most likely due to a technical error in the neutralising antibody assay or degradation of Ig during processing or storage of serum samples from B cell conditional *Fcrl6*$^{-/-}$ mice. GC formation in addition to the presence of class switched and effective neutralising antibodies in *Fcrl6*$^{-/-}$ mice and B cell conditional *Fcrl6*$^{-/-}$ mice suggests that processes such as SHM and CSR remain unaffected by overall or B cell specific deletion of FCRL6. Thus, our results demonstrate that deletion of *Fcrl6* during early B cell development does not affect the B cell response to T-dependent type 1 antigens.

4.4.3 Future work

Whilst B cell development is normal in the absence of *Fcrl6*, whole transcriptome sequencing of B cell conditional *Fcrl6*$^{-/-}$ pro-B and pre-B cells could be carried out in future studies to detect subtle differences that could have arisen due to the absence of *Fcrl6.* Differentially regulated genes could be further investigated using pathway analysis to give an indication of potential phenotypes that may be evident in these cells due to deletion of *Fcrl6*. Pro-B and pre-B cells represent crucial stages of B cell development where somatic recombination of V_H, D_H and J_H gene segments at the IgH and V_L and J_L gene segments at the IgL loci drives the generation a diverse range of BCRs (Chaudhary & Wesemann 2018). As *Fcrl6* is expressed by these cells, its absence in *Fcrl6*-deficient mice could affect this process. Thus, the BCR repertoire of B cell conditional *Fcrl6*$^{-/-}$ mice could also be sequenced in future studies to identify potential changes caused by *Fcrl6* deletion.

It is well-established that two populations of B cells – B1 and B2 – exist in mice. B2 cells are continually generated in the bone marrow and circulate to secondary lymphoid organs such as the spleen where they form follicular and marginal zone B cells that respond to T-dependent and T-independent antigens (Tangye 2013). We were unable to find differences in the development or functioning of B2 cells in response to T-dependent type 1 antigens in the absence of *Fcrl6*.

However, FCRL6 could have a role in the development and function of B1 cells which are predominantly found in peritoneal and pleural cavities, and represent a distinct lineage of B cells that self-renew following generation from stem cells at early stages of life (Montecino-Rodriguez & Dorshkind 2012). Future studies should aim to investigate the expression of FCRL6 in B1 cells as well as analyse their proportions in the aforementioned compartments in *Fcrl6*$^{-/-}$ mice to identify differences in their development that could arise as result of *Fcrl6* deletion. B1 cells are considered to be the major producers of 'natural' IgM and IgG3 in mouse serum (Baumgarth 2017; Kantor & Herzenberg 1993). Although we did not identify a difference in the serum IgM level of unchallenged *Fcrl6*$^{-/-}$ mice, there could be differences in serum IgG3 levels and *in vivo* activation of B1 cells due to deletion of *Fcrl6* which could be examined by future studies to determine the role of this receptor in context of B1 cells.

We identified that deletion of *Fcrl6* during development does not affect the generation of an effective B cell response to T-dependent type 1 antigens. However, we did not analyse the formation of plasma cells and memory B cells following challenge of T-dependent antigens in *Fcrl6*-deficient mice. It is unlikely that plasma cell formation is affected by the absence of *Fcrl6* as *Fcrl6*$^{-/-}$ and B cell conditional *Fcrl6*$^{-/-}$ mice do not display a difference in serum levels of virus-specific antibodies. Nonetheless, short- and long-lived plasma cell proportions should be examined in these mice to confirm normal differentiation of these populations following B cell activation despite deletion of *Fcrl6*. Memory B cell formation could also be affected by the deletion of FCRL6 during development and should be examined in B cell conditional *Fcrl6*$^{-/-}$ mice through immunisation and rechallenge with a T-dependent antigen such as NP-CGG. Additionally, future work should also involve analysing the B cell response to antigens such as NP-LPS (T-independent type 1) and NP-Ficoll (T-independent type 2) in B cell conditional *Fcrl6*$^{-/-}$ mice to determine if the expression of FCRL6 during development affects generation of effective T-independent B cell responses. Additionally, as we were unable to characterise the expression of FCRL6 in plasma and memory B cell populations, future studies should analyse FCRL6 expression in these cells to obtain a full expression profile of this receptor in context of B cells.

Chapter 5. Role of FCRL6 in the development and function of NK cells

5.1 Introduction

5.1.1 NK cell development

NK cells are an indispensable component of the innate immune response and constitute the first line of defence against microbial pathogens and tumours. NK cells like B and T lymphocytes, are derived from CLPs and develop in the BM. NK cell development has also been reported to occur in other anatomical locations such as the liver and thymus. However, these developmental pathways will not be described in this thesis and further reference to NK development is indicative of their development in the BM. Unlike the somatically rearranged receptors expressed by B and T lymphocytes, NK cell 'antigen receptors' consist of germ line encoded self MHCI binding inhibitory receptors, and activating receptors that recognise ligands associated with cellular stress. These receptors are expressed in a stochastic pattern resulting in subsets of functionally distinct NK cells. During their development, NK cells undergo an 'education' process where they learn to recognise an absence of self MHCI molecules on target cells also known as 'missing self' via expression of their inhibitory receptors. This ability alongside their expression of activating receptors allows NK cells to target compromised cells that have downregulated MHCI and upregulated expression of NK activating ligands due to infection or malignancy.

5.1.1.1 NK cell development in the bone marrow

Development of NK-lineage progenitors

NK cells are the founding members of a specialised group of leukocytes known as innate lymphoid cells (ILCs). ILCs are divided into three subsets; ILC1, ILC2 and ILC3 as defined by expression of key transcription factors and functional profile. NK cells along with ILC1 cells constitute the

ILC1 subset that is characterised by constitutive T-bet expression and the ability to produce T_{H1} cytokines following stimulation with IL-12, IL15 or IL-18. All ILCs are derived from CLPs which differentiate into common ILC precursor (CILCP) cells that can be identified by their expression of the transcription factor Tcf-1 (Maloy & Uhlig 2013; Yang *et al.* 2015b; Yu *et al.* 2013). Notch signalling through the ligands Jagged1 and Jagged2 has been shown to drive the development of NK cells from the CLP stage (Maillard *et al.* 2005). The development of CLPs is discussed in section 4.1.1.1 of the thesis. CILCPs then form αLP cells which are able to differentiate into progenitors of both NK and ILC-linage cells (Constantinides *et al.* 2015). Subsequently, αLP cells destined for the NK lineage upregulate their expression of CD122, the β chain of the IL-15 receptor, and develop into NK precursor (NKP) cells (Geiger & Sun 2016). IL-15 plays a crucial role in the development of NK cells highlighted by the absence of mature NK cells in *IL-15*$^{-/-}$ mice (Kennedy *et al.* 2000).

Development of NK-lineage cells

NK cells are reliant on multiple cytokines and transcription factors for the promotion and regulation of their development. Nfil3 is a critical factor for controlling NK cell lineage commitment and is expressed from the CLP stage in developing lymphocytes (Male *et al.* 2014). However, its expression is only crucial during the NKP stage of NK cell development as conditional deletion of Nfil3 at the subsequent stage of NK development does not impact the number of mature NK cells or their effector function (Firth *et al.* 2013). Nfil3 expression at the NKP stage is driven by IL-15 through the PDK1 kinase and its downstream target mTOR as NK conditional deletion of mTOR results in a NK developmental block in the bone marrow and absence of peripheral NK cells (Marçais *et al.* 2014; Yang *et al.* 2015a). NKP cells lack expression of common NK lineage markers such as NK1.1 and CD49b but can be identified by their expression of CD122 as well as an absence of common lineage markers. CD122 expression may by driven in these cells by the transcription factors, Runx3 and Cbfβ as NKP cells deficient in these factors do not generate peripheral NK cells in foetal liver chimeras (Guo *et al.* 2008a). T-bet and Eomesodermin (Eomes) expression has also been shown to drive CD122 expression and mice with an absence of both

factors are deficient in NK cells due to lack of IL-15 signalling (Intlekofer *et al.* 2005). The NKP population also expresses the α chain of the IL-7 receptor which is subsequently lost following their differentiation into immature NK (iNK) cells. iNK cells acquire expression of NK1.1 and CD335 but still do not express the remaining NK lineage marker, CD49b. Runx3 expression has been shown to be vital following the expression of CD335 as deletion of the factor following CD335 expression results in the absence of peripheral mature NK cells (Ebihara *et al.* 2015). Next, iNK cells differentiate into the mature NK cell (mNK) cells and start expressing CD11b, CD43, various activating and inhibitory receptors, and CD49b. The transcription factor ID2 has been shown to be important for this transition as its absence results in a developmental arrest of NK linage cells at the iNK stage (Boos *et al.* 2007; Yokota *et al.* 1999). T-bet and Eomes are also important for the transition of iNK cells to mNK cells due to roles in the expression of the BM egress receptor, S1P5 and Ly49 receptors, respectively (Gordon *et al.* 2012; Jenne *et al.* 2009). mNK cells also acquire functional competence in cytotoxicity and IFNγ production and egress from the BM.

5.1.1.2 Development of NK-lineage cells in the periphery

Peripheral NK cells undergo a maturation program that is associated with an increase in their cytotoxic alongside a reduction in their proliferative capacity. This maturation process can be divided into four stages dependent on the expression of CD11b and CD27: NK cells progress from $CD11b^-$ $CD27^-$→$CD11b^-$ $CD27^+$→$CD11b^+$ $CD27^+$→$CD11b^+$ $CD27^-$. $CD11b^+$ $CD27^-$ NK cells represent the most cytotoxic and differentiated NK cell subset in mice under steady state conditions. However, $CD11b^+$ $CD27^+$ NK cells have a greater potential for cytokine production compared to $CD11b^+$ $CD27^-$ NK cells. Thus, mNK subsets in the periphery likely perform distinct immunological roles but also represent sequential stages of NK cell maturation. Aiolos, an Ikaros family member, is important for this process as Aiolos-deficient mice present with a reduced number of $CD11b^+$ $CD27^-$ NK cells and increased numbers of $CD11b^-$ $CD27^+$ and $CD11b^+$ $CD27^+$ NK cells. Irf2 is equally required for peripheral NK maturation as its deletion results in reduced $CD11b^+$ $CD27^-$ NK cells and an overall reduction in peripheral NK cell number without a change

in bone marrow NK lineage cells (Chiossone *et al.* 2009b; Holmes *et al.* 2014; Lohoff *et al.* 2000; Taki *et al.* 2005). Although an in-depth discussion relating to the formation of memory NK cells is beyond the scope of this thesis, memory NK cells are briefly discussed below.

NK cells are traditionally considered to be a part of the innate immune system. However, NK cells with memory cell-like features have been detected following cytokine stimulation of NK cells with IL-12 and IL-18 as well as following mouse cytomegalovirus virus (MCMV) infection (Dokun *et al.* 2001; Keppel *et al.* 2013). Thus, these memory-like NK cells could be considered the final stage of NK maturation. However, it is unclear if memory NK cells form as part of linear developmental pathway or arise from the peripheral mNK pool that includes cells at multiple stages of maturation, as result of the stimulatory milieu. It is likely that the latter is closer to the truth as two NK subsets with inherently different potentials of becoming memory cells are observed following infection with MCMV; killer cell lectin-like receptor G1 (KLRG1)^{lo} NK cells appeared to have a greater probability of becoming memory NK cells compared to their KLRG1^{hi} counterparts (Kamimura & Lanier 2015). In agreement with this finding, expression of RAG enzymes in developing NK cells has been found to be associated with lower peripheral expression of KLRG1 and consequently, increased potential of these cells to acquire a memory phenotype (Karo *et al.* 2014).

5.1.1.3 NK cell education

The expression of multiple activating receptors on NK cells that bind self-ligands raises the possibility of autoimmunity unless balanced by inhibitory signals. Thus, tolerance to self-molecules is required, and achieved by expression of inhibitory receptors that recognise self MHCI and restrain NK cell effector function. This recognition of self MHCI via inhibitory receptors is also required for the acquisition of functional effector NK cells. The mechanism by which NK cells gain functional competence as well as self-tolerance is known as NK cell education and numerous models have been hypothesised to explain the process (Boudreau *et al.* 2018). These models are briefly discussed below.

One of the models known as the “disarming model” suggests that NK cells are inherently responsive to self-ligands and become tolerant following acquisition of self MHCI binding inhibitory receptors. NK cells that fail to acquire these inhibitory receptors become hyporesponsive due to chronic stimulation by normal cells (Gasser & Raulet 2006). Another model known as the “arming model” suggests the opposite of the disarming model as it states that NK cells are initially hyporesponsive and become responsive or ‘armed’ following engagement of inhibitory receptors with self MHCI during development that leads to transmission of undefined activating signals (Kim *et al.* 2005). Additionally, another model known as the tuning model suggests an altogether different mechanism wherein the NK cell response is tuned by the number of self MHCI binding inhibitory receptors and affinity of these receptors for their cognate ligands (Brodin *et al.* 2009).

Thus, NK cell education is likely to be a quantitative process where functional capacity is determined the strength of the activating and inhibitory signals. NK cells in which activating signals are strongly opposed by inhibitory signals are maintained in a high responsive state whilst NK cells in which inhibitory signals are outweighed by activating signals are kept in a hyporesponsive state due to chronic stimulation. Unlike B and T lymphocyte development, potentially autoreactive NK cells are not clonally deleted in the bone marrow or the periphery but maintained in their hyporesponsive state at least under steady state conditions (Orr & Lanier 2010).

5.1.2 NK cell activation

The activation of NK cells and their effector function depends upon the integration of signals from multiple inhibitory and activating receptors. Healthy cells express MHCI molecules on their surface that act as ligands for the inhibitory receptors of NK cells and contribute to their self-tolerance. However, virally-infected cells as well as tumour cells may lose expression of MHCI thereby reducing inhibitory signals delivered to NK cells through their self MHCI recognising inhibitory receptors. Concurrently, cellular stress associated with these scenarios due to the DNA

damage response, senescence program or tumour suppressor gene activation can result in the surface expression of ligands binding the activating receptors of NK cells. Consequently, absence of inhibitory signalling alongside signalling through activating receptors shifts the balance of NK cells towards activation and elimination of compromised cells through direct cytotoxicity or secretion of cytokines and chemokines (Paul & Lal 2017).

5.1.2.1 Activating receptors

Full NK cell activation is only achieved following loss of self MHCI derived inhibitory signalling and recognition of stress induced molecules on target cells by activating NK receptors. A majority of the NK activating receptors contain an ITAM within their cytoplasmic regions. Ligand engagement of these ITAM bearing receptors causes phosphorylation of the tyrosine residue within the motif by tyrosine kinases of the Src family such as Lck and Fyn which in turn causes recruitment and activation of the tyrosine kinase Syk and Zap70. The succeeding downstream signalling pathway leads to an activation of MAP kinases and ERKs which cause an increase in intracellular calcium. This increase enables release of cytotoxic granules containing perforin and granzymes and also elevates transcription of cytokines and chemokines such as IL-5, IL-10, IL-13, IFNγ, TNFα, GM-CSF, MIP-1α, MIP-1β, IL-8, and RANTES (Martinez-Lostao *et al.* 2015; Paul & Lal 2017). An important NK activating receptor is the natural-killer group 2, member D (NKG2D) which binds a range of highly polymorphic ligands that are structural homologs of MHCI molecules. These ligands are expressed at low levels on healthy tissue but can be upregulated on tumours from a range of different tissues (Jamieson *et al.* 2002; Takada *et al.* 2008). NKp46 also known as CD335 is another important activating receptor expressed by mouse NK cells. Although NKp46 does not contain an ITAM within its cytoplasmic region, it associates with ITAM bearing adaptor proteins in order to transduce its activation signal. Its importance in NK activation is highlighted by its ability to recognise a wide range of ligands on target cells ranging from bacterial, parasite and viral proteins to molecules expressed by tumours and other cells of the host (Kruse *et al.* 2014). CD226 is a crucial NK activating receptor for induction of the anti-tumour response of NK cells. The ligands of this receptor, CD155 and CD112 are expressed on normal tissue but are

upregulated in response to cellular stress particularly on tumours of epithelial origin such as melanomas. The engagement of CD226 with its ligands causes phosphorylation and inactivation of the transcription factor FOXO1, which negatively regulates NK cell effector function (Du *et al.* 2018). The expression of multiple activating receptors suggests that cytokine and chemokine release from NK cells as well as NK mediated cytotoxicity may require synergistic stimulation of a range of these receptors in order to surpass given activation threshold (Bryceson *et al.* 2006).

5.1.2.2 Inhibitory receptors

The majority of NK inhibitory receptors signal through ITIMs present in their cytoplasmic regions. Following binding of a ligand, ITIMs undergo phosphorylation of their tyrosine residue which in turn results in recruitment of phosphatases such as Src homology-containing tyrosine phosphatase 1 (Shp-1), Shp-2, and lipid phosphatase SH2 domain-containing inositol-5-phosphatase (Ship). These phosphatases mediate their inhibitory function through multiple pathways including dephosphorylation of signalling components such as Lck, Fyn, Syk, Zap70 due to their importance in pathways associated with activating NK receptors. Ly-49 receptors comprise one of the largest families of mouse NK inhibitory receptors. Members of this family belong to the type II glycoprotein of C-type lectin-like superfamily and contain a carboxy-terminal lectin domain also known as NK domain (NKD). Recognition of self MHCI by Ly-49 receptors is mediated through the NKD in an MHC-peptide independent manner. The Ly-49 receptor family is highly polymorphic resulting in heterogenous expression in the various inbred mouse strains. (Dam *et al.* 2003; Paul & Lal 2017; Wong *et al.* 1991). NK cells also possess other ITIM bearing inhibitory receptors such as CD94-natural-killer group 2, member A (NKG2A) that recognise non-classical MHC molecules on healthy cells to prevent their killing (Vance *et al.* 1998). ITIM bearing KLRG1 is also an important NK inhibitory receptor that functions by binding three members of the mouse classical cadherin family. Importantly, KLRG1 expression on NK cells is upregulated following their viral infection which suggests that this receptor acts to increase the activation threshold of 'antigen experienced' NK cells to limit excessive damage to healthy tissue expressing its ligands, and possibly even terminate the NK cell response (Ito *et al.* 2006). Thus, NK cells

possess multiple inhibitory receptors that bind a range of ligands to guard against inappropriate NK cell activation.

5.2 Aims

We identified the expression of FCRL6 via qRT-PCR in mature NK cells from the bone marrow and spleen. The expression of FCRL6 in peripheral mature NK cells correlates with their differentiation as the highest expression is detected in the most mature and cytotoxic NK subset. Although we were unable to analyse the expression of FCRL6 in developing NK cells, we hypothesised that it is conceivable that expression of the receptor precedes the mature NK cell stage in the bone marrow. Thus, we aimed to investigate the consequence of FCRL6 deletion on NK cell development and maturation by analysing developing and mature NK cell populations in *Fcrl6*$^{-/-}$ mice. Additionally, we also examined reconstitution of mature NK cells derived from *Fcrl6*-deficient bone marrow in competitive mixed bone marrow chimeras to identify the impact of cell intrinsic FCRL6 deletion on the bone marrow output of NK cells and their maturation. The expression of FCRL6 in mature NK cells suggests that it may also play a role in regulating NK cell effector function. Accordingly, we investigated the response of *Fcrl6*$^{-/-}$ and NK cell conditional *Fcrl6*$^{-/-}$ NK cells in a chronic retroviral infection model as well as in a melanoma model where NK cell-mediated immunity has been demonstrated to play an important role, thereby revealing potential cell extrinsic or intrinsic FCRL6-mediated mechanisms that could affect *in vivo* NK cell function.

5.3 Results

5.3.1 Analysis of NK cell development in the absence of *Fcrl6* using competitive mixed bone marrow chimeras and in *Fcrl6*$^{-/-}$ mice

We analysed the number and percentage of developing and mature NK cell populations in the bone marrow and spleen under steady-state conditions via flow cytometry. The analysis included NK cell precursors, immature NK cells and mature NK cells from the bone marrow in addition to mature NK cells from the spleen. The number and percentage of all analysed populations remained unchanged in *Fcrl6*$^{-/-}$ mice compared to their WT counterparts (Figure 21a and 21b).

We next examined the maturation of NK cells in the bone marrow and spleen by analysing the surface expression of CD11b and CD27 on mature NK cells from these organs. The percentage of CD11b^{-} CD27^{+} NK cells in the bone marrow of *Fcrl6*$^{-/-}$ mice was marginally higher than that observed in WT mice. Consequently, the percentage of more differentiated CD11b^{+} CD27^{+} and CD11b^{+} CD27^{-} NK cells in the bone marrow of *Fcrl6*$^{-/-}$ mice was lower compared to WT mice (Figure 21c). The maturation of NK cells in the periphery was also slightly affected in the absence of *Fcrl6.* We detected a lower percentage of CD11b^{-} CD27^{+} and CD11b^{+} CD27^{+} NK cells in the spleen of *Fcrl6*$^{-/-}$ mice compared to WT mice. However, the percentage of the most mature and cytotoxic NK subset in the spleen, CD11b^{+} CD27^{-} NK cells remained unchanged in *Fcrl6*$^{-/-}$ mice compared to their WT counterparts (Figure 21d).

We decided to further investigate maturation of NK cells using mixed bone marrow chimeras. CD45.2^{+} *Fcrl6*$^{-/-}$ or WT bone marrow cells were mixed with CD45.1^{+} WT bone marrow cells and injected into myeloablated CD45.1/2^{+} WT recipient mice to detect developmental abnormalities arising due to the absence of *Fcrl6*. The mixed bone marrow chimeras were created at a ratio of 55:45% with respect to CD45.2^{+} and CD45.1^{+} cells. *Fcrl6*-deficient bone marrow performed similarly to WT bone marrow at reconstituting NK cells in the spleen. We also did not observe differences in the maturation of *Fcrl6*$^{-/-}$ bone marrow-derived NK cells in the spleen compared to WT-derived NK cells (Figure 21e). We concluded following evaluation of cell surface markers in

mixed bone marrow chimeras and *Fcrl6*$^{-/-}$ mice that development of NK cells from NK cell precursors to fully differentiated CD11b^{+} CD27^{-} NK cells remains broadly unaffected by the absence of *Fcrl6* (Figure 24).

Figure 21: There are minor differences in NK maturation in the bone marrow and spleen in the absence of *Fcrl6*.

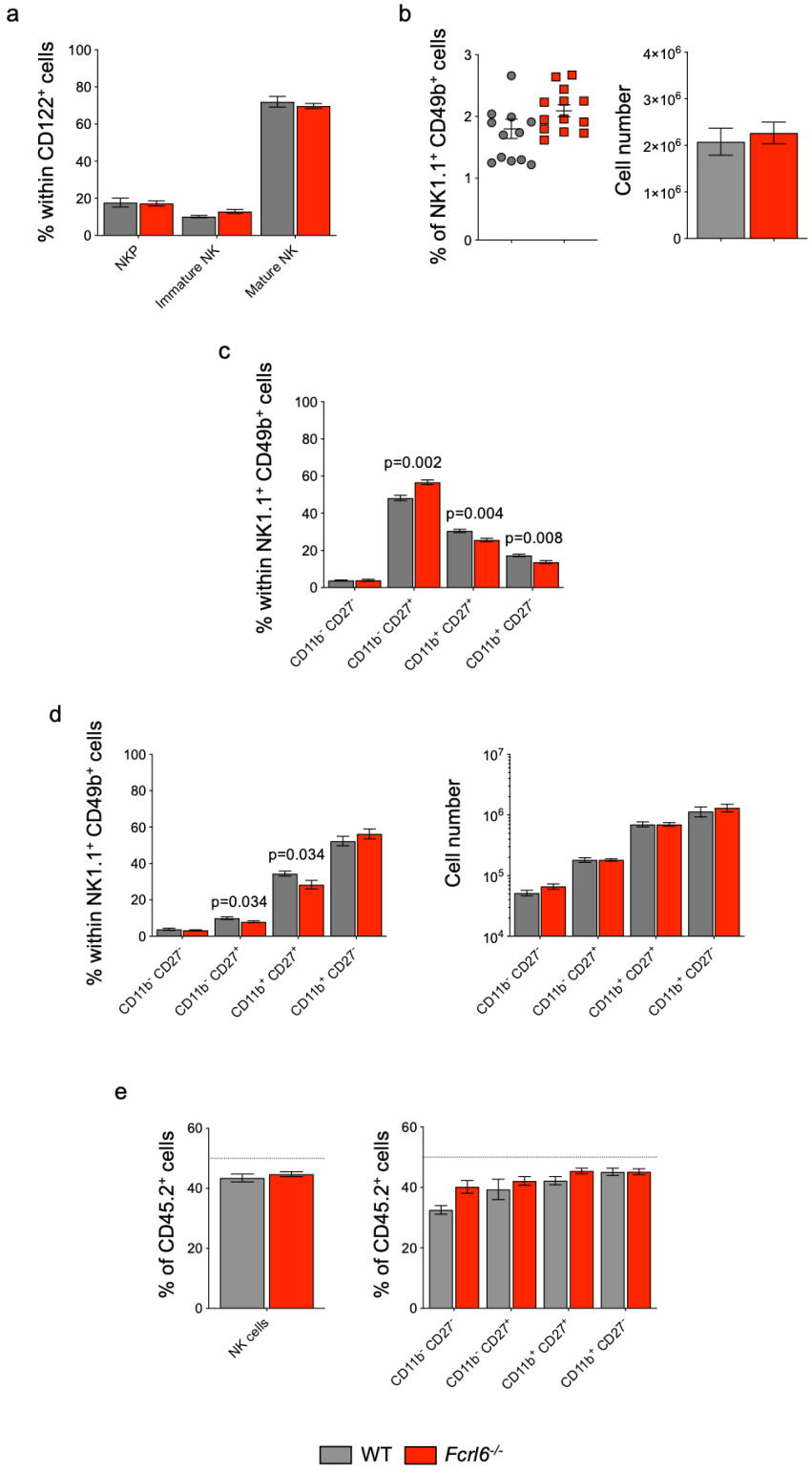

(a) Percentage of developing and mature NK cells in the bone marrow of *Fcrl6*$^{-/-}$ and WT mice under steady state conditions. Bars represent mean ± SEM of 5 biological repeats per genotype

(b) Number and percentage of mature NK cells in the spleen of *Fcrl6*$^{-/-}$ and WT mice under steady state conditions. Bars and symbols represent mean ± SEM of 13 biological repeats per genotype from 3 independent experiments. (c) Percentage of maturing NK cells in the bone marrow of *Fcrl6*$^{-/-}$ and WT mice under steady state conditions. Bars represent mean ± SEM of 5 biological repeats per genotype. (d) Percentage and number of maturing NK cells in the spleen of *Fcrl6*$^{-/-}$ and WT mice under steady state conditions. Bars represent mean ± SEM of 13 biological repeats per genotype from 3 independent experiments. All populations were analysed via flow cytometry and gated as depicted in Figure 24. (e) Relative proportions of *Fcrl6*$^{-/-}$ and WT derived mature NK cells and their maturation from mixed bone marrow chimeras. Bone marrow from CD45.2^{+} *Fcrl6*$^{-/-}$ and WT mice was mixed with bone marrow from CD45.1^{+} WT mice (55% CD45.2^{+} cells) and injected intravenously into myeloablated CD45.1/2^{+} WT recipient mice. Reconstitution was analysed 8 weeks later via flow cytometry. Bars represent mean ± SEM of 4 (WT) and 14 (*Fcrl6*$^{-/-}$) biological replicates. Cell populations were gated as depicted in Figure 24 with additional gating for CD45.1 and CD45.2. Dotted line indicates injected percentage of CD45.2^{+} cells. NK, natural killer; NKP, natural killer precursor.

5.3.2 Analysis of NK cell development in NK conditional *Fcrl6*$^{-/-}$ mice

Next, we created NK conditional *Fcrl6*$^{-/-}$ mice to investigate NK cell-specific function of FCRL6 We generated the NK conditional *Fcrl6*$^{-/-}$ strain by crossing *Fcrl6*$^{tm1c(KOMP)Wtsi}$ mice with C57BL/6-*Ncr1*$^{tm1.1(icre)Viv}$ mice. The product of *Ncr1,* NKP46 (CD335) is expressed exclusively in NK-lineage cells following expression of CD122 at the NK cell precursor stage but prior to the expression of CD49b at the mature NK cell stage (Narni-Mancinelli *et al.* 2011). Thus, *Fcrl6* should be deleted in NK conditional *Fcrl6*$^{-/-}$ mice at the immature NK cell stage in the bone marrow. Despite the absence of major NK developmental differences in *Fcrl6*$^{-/-}$ mice, we decided to investigate if there are differences in NK development due to the conditional nature of *Fcrl6* deletion in these mice. We analysed the number and percentage of developing and mature NK cell populations in the bone marrow and spleen under steady-state conditions via flow cytometry. As with *Fcrl6*$^{-/-}$ mice, the analysis included NK cell precursors, immature NK cells and mature NK cells from the bone marrow in addition to mature NK cells from the spleen. The percentage of NK cell precursors, immature NK cells and mature NK cells in the bone marrow remained unchanged in NK conditional *Fcrl6*$^{-/-}$ mice compared to their litter mate WT counterparts (Figure 22a). However, the number and percentage of mature NK cells in the spleen was lower in NK conditional *Fcrl6*$^{-/-}$ mice compared to litter mate WT mice (Figure 22b). We then examined the maturation of NK cells in the bone marrow and spleen and found that it remained unchanged in NK conditional *Fcrl6*$^{-/-}$ mice compared to litter mate WT mice (Figure 22c and 22d). We also analysed the expression of select surface activation and inhibitory markers on NK cells from NK conditional *Fcrl6*$^{-/-}$ and litter mate WT mice under steady state conditions. The percentage of KLRG1^{+}, CD226^{+} and Lag-3^{+} NK cells remained unchanged in NK conditional *Fcrl6*$^{-/-}$ mice compared to litter mate WT mice. Additionally, we did not find differences in IFNγ or GzmB levels in NK cells from NK conditional *Fcrl6*$^{-/-}$ and litter mate WT mice following *ex vivo* restimulation of splenocytes obtained under steady state conditions (Figure 23a and 23b). We determined following evaluation of cell surface markers that conditional absence of *Fcrl6* in NK cells does not affect their development or maturation in the bone marrow as well as peripheral maturation in the spleen. However, NK cell specific deletion of *Fcrl6* does appear to cause a reduction in the percentage and number of NK cells in the spleen by an as of yet unknown mechanism (Figure 24).

Figure 22: NK conditional *Fcrl6*$^{-/-}$ mice have a reduction in the percentage and number of NK cells in the spleen.

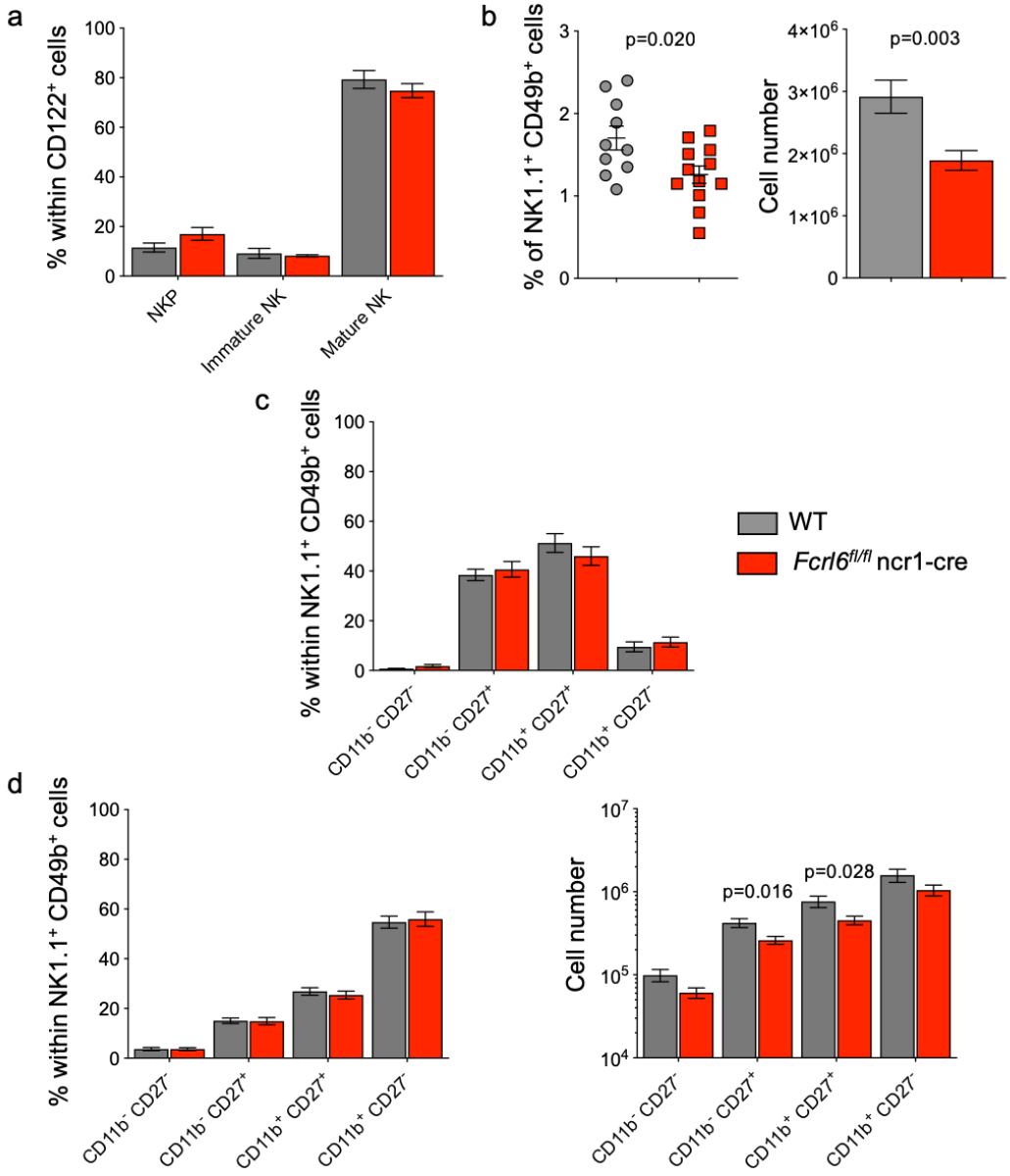

(a) Percentage of developing and mature NK cells in the bone marrow of unchallenged *Fcrl6* $^{fl/fl}$ ncr1-cre^{+} and WT mice. Bars represent mean ± SEM of 5 biological repeats per genotype (b) Number and percentage of mature NK cells in the spleen of unchallenged NK conditional *Fcrl6*$^{-/-}$ and WT mice. Bars and symbols represent mean ± SEM of 10 (WT) and 12 (*Fcrl6* $^{fl/fl}$ ncr1-cre^{+}) biological repeats. (c) Percentage of maturing NK cells in the bone marrow of unchallenged *Fcrl6* $^{fl/fl}$ ncr1-cre^{+} and WT mice. Bars represent mean ± SEM of 5 biological repeats per genotype (d)

Percentage and number of maturing NK cells in the spleen of unchallenged NK conditional *Fcrl6*$^{-/-}$ and WT mice. Bars represent mean ± SEM of 10 (WT) and 12 (*Fcrl6* $^{fl/fl}$ ncr1-cre^{+}) biological repeats. All populations were analysed via flow cytometry and gated as depicted in Figure 24. NK, natural killer; NKP, natural killer precursor.

Figure 23: NK conditional *Fcrl6*$^{-/-}$ mice show normal surface activation and inhibition marker expression.

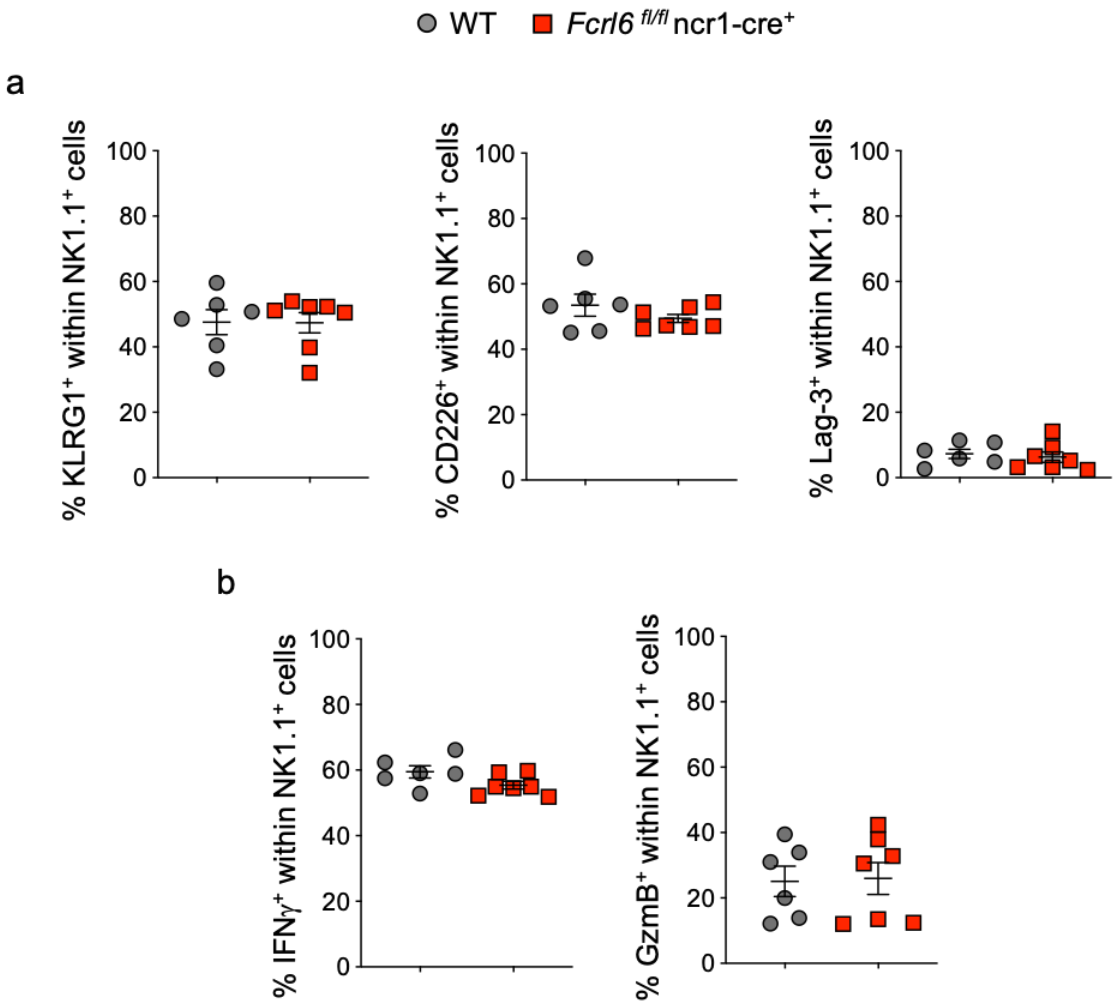

(a) Percentage of KLRG1^{+}, CD226^{+}, Lag-3^{+} NK cells in the spleens of unchallenged WT and *Fcrl6* $^{fl/fl}$ ncr1-cre^{+} mice. (b) Percentage of IFNg^{+} and GzmB^{+} NK cells following *ex vivo* restimulation of splenocytes from unchallenged WT and NK conditional *Fcrl6*$^{-/-}$. Symbols show mean ± SEM of 6 (WT) and 7 (*Fcrl6* $^{fl/fl}$ ncr1-cre^{+}) biological replicates per genotype.

Figure 24: *Fcrl6*$^{-/-}$ mice show slight differences in NK cell maturation whilst NK conditional *Fcrl6*$^{-/-}$ show a reduction in the percentage and number of mature NK cells.

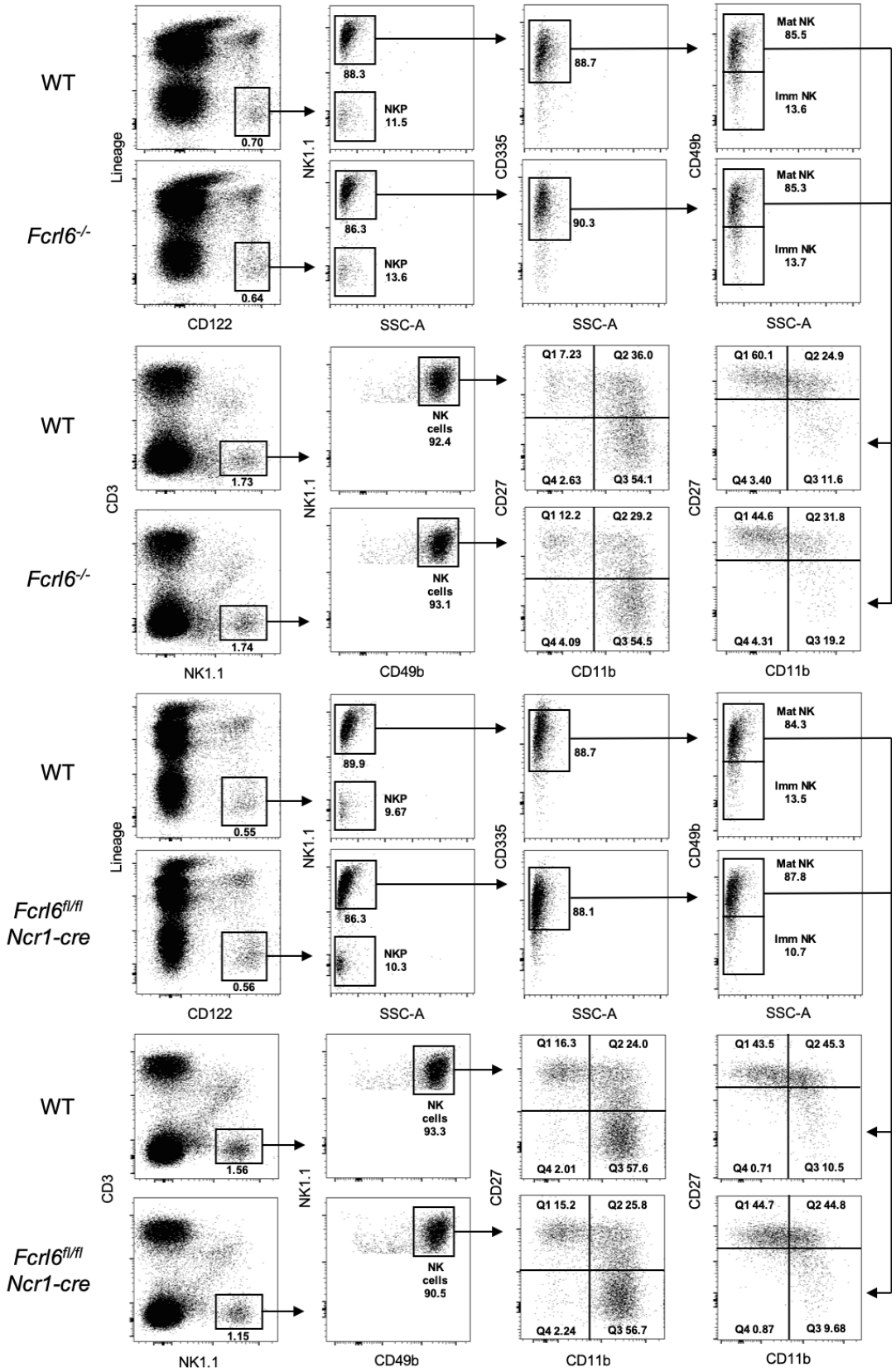

Flow cytometric gating strategy used for analysis and sorting of developing and mature NK cell populations in Figures 7, 22 and 23. Names are indicated by text next to the gates whilst numbers represent population percentage within that plot. Gating strategies were as follows: bone marrow – Imm NK, immature NK ($CD122^+$ $NK1.1^+$ $CD335^+$ $CD49b^-$) Mat NK, mature natural killer ($CD122^+$ $NK1.1^+$ $CD335^+$ $CD49b^+$) and NKP, natural killer precursor ($CD122^+$ $NK1.1^-$); spleen – NK cells ($NK1.1^+$ $CD49b^+$). CD11b and CD27 were used to delineate NK maturation in the bone marrow and spleen in the following order: $CD11b^-$ $CD27^-$ → $CD11b^-$ $CD27^+$ → $CD11b^+$ $CD27^+$ → $CD11b^+$ $CD27^-$.

5.3.3 Analysis of viral load during the initial phase of FV infection in *Fcrl6*$^{-/-}$ mice

We focused on identifying a difference during the acute phase of FV infection as a result of the early immune response to the virus. This was of particular interest due to the expression of *Fcrl6* in NK cells and their protective role during the initial phase of the infection (Littwitz *et al.* 2013). We infected *Fcrl6*$^{-/-}$ and WT mice intravenously with FV and analysed the viral load in the bone marrow and spleen at day 7 following infection, which represents the peak of infection in C57BL/6 mice (Marques *et al.* 2008). During the acute phase of FV infection, there is an expansion of erythroid precursor (nucleated Ter119^{+}) cells, which are the primary targets of FV (Hasenkrug *et al.* 1998). We did not find differences in the percentage of Ter119^{+} cells in the spleen of *Fcrl6*$^{-/-}$ and WT mice at day 7 following infection (Figure 25b). Thereafter, we analysed the percentage FV-infected (glyco-Gag^{+}) Ter119^{+} cells in the bone marrow and spleen at this time point. We did not observe a difference in the percentage of glyco-Gag^{+} Ter119^{+} cells in the bone marrow of *Fcrl6*$^{-/-}$ mice compared to WT mice (Figure 25a and 25c). However, the percentage of glyco-Gag^{+} Ter119^{+} cells was lower in the spleen of *Fcrl6*$^{-/-}$ mice compared to their WT counterparts (Figure 25a and 25d). Similarly, splenocytes from *Fcrl6*$^{-/-}$ mice at day 7 following infection had lower FV *env* DNA copy numbers compared to WT mice (Figure 25e). Thus, we determined that absence of FCRL6 increases the natural resistance of C57BL/6 mice to FV infection possibly due to an augmented NK cell response.

Figure 25: *Fcrl6*$^{-/-}$ mice show reduced infection during the initial phase of Friend virus infection.

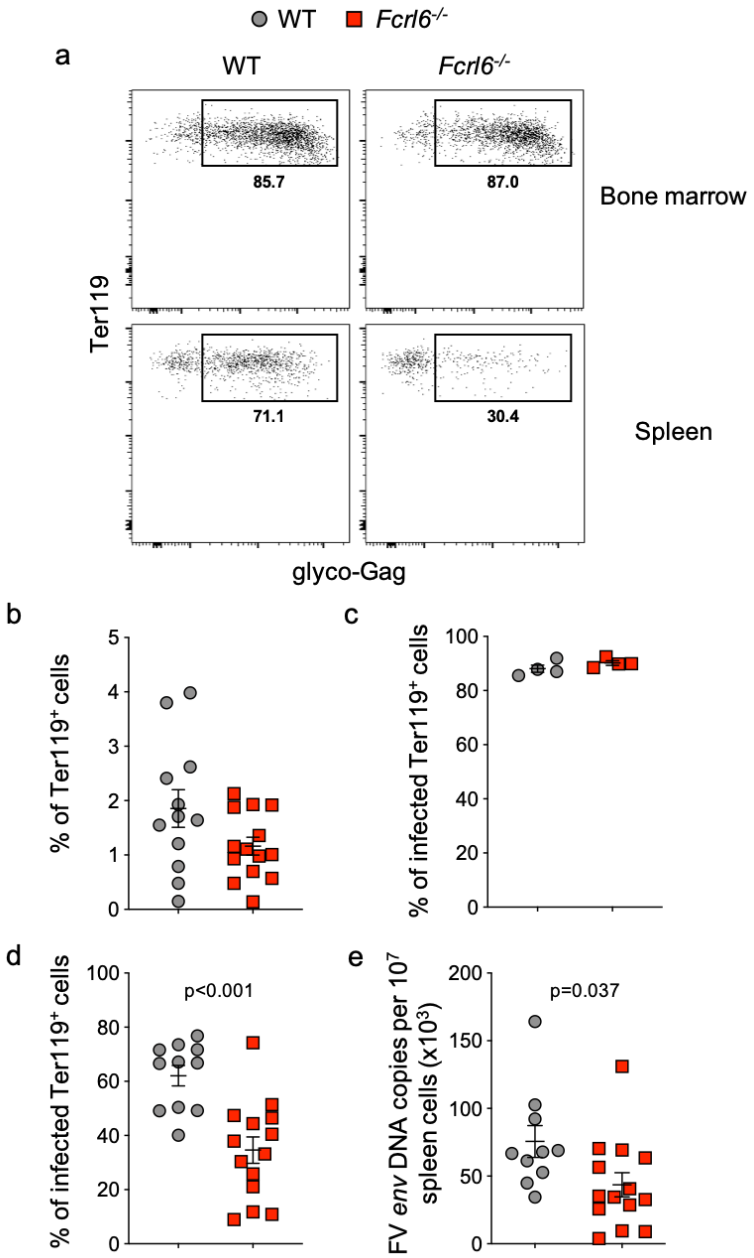

(a) Representative infection in the bone marrow and spleen of *Fcrl6*$^{-/-}$ and WT mice at day 7 following FV infection. (b) Percentage of Ter119^{+} cells in the spleen at day 7 following FV infection. (c) Percentage of infected Ter119^{+} cells in the bone marrow at day 7 following FV infection. (d) Percentage of infected Ter119^{+} cells in the spleen at day 7 following FV infection. (e) Copies of FV envelope DNA in the spleen at day 7 following FV infection. Symbols show mean ± SEM of 4-11 (WT) and 4-14 (*Fcrl6*$^{-/-}$) biological repeats per genotype from 3 independent experiments.

Fcrl6$^{-/-}$ or WT mice were infected with 1000 spleen focus-forming units of Friend virus by intravenous injection. Infected Ter119^{+} cells were gated as B220^{-} Ter119^{+} glyco-Gag^{+}.

5.3.4 NK cell response in the absence of FCRL6

5.3.4.1 Analysis of the NK cell response to B16 melanoma cells in Fcrl6$^{-/-}$ mice

In addition to being critical for host defence against viral infection, NK cells also play an important role in mediating anti-tumour immunity. Consequently, we used the B16 melanoma model where NK depletion augments B16 lung metastasis to further investigate the function of FCRL6 in NK cells (Takeda *et al.* 2011). We first injected *Fcrl6*$^{-/-}$ and WT mice intravenously with B16 melanoma cells and counted the number of lung colonies at day 14 following inoculation. We found that *Fcrl6*$^{-/-}$ mice developed a lower number of colonies on their lungs at this time point compared to WT mice (Figure 26a and 26b).

Next, we characterised the NK cell response in the lungs of these mice to identify differences resulting from *Fcrl6* deletion that could account for the reduced number of lung colonies detected in *Fcrl6*$^{-/-}$ mice. However, we did not find a difference in the percentage of NK cells in the lungs of *Fcrl6*$^{-/-}$ and WT mice (Figure 26c). Similarly, maturation of lung NK cells did not show a difference between *Fcrl6*$^{-/-}$ and WT mice (Figure 26d). Thereafter, we analysed the activation of lung NK cells from both genotypes at this time point. We did not find a difference in the percentage of CD226^{+} and KLRG1^{+} NK cells in the lungs of *Fcrl6*$^{-/-}$ and WT mice (Figure 26e). We also did not find a difference in the percentage of IFNγ^{+} and GzmB^{+} NK cells following *ex vivo* restimulation of lung cell suspensions from B16 inoculated *Fcrl6*$^{-/-}$ and WT mice (Figure 26f). These results indicate that NK cell function is not affected by the absence of *Fcrl6* in this tumour model. However, it is possible that the effects of FCRL6 deletion on NK cell expansion and activation may be masked by compensatory mechanisms due to the germline deletion of FCRL6 in *Fcrl6*$^{-/-}$ mice. Thus, we next investigated the NK cell response following FV infection in NK conditional *Fcrl6*$^{-/-}$ mice.

Figure 26: *Fcrl6*$^{-/-}$ mice show reduced lung colony formation in a model of multiple pulmonary melanoma metastases

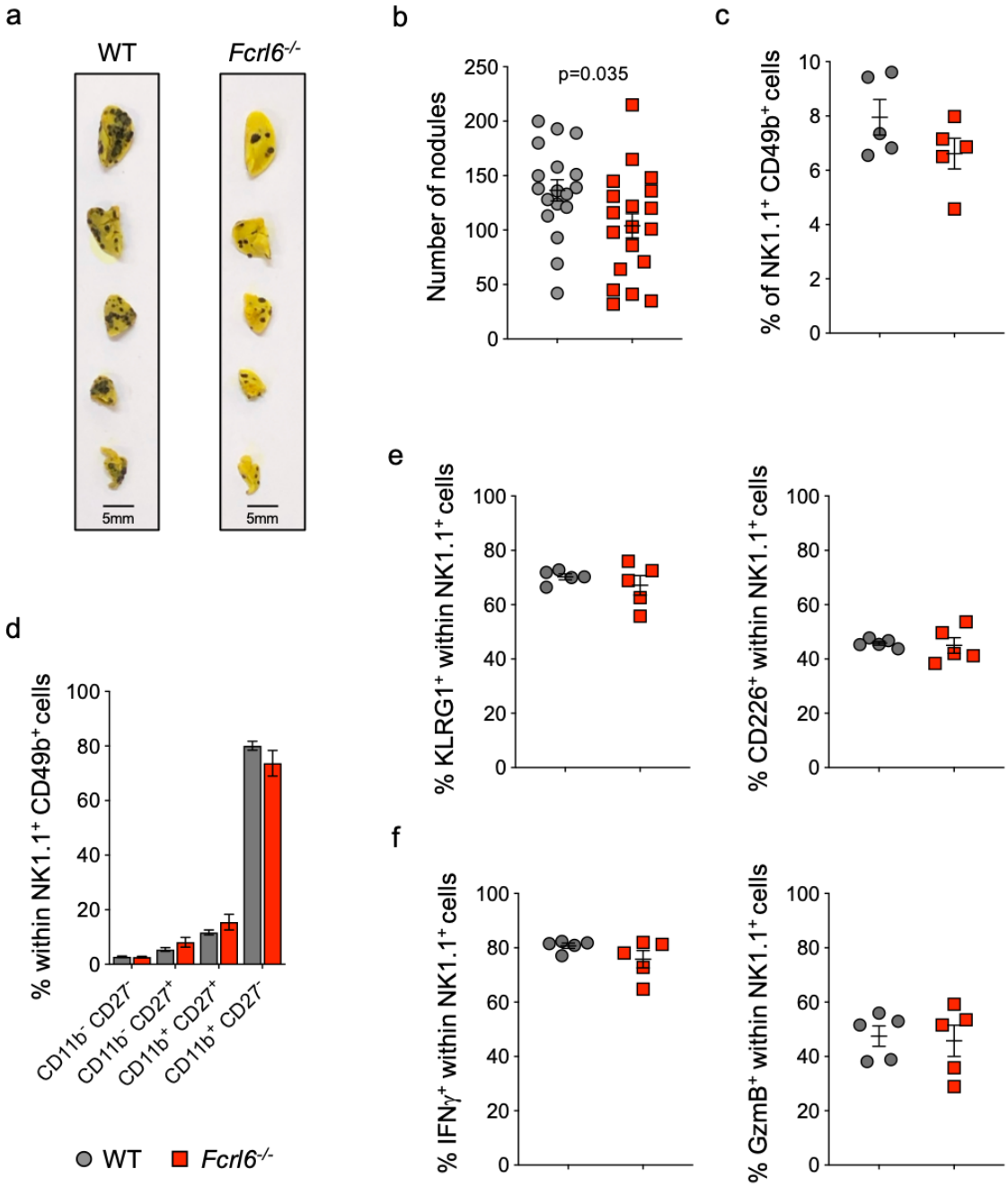

(a) Lung colony formation in *Fcrl6*$^{-/-}$ and WT mice at day 14 following B16F0 challenge. (b) Number of pulmonary nodules at day 14 following B16F0 challenge. (c) Percentage of NK cells in the lung at day 14 following B16F0 challenge (d) Maturation of NK cells in the lung at day 14 following B16F0 challenge (e) Percentage of KLRG1^{+} and CD226^{+} NK cells in the lung at day 14 following B16F0 challenge. (f) Percentage of IFNg^{+} and GzmB^{+} NK cells following *ex vivo*

restimulation of lung cell suspension at day 14 following B16F0 challenge. *Fcrl6*$^{-/-}$ or WT mice were challenged with 2.0x10^5 cells by intravenous injection following which lungs were excised 14 days later to analyse nodule development. Symbols show mean ± SEM of 18 (WT) and 19 (*Fcrl6*$^{-/-}$) biological replicates from 4 independent experiments.

5.3.4.2 Analysis of the NK cell response to FV in NK conditional Fcrl6$^{-/-}$ mice

We were interested in examining how the conditional absence of *Fcrl6* in NK cells alongside the reduced percentage and number of these cells in NK conditional *Fcrl6*$^{-/-}$ mice would affect the early immune response to FV. We infected NK conditional *Fcrl6*$^{-/-}$ and litter mate WT mice intravenously with FV and analysed the viral load at the peak of infection. As observed in *Fcrl6*$^{-/-}$ mice, we did not see a difference in the percentage of Ter119^{+} cells in the spleen of NK conditional *Fcrl6*$^{-/-}$ mice at day 7 following FV infection compared to litter mate WT mice (Figure 27b). Similarly, we did not detect a difference in the percentage of glyco-Gag^{+} Ter119^{+} cells in the bone marrow of NK conditional *Fcrl6*$^{-/-}$ mice compared to litter mate WT mice at this time point. However, unlike *Fcrl6*$^{-/-}$ mice we did not observe a difference in the percentage of glyco-Gag^{+} Ter119^{+} cells in the spleen of NK conditional *Fcrl6*$^{-/-}$ mice at day 7 following infection compared to litter mate WT mice (Figure 27a and 27c).

We also characterised NK cells at this time point and found they were expanded in terms of percentage and number following FV infection in the spleen of both genotypes compared to the steady state. The lower percentage of NK cells observed in the spleen of NK conditional *Fcrl6*$^{-/-}$ mice compared to litter mate WT mice during steady state conditions was maintained at day 7 following FV infection. However, an identical difference in the number of NK cells in the spleen of NK conditional *Fcrl6*$^{-/-}$ mice was not apparent following FV infection at this timepoint (Figure 27d). Maturation of NK cells in the spleen at day 7 following FV infection appeared similar between NK conditional *Fcrl6*$^{-/-}$ mice and litter mate WT mice (Figure 27e). We did not detect a difference in the activation of splenic NK cells at this time point following FV infection of NK conditional *Fcrl6*$^{-/-}$ and litter mate WT mice as measured by CD69 and KLRG1 expression (Figure 27f). There were also no differences in IFNγ and GzmB levels in NK cells following *ex vivo* restimulation of splenocytes from FV infected NK conditional *Fcrl6*$^{-/-}$ and litter mate WT mice (Figure 27g). The data obtained following FV infection of NK conditional *Fcrl6*$^{-/-}$ mice helped us determine that the increased natural resistance to FV in *Fcrl6*$^{-/-}$ mice was not exclusively linked to NK cell function. Additionally, we also concluded that conditional absence of *Fcrl6* in NK cells does not appear to alter their response in this retroviral infection model.

Figure 27: NK conditional *Fcrl6*$^{-/-}$ mice do now show reduced infection during the early phase of Friend virus infection.

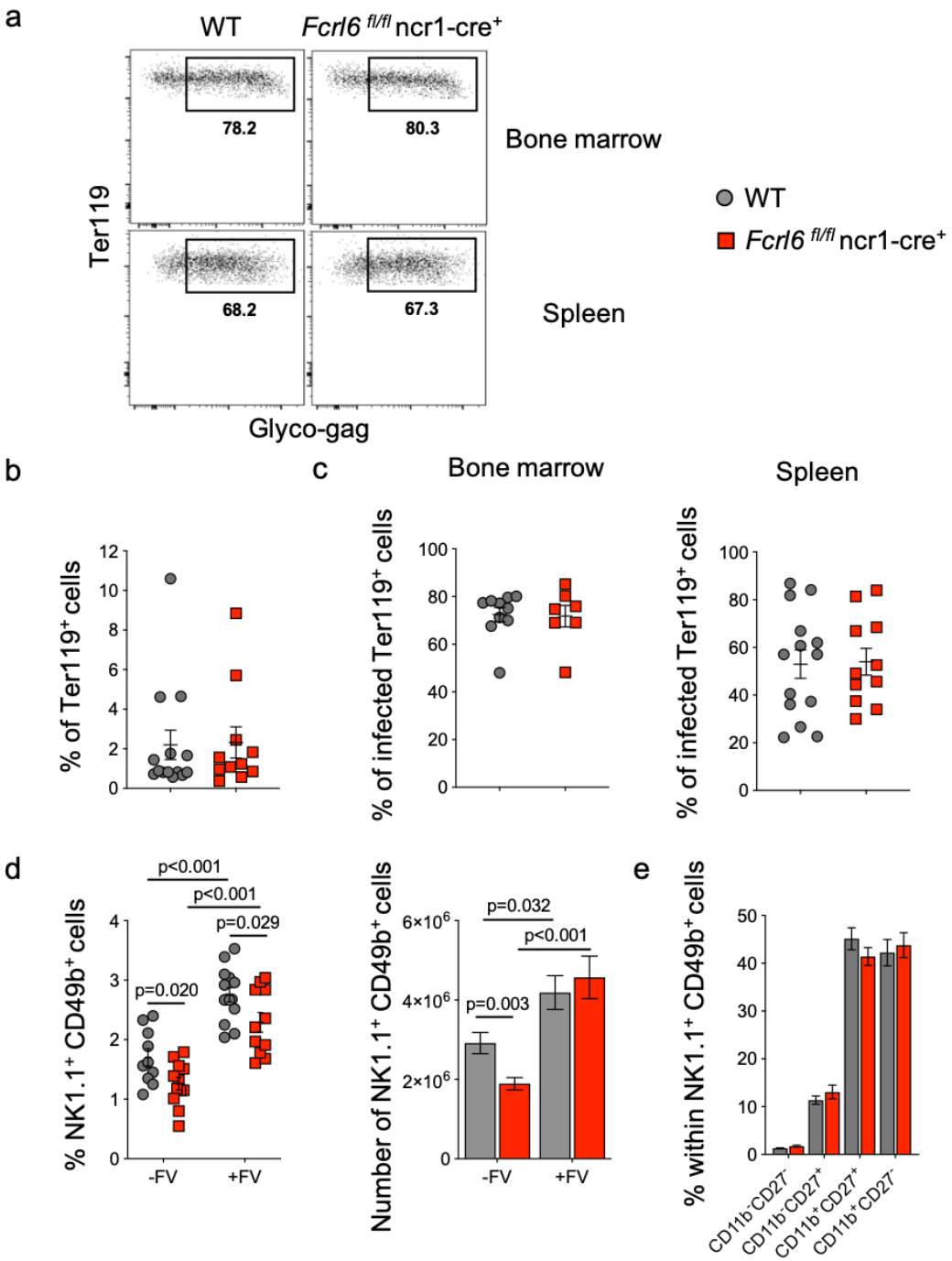

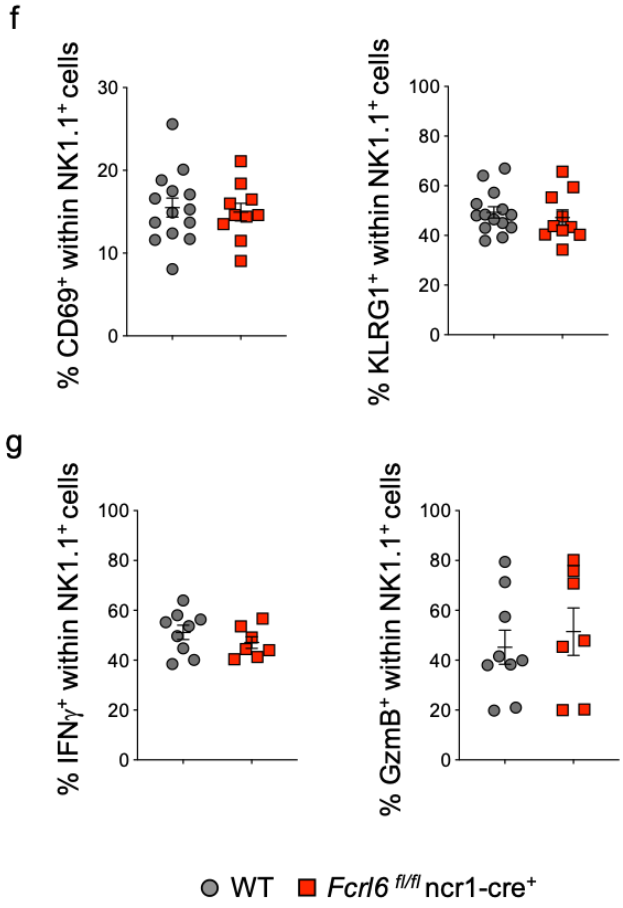

(a) Infected Ter119$^+$ cells in the bone marrow and spleen of *Fcrl6* $^{fl/fl}$ ncr1-cre$^+$ and WT mice at day 7 following FV infection. (b) Percentage of Ter119$^+$ cells in the spleen at day 7 following FV infection (c) Percentage of infected Ter119$^+$ cells in the bone marrow and spleen at day 7 following FV infection (d) Percentage and number of NK cells in the spleen at steady state and day 7 following FV infection. (e) Maturation of NK cells in the spleen at day 7 following FV infection (f) Percentage of CD69$^+$ and KLRG1$^+$ NK cells in the spleen at day 7 following FV infection (g) Percentage of IFNg$^+$ and GzmB$^+$ NK cells following *ex vivo* restimulation of splenocytes at day 7 following FV infection. *Fcrl6*$^{-/-}$ or WT mice were infected with 1000 spleen focus-forming units of FV by intravenous injection. Symbols and bars show mean ± SEM of 14 (WT) and 11 (*Fcrl6* $^{fl/fl}$ ncr1-cre$^+$) biological replicates per genotype from four independent experiments. Infected Ter119$^+$ cells were gated as B220$^-$ Ter119$^+$ glyco-Gag$^+$.

5.4 Discussion

Human FCRL6 expression is confined to $CD56^{dim}$ NK cells which represent the most differentiated NK cell subset in humans (Moretta 2010; Schreeder *et al.* 2008; Wilson *et al.* 2007b). The expression of *Fcrl6* in peripheral mature NK cells correlated with their differentiation as the highest expression was detected in $CD11b^{+}$ $CD27^{-}$ NK cells which represent the most differentiated NK cell subset in mice (Chiossone *et al.* 2009a). Thus, the expression of mouse FCRL6 in NK cells appears similar to that of its human counterpart. Despite being unable to analyse *Fcrl6* expression in developing NK cells in the bone marrow, we hypothesised that expression may occur during NK cell development in the bone marrow and examined developing NK cell populations in *Fcrl6*$^{-/-}$ and NK conditional *Fcrl6*$^{-/-}$ mice to identify differences arising due to the deletion of FCRL6. The expression of *Fcrl6* in peripheral mature NK cells suggests that the receptor may influence NK cell function. Accordingly, we investigated the response of *Fcrl6*$^{-/-}$ and NK cell conditional *Fcrl6*$^{-/-}$ NK cells in a chronic retroviral infection model as well as a melanoma model where NK cell-mediated immunity has been demonstrated to play an important role, thereby revealing potential cell extrinsic or intrinsic FCRL6-mediated mechanisms that could affect *in vivo* NK cell function.

5.4.1 FCRL6 and NK cell development

Firstly, we analysed developing and mature NK cell populations in the bone marrow of *Fcrl6*$^{-/-}$ mice and did not identify a difference in the percentage of NK cell precursors, immature NK cells and mature NK cells compared to WT mice. Similarly, we did not detect a difference in the number and percentage of mature NK cells in the spleen of *Fcrl6*$^{-/-}$ mice compared to WT mice. We next examined the surface expression of CD11b and CD27 on mature NK cells from the bone marrow to analyse their maturation. The proportion of $CD11b^{+}$ $CD27^{-}$ cells within the bone marrow mature NK cell pool from *Fcrl6*$^{-/-}$ mice was slightly reduced compared to WT mice. Consequently, the percentages of the preceding stages of maturing NK cells in the bone marrow of *Fcrl6*$^{-/-}$ mice were increased compared to WT mice. Although the number and percentage of total NK cells in the spleen remained unaffected in *Fcrl6*$^{-/-}$ mice, the proportion of terminally differentiated NK cells

within the mature NK cell pool may be reduced due to the absence of FCRL6. Thus, we next analysed the maturation of splenic NK cells as their development is believed to occur largely if not exclusively in the bone marrow (Sojka *et al.* 2014), and identified that the percentage of $CD11b^{-}$ $CD27^{+}$ and $CD11b^{-}$ $CD27^{+}$ subsets within mature NK cells were marginally lower in *Fcrl6*$^{-/-}$ mice compared to WT mice. However, the percentage of the most mature $CD11b^{+}$ $CD27^{-}$ subset remained unchanged in *Fcrl6*$^{-/-}$ mice compared to WT mice. Thus, the absence of FCRL6 does not appear to significantly slow down or arrest the terminal maturation of NK cells. Nonetheless, we investigated the maturation of *Fcrl6*$^{-/-}$ bone marrow-derived NK cells in mixed bone marrow chimeras in order to reveal minor differences that could become more apparent due to direct competition with WT cells in this setting. Similar to the result observed in *Fcrl6*$^{-/-}$ mice, the proportion of *Fcrl6*$^{-/-}$ bone marrow-derived NK cells in the spleen was identical to that of their WT counterparts. We did not detect a difference in the maturation of *Fcrl6*$^{-/-}$ NK cells under competition with WT cells in mixed bone marrow chimeras. This result supports our conclusion that germline deletion of FCRL6 does not appear to affect the development of NK cells or their terminal maturation.

Although the differences observed in NK cell maturation during comparison of *Fcrl6*$^{-/-}$ and WT mice are statistically significant, the presence of an unaffected mature $CD11b^{+}$ $CD27^{-}$ NK population in the spleen of *Fcrl6*$^{-/-}$ mice alongside minor differences in the preceding NK cell subsets suggests that the differences observed during comparison of *Fcrl6*$^{-/-}$ and WT mice are likely to be a false positive potentially due to the use of non-litter mate WT control mice. Thus, it is probable that 1) FCRL6 is not expressed by developing NK cell populations or their precursors, thereby negating an effect of its deletion on NK cell development or 2) FCRL6 is expressed by NK-lineage cells as well as their precursors and the germline nature of *Fcrl6* deletion in *Fcrl6*$^{-/-}$ mice results in the emergence of alternative mechanisms that effectively counteract the absence of FCRL6 and result in broadly unaffected NK cell development and maturation.

To address this, we analysed developing and mature NK cell populations as well as their differentiation in NK conditional *Fcrl6*$^{-/-}$ mice where *Fcrl6* is exclusively deleted in NK-lineage cells

from the immature NK cell stage in the bone marrow, thereby allowing us to examine the effect of *Fcrl6* deletion at a later stage of NK cell development. As with *Fcrl6*$^{-/-}$ mice, we did not observe differences in NK cell development in the bone marrow of NK conditional *Fcrl6*$^{-/-}$ mice and litter mate WT mice. However, we detected that the number and percentage of mature NK cells was reduced in the spleen of NK conditional *Fcrl6*$^{-/-}$ mice compared to their WT litter mate counterparts. Further analysis revealed a reduction in the number of all individual maturing NK cell populations in the spleen of NK conditional *Fcrl6*$^{-/-}$ mice compared to litter mate WT mice. However, we did not observe differences in the percentage of these maturing NK cell populations within the pool of mature NK cells from the bone marrow and spleen NK conditional *Fcrl6*$^{-/-}$ and litter mate WT mice.

This alongside data obtained from *Fcrl6*$^{-/-}$ mice suggests that despite expression of FCRL6 in mature NK cells, its absence does not affect the maturation program of NK cells and thus, it does not appear to have a role in the regulation of this process. We did not detect differences in NK cell development in *Fcrl6*$^{-/-}$ and NK conditional *Fcrl6*$^{-/-}$ mice, this would suggest that FCRL6 is not expressed by developing NK cells and does not have a role during their development. Alternatively, it is also likely that FCRL6 is expressed and has a function during NK cell development that is successfully compensated in *Fcrl6*$^{-/-}$ mice due to its germline deletion possibly by mechanisms such as increased expression of receptors with similar binding and/or signalling capabilities. It could be argued that this is not the case as we did not detect differences during NK cell development in NK conditional *Fcrl6*$^{-/-}$ mice where FCRL6 is deleted at a later stage, thereby reducing the possibility of the emergence of compensatory mechanisms to counteract the loss of the receptor due to the non-germline nature of this deletion. However, NK cell development may have proceeded normally in these mice due to the deletion of FCRL6 at the immature NK cell stage, thereby permitting its possible expression in preceding NK-lineage cells which could be sufficient to allow for unperturbed NK cell development in the bone marrow of NK conditional *Fcrl6*$^{-/-}$ mice. Eventual loss of FCRL6 expression in NK-lineage cells in NK conditional *Fcrl6*$^{-/-}$ mice may occur due to degradation without replacement as part of normal protein turnover. This may account for the reduced number and percentage of splenic mature NK cells observed

in NK conditional *Fcrl6*$^{-/-}$ mice. Thus, absence of FCRL6 possibly combined with a lack of compensatory mechanisms in these mice highlights a potential role of the receptor in bone marrow generated NK cells or specifically mature splenic NK cells.

The decrease in number and hence percentage of splenic NK cells in NK conditional *Fcrl6*$^{-/-}$ mice does not appear to be driven by a reduction in the bone marrow output of NK cells due to the possible aforementioned reasons and also as we did not observe differences in developing and mature NK cell populations in the bone marrow of NK conditional *Fcrl6*$^{-/-}$ mice. The drop in splenic NK cells also cannot be attributed to a block in peripheral maturation as the percentage of individual maturing NK cell subsets did not differ between NK conditional *Fcrl6*$^{-/-}$ and litter mate WT mice. Consequently, other possibilities such as reduced migration of NK cells to the spleen following entry into circulation from the bone marrow may be responsible for the reduction in the splenic NK cell population of NK conditional *Fcrl6*$^{-/-}$ mice and should be investigated in future studies. Additionally, it also remains unclear if FCRL6 plays a role during NK cell development in mice, this could also be addressed in future studies by some of the strategies discussed below.

5.4.2 FCRL6 and the NK cell response

As the absence of FCRL6 did not affect NK cell development or their maturation, we were interested in identifying if mouse FCRL6 had a potential role in regulating NK cell function due to the inhibitory potential of human FCRL6 in NK cells (Johnson *et al.* 2018b). Thus, we infected *Fcrl6*$^{-/-}$ and WT mice with FV and focused on identifying a difference in viral load during the acute phase of the infection. This was of particular interest due to the expression of FCRL6 in mature NK cells and their protective role during the initial phase of FV infection (Littwitz *et al.* 2013). We analysed the viral load in the bone marrow and spleen of infected mice at day 7 following infection, as this represents the peak of infection in C57BL/6 mice (Marques *et al.* 2008). During the acute phase of FV infection, there is an expansion of erythroid precursor (nucleated Ter119^{+}) cells, which are the primary targets of FV (Hasenkrug *et al.* 1998). We did not observe a difference in the percentage of FV infected Ter119^{+} cells in the bone marrow of *Fcrl6*$^{-/-}$ mice compared to WT

mice. However, the percentage of FV infected Ter119$^+$ cells was significantly lower in the spleen of *Fcrl6*$^{-/-}$ mice compared to their WT counterparts. This was further confirmed by lower FV *env* DNA copy numbers in splenocytes from *Fcrl6*$^{-/-}$ mice compared to WT mice.

Effective clearance of FV infection is primarily dependent upon the function of B cells, NK cells and T cells (Dittmer *et al.* 1999; Littwitz *et al.* 2013; Messer *et al.* 2004). FV-specific cytotoxic T cells are not observed until about 10 days after FV infection (Zelinskyy *et al.* 2009) whilst a significant titre of FV-specific neutralising antibodies is not detected until day 21 after infection (own analysis). Thus, we determined that absence of FCRL6 increases the natural resistance of C57BL/6 mice to FV infection possibly due to an augmented NK cell response as T and B cell responses may not yet be fully developed at the analysed time point.

In addition to being critical for host defence against viral infection, NK cells are also vital for anti-tumour immunity. Consequently, we used the B16 melanoma model where NK cell depletion has been demonstrated to augment B16 lung metastasis to further investigate the function of FCRL6 in NK cells (Takeda *et al.* 2011). We analysed the tumour burden as well as the NK cell response at day 14 following inoculation of *Fcrl6*$^{-/-}$ mice with B16 melanoma cells. We observed that *Fcrl6*$^{-/-}$ mice had a slightly lower number of colonies on their lungs at this time point compared to WT mice. Next, we characterised the lung NK cell response in these mice to identify if this difference could be driven by alterations in their expansion and activation. We identified that the mature lung NK cell population was composed of a much greater proportion of CD11b$^+$ CD27$^-$ NK cells in both genotypes compared to the mature splenic NK cell population perhaps due to the critical role of NK cells in mediating pulmonary immune responses. However, we did not find differences in the percentage or maturation of NK cells in the lungs of *Fcrl6*$^{-/-}$ mice. Next, we examined the activation of lung NK cells via analysis of surface markers and did not find differences in their expression on NK cells from *Fcrl6*$^{-/-}$ mice. Similarly, we also did not find a difference in the levels of IFNγ and GzmB in *Fcrl6*$^{-/-}$ lung NK cells following *ex vivo* restimulation. These results indicate that NK cell function is unaffected by the absence of FCRL6 in this tumour model and thus, it is probable that the difference in tumour burden observed in *Fcrl6*$^{-/-}$ mice is not due to alterations in NK cell

function. However, it is conceivable that the effects of FCRL6 deletion on NK cell expansion and activation may be masked by compensatory mechanisms due to the germline deletion of FCRL6 in *Fcrl6*$^{-/-}$ mice. Thus, we next investigated the function of FCRL6 in NK cells using NK conditional *Fcrl6*$^{-/-}$ mice.

We infected NK conditional *Fcrl6*$^{-/-}$ and litter mate WT mice with FV and analysed the viral load as well as NK cell activation at day 7 following infection. Contrary to our finding in *Fcrl6*$^{-/-}$ mice, we did not detect a difference in the percentage of FV infected Ter119^{+} cells in the spleen of NK conditional *Fcrl6*$^{-/-}$ mice. Subsequently, we characterised NK cell expansion and observed that splenic NK cells were expanded in terms of percentage and number following infection in both genotypes compared to the steady state. However, the percentage of NK cells remained lower in the spleen of NK conditional *Fcrl6*$^{-/-}$ mice compared to WT mice following infection as observed during steady state conditions. The maturation of splenic NK cells was unaffected by the absence of FCRL6 in NK conditional *Fcrl6*$^{-/-}$ mice following infection as also observed during steady state conditions. This further suggested that FCRL6 is dispensable for NK cell maturation whilst possibly affecting other processes that result in a reduced percentage of splenic NK cells in NK conditional *Fcrl6*$^{-/-}$ mice. Next, we analysed NK cell activation via expression of surface markers and did not identify differences in their expression on NK conditional *Fcrl6*$^{-/-}$ NK cells. We also did not find differences in the levels of IFNγ and GzmB in splenic NK conditional *Fcrl6*$^{-/-}$ NK cells following *ex vivo* restimulation. This alongside the equivalent viral load in NK conditional *Fcrl6*$^{-/-}$ mice compared to their WT counterparts indicates that FCRL6 is not involved in regulating NK cell function at least in this retroviral infection model. Thus, the increased natural resistance to FV in *Fcrl6*$^{-/-}$ mice is not specifically driven by the deletion of FCRL6 in NK cells.

Collectively, the data obtained following challenge of *Fcrl6*$^{-/-}$ and NK conditional *Fcrl6*$^{-/-}$ mice with FV and B16 melanoma cells suggests that despite the inhibitory potential of human FCRL6 in NK cells, mouse FCRL6 does not seem to possess immunoregulatory functionality as NK cell expansion and activation in the aforementioned models was unaffected in its absence. However, it is possible that the receptor possesses other functionality due to the lower percentage and

number of mature NK cells in the spleen of NK conditional *Fcrl6*$^{-/-}$ mice.

5.4.3 Future work

We were unable to determine if FCRL6 played an important role during NK cell development primarily due to a lack of data regarding its expression in developing NK cells. Thus, it would be of interest to future studies to determine the expression of FCRL6 in developing NK-lineage cells as well as NK-lineage committed precursor cells to assist in understanding if the receptor has a role during NK cell development. If expression is detected in developing NK cells or their precursors, then it is likely that compensatory mechanisms exist in *Fcrl6*$^{-/-}$ mice that allow normal NK cell development and negates further use of these mice to elucidate the function of FCRL6 during NK cell development. In this case, the expression of FCRL6 should be examined in NK conditional *Fcrl6*$^{-/-}$ mice to identify the stage at which FCRL6 surface expression is lost in these mice, and determine if they are an appropriate model study the role of this receptor during NK cell development. It is possible that a role of FCRL6 prior to its deletion at the immature NK cell stage in these mice or its residual expression on NK cells after its deletion could allow normal NK cell development. Thus, it may become imperative to generate NK conditional *Fcrl6*$^{-/-}$ mice where deletion of the receptor is not germline-induced but occurs prior to its expression in NK-lineage cells to effectively study its role during NK cell development.

Conditional deletion of FCRL6 in NK cells resulted in a reduced percentage and number of these cells in the spleen during steady state conditions. A similar decrease in the percentage of mature NK cells in the spleen was also observed following FV infection of NK conditional *Fcrl6*$^{-/-}$ mice. Whole transcriptome sequencing of NK cells from these mice could aid in identifying differentially regulated genes and potential pathways responsible for the observed phenotype, thereby assisting in our understanding of the function of FCRL6 in NK cells. Migration of NK cells could be affected as FCRL6 may bind potential ligands to induce signalling that facilitates entry of these cells out of the circulation and into organs. This could be explored in future studies by identifying the number of NK cells in the circulation as well as in other organs of NK conditional *Fcrl6*$^{-/-}$ mice.

Potential ligands of FCRL6 could be identified by engineering a chimeric molecule consisting of the extracellular region of mouse FCRL6 coupled to an intracellular region that permits signal transduction and induces expression of a marker such as GFP following engagement of the receptor by a ligand. Cells expressing this chimeric mouse FCRL6 molecule can then be cultured with cell suspensions from different tissues to identify potential ligands of the receptor. Although *in vivo* activation and production of IFNγ and GzmB following *ex vivo* restimulation remained unaffected by the absence of FCRL6, killing of a NK sensitive target cell line such as K562 cells as well as Granzyme B production by NK conditional *Fcrl6*$^{-/-}$ NK cells could be assessed in an *in vitro* cytotoxicity assay to identify differences due to the absence of FCRL6. The expression of FCRL6 should also be analysed in NK cells from other anatomical locations in order to determine if its expression is specific to bone marrow produced and spleen residing NK cells.

NK cells are primarily activated following loss of signalling through inhibitory receptors due to MHC class I downregulation that occurs during infection or malignancy (Pegram *et al.* 2011). In addition to MHC class I binding inhibitory receptors, NK cells also express other inhibitory receptors that bind non-MHC class I molecules to regulate NK cell activation (He & Tian 2017). The inhibitory potential of human FCRL6 and its capability of engaging with HLA-DR suggests that it could function as one of these receptors, thereby allowing NK cells to target tumours from certain tissues that downregulate MHC class II expression to evade CD4^{+} T cell immunity (Mottok *et al.* 2015; Steidl *et al.* 2011a, 2011b). This hypothesis could be tested in future studies by challenging Tg mice that express human FCRL6 on NK cells with a NK sensitive tumour cell line that has been transduced with HLA-DR and analysing its clearance. It should be noted that mouse and human FCRL6 possess slightly different extracellular and intracellular regions and thus potential roles of either of these proteins may not be shared by the other.

Chapter 6. Role of FCRL6 in the development and function of T cells

6.1 Introduction

6.1.1 T cell development

Self-determination and maintenance of diversity form the central principles of T cell development. The T cell repertoire must be able to respond to a wide range of pathogens whilst maintaining tolerance to self-antigens. As with B cell development, multiple mechanisms function during T cell development to increase the diversity of the TCR as well as eliminate potentially dysfunctional T cells. These processes necessitate T cells to maintain a balance between the ability to recognise self and overt self-reactivity. Early mammalian T cell development occurs in the BM following which, T cells traffic to the thymus in order to complete their development and subsequently integrate into the pool of naïve, mature T cells that survey their environment for cognate antigen.

6.1.1.1 T cell development in the bone marrow

Development of T-lineage progenitors

The development of CLPs is discussed in section 4.1.1.1 of the thesis. The primary site of T cell development is the thymus. However, this requires a continuous supply of T-lineage committed CLPs from the bone marrow. Whilst CLPs are unable to form myeloid cells, they can commit to any cell type within the lymphoid lineage comprised of B, NK and T cells. The process involving commitment to the T-linage remains to be fully understood but it is believed that Notch signalling via delta-like ligands plays a crucial role. Notch signalling initiation in CLPs has been shown to block B and NK cell development and favour commitment to the T-linage (Guo *et al.* 2008b; Maillard *et al.* 2005; Radtke *et al.* 1999). T lineage committed CLPs subsequently migrate to the thymus via processes that also remain to be fully understood. Once in the outer cortical region of

the thymus, T lineage committed CLPs undergo several rounds of cellular division as a result of Notch and IL-7 signalling, and begin thymic T cell development (Patra *et al.* 2013; Zúñiga-Pflücker 2004).

6.1.1.2 Development of T-lineage cells in the thymus

The development of T cells in the thymus occurs through a spatially organised process in which developing T cells or thymocytes navigate from the outer cortex to the medullary regions of the thymus to complete their development. During this migration, thymocytes generate their TCR and undergo selection mechanisms in distinct thymic microenvironments that allow them to continue to the next developmental stage. As observed during B-lymphopoiesis, only a fraction of thymocytes integrate into the mature T lymphocyte pool.

T cell differentiation has been extensively characterised by the analysis of surface marker expression using flow cytometry. Primarily, cluster of differentiation (CD)4 and CD8 are used to delineate developing T cell populations with the most immature thymocytes being identified as $CD4^-$ $CD8^-$ and termed double negative (DN). DN thymocytes do not express the TCR on their surface, possess non-recombined TCR gene segments and maintain the potential to develop into both $\alpha\beta$ or $\gamma\delta$ T lymphocytes. DN thymocytes migrate from the outer to the inner cortex of the thymus, a transition that is associated with changes in their surface expression of CD25 and CD44. These changes can be used to further divide DN thymocytes into DN1 ($CD44^+CD25^-$), DN2 ($CD44^+CD25^+$), DN3 ($CD44^-CD25^+$) and DN4 ($CD44^-CD25^-$) subsets (Aldrich & Kellems 2001; Germain 2002; Godfrey *et al.* 1993). Thymocytes begin recombination of their TCR β, δ and γ loci at the DN3 stage of T cell development. Successful rearrangement within the TCR γ and δ loci leads to the surface expression of a $\gamma\delta$ TCR. Subsequent engagement of this receptor results in commitment towards the $\gamma\delta$ T-lineage via expression of ERK1 and 2, early growth response proteins and inhibitor of differentiation 3. It has been identified that strong signalling through the $\gamma\delta$ TCR is crucial for development of the $\gamma\delta$ T-lineage as attenuated signalling through

the γδ TCR has been shown to result in a commitment switch towards the αβ T-lineage (Haks *et al.* 2005; Prinz *et al.* 2006). Thus, strict temporal signalling guidelines exist to instruct commitment towards the γδ T-lineage.

Unlike γ and δ TCR chains, α and β TCR chains are expressed in a successive manner with rearrangement and expression of the TCRβ chain occurring prior to that of the TCRα chain (Krangel 2009). The rearranged TCRβ chain is expressed from the DN3 stage of T cell development as part of the pre-TCR complex alongside an invariant surrogate α chain (von Boehmer & Fehling 1997). Signalling through the pre-TCR complex leads to allelic exclusion of the other TCRβ locus thereby ensuring expression of a single recombined TCRβ chain. Subsequently, thymocytes undergo IL-7 dependent cellular proliferation and commence recombination of their TCRα loci (Robey & Fowlkes 1994). Following successful rearrangement of their TCRα loci, thymocytes substitute the surrogate α chain in the pre-TCR complex for a recombined TCRα chain. This substitution leads to the assembly of the mature TCR complex comprised of the TCRα and β chains, two CD3ζ chains and the CD3 co receptor composed of CD3γ, CD3δ and two CD3ε chains (Strominger 1989). Subsequently, DN thymocytes become $CD4^+$ $CD8^+$ and commit to the αβ T-lineage. The dual expression of CD4 and CD8 leads to these thymocytes being referred to as double positive (DP).

Germline TCRα and TCRβ loci like IgL and IgH loci are composed of genetic regions that encode distinct TCR gene families known as variable (V), diversity (D), joining (J) and constant (C) regions. V, D, and J families are composed of multiple gene segments with only a single segment from each family being required in addition to a C segment to form the α or β chain that makes up the TCR. Thus, somatic recombination of V and J segments of TCRα and V, D and J segments of TCRβ loci is required to produce a functional TCR and contributes to the genetic diversity of the TCR due to its combinatorial nature. As observed during recombination of IgH loci, TCRβ chain recombination proceeds with D-J rearrangement occurring prior to V to DJ rearrangement (Janeway 2001). RAG1 and RAG2 expression is critical for the recombination of TCRα and

TCRβ loci. These enzymes function by binding recombination signal sequences (RSS) that flank individual TCR gene segments and causing double stranded DNA breaks that are subsequently repaired by non-homologous end joining(Krangel 2009; Oettinger *et al.* 1990; Schatz *et al.* 1989). Specific nucleotide sequences known as spacer sequences are present within the RSS and differ in length, consisting of either 12 base-pairs (bp) or 23 bp depending on the gene family. This difference in spacer sequence length is critical for generating diversity during recombination as pairing only occurs between gene segments that contain 12bp and 23bp terminal spacer sequences thereby, maximising the potential for diverse rearrangements (Janeway 2001; van Gent *et al.* 1996). Additional TCR diversity is generated by the addition of random nucleotides to VDJ and VJ junctions of TCRβ and TCRα loci, respectively by the enzyme TdT as well as by combination of different TCRα and TCRβ chains. These processes along with somatic recombination lead to the generation of highly variable complementary determining regions (CDR) within the TCR which determine the antigen specificity of the receptor. Specifically, CDR3 is crucial for peptide specificity and binds the antigen whilst CDR1 and 2 are responsible for the binding of the TCR to major histocompatibility complex (MHC) molecules (Cabaniols *et al.* 2001; Davis & Bjorkman 1988; Marrack *et al.* 2008).

The theoretical TCR diversity generated by somatic recombination, TdT and pairing of different TCRα and TCRβ chains far outweighs the actual diversity observed in hosts (Davis & Bjorkman 1988). This is primarily due to selection events during T lymphocyte development that remove non-functional and dysfunctional T cells. Thymocytes are screened against a range of self-peptides also known as peripheral tissue antigens (PTA) presented on thymic APCs due to action of the transcription factor autoimmune regulator (AIRE) in a process known as thymic selection. AIRE binds to polymerase complexes associated with promoter regions of PTA genes and acts to inhibit RNA polymerase inactivation thereby, driving transcription of PTAs in thymic APCs (Giraud *et al.* 2012).

Thymic selection occurs at the DP stage and involves positive and negative selection which examine TCRs of individual T cell clones for their MHC restriction as well as signalling capacity

(Surh & Sprent 1994). These selection processes drive development of a particular T cell clone towards one of four possible outcomes; death by neglect, positive selection, negative selection or integration into the mature T cell pool. Positive selection occurs prior to negative selection in the cortex of the thymus and is dependent on thymic APCs known as cortical thymic epithelial cells (cTECs). The vast majority of thymocytes interact weakly with cTECs via their TCRs and as a result fail positive selection and die by neglect. Approximately, 10% of thymocytes undergoing this process meet the TCR signalling requirement and are positively selected to progress onto the next stage of T lymphocyte development in the medullary regions of the thymus. Here, thymocytes undergo negative selection which involves interactions of their TCRs with PTAs expressed on medullary thymic epithelial cells (mTECs), thymic and migratory DCs. T cell clones that react too strongly with self-antigen undergo clonal deletion which involves cell death via apoptosis (Klein *et al.* 2014; Mandl *et al.* 2013; Yasutomo *et al.* 2000).. Thus, T cell clones possessing an optimal range of TCR signalling that allows them to successfully navigate positive and negative selection are able to integrate into the mature T cell pool.

In addition to clonal deletion, thymocytes possessing strong signalling self-reactive TCRs can also be diverted to the regulatory T cell (T_{reg}) lineage. The specific conditions instructing T_{reg} development remain to be fully elucidated however, it is believed to be dependent on high levels of TCR signalling which induces IL-7 signalling and increased expression of Bcl-2. This is thought to provide protection against clonal deletion and allows continued TCR signalling that drives Forkhead box P3 and IL-2 receptor upregulation which are critical for acquirement of the T_{reg} lineage (Fan *et al.* 2018; Mazzucchelli *et al.* 2008; Tischner *et al.* 2012; Ziegler & Buckner 2009).

CD4/8 lineage commitment is entwined with thymic selection processes. The specific mechanisms relating to the transition of DP thymocytes to either CD4 single positive (SP) or CD8 SP thymocytes have been extensively debated. Historically, two models known as the instructive and the stochastic model have been used to explain the mechanism underlying this transition. The instructive model suggests that CD4/8 lineage commitment is determined by the interaction of the TCR with different classes of MHC molecules thereby, suggesting that commitment is

driven by the class of the interacting MHC molecule. The stochastic model suggests lineage commitment is predetermined prior to recombination of TCR gene segments with CD4/8 lineage commitment occurring in a TCR independent manner. DP thymocytes that interact with the wrong class of MHC molecule are said to be MHC mismatched and are eliminated (Kappes *et al.* 2005). Recently, new models have emerged to explain CD4/8 lineage known as the strength and duration of signal models in which commitment is instructed by the strength, duration and quality of TCR signalling. High levels of sustained TCR signalling that occur following interaction with MHCII molecules cause increased intracellular calcium levels and ERK signalling which drive CD4 commitment whilst low levels of TCR signalling for shorter periods of time following interaction with MHCI molecules cause CD8 commitment (Singer *et al.* 2008). Irrespective of the specific mechanism instructing CD4/8 choice, specific lineage commitment requires expression of lineage specific transcription factors; Th-inducing POK, thymocyte selection-associated high mobility group box protein TOX and GATA3 instruct $CD4^+$ T cell lineage whilst runt-related transcription factor 3 (RUNX3) is associated with $CD8^+$ T cell lineage (Naito & Taniuchi 2010). Following lineage commitment, CD4 and CD8 SP thymocytes travel from the medulla to peripheral sites and integrate into the mature T cell pool (Germain 2002).

6.1.2 T cell activation

$CD4^+$ and $CD8^+$ T cell activation requires interaction of the TCR with cognate antigen as well as specific cell-to-cell contacts. Naïve T cells continually travel between lymphoid organs and sample MHC molecules on the encountered APCs. Following infection, APCs become activated and start expressing peptides fragments derived from invading pathogens on their surface in concert with MHC molecules. T cell activation is dependent on two signals; recognition of cognate antigen via the TCR and delivery of co-stimulatory signals. The initial binding of the TCR with pMHC which results in activation of the T cell is known as priming. However, priming alone is insufficient to sustain T cell activation and results in anergy if not supplemented with costimulatory signals delivered by APCs. The three main types of professional APCs are B cells, DCs and macrophages. DCs are vital for T cell activation as these cells migrate to secondary lymphoid organs following

their activation and present antigen on MHCI and MHCII molecules to activate $CD4^+$ and $CD8^+$ T cells (Pennock *et al.* 2013). Activation and differentiation of $CD4^+$ and $CD8^+$ T cells is discussed below.

6.1.2.1 $CD4^+$ and $CD8^+$ T cell activation

The activation of $CD4^+$ and $CD8^+$ T cells is initiated following recognition of cognate pMHCII and pMHCI complexes, respectively on APCs by the TCR of specific clones. The early signalling events surrounding this event remain to be fully elucidated however, phosphorylation of tyrosine residues in immune-receptor tyrosine-based activation motifs (ITAMs) present on covalently associated CD3 subunits of the TCR has been shown to be critical in initiating the ensuing downstream signalling process. Phosphorylation of these ITAMs leads to the recruitment of kinases to cytoplasmic domains within the TCR complex and initiation of a signalling cascade involving CD45, lymphocyte protein tyrosine kinase and Zeta Chain of T Cell receptor associated protein kinase which cause calcium fluxing thereby, regulating the activity of calcineurin, a calcium sensitive phosphatase that is responsible for the transcription of multiple genes associated with T cell activation (Fracchia *et al.* 2013). Costimulation is provided by the interaction of CD28 on T cells with its ligands, CD80 or CD86. These ligands of CD28 differ in their expression pattern with CD86 being constitutively expressed by APCs and thus, playing a more important role during activation of T cells compared to CD80 which is upregulated on APCs following their activation (Esensten *et al.* 2016). The activation of the TCR also leads to reorganisation of TCR-pMHC complexes into large clusters at the T cell-APC interface which ultimately form an even larger structure known as the supra-molecular activation cluster (SMAC) or immunological synapse. The TCR-pMHC complexes form the core of the SMAC and are referred to as central SMAC (cSMAC) whilst adhesion proteins such as lymphocyte function-associated 1, talin and intracellular adhesion molecule 1 form scaffolding structures that constitute the peripheral SMAC (pSMAC). The outermost cluster of proteins that form the SMAC are referred to as the distal SMAC (dSMAC) and consist of CD43 and CD45 molecules. This organisational structure is postulated to be important for many functions one of which, includes amplification of signalling following T cell

activation. However, SMAC formation has been shown to not be essential for T cell activation (Dustin 2002; Lin *et al.* 2005).

6.1.2.2 $CD4^+$ T cell differentiation

The activation of naïve $CD4^+$ T cells induces transcriptional changes that allows their differentiation into an array of T helper (T_H) effector subsets that perform different immune functions: T_{H1}, T_{H2}, T_{H17}, T_{reg}, T_{FH} and T_{H9}. This differentiation requires the expression of distinct signal transducers and activators of transcription (STAT) proteins and transcription factors, and is thought to be influenced by TCR signalling quality, cytokine milieu as well as the activating APC. Each T_H subset is defined by the expression of a lineage specific transcription factor, cytokine expression profile and consequently, functionality (Saravia *et al.* 2019).

T_{H1} differentiation is induced by IL-12 and IFNγ and is directed by the lineage specific transcription factor T-bet. T_{H1} cells are able to produce IL-2, IFNγ and TNFα/β all of which allow these cells to specifically stimulate and activate cellular immunity by macrophages and $CD8^+$ T cells (Zhang *et al.* 2014).

T_{H2} differentiation requires IL-2 and IL-4 and is driven by the lineage specific transcription factor GATA3. The hallmark cytokines produced by T_{H2} cells are IL-4, IL-5 and IL-13 which alongside their collaboration with B cells allows them to mediate humoral immunity and allergic responses (Walker & McKenzie 2018).

T_{H17} differentiation can be induced by the dual actions of TGFβ and IL-6 or TGFβ and IL-21, and driven by the lineage specific transcription factor RORγt. These cells can also be identified by their expression of IL-17A and IL- 17F and are vital for regulating neutrophil and macrophage responses in addition to contributing to the immune response against extracellular pathogens (Sandquist & Kolls 2018).

T_{FH} differentiation is promoted by interactions of naïve $CD4^+$ T cells with B cells in the interfollicular zone of secondary lymphoid organs and requires IL-6 signalling with lineage commitment being driven by the transcription factor Bcl-6. T_{FH} cells produce IL-21 and express CXCR5 both of which are crucial for their role in the germinal centre reaction and production of somatically hypermutated class switched antibodies (Crotty 2014).

T_{H9} cells are a recently identified T_H effector subset characterised by their expression of IL-9 and are responsible for multiple functions in immunity and immunopathology. Their differentiation appears to be driven by the transcription factor PU.1(Kaplan *et al.* 2015).

Following resolution of infection, the vast majority of differentiated $CD4^+$ T cells die via apoptosis. However, a small percentage of clonally expanded cells survive and differentiate into memory $CD4^+$ T cells. These cells underpin the basis of immunological memory and generate rapid recall responses following infection by the same pathogen.

6.1.2.3 $CD8^+$ T cell differentiation

The $CD8^+$ T cell response is characterised by three phases; activation, contraction and establishment of immunological memory. The initial activation of naïve $CD8^+$ T cells is followed by an expansion phase in which activated $CD8^+$ T cells increase by about 10^4- to 10^5-fold, with cells dividing approximately every 6 to 8 hours at the peak of proliferation. The transcription profile of activated $CD8^+$ T cells is dramatically altered compared to their naïve counterparts. In early activated $CD8^+$ T cells, various transcription factors including T-bet, BLIMP1, ID2 and STAT4 cooperate to induce a differentiation program that results in the generation of effector $CD8^+$ T cells which perform a critical role in the immune response against viruses, intracellular bacteria, and tumours (Kaech & Cui 2012).

Effector $CD8^+$ T cells gain the ability to rapidly produce cytokines such as IL-2, IFNγ and TNFα as well as traffic to nonlymphoid tissues via expression of the chemokine receptors CXCR3 and

CXCR4. Following recognition of cognate pMHCI complexes on compromised cells, effector $CD8^+$ T cells upregulate their expression of cytotoxic granules containing perforin and granzymes, and become cytotoxic. These granules are only released towards the direction of a target cell, aligned with the immunological synapse in order to avoid non-specific killing of nearby healthy cells. Perforin functions by forming a pore in the membrane of a target cell thereby allowing entry of granzymes also present within cytotoxic granules into the cytoplasm of the target cell. Granzymes are serine proteases that activate caspases and ultimately, cause cell death of compromised cells via apoptosis. Effector $CD8^+$ T cells are also able to kill compromised cells due to their expression of Fas ligand which can bind to its receptor, Fas on target cells and result in the activation of a caspase-mediated cascade that kills compromised cells via apoptosis (Groom & Luster 2011; Harty *et al.* 2000; Wang *et al.* 2014).

Following clearance of a pathogen, effector $CD8^+$ T cells undergo a contraction phase in which a majority of the expanded pathogen-specific population dies as a result of apoptosis. A small minority of these cells, approximately 5-10% survive this contraction phase and further mature into long-lived memory $CD8^+$ T cells. The survival and integration of effector $CD8^+$ T cells into the memory pool is not a random process as certain effector cells are intrinsically better at persisting and becoming memory cells than others. Thus, the initial pool of effector $CD8^+$ T cells generated following activation of naïve $CD8^+$ T cells is heterogenous and can be divided into subsets with distinct effector and memory potential and consequently, gene expression, function, migratory pattern, proliferative capacity and long-term fate. However, other subsets also exist within the effector $CD8^+$ T cell pool with intermediate differentiation states that have mixed phenotypes. Long-lived memory $CD8^+$ T cells are maintained following an infection in an antigen independent-cytokine dependent manner involving IL-7 and IL-15 which promote homeostatic basal proliferation resulting in self-renewal and survival (Kaech & Cui 2012; Wherry & Ahmed 2004).

There are two broad subsets of memory $CD8^+$ T cells; central memory T (T_{CM}) and effector memory T (T_{EM}) cells as defined by their expression of surface markers, anatomical location and function. T_{CM} cells are mainly found in secondary lymphoid organs and the bone marrow whilst

T_{EM} cells are primarily found in circulation and non-lymphoid tissues. As mentioned previously, these cells also differ in their functional capacity with T_{CM} cells possessing a greater proliferative potential and increased capacity for IL-2 production compared to T_{EM} cells which produce cytokines and cytotoxic granules at a much faster rate than T_{CM} cells. Recently, a third subset of memory $CD8^+$ T cells known as tissue resident memory T (T_{RM}) cells has emerged. These cells permanently reside in peripheral tissue following pathogen clearance and provide site specific protection against rechallenge by the same pathogen. T_{RM} cells are characterised by their lack of tissue egress receptors, sustained granzyme B production and high mRNA levels of IL-2, IFNγ and TNFα (Chen *et al.* 2018; Weisel *et al.* 2016).

6.2 Aims

We did not identify the expression of FCRL6 via qRT-PCR in developing or mature $CD4^+$ and $CD8^+$ T cells from the thymus and the spleen. However, we examined publicly available expression data and discovered the expression of FCRL6 in medullary thymic epithelial cells, thereby raising the possibility that it could potentially affect T cell development in the thymus. Thus, we aimed to investigate the consequence of FCRL6 deletion on T cell development by analysing developing and mature $CD4^+$ and $CD8^+$ T cell populations in *Fcrl6*$^{-/-}$ mice. Due to the absence of FCRL6 expression in mature mouse T cells, we generated Tg mice expressing human FCRL6 and challenged T cells from these mice in multiple *in vitro* and *in vivo* settings to explore the function of human FCRL6 in the context of T cells.

6.3 Results

6.3.1 T cell development in *Fcrl6*$^{-/-}$ mice

Our analysis showed that the expression of mouse FCRL6 in major immune populations is restricted to developing B cells and mature NK cells. However, *Fcrl6* could also be expressed by non-immune cells. Accordingly, we examined publicly available expression data for the expression of *Fcrl6* by non-immune cells. We discovered medullary thymic epithelial cells (mTECs) expressed *Fcrl6* at comparable levels to splenic NK cells (ImmGen consortium – data not shown). The crucial role of mTECs in central tolerance raises the possibility that deletion of *Fcrl6* in these cells could potentially affect T cell development in the thymus (Derbinski *et al.* 2001). Thus, we proceeded to investigate the effect of *Fcrl6* deletion on T cells using *Fcrl6*$^{-/-}$ mice.

We started by investigating if there are differences in the relative proportion of thymocytes or mature CD4^{+} and CD8^{+} T cells in *Fcrl6*$^{-/-}$ mice under steady state conditions. We did not detect a difference in the percentage of DN subsets in the thymus of *Fcrl6*$^{-/-}$ mice compared to WT mice. Moreover, the proportion and number of thymocytes in *Fcrl6*$^{-/-}$ mice remained unchanged compared to WT mice. (Figure 28a and 28b). We did not observe a difference in the number and percentage of total as well as naïve, memory and regulatory CD4^{+} T cells in the spleen of *Fcrl6*$^{-/-}$ mice compared to WT mice. Similarly, the number and percentage of total, naïve and memory CD8^{+} T cells in the spleen were also comparable in *Fcrl6*$^{-/-}$ and WT mice (Figure 29a and 29b). Furthermore, we were not able to observe the development of autoimmune phenotypes in *Fcrl6*$^{-/-}$ mice. Thus, we concluded following evaluation of developing and mature T cell populations in *Fcrl6*$^{-/-}$ mice, and due to a lack of spontaneous autoimmunity in these mice that deletion of *Fcrl6* does not affect T cell development and potentially their phenotype (Figure 30). Due to an absence of *Fcrl6* expression in T-lineage cells under steady state conditions and following activation, we did not perform further experiments involving analysis of the functional capacity of T cells in *Fcrl6*$^{-/-}$ mice.

Figure 28: There are no differences during T cell development in the absence of *Fcrl6*

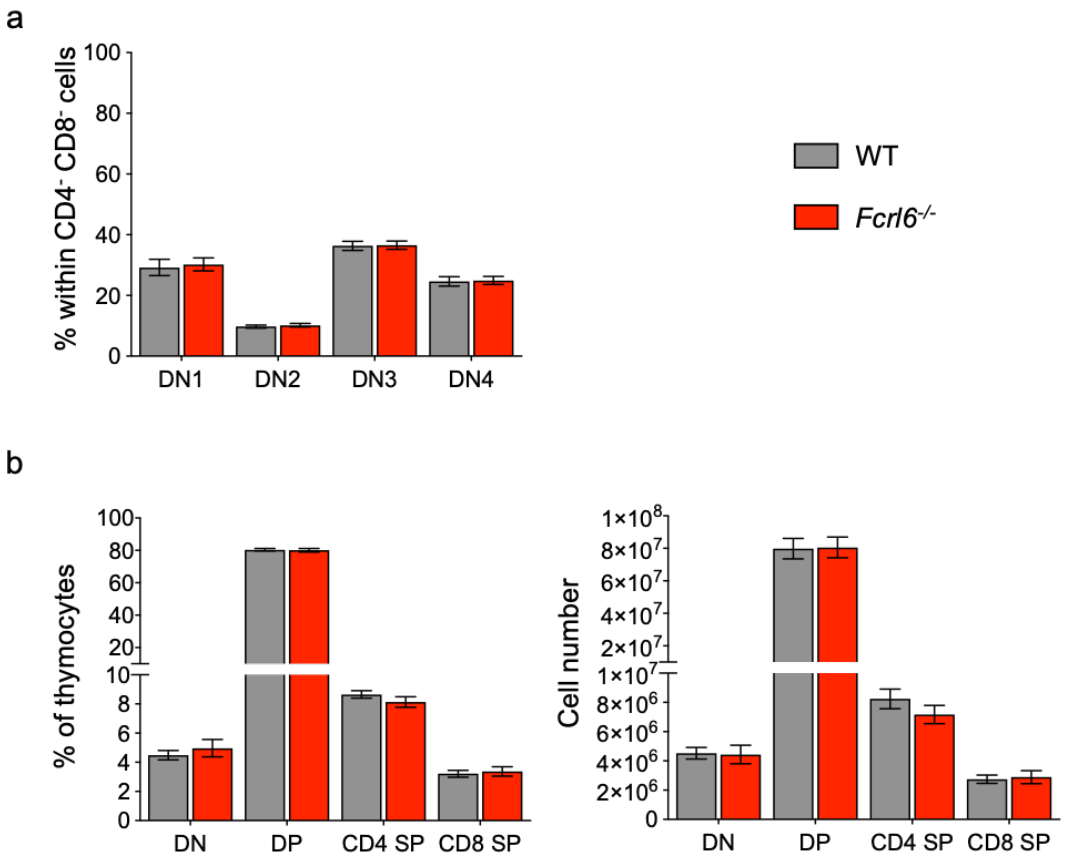

(a) Percentage of DN subsets in unchallenged *Fcrl6*$^{-/-}$ and WT mice analysed via flow cytometry. (b) Number and percentage of thymocytes in unchallenged *Fcrl6*$^{-/-}$ and WT mice analysed via flow cytometry. Cell populations were gated as depicted in Figure 30. Bars represent mean ± SEM of 13 biological repeats per genotype from 3 independent experiments. CD4 SP, CD4 single positive; CD8 SP, CD8 single positive; DN, double negative; DN1 double negative 1; DN2 double negative 2; DN3 double negative 3; DN4 double negative 4; DP, double positive.

Figure 29: There are no differences in mature T cells in the absence of *Fcrl6*.

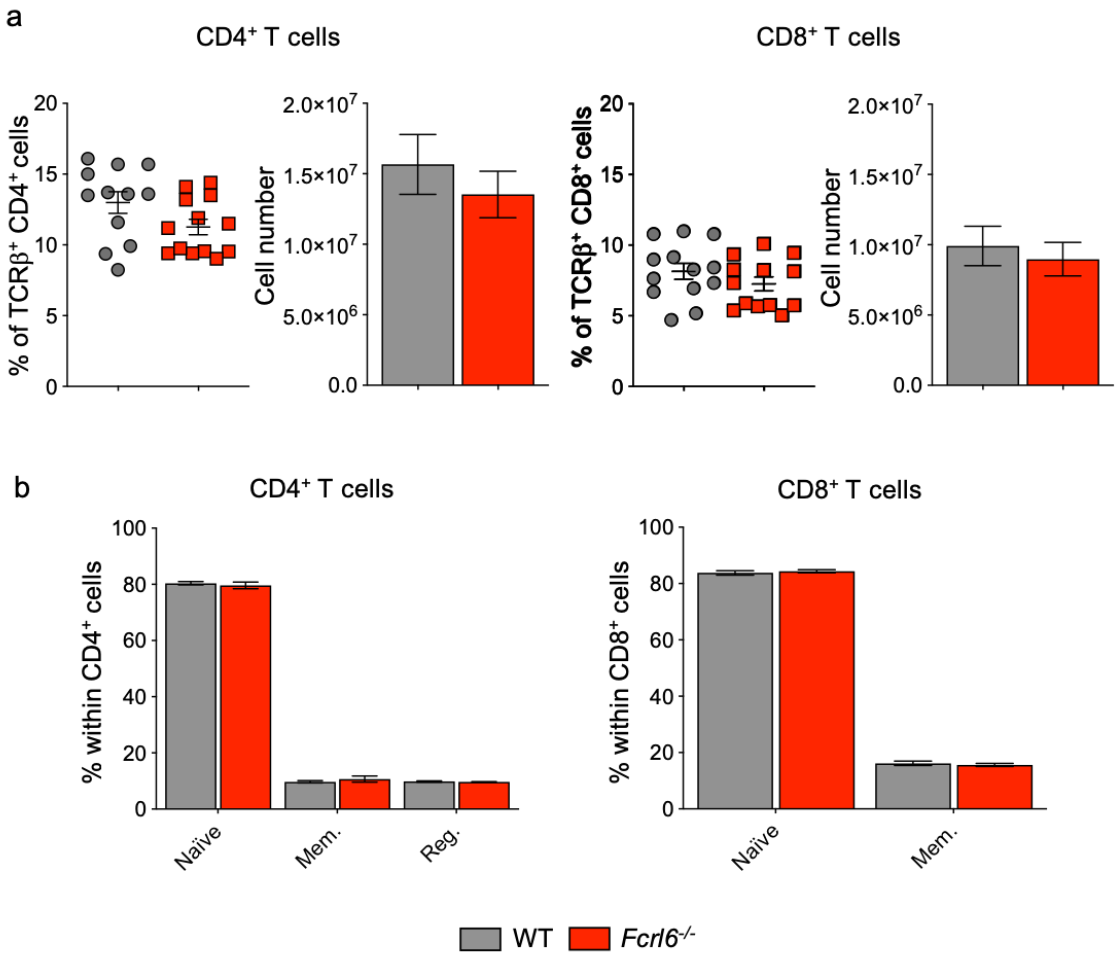

(a) Number and percentage of total CD4+ and CD8+ T cells in the spleen of unchallenged Fcrl6-/- and WT mice analysed via flow cytometry. (b) Percentage of CD4+ and CD8+ T cell subsets in the spleen of unchallenged Fcrl6-/- and WT mice analysed via flow cytometry. Cell populations were gated as depicted in Figure 30. Bars and symbols represent mean ± SEM of 13 biological repeats per genotype from 3 independent experiments. Mem., memory; Reg., regulatory.

Figure 30: *Fcrl6*$^{-/-}$ mice show normal T cell development.

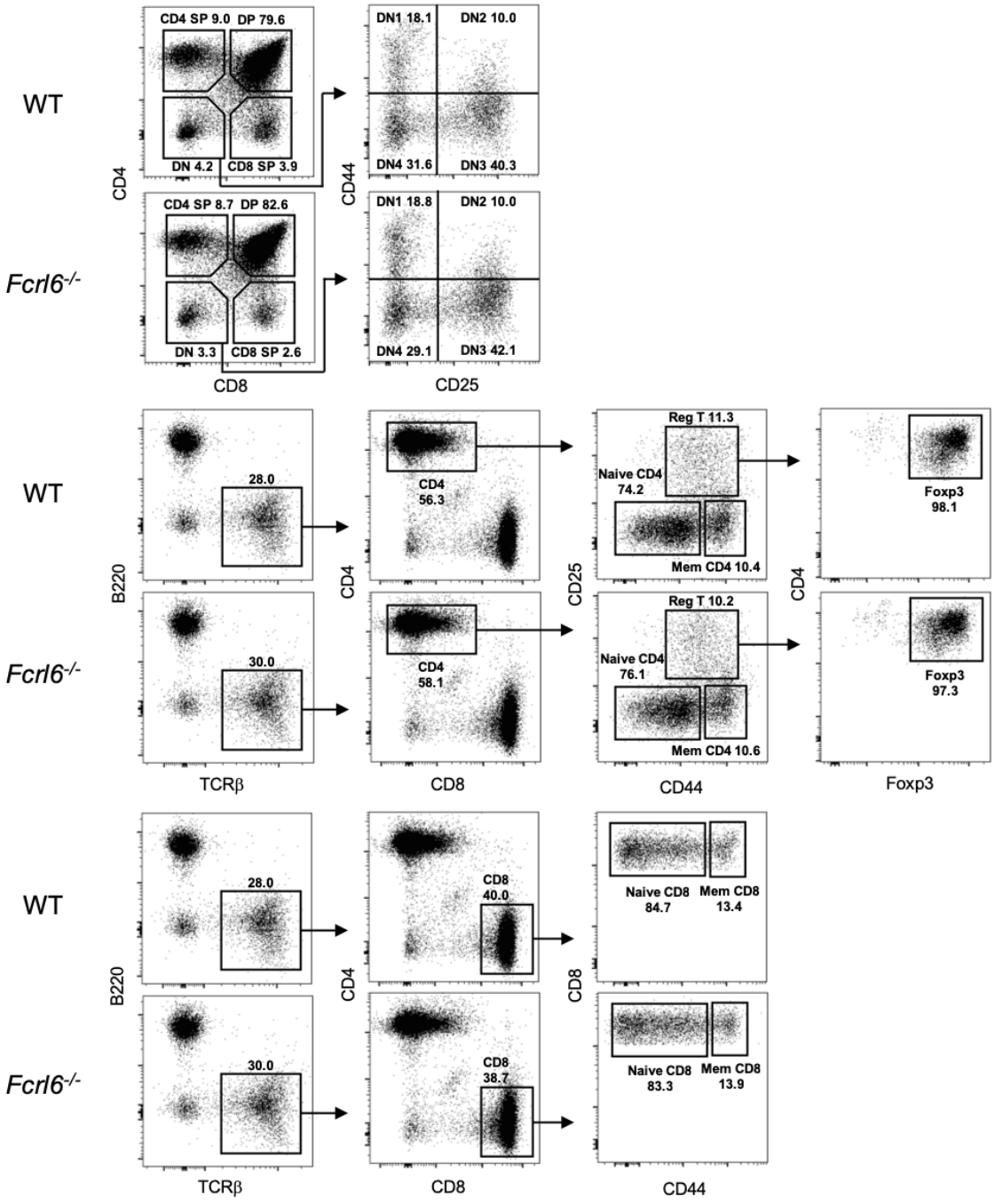

Flow cytometric gating strategy used for analysis and sorting of developing and mature T cell populations in Figures 7, 28 and 29. Names are indicated by text next to the gates whilst numbers represent population percentage within that plot. Gating strategies were as follows: thymus – CD4 SP, CD4 single positive ($CD4^+$ $CD8^-$); CD8 SP, CD8 single positive ($CD4^-$ $CD8^+$); DN, double negative ($CD4^-$ $CD8^-$); DN1 double negative 1 ($CD4^-$ $CD8^-$ $CD25^-$ $CD44^+$); DN2 double negative 2

($CD4^-$ $CD8^-$ $CD25^+$ $CD44^+$); DN3 double negative 3 ($CD4^-$ $CD8^-$ $CD25^+$ $CD44^-$); DN4 double negative 4 ($CD4^-$ $CD8^-$ $CD25^-$ $CD44^-$) and DP, double positive ($CD4^+$ $CD8^+$); spleen – $CD4^+$ T cells ($TCR\beta^+$ $CD4^+$); Naïve $CD4^+$ T cells ($TCR\beta^+$ $CD4^+$ $CD25^-$ $CD44^-$); Mem CD4, memory $CD4^+$ T cells ($TCR\beta^+$ $CD4^+$ $CD25^-$ $CD44^+$); Reg T, regulatory T cells ($TCR\beta^+$ $CD4^+$ $CD25^+$ $Foxp3^+$); $CD8^+$ T cells ($TCR\beta^+$ $CD8^+$); Naïve $CD8^+$ T cells ($TCR\beta^+$ $CD8^+$ $CD44^-$) and Mem CD8, memory $CD8^+$ T cells ($TCR\beta^+$ $CD8^+$ $CD44^-$).

6.3.2 Generation of a human FCRL6 transgenic mouse strain

Due to structural differences between human and mouse FCRL6 and the absence of *Fcrl6* expression during development or following activation of $CD4^+$ and $CD8^+$ T cells, we decided to generate a human FCRL6 (hFCRL6) expressing Tg mouse in order to study the function of this receptor in T lymphocytes. hFCRL6 expressing Tg mice were created by inserting cDNA encoding the canonical hFCRL6 isoform into the hCD2-VA expression cassette and integrating it into the DNA of fertilized B6 oocytes via pronuclear microinjection. The hCD2-VA expression cassette incorporates a 5 kilobase (kb) 5' promoter region as well as a 5.5 kb 3' locus control region containing a strong T cell specific enhancer and additional regulatory elements required for the establishment of an active chromatin domain in T cells (Zhumabekov *et al.* 1995). Thus, the use of this expression cassette allows for robust expression of hFCRL6 in $CD4^+$ and $CD8^+$ T cells in a transgene copy number dependent, position integration independent manner. Tg founder mice were identified via genotyping and confirmed by flow cytometry for the presence of human FCRL6 (Figure 31).

Figure 31: Human FCRL6 transgenic mice show robust expression of human FCRL6 on CD4$^+$ and CD8$^+$ T cells.

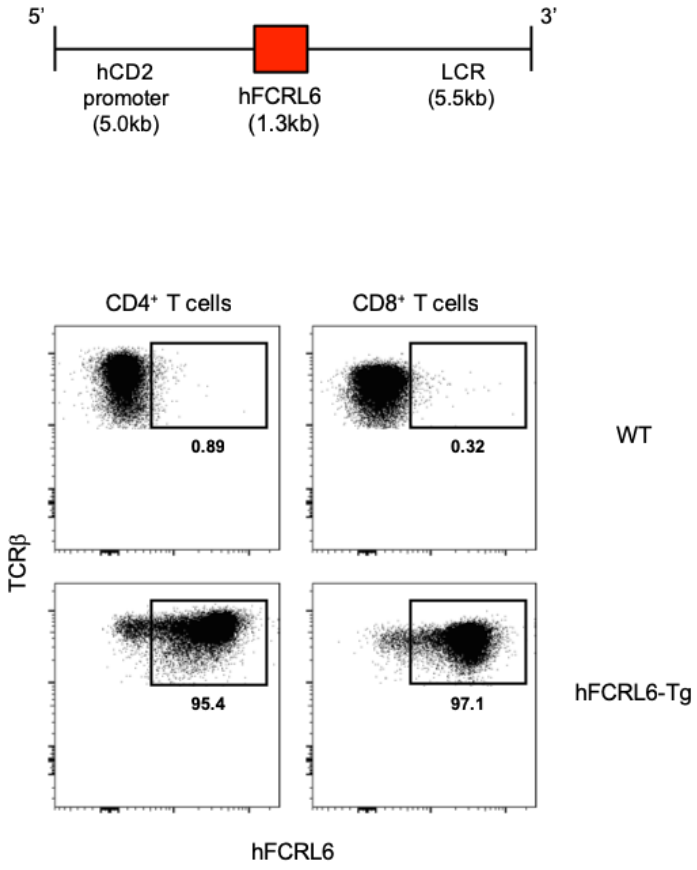

cDNA encoding the canonical human FCRL6 (hFCRL6) isoform was inserted into the hCD2-VA expression cassette and integrated into the DNA of fertilized B6 oocytes via pronuclear microinjection. Transgenic founders were identified by genotyping and flow cytometry for the presence of hFCRL6. CD4$^+$ and CD8$^+$ T cells were gated as TCRβ^+ CD4$^+$ and TCRβ^+ CD8$^+$, respectively.

6.3.2.1 T cell development in hFCRL6-Tg mice

To the best of our knowledge, this was the first attempt at generating a hFCRL6 expressing Tg mouse strain. The expression of hFCRL6 in hFCRL6-Tg mice occurs from at least the double negative stage in the thymus. Thus, we needed to first assess if the expression of hFCRL6 affected T cell development in mice by possibly altering the threshold for positive selection due to its predicted inhibitory nature. As before, we started by investigating if there are differences in the relative proportion of thymocytes or mature $CD4^+$ and $CD8^+$ T cells in hFCRL6-Tg mice under steady state conditions. The proportion and number of thymocytes in hFCRL6-Tg mice remained unchanged compared to WT mice. (Figure 32a). Next, we analysed mature $CD4^+$ and $CD8^+$ T cells in hFCRL6-Tg mice under steady state conditions. We did not observe a difference in the number and percentage of total $CD4^+$ and $CD8^+$ T cells in the spleen of hFCRL6-Tg mice compared to WT mice. We also did not find a difference in the percentage of naïve $CD4^+$ T, memory $CD4^+$ T and regulatory $CD4^+$ T cells in the spleen of hFCRL6-Tg mice compared to WT mice. Similarly, we did not identify a difference in the percentage of naïve $CD8^+$ T and memory $CD8^+$ T cells in the spleen of hFCRL6-Tg mice compared to WT mice (Figure 32b). Overall, these results suggested that transgene expression of hFCRL6 does not affect $CD4^+$ and $CD8^+$ T cell development (Figure 33).

Figure 32: There are no differences in developing and mature T cells in human FCRL6 transgenic mice.

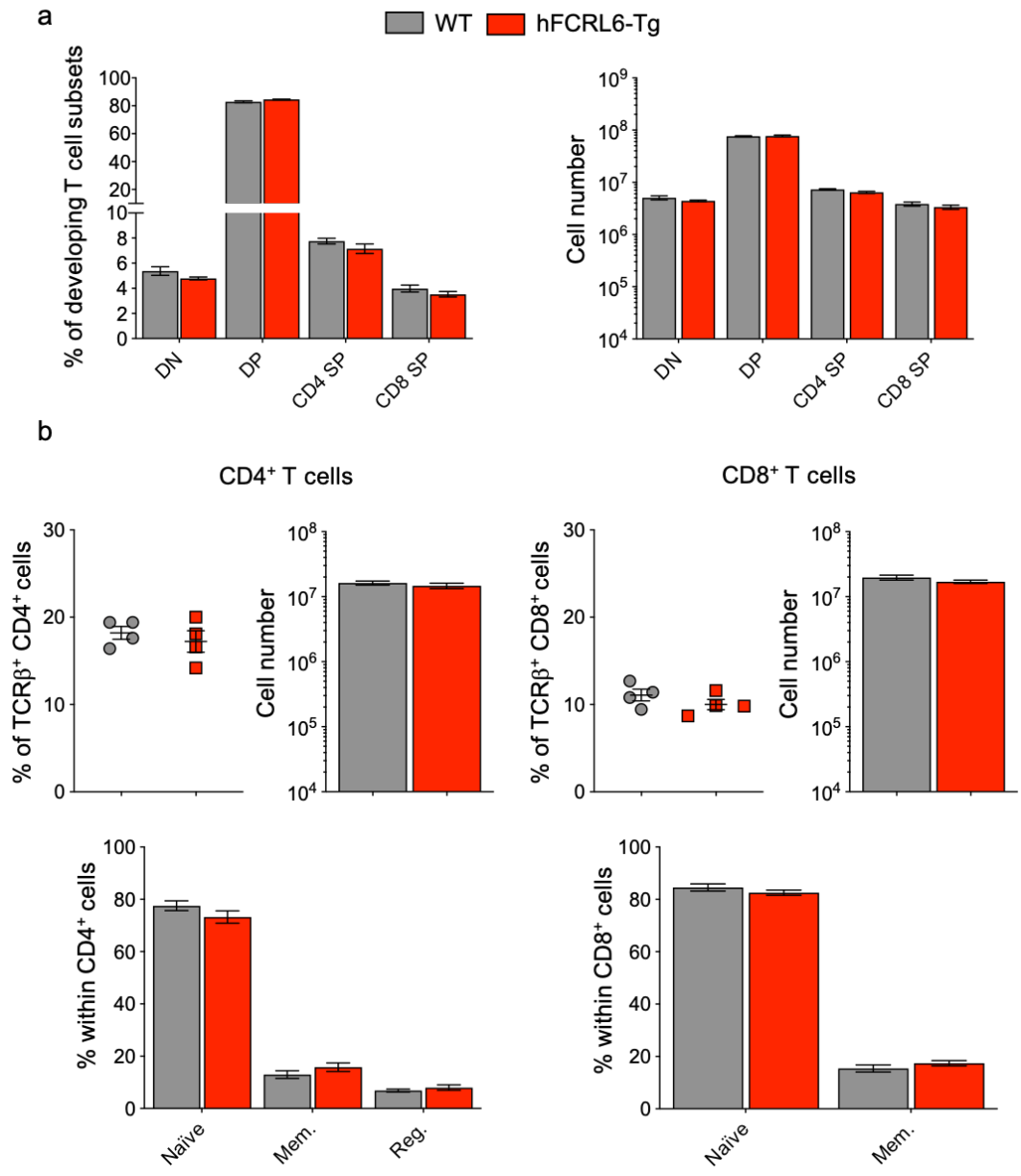

(a) Number and percentage of developing T cells in unchallenged hFCRL6-Tg and WT mice analysed via flow cytometry. Cell populations were gated as depicted in Figure 33. Bars represent mean ± SEM of 5 biological repeats per genotype. (b) Number and percentage of mature T cells in the spleens of unchallenged hFCRL6-Tg and WT mice analysed via flow cytometry. Cell populations were gated as depicted in Figure 33. Bars and symbols represent mean ± SEM of 4-6 biological repeats per genotype. CD4 SP, CD4 single positive; CD8 SP, CD8 single positive; DN, double negative; DP, double positive; Mem., memory; Reg., regulatory.

Figure 33: Human FCRL6 transgenic mice show normal T cell development.

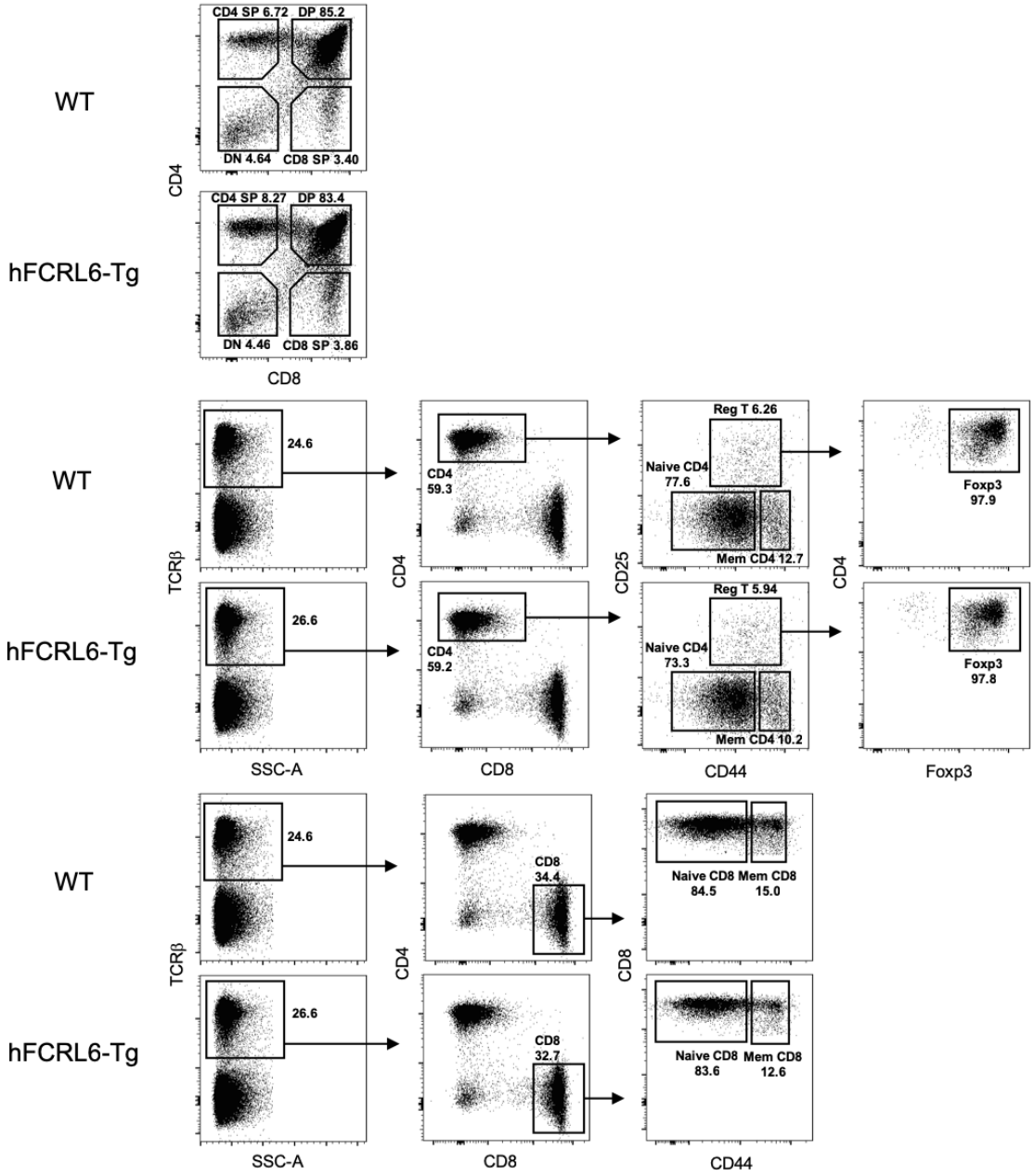

Flow cytometric gating strategy used for analysis of developing and mature T cell populations in Figure 32. Names are indicated by text next to the gates whilst numbers represent population percentage within that plot. Gating strategies were as follows: thymus – CD4 SP, CD4 single positive ($CD4^+$ $CD8^-$); CD8 SP, CD8 single positive ($CD4^-$ $CD8^+$); DN, double negative ($CD4^-$ $CD8^-$); DN1 double negative 1 ($CD4^-$ $CD8^-$ $CD25^-$ $CD44^+$); DN2 double negative 2 ($CD4^-$ $CD8^-$ $CD25^+$ $CD44^+$); DN3 double negative 3 ($CD4^-$ $CD8^-$ $CD25^+$ $CD44^-$); DN4 double negative 4 ($CD4^-$ $CD8^-$ $CD25^-$ $CD44^-$) and DP, double positive ($CD4^+$ $CD8^+$); spleen – $CD4^+$ T cells ($TCR\beta^+$ $CD4^+$);

Naïve $CD4^+$ T cells ($TCR\beta^+$ $CD4^+$ $CD25^-$ $CD44^-$); Mem CD4, memory $CD4^+$ T cells ($TCR\beta^+$ $CD4^+$ $CD25^-$ $CD44^+$); Reg T, regulatory T cells ($TCR\beta^+$ $CD4^+$ $CD25^+$ $Foxp3^+$); $CD8^+$ T cells ($TCR\beta^+$ $CD8^+$); Naïve $CD8^+$ T cells ($TCR\beta^+$ $CD8^+$ $CD44^-$) and Mem CD8, memory $CD8^+$ T cells ($TCR\beta^+$ $CD8^+$ $CD44^-$). hFCRL6, human FCRL6.

6.3.3 Function of human FCRL6 in T cells

6.3.3.1 In vitro activation of hFCRL6 expressing CD4$^+$ and CD8$^+$ T cells with anti-CD3/CD28 beads

Next, we aimed to investigate the effect of hFCRL6 expression during the activation of T cells. We stimulated splenocyte suspensions from hFCRL6-Tg and WT mice with anti-CD3/CD28 beads and analysed cell surface expression of T cell associated activation markers. We did not find a difference in the expression of CD25, CD44 and CD69 on CD4$^+$ and CD8$^+$ T cells from hFCRL6-Tg mice compared to WT mice at the analysed time points following activation (Figure 34a). Additionally, we loaded splenocyte suspensions from hFCRL6-Tg and WT mice with CellTrace Violet (CTV) prior to *in vitro* activation with anti-CD3/CD28 beads in order to identify differences in T cell proliferation. We did not identify a difference in the number of divisions of CD4$^+$ and CD8$^+$ T cells from hFCRL6-Tg mice compared to WT mice at day 3 following activation (Figure 34b).

Figure 34: Human FCRL6 transgenic CD4⁺ and CD8⁺ T show normal *in vitro* activation with anti-CD3/CD28 beads

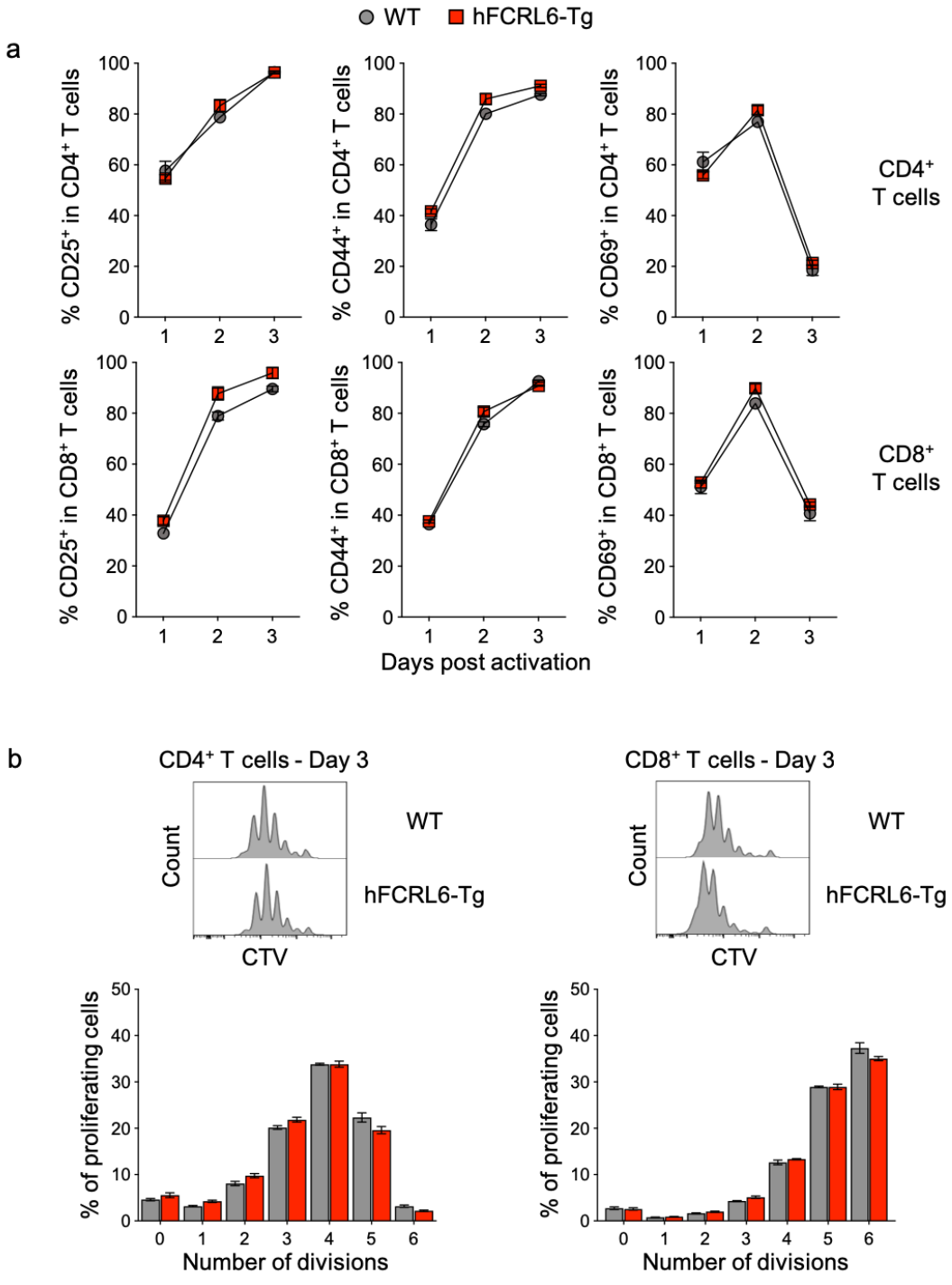

(a) Percentage of CD25⁺, CD44⁺ and CD69⁺ T cells following *in vitro* activation of splenocytes from hFCRL6-Tg and WT mice with anti-CD3/CD28 beads. (b) Percentage of CTV^{low} T cells at day 3 following *in vitro* activation of splenocytes from hFCRL6-Tg and WT mice with anti-

CD3/CD28 beads. Symbols and bars represent mean ± SEM of 3 biological repeats per genotype from 3 independent experiments.

6.3.3.2 In vivo activation of hFCRL6 expressing CD4⁺ T cells in response to a minor alloantigen mismatch

Minor histocompatibility antigens refer to small polymorphic peptides that are present on the cell surface in association with MHC class I and II molecules. Single amino acid differences in these peptides can be detected by T cells which become immunoreactive and can ultimately cause graft-versus-host disease (Roy & Perreault 2017). As *in vitro* polyclonal activation of $CD4^+$ and $CD8^+$ T cells remained unaffected by the presence of hFCRL6, we examined the effect of hFCRL6 expression on *in vivo* activation of $CD4^+$ T cells. We isolated and mixed $CD4^+$ T cells from $CD45.2^+$ hFCRL6-Tg and litter mate WT mice at a ratio of 52:48% with respect to WT and hFCRL6-Tg cells. Subsequently, we transferred this mixed suspension into B and T cell-deficient minor histocompatibility antigen mismatched recipient mice and analysed the expansion of WT and hFCRL6-Tg $CD4^+$ T cells as well as the expression of T cell associated activation markers. The expression of hFCRL6 did not affect the expansion of $CD4^+$ T cells following activation due to minor histocompatibility antigens as the percentage of hFCRL6-Tg $CD4^+$ T cells was similar to WT $CD4^+$ T cells at day 14 following transfer into recipient mice. Consequently, the ratio of WT to hFCRL6-Tg $CD4^+$ T cells at day 14 following transfer remained relatively unchanged compared to the initial ratio (Figure 35a). We also did not detect differences in the surface expression of CD25, CD43 and CD44 on hFCRL6-Tg $CD4^+$ T cells compared to WT $CD4^+$ T cells (Figure 35b).

Figure 35: Human FCRL6 transgenic CD4⁺ T cells show normal *in vivo* activation.

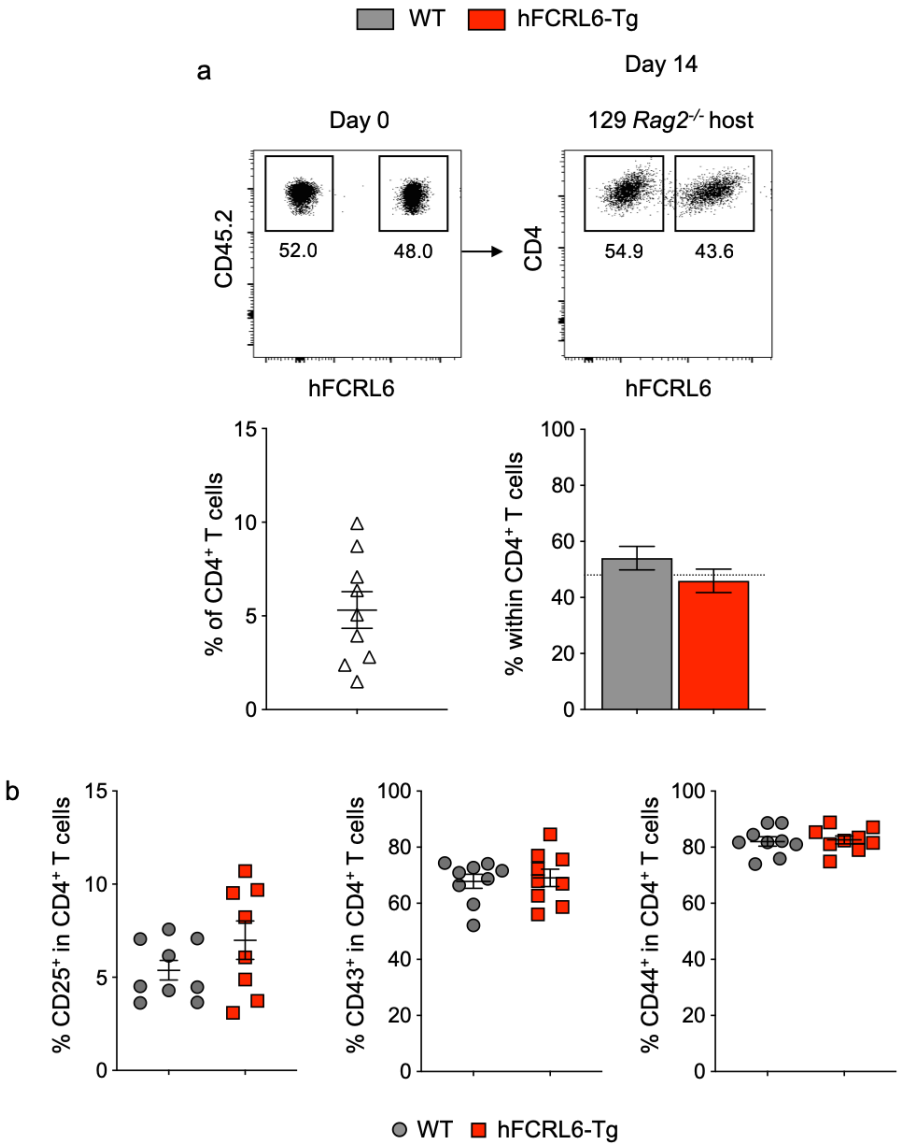

(a) Expansion of CD4⁺ T cells at day 14 in response to alloantigens following transfer into B and T cell-deficient minor histocompatibility antigen mismatched recipient mice. Dotted line indicates injected percentage of hFCRL6-Tg CD4⁺ T cells (b) Percentage of CD25⁺, CD43⁺ and CD44⁺ WT and hFCRL6-Tg CD4⁺ T cells at day 14 following transfer into recipient mice. Symbols and bars represent mean ± SEM of 9 biological repeats. CD4⁺ T cells were isolated as described in section 2.2.4 of materials and methods. CD45.2⁺ WT CD4⁺ T cells were mixed with CD45.2⁺ hFCRL6-Tg CD4⁺ T cells (48% hFCRL6-Tg CD4⁺ T cells) and injected intravenously into recipient mice. Expansion and activation were analysed 14 days later via flow cytometry. CD4+ T cells were gated as CD45.2⁺ TCRβ⁺ CD4⁺.

6.3.3.3 In vitro activation of EF4.1 human FCRL6 TCRβ-double transgenic CD4⁺ T cells with a cognate peptide

Thus far, we have analysed the potential role of hFCRL6 in the context of polyclonal activation of T cells. Next, we investigated the role of hFCRL6 in the context of antigen-specific T cell activation by crossing hFCRL6-Tg mice with EF4.1 mice, a TCRβ-Tg strain previously generated in our lab (Antunes *et al.* 2008) to create EF4.1 hFCRL6 TCRβ-double Tg (dTg) mice. This TCR–Tg system allowed us to study the $CD4^+$ T cell response to the A^b-restricted $env_{122-141}$ epitope derived from the gp70 envelope glycoprotein of FV. The use of EF4.1 mice also had an additional benefit as pairing of the TCRβ transgene in these mice with endogenous TCRα chains results in an increased frequency of FV specific $CD4^+$ T cells in these mice compared to WT mice (Antunes *et al.* 2008), thereby allowing us to use EF4.1 hFCRL6 TCRβ-dTg mice as a source of hFCRL6 expressing antigen-specific $CD4^+$ T cells

We first used $CD4^+$ T cells from EF4.1 hFCRL6 TCRβ-dTg mice to investigate the effect of hFCRL6 expression on *in vitro* $CD4^+$ T cell activation in response to varying levels of peptide stimulation. Accordingly, we activated splenocytes from EF4.1 hFCRL6 TCRβ-dTg and EF4.1 TCRβ-Tg mice with different concentrations of the $env_{122-141}$ F-MLV peptide, and analysed surface expression of T cell associated activation markers. $CD4^+$ T cells from both genotypes were also loaded with CTV prior to activation in order to investigate the effect of hFCRL6 expression on proliferation following stimulation.

We did not identify a difference in the initial activation of EF4.1 hFCRL6 TCRβ-dTg $CD4^+$ T cells as expression of the early T cell activation marker CD69 on these cells was comparable to that observed on EF4.1 TCRβ-Tg $CD4^+$ T cells (Figure 36a and 36b). The TCR Vα2 family possesses greater avidity for the $env_{122-141}$ peptide compared to other Vα families, and although Vα2 T cells are a minority in the naïve repertoire, these high-avidity T cells become the dominant subset at the peak of the *in vivo* response (Ploquin *et al.* 2011). Thus, we next examined the proportion of $V\alpha2^+$ cells within the responding population ($CD69^+$ $CD4^+$ T cells) from both genotypes at day 1

following activation. The percentage of Vα2 *env*-reactive cells within the responding EF4.1 hFCRL6 TCRβ-dTg $CD4^+$ T cell population remained similar to that observed in the responding population of EF4.1 TCRβ-Tg $CD4^+$ T cells (Figure 36b). Subsequently, we did not detect a difference in the percentage of CTV^{low} EF4.1 hFCRL6 TCRβ-dTg and CTV^{low} EF4.1 TCRβ-Tg $CD4^+$ T cells on day 3 following activation at all used concentrations of the $env_{122\text{-}141}$ peptide (Figure 36a and 36c). Similarly, the percentage of Vα2 *env*-reactive cells within the responding population (CTV^{low} $CD4^+$ T cells) of both genotypes also did not differ at this time point (Figure 36c).

Figure 36: EF4.1 human FCRL6 TCRβ-double transgenic CD4⁺ T cells show normal *in vitro* activation with env$_{122-141}$ peptide.

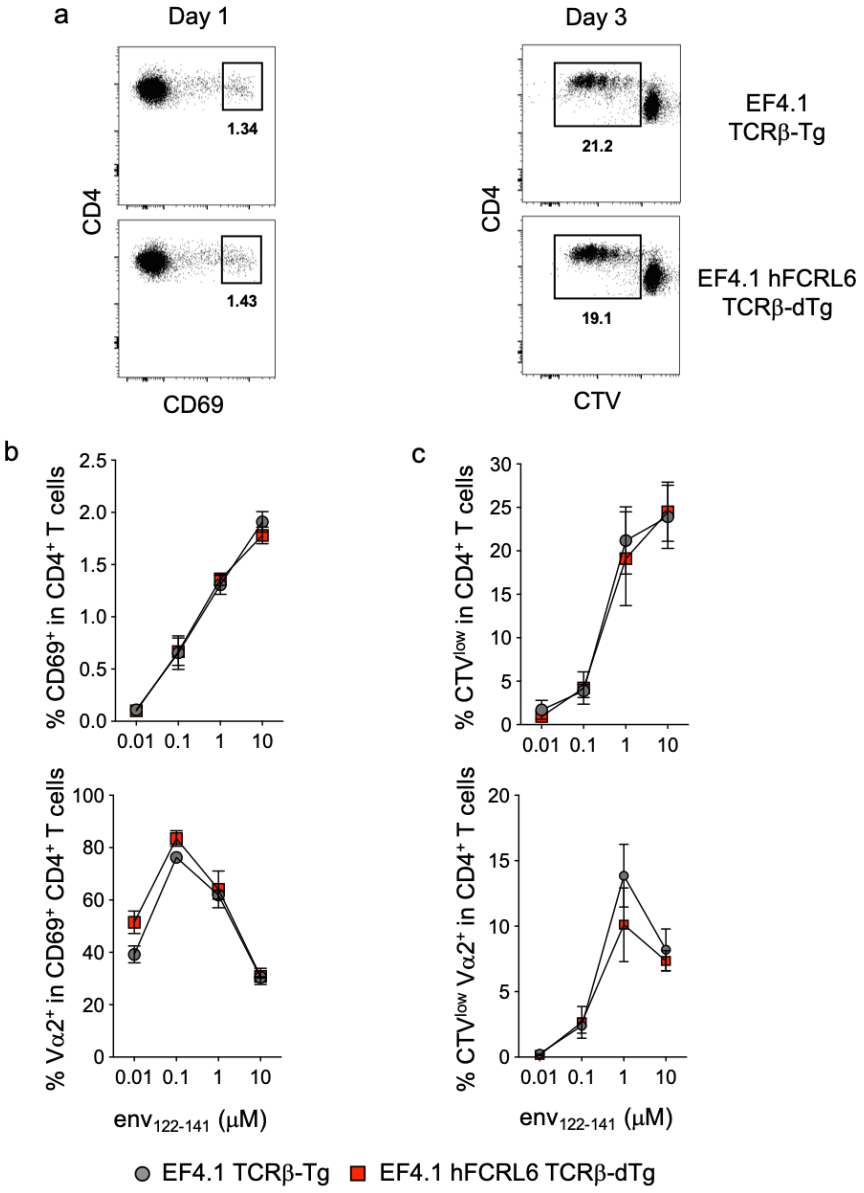

(a) Dot plots showing representative activation of EF4.1 TCRβ-Tg and EF4.1 hFCRL6 TCRβ-dTg cells at day 1 and 3 with 1mM env$_{122-141}$ peptide. (b) Percentage of CD69⁺ and Va2 *env*-reactive (CD69⁺) CD4⁺ T cells from EF4.1 TCRβ-Tg and EF4.1 hFCRL6 TCRβ-dTg mice at day 1 following *in vitro* activation with a range of env$_{122-141}$ peptide concentrations. (c) Percentage of CTV^{low} and Va2 *env*-reactive (CTV^{low}) CD4⁺ T cells CD4⁺ T cells from EF4.1 TCRβ-Tg and EF4.1 hFCRL6 TCRβ-dTg mice at day 3 following *in vitro* activation with a range of env$_{122-141}$ peptide concentrations. Symbols represent mean ± SEM of 3 biological repeats per genotype. CD4⁺ T

cells from EF4.1 TCRβ-Tg and EF4.1 hFCRL6 TCRβ-dTg were activated by directly adding varying concentrations of $env_{122-141}$ peptide to splenocyte suspensions.

6.3.3.4 In vivo activation of EF4.1 human FCRL6 TCRβ-double transgenic CD4⁺ T cells to a high affinity antigen in immunodeficient mice

Next, we used CD4⁺ T cells from EF4.1 hFCRL6 TCRβ-dTg mice to examine the effect of hFCRL6 expression during activation by a high affinity antigen. We isolated and mixed CD4⁺ T cells from EF4.1 TCRβ-Tg and EF4.1 hFCRL6 TCRβ-dTg mice at a ratio of 52:48% with respect to EF4.1 TCRβ-Tg and EF4.1 hFCRL6 TCRβ-dTg cells. Subsequently, we adoptively transferred this mixed suspension into B and T cell-deficient *Rag2*$^{-/-}$ recipient mice followed by infection with 1000 spleen focus-forming units of FV, and analysed the expansion of EF4.1 TCRβ-Tg and EF4.1 hFCRL6 TCRβ-dTg CD4⁺ T cells as well as the expression of T cell associated activation markers.

The expression of hFCRL6 did not affect the expansion of CD4⁺ T cells following FV infection as the percentage of EF4.1 hFCRL6 TCRβ-dTg CD4⁺ T cells was similar to EF4.1 TCRβ-Tg CD4⁺ T cells at day 14 following transfer into recipient mice. Consequently, the ratio of EF4.1 TCRβ-Tg to EF4.1 hFCRL6 TCRβ-dTg CD4⁺ T cells at day 14 following transfer remained relatively unchanged compared to the initial ratio (Figure 37a). We also did not detect differences in the surface expression of CD44 and co-expression of PD1 and LAG3 on EF4.1 hFCRL6 TCRβ-dTg and EF4.1 TCRβ-Tg CD4⁺ T cells in both recipient mice. Subsequently, we examined the proportion of Vα2⁺ cells within the responding CD4⁺ T cell population (CD44⁺ CD4⁺ T cells) from both genotypes at this time point. The percentage of Vα2 *env*-reactive cells within the responding EF4.1 hFCRL6 TCRβ-dTg CD4⁺ T cell population remained similar to that observed in the responding population of EF4.1 TCRβ-Tg CD4⁺ T cells (Figure 37b).

Figure 37: EF4.1 human FCRL6 TCRβ-double transgenic CD4⁺ T cells show normal *in vivo* activation to a high affinity antigen in immunodeficient mice.

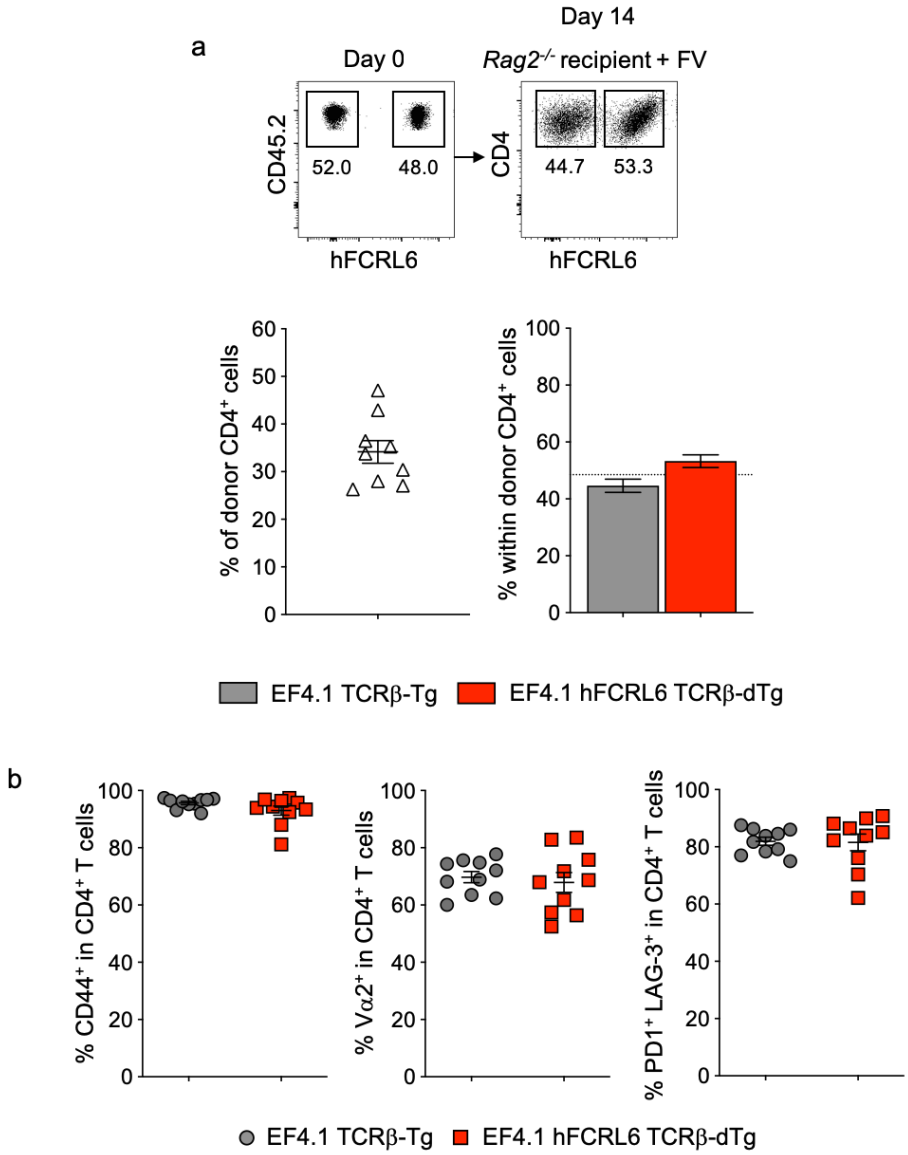

(a) Expansion of CD4⁺ T cells at day 14 following adoptive transfer into B and T cell-deficient recipient mice and FV infection. Dotted line indicates injected percentage of EF4.1 hFCRL6 TCRβ-dTg CD4⁺ T cells (b) Percentage of CD44⁺, Va2 *env*-reactive (CD44⁺) and PD1⁺ LAG-3⁺ EF4.1 TCRβ-Tg and EF4.1 hFCRL6 TCRβ-dTg CD4⁺ T cells at day 14 following transfer into recipient mice. Symbols and bars represent mean ± SEM of 10 biological repeats. CD4⁺ T cells were isolated as described in section 2.2.4 of materials and methods. CD45.2⁺ EF4.1 TCRβ-Tg CD4⁺ T cells were mixed with CD45.2⁺ EF4.1 hFCRL6 TCRβ-dTg CD4⁺ T cells (48% EF4.1 hFCRL6 TCRβ-dTg CD4⁺ T cells) and injected intravenously into recipient mice alongside 1000

spleen focus-forming units of FV. Expansion and activation were analysed 14 days later via flow cytometry. CD4+ T cells were gated as CD45.2^{+} TCRβ^{+} CD4^{+}.

6.3.3.5 In vivo activation of EF4.1 human FCRL6 TCRβ-double transgenic CD4+ T cells to a high affinity antigen in immunocompetent mice

We next investigated the effect of hFCRL6 expression during activation of $CD4^+$ T cells by a high affinity antigen in immunocompetent mice. We crossed hFCRL6-Tg mice with $CD45.1^{+/}CD45.2^+$ WT mice to generate $hFCRL6^+$ recipient mice in order to control for immune rejection of the hFCRL6 molecule by recipient mice. We isolated and mixed $CD4^+$ T cells from EF4.1 TCRβ-Tg and EF4.1 hFCRL6 TCRβ-dTg mice at a ratio of 46:54% with respect to EF4.1 TCRβ-Tg and EF4.1 hFCRL6 TCRβ-dTg cells. Subsequently, we adoptively transferred this mixed suspension into FV-infected immunocompetent recipient mice, and analysed the expansion of EF4.1 TCRβ-Tg and EF4.1 hFCRL6 TCRβ-dTg $CD4^+$ T cells as well as the expression of T cell associated activation markers and T cell differentiation.

The expression of hFCRL6 did not affect the expansion of $CD4^+$ T cells following FV infection as the percentage of EF4.1 hFCRL6 TCRβ-dTg $CD4^+$ T cells was similar to EF4.1 TCRβ-Tg $CD4^+$ T cells at day 7 following transfer into recipient mice. Consequently, the ratio of EF4.1 TCRβ-Tg to EF4.1 hFCRL6 TCRβ-dTg $CD4^+$ T cells at day 7 following transfer remained relatively unchanged compared to the initial ratio (Figure 38a). We also did not detect differences in the surface expression of CD44 and co-expression of PD1 and LAG3 on EF4.1 hFCRL6 TCRβ-dTg and EF4.1 TCRβ-Tg $CD4^+$ T cells. Thereafter, we examined the proportion of $V\alpha2^+$ cells within the responding $CD4^+$ T cell population ($CD44^+$ $CD4^+$ T cells) from both genotypes at this time point. The percentage of Vα2 *env*-reactive cells within the responding EF4.1 hFCRL6 TCRβ-dTg $CD4^+$ T cell population remained similar to that observed in the responding population of EF4.1 TCRβ-Tg $CD4^+$ T cells (Figure 38b). The differentiation of $CD4^+$ T cells also did not differ in the presence of hFCRL6 as a similar percentage of T_{H1} and T_{FH} cells were detected following activation of EF4.1 hFCRL6 TCRβ-dTg and EF4.1 TCRβ-Tg $CD4^+$ T cells at day 7 following transfer in recipient mice (Figure 38c).

Figure 38: EF4.1 human FCRL6 TCRβ-double transgenic CD4⁺ T cells show normal *in vivo* activation to a high affinity antigen in immunocompetent mice.

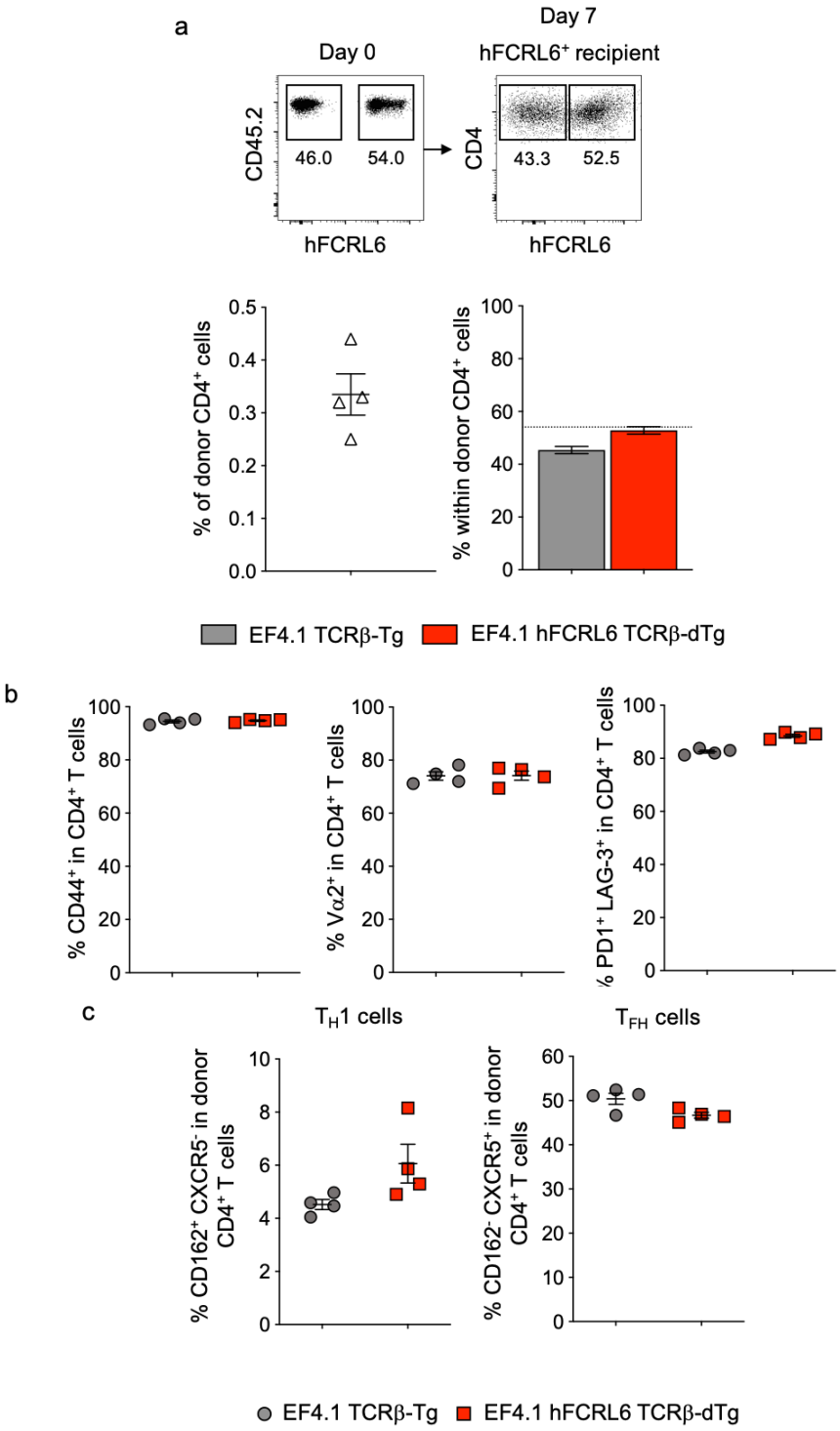

(a) Expansion of CD4⁺ T cells at day 7 following adoptive transfer into immunocompetent hFCRL6⁺ recipient mice and FV infection. Dotted line indicates injected percentage of EF4.1 hFCRL6 TCRβ-dTg CD4⁺ T cells (b) Percentage of CD44⁺, Va2 *env*-reactive (CD44⁺) and PD1⁺

LAG-3$^+$ EF4.1 TCRβ-Tg and EF4.1 hFCRL6 TCRβ-dTg CD4$^+$ T cells at day 7 following transfer into hFCRL6$^+$ recipient mice. (c) Differentiation of EF4.1 TCRβ-Tg and EF4.1 hFCRL6 TCRβ-dTg CD4$^+$ T cells at day 7 following transfer into hFCRL6$^+$ recipient mice. Symbols and bars represent mean ± SEM of 4 biological repeats. CD4$^+$ T cells were isolated as described in section 2.2.4 of materials and methods. CD45.2$^+$ EF4.1 TCRβ-Tg CD4$^+$ T cells were mixed with CD45.2$^+$ EF4.1 hFCRL6 TCRβ-dTg CD4$^+$ T cells (54% EF4.1 hFCRL6 TCRβ-dTg CD4$^+$ T cells) and injected intravenously into recipient mice alongside 1000 spleen focus-forming units of FV. Expansion and activation were analysed 7 days later via flow cytometry. CD4+ T cells were gated as CD45.2$^+$ TCRβ$^+$ CD4$^+$.

6.3.3.6 In vivo activation of EF4.1 human FCRL6 TCRβ-double transgenic CD4⁺ T cells to a low affinity antigen

Next, to exclude that the FCRL6 function may be hindered by our experimental conditions, we examined the effect of hFCRL6 expression during sub-optimal *in vivo* activation with a low affinity antigen. *Emv2* is a single copy endogenous retrovirus which has been identified in the genome of C57BL/6J and related strains of mice (Jenkins *et al.* 1982). *Emv2* encodes a full-length provirus that is unable to produce infectious particles due to an inactivating mutation in the *pol* gene (King *et al.* 1988). However, *Emv2* retains the ability for *env* expression, and, notably, the *env* epitope of *Emv2* is almost identical to that of F-MLV apart from a single amino acid substitution. Previous work in our lab has identified that CD4$^+$ T cells from EF4.1 TCRβ-Tg mice can be activated by the *env* of *Emv2*, albeit less potently than by the *env* of F-MLV (Young *et al.* 2012). We isolated and mixed CD4$^+$ T cells from EF4.1 TCRβ-Tg and EF4.1 hFCRL6 TCRβ-dTg mice at a ratio of 52:48% with respect to EF4.1 TCRβ-Tg and EF4.1 hFCRL6 TCRβ-dTg cells. We adoptively transferred this mixed suspension into B and T cell-deficient *Rag1*$^{-/-}$ and *Rag2*$^{-/-}$ recipient mice on the C57BL/6J background which have different levels of *Emv2* expression, and analysed the expansion of EF4.1 TCRβ-Tg and EF4.1 hFCRL6 TCRβ-dTg CD4$^+$ T cells as well as the expression of T cell associated activation markers.

hFCRL6 expression did not affect CD4$^+$ T cells expansion following activation by the *env* of *Emv2* as the percentage of EF4.1 hFCRL6 TCRβ-dTg CD4$^+$ T cells was similar to EF4.1 TCRβ-Tg CD4$^+$ T cells at day 14 following transfer in both recipient mice. Consequently, the ratio of EF4.1 TCRβ-Tg to EF4.1 hFCRL6 TCRβ-dTg CD4$^+$ T cells at day 14 following transfer remained relatively unchanged compared to the initial ratio in both recipient mice (Figure 39a). We also did not detect differences in the surface expression of CD44 and co-expression of PD1 and LAG3 on EF4.1 hFCRL6 TCRβ-dTg and EF4.1 TCRβ-Tg CD4$^+$ T cells in both recipient mice. We next examined the proportion of Vα2$^+$ cells within the responding CD4$^+$ T cell population (CD44$^+$ CD4$^+$ T cells) from both genotypes at this time point. The percentage of Vα2 *env*-reactive cells within the

responding EF4.1 hFCRL6 TCRβ-dTg $CD4^+$ T cell population remained similar to that observed in the responding population of EF4.1 TCRβ-Tg $CD4^+$ T cells in both recipient mice (Figure 39b). The obtained results were comparable in both *Rag1*$^{-/-}$ and *Rag2*$^{-/-}$ mice, thereby suggesting that not only the quality but also the quantity of available antigen does not affect the activation of hFCRL6 expressing $CD4^+$ T cells.

Figure 39: EF4.1 human FCRL6 TCRβ-double transgenic CD4⁺ T cells show normal *in vivo* activation in response to a low affinity antigen in immunodeficient mice.

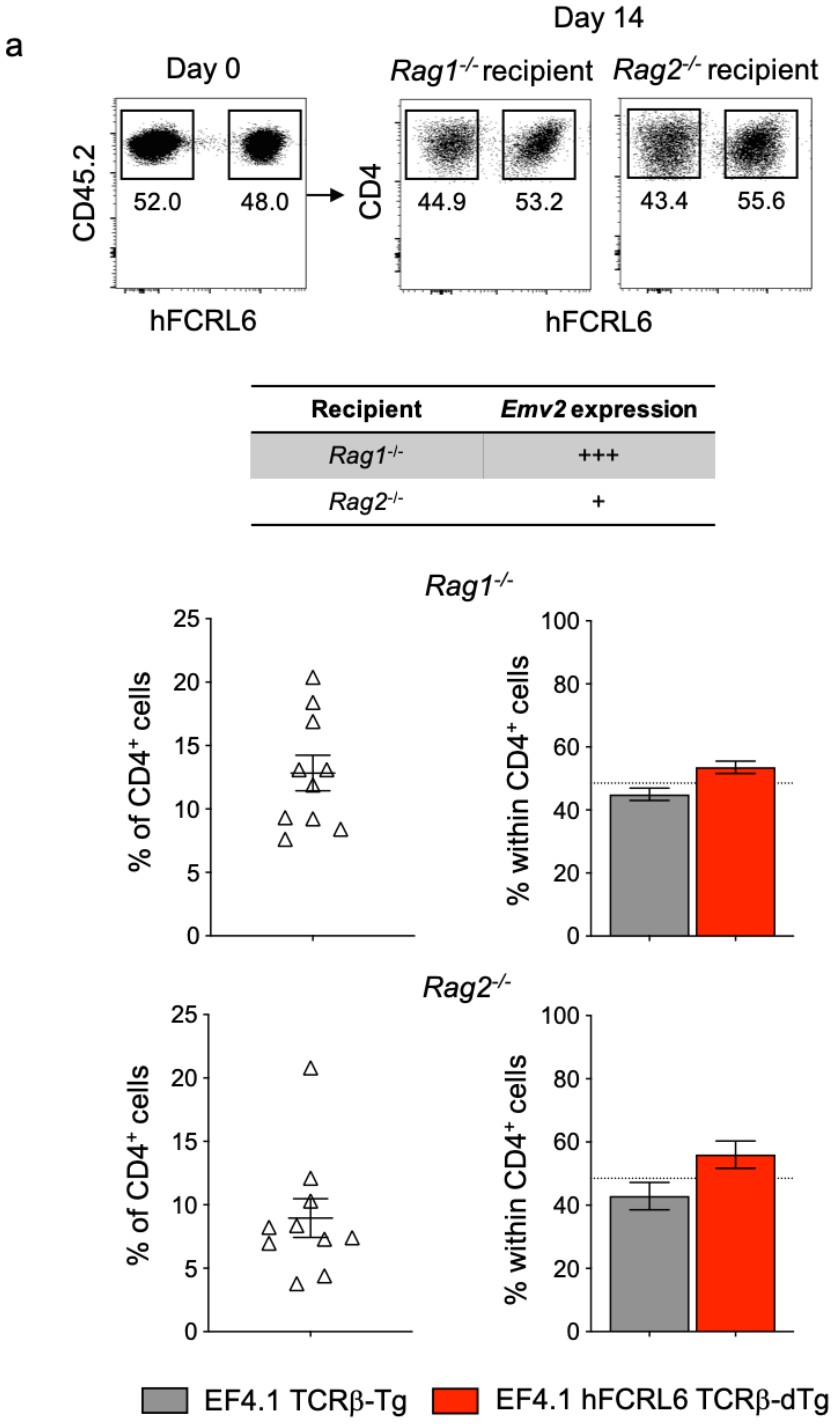

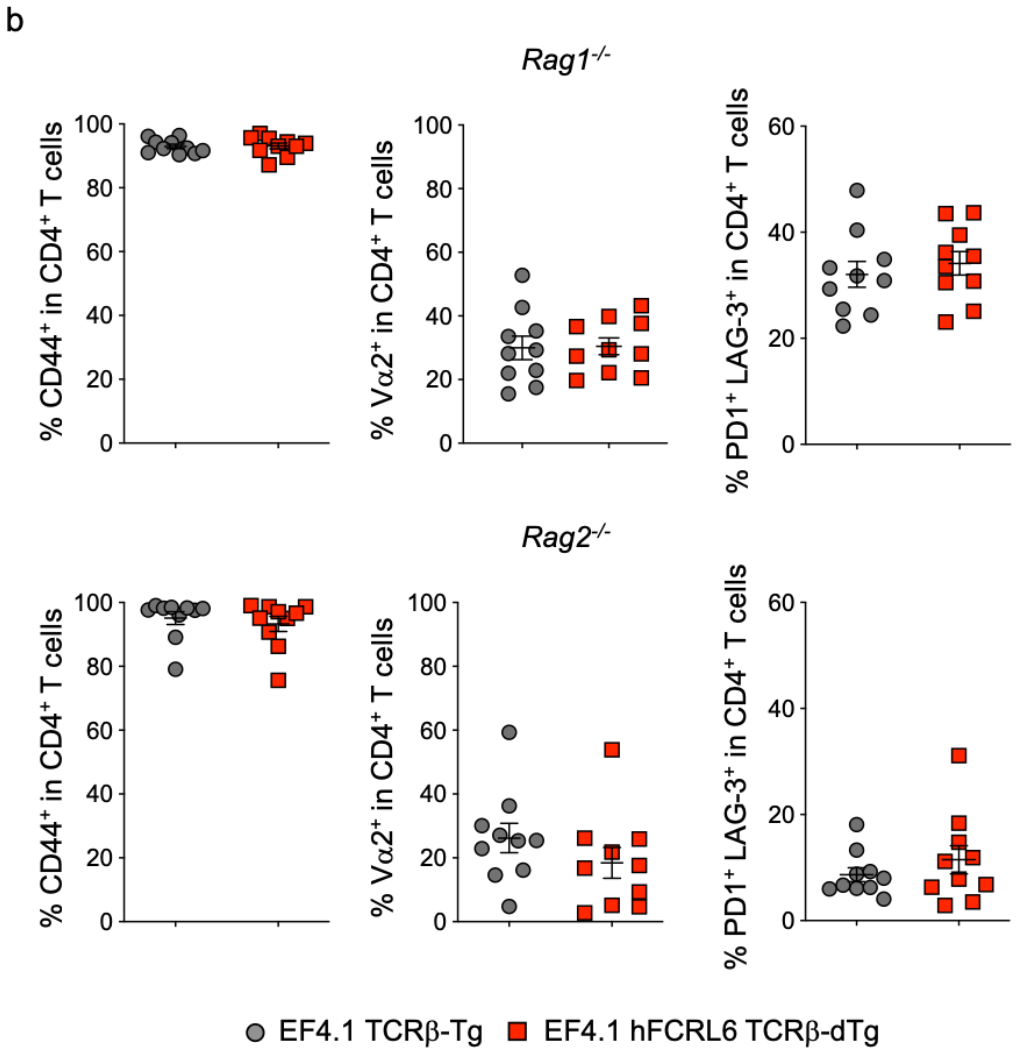

(a) Expansion of CD4⁺ T cells at day 14 following adoptive transfer into *Emv2* expressing B and T cell-deficient recipient mice. Dotted line indicates injected percentage of EF4.1 hFCRL6 TCRβ-dTg CD4⁺ T cells (b) Percentage of CD44⁺, Va2 *env*-reactive (CD44⁺) and PD1⁺ LAG-3⁺ EF4.1 TCRβ-Tg and EF4.1 hFCRL6 TCRβ-dTg CD4⁺ T cells at day 14 following transfer into recipient mice. Symbols and bars represent mean ± SEM of 10 biological repeats. CD4⁺ T cells were isolated as described in section 2.2.4 of materials and methods. CD45.2⁺ EF4.1 TCRβ-Tg CD4⁺ T cells were mixed with CD45.2⁺ EF4.1 hFCRL6 TCRβ-dTg CD4⁺ T cells (48.5% EF4.1 hFCRL6 TCRβ-dTg CD4⁺ T cells) and injected intravenously into recipient mice. Expansion and activation were analysed 14 days later via flow cytometry. CD4+ T cells were gated as CD45.2⁺ TCRβ⁺ CD4⁺.

6.3.3.7 In vitro activation of EF4.1 human FCRL6 TCRβ-double transgenic CD4+ T cells by B3 MHCII cells transduced with human leukocyte antigen-DR and a cognate peptide

In our hands, transgene expression of hFCRL6 did not seem to affect *in vitro* or *in vivo* $CD4^+$ T cell activation. Since hFCRL6 has been suggested to act as an inhibitory receptor, we hypothesized that the lack of effect may be due to the absence of a physiological ligand of hFCRL6 in our experimental conditions. Human leukocyte antigen-DR (HLA-DR), an MHC Class II surface receptor, has been previously identified as a ligand for hFCRL6 (Schreeder *et al.* 2010). To examine the effect of hFCRL6 and HLA-DR interaction, we transduced B3 cells, a pro-B leukaemia cell line (Fisher *et al.* 1995) with retroviral vectors expressing the α and β chains of HLA-DR as well as the α and β chains of mouse H2-Ab and used them as antigen presenting cells in co-culture assays.

The expression of hFCRL6 on $CD4^+$ T cells and HLA-DR on B3 MHCII cells did not affect early CD69 expression on EF4.1 hFCRL6 TCRβ-dTg $CD4^+$ T cells compared to EF4.1 TCRβ-Tg $CD4^+$ T cells at day 1 following activation at all tested concentrations of the $env_{122\text{-}141}$ peptide (Figure 40a). Thereafter, we investigated $CD4^+$ T cell proliferation at day 3 following activation and identified that the expression of hFCRL6 on $CD4^+$ T cells and HLA-DR on B3 MHCII cells resulted in a reduced percentage of CTV^{low} EF4.1 hFCRL6 TCRβ-dTg $CD4^+$ T cells compared to CTV^{low} EF4.1 TCRβ-Tg $CD4^+$ T cells with increasing concentrations of $env_{122\text{-}141}$ peptide. This difference was not detected when analysing the percentage of CTV^{low} $CD4^+$ T cells from both genotypes in the absence of HLA-DR expression on B3 MHCII cells at this time point (Figure 40b). An identical result was observed at day 6 following activation where a greater difference in the percentage of CTV^{low} cells was detected between EF4.1 TCRβ-Tg and EF4.1 hFCRL6 TCRβ-dTg $CD4^+$ T cells in the presence of HLA-DR on B3 MHCII cells at all concentrations of $env_{122\text{-}141}$ peptide. As observed at day 3 following activation, this difference was not replicated in the absence of HLA-DR expression on B3 MHCII cells (Figure 40c). Overall, these data suggested that whilst early T

activation is not affected, the interaction of hFCRL6 with its ligand HLA-DR could limit long term T cell activation and proliferation.

Figure 40: EF4.1 human FCRL6 TCRβ-double transgenic CD4⁺ T cells show reduced *in vitro* activation in presence of HLA-DR when activated with B3 MHCII and env$_{122-141}$ peptide.

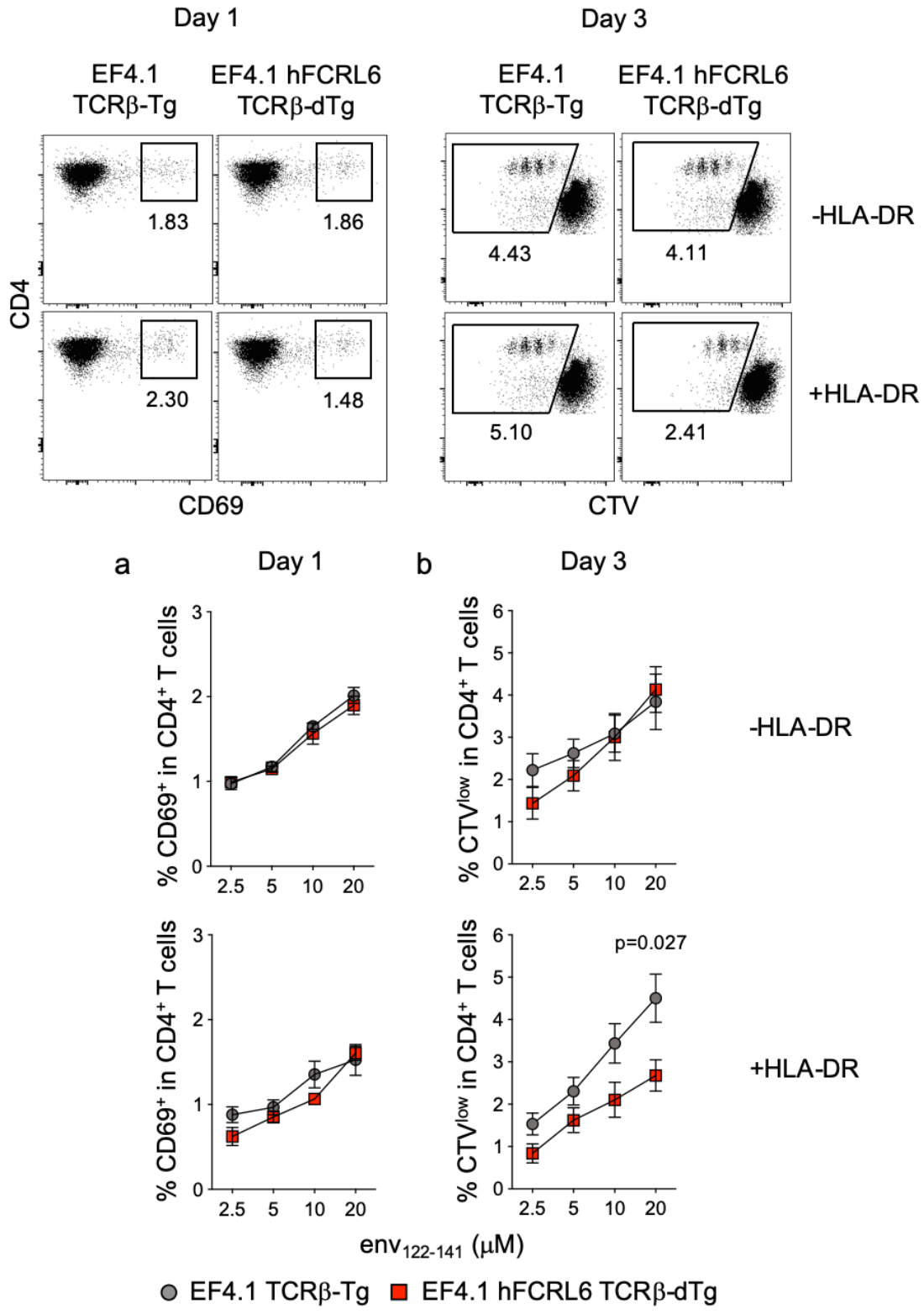

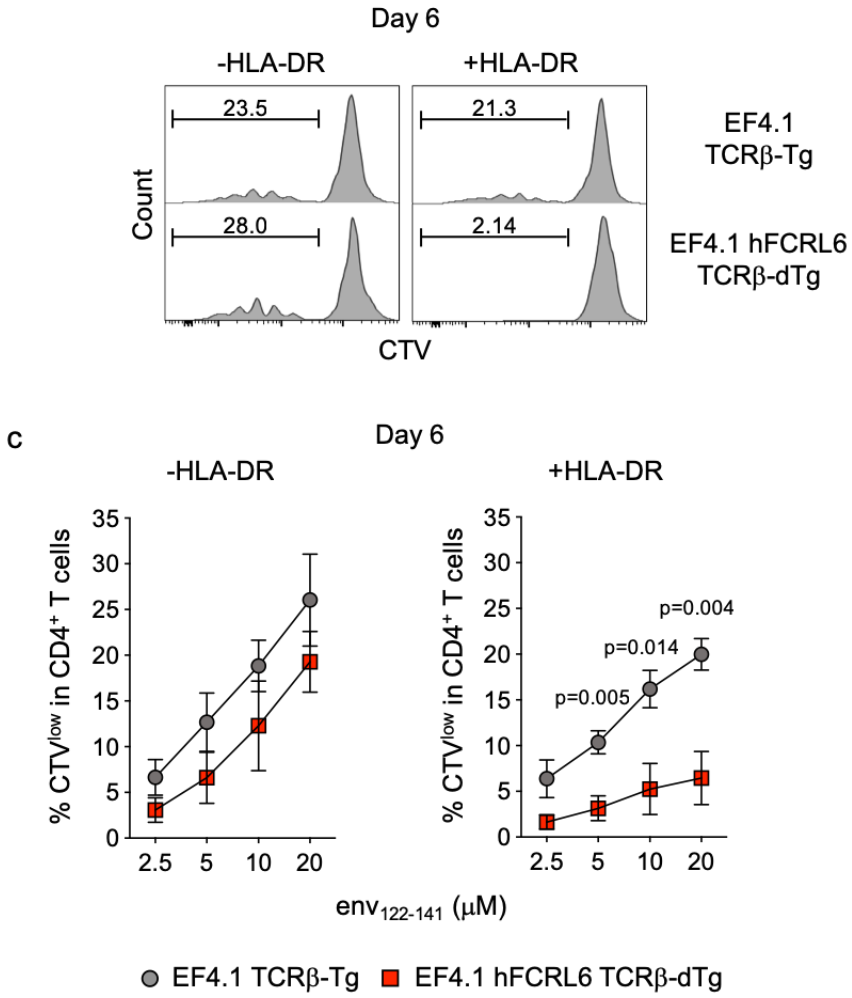

(a) Percentage of $CD69^+$ EF4.1 TCRβ-Tg and EF4.1 hFCRL6 TCRβ-dTg $CD4^+$ T cells at day 1 following *in vitro* activation with B3 MHCII and varying concentrations of $env_{122-141}$ peptide (b) Percentage of CTV^{low} EF4.1 TCRβ-Tg and EF4.1 hFCRL6 TCRβ-dTg $CD4^+$ T cells at day 3 following *in vitro* activation with B3 MHCII and varying concentrations of $env_{122-141}$ peptide. (c) Percentage of CTV^{low} EF4.1 TCRβ-Tg and EF4.1 hFCRL6 TCRβ-dTg $CD4^+$ T cells at day 6 following *in vitro* activation with B3 MHCII and varying concentrations of $env_{122-141}$ peptide. Symbols represent mean ± SEM of 5 biological repeats per genotype from 2 independent experiments. Dot plots and histogram show representative activation with 20mM $env_{122-141}$ peptide. $CD4^+$ T cells were isolated as described in section 2.2.4 of materials and methods. EF4.1 TCRβ-Tg and EF4.1 hFCRL6 TCRβ-dTg $CD4^+$ T cells were incubated with $HLA\text{-}DR^+$ or $HLA\text{-}DR^-$ B3 MHCII and $env_{122-141}$ peptide to analyse the effect of hFCRL6 and HLA-DR interaction on CD4+ T cell activation.

6.3.3.8 In vitro activation of EF4.1 human FCRL6 TCRβ-double transgenic CD4+ T cells by B3 MHCII$^{env123-139}$ cells transduced with human leukocyte antigen-DR, a known ligand of human FCRL6

Thus far, our data suggested that, whilst early T activation is not affected, the interaction of hFCRL6 with its ligand HLA-DR could limit long-term T cell activation and proliferation. To confirm our observation, we stimulated CD4$^+$ T cells from EF4.1 hFCRL6 TCRβ-dTg and EF4.1 TCRβ-Tg mice with B3 MHCII$^{env123-139}$, a variant of the B3 cell line transduced with retroviral vectors expressing the H2-A^b α and β chains covalently linked to the env$_{123-139}$ peptide recognised by EF4.1 TCRβ-Tg CD4$^+$ T cells, as well as the α and β chains of HLA-DR, and analysed the surface expression of T cell associated activation markers. The covalently bound peptide expressed by these cells is similar to env$_{122-141}$ as it retains all of the important TCR contact residues present in env$_{122-141}$ (Shimizu *et al.* 1994). The rationale behind this approach involved mimicking persistent and strong antigen stimulation that would be experienced by these cells *in vivo* in states of chronic immune activation thereby, allowing us to investigate the inhibitory potential of hFCRL6 in this setting. CD4$^+$ T cells from both genotypes were also loaded with CTV prior to activation in order to investigate the effect of hFCRL6 expression on proliferation following stimulation.

The expression of hFCRL6 on CD4$^+$ T cells and HLA-DR on B3 MHCII$^{env123-139}$ appeared to slightly reduce CD69 expression on EF4.1 hFCRL6 TCRβ-dTg CD4$^+$ T cells compared to EF4.1 TCRβ-Tg CD4$^+$ T cells at day 1 following activation. A similar decrease was not observed in the absence of HLA-DR expression on B3 MHCII$^{env123-139}$ (Figure 41a). Next, we investigated CD4$^+$ T cell proliferation at day 3 following activation and identified that the expression of hFCRL6 on CD4$^+$ T cells and HLA-DR on B3 MHCII$^{env123-139}$ resulted in a reduced percentage of CTV^{low} EF4.1 hFCRL6 TCRβ-dTg CD4$^+$ T cells compared to CTV^{low} EF4.1 TCRβ-Tg CD4$^+$ T cells. This difference was not detected when analysing the percentage of CTV^{low} CD4$^+$ T cells from both genotypes in the absence of HLA-DR expression on B3 MHCII$^{env123-139}$ at this time point (Figure 41b). A similar result was also observed at day 6 following activation where a significant difference in the percentage of CTV^{low} cells was detected between EF4.1 TCRβ-Tg and EF4.1 hFCRL6

TCRβ-dTg $CD4^+$ T cells in the presence of HLA-DR on B3 $MHCII^{env123-139}$. As observed at day 3 following activation, this difference was not replicated in the absence of HLA-DR expression on B3 $MHCII^{env123-139}$ (Figure 41c).

Figure 41: EF4.1 human FCRL6 TCRβ-double transgenic CD4⁺ T cells show reduced *in vitro* activation in presence of HLA-DR when activated with B3 MHCII$^{env123-139}$.

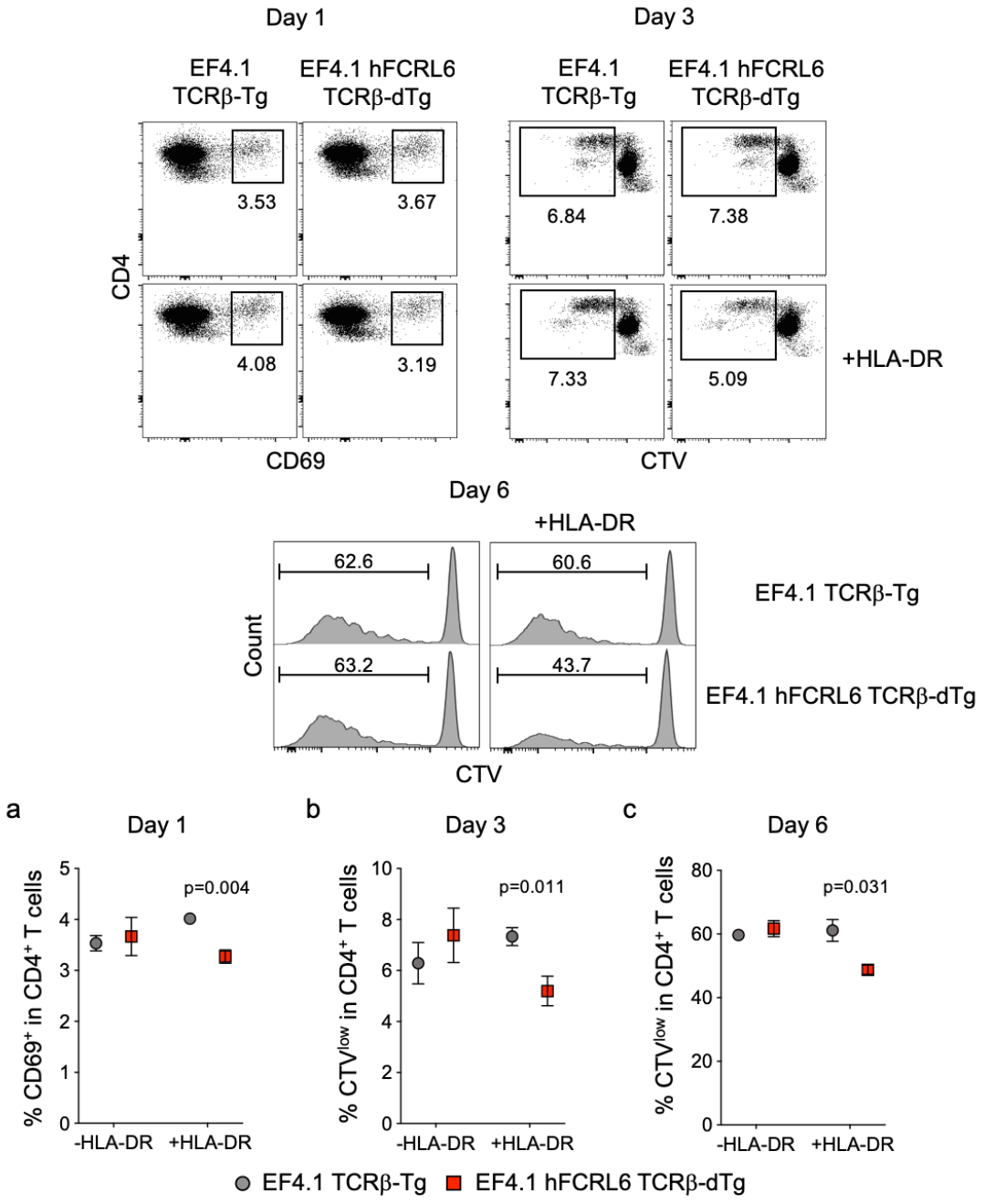

(a) Percentage of CD69⁺ EF4.1 TCRβ-Tg and EF4.1 hFCRL6 TCRβ-dTg CD4⁺ T cells at day 1 following *in vitro* activation with B3 MHCII$^{env123-139}$ (b) Percentage of CTV^{low} EF4.1 TCRβ-Tg and EF4.1 hFCRL6 TCRβ-dTg CD4⁺ T cells at day 3 following *in vitro* activation with B3 MHCII$^{env123-139}$. (c) Percentage of CTV^{low} EF4.1 TCRβ-Tg and EF4.1 hFCRL6 TCRβ-dTg CD4⁺ T cells at day

6 following *in vitro* activation with B3 MHCII$^{env123-139}$. Symbols represent mean ± SEM of 2-3 biological repeats per genotype from 3 independent experiments. Dot plots and histogram show representative activation. CD4$^+$ T cells were isolated as described in section 2.2.4 of materials and methods. EF4.1 TCRβ-Tg and EF4.1 hFCRL6 TCRβ-dTg hFCRL6 CD4$^+$ T cells were incubated with HLA-DR$^+$ or HLA-DR$^-$ B3 MHCII$^{env123-139}$ cells to analyse the effect of hFCRL6 and HLA-DR interaction on CD4$^+$ T cell activation.

6.3.3.9 In vivo activation of EF4.1 human FCRL6 TCRβ-double transgenic CD4⁺ T cells by B3 MHCII$^{env123-139}$ transduced with human leukocyte antigen-DR

Since the interaction of HLA-DR and hFCRL6 appears to have a selective inhibitory effect on *in vitro* T cell proliferation, we next aimed to investigate if this effect could be recapitulated in an *in vivo* setting. For this reason, we isolated and mixed CD4⁺ T cells from EF4.1 TCRβ-Tg and EF4.1 hFCRL6 TCRβ-dTg mice at a ratio of 61:39% with respect to EF4.1 TCRβ-Tg and EF4.1 hFCRL6 TCRβ-dTg cells. Subsequently, we adoptively transferred this mixed suspension into immunocompetent recipient mice immunised with B3 MHCII$^{env123-139}$ cells, and analysed the relative expansion of EF4.1 TCRβ-Tg and EF4.1 hFCRL6 TCRβ-dTg CD4⁺ T cells as well as the expression of T cell associated activation markers.

hFCRL6 expression on CD4⁺ T cells and HLA-DR on B3 MHCII$^{env123-139}$ cells did not affect CD4⁺ T cell expansion as the percentage of EF4.1 hFCRL6 TCRβ-dTg CD4⁺ T cells was similar to EF4.1 TCRβ-Tg CD4⁺ T cells at day 7 following transfer in recipient mice injected with HLA-DR⁺ B3 MHCII$^{env123-139}$ cells. Consequently, the ratio of EF4.1 TCRβ-Tg to EF4.1 hFCRL6 TCRβ-dTg CD4⁺ T cells at day 7 following transfer remained unchanged compared to the initial ratio in recipient mice injected with HLA-DR⁺ or HLA-DR⁻ B3 MHCII$^{env123-139}$ cells. However, we observed an overall reduction in percentage of CD4⁺ T cells in the spleen of recipient mice injected with HLA-DR⁺ B3 MHCII$^{env123-139}$ cells compared to those injected with HLA-DR⁻ B3 MHCII$^{env123-139}$ cells (Figure 42a). We did not detect differences in the expression of CD44 and PD1 on EF4.1 hFCRL6 TCRβ-dTg and EF4.1 TCRβ-Tg CD4⁺ T cells at day 7 following transfer in recipient mice injected with HLA-DR⁺ or HLA-DR⁻ B3 MHCII$^{env123-139}$ cells. We also did not detect a difference in intracellular granzyme B in EF4.1 hFCRL6 TCRβ-dTg and EF4.1 TCRβ-Tg CD4⁺ T cells at day 7 following transfer in recipient mice injected with HLA-DR⁺ or HLA-DR⁻ B3 MHCII$^{env123-139}$ cells. Next, we examined the proportion of Vα2⁺ cells within the responding CD4⁺ T cell population (CD44⁺ CD4⁺ T cells) at this time point in recipient mice injected with HLA-DR⁺ and HLA-DR⁻ B3 MHCII$^{env123-139}$ cells. The percentage of Vα2 *env*-reactive cells within the responding EF4.1 hFCRL6 TCRβ-dTg CD4⁺ T cell population remained similar to that observed in the responding

population of EF4.1 TCRβ-Tg CD4$^+$ T cells in recipient mice injected with HLA-DR$^+$ or HLA-DR$^-$ B3 MHCII$^{env123-139}$ cells (Figure 42b). We also analysed the expression of intracellular interleukin-2 (IL-2) and interferon γ (IFNγ) following *ex vivo* restimulation of EF4.1 hFCRL6 TCRβ-dTg and EF4.1 TCRβ-Tg CD4$^+$ T cells obtained from the spleen of recipient mice injected with HLA-DR$^+$ and HLA-DR$^-$ B3 MHCII$^{env123-139}$ cells. We did not see a difference in the level of IL-2 and IFNγ expression in EF4.1 hFCRL6 TCRβ-dTg and EF4.1 TCRβ-Tg CD4$^+$ T cells at day 7 following transfer in recipient mice injected with HLA-DR$^+$ or HLA-DR$^-$ B3 MHCII$^{env123-139}$ cells (Figure 42c).

Figure 42: EF4.1 human FCRL6 TCRβ–double transgenic CD4⁺ T cells show normal *in vivo* activation in presence of HLA-DR when activated with B3 MHCII$^{env123-139}$.

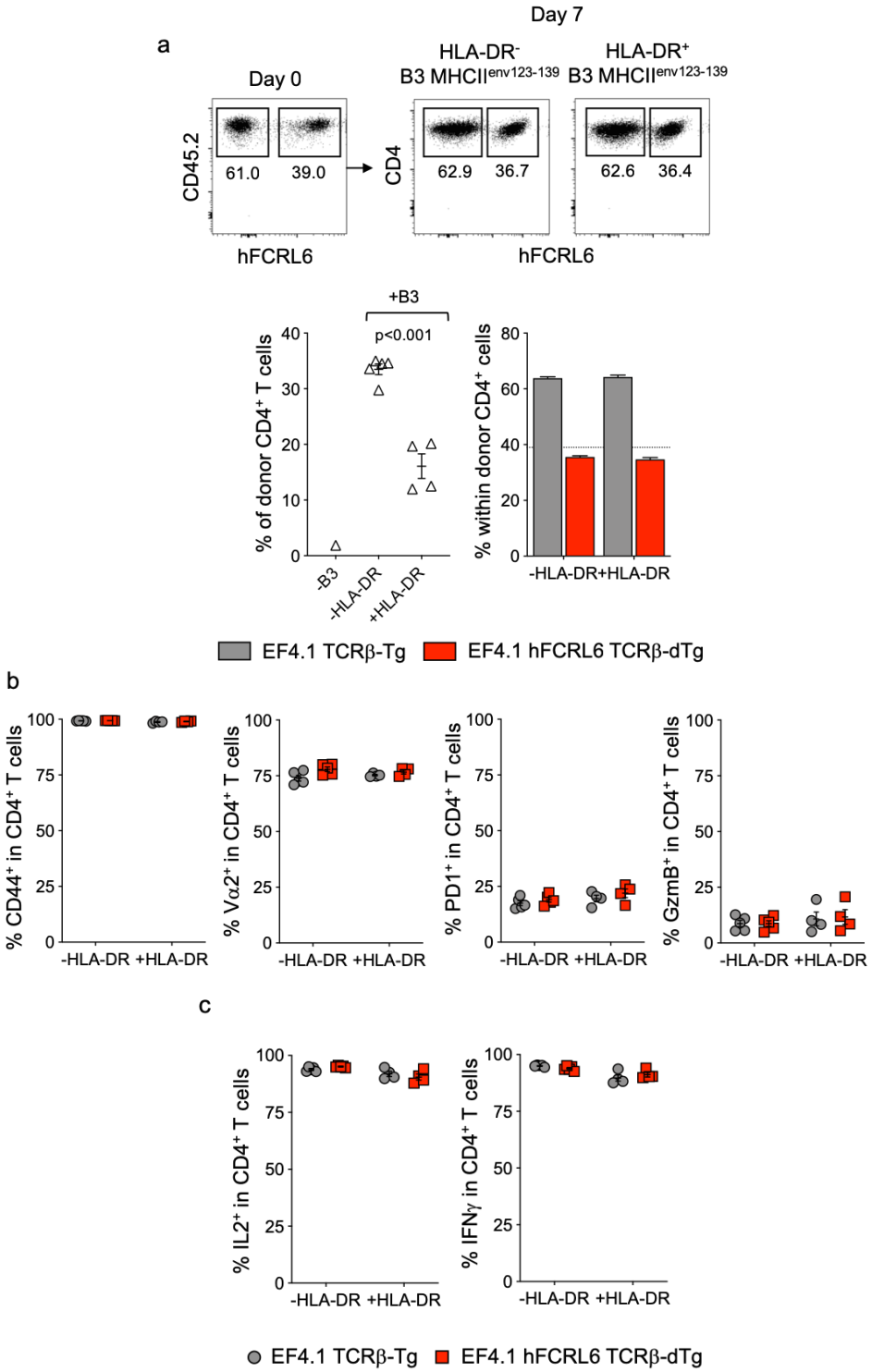

(a) Expansion of EF4.1 TCRβ-Tg and EF4.1 hFCRL6 TCRβ-dTg CD4⁺ T cells at day 14 following adoptive transfer into B and T cell-deficient recipient mice. Dotted line indicates injected

percentage of EF4.1 hFCRL6 TCRβ-dTg cells. (b) Percentage of $CD44^+$, Va2 *env*-reactive ($CD44^+$) and $PD1^+$ and $GzmB^+$ EF4.1 TCRβ-Tg and EF4.1 hFCRL6 TCRβ-dTg $CD4^+$ T cells at day 7 following transfer into recipient mice. (c) Percentage of $IL2^+$ and $IFNg^+$ EF4.1 TCRβ-Tg and EF4.1 hFCRL6 TCRβ-dTg $CD4^+$ T cells following *ex vivo* restimulation at day 7 following transfer into recipient mice. Symbols represent mean ± SEM of 4-6 biological repeats per genotype. $CD4^+$ T cells were isolated as described in section 2.2.4 of materials and methods. $CD45.2^+$ EF4.1 TCRβ-Tg $CD4^+$ T cells were mixed with $CD45.2^+$ EF4.1 hFCRL6 TCRβ-dTg $CD4^+$ T cells (39.0% EF4.1 hFCRL6 TCRβ-dTg $CD4^+$ T cells) and injected intravenously into recipient mice alongside HLA-DR^+ or HLA-DR^- $1.5x10^6$ B3 $MHCII^{env123-139}$ cells. Expansion and activation were analysed 7 days later via flow cytometry. CD4+ T cells were gated as $CD45.2^+$ $TCR\beta^+$ $CD4^+$.

6.3.3.10 In vivo killing of B3 MHCII$^{env123-139}$ cells transduced with human leukocyte antigen-DR by EF4.1 human FCRL6 TCRβ-double transgenic CD4$^+$ T cells

Despite the absence of an inhibitory effect during *in vivo* activation and expansion of EF4.1 hFCRL6 TCRβ-dTg CD4$^+$ T cells in the presence of HLA-DR, we decided to explore the functionality of these cells in this setting. Since CD4$^+$ T cells acquire cytotoxic activity in immunocompromised mice (Takeuchi *et al.* 2016) and the fact that B3 cells grow in the bone marrow and spleen of these mice (Merkenschlager *et al.* 2019), we examined if CD4$^+$ T cell cytotoxicity was somehow affected by the hFCRL6:HLA-DR axis. We mixed HLA-DR$^+$ and HLA-DR$^-$ B3 MHCII$^{env123-139}$ cells (51.6% HLA-DR$^+$ B3 MHCII$^{env123-139}$ cells) and injected the resulting cell suspension intravenously into B and T cell-deficient *Rag2*$^{-/-}$ recipient mice on the C57BL/6J background. This was followed 4 days later by the intravenous injection of CD45.2$^+$ EF4.1 TCRβ-Tg or EF4.1 hFCRL6 TCRβ-dTg CD4$^+$ T cells. We analysed the percentage of B3 MHCII$^{env123-139}$ cells as well as the proportion of HLA-DR$^+$ and HLA-DR$^-$ B3 MHCII$^{env123-139}$ cells in the spleen of recipient mice in addition to the expansion of EF4.1 TCRβ-Tg and EF4.1 hFCRL6 TCRβ-dTg CD4$^+$ T cells.

Consistent with previous findings in our lab (unpublished data), the accumulation of B3 MHCII$^{env123-139}$ cells in the spleen of *Rag2*$^{-/-}$ mice was completely abrogated in the presence of EF4.1 CD4$^+$ T cells, independent of the T cell genotype or HLA-DR expression on B3 cells (Fig. 44b). Consequently, the ratio of HLA-DR$^+$ and HLA-DR$^-$ B3 MHCII$^{env123-139}$ at day 7 following CD4$^+$ T cell transfer remained relatively unchanged compared to the initial ratio in the spleen of recipient mice injected with EF4.1 TCRβ-Tg or EF4.1 hFCRL6 TCRβ-dTg CD4$^+$ T cells (Figure 43a and 43b). We only observed a slight reduction in percentage of CD4$^+$ T cells in the spleen of recipient mice injected with EF4.1 hFCRL6 TCRβ-dTg compared to EF4.1 TCRβ-Tg CD4$^+$ T cells (Figure 43c).

Figure 43: EF4.1 human FCRL6 TCRβ-double transgenic CD4⁺ T cells show normal killing of B3 MHCII$^{env123-139}$ cells in presence of HLA-DR.

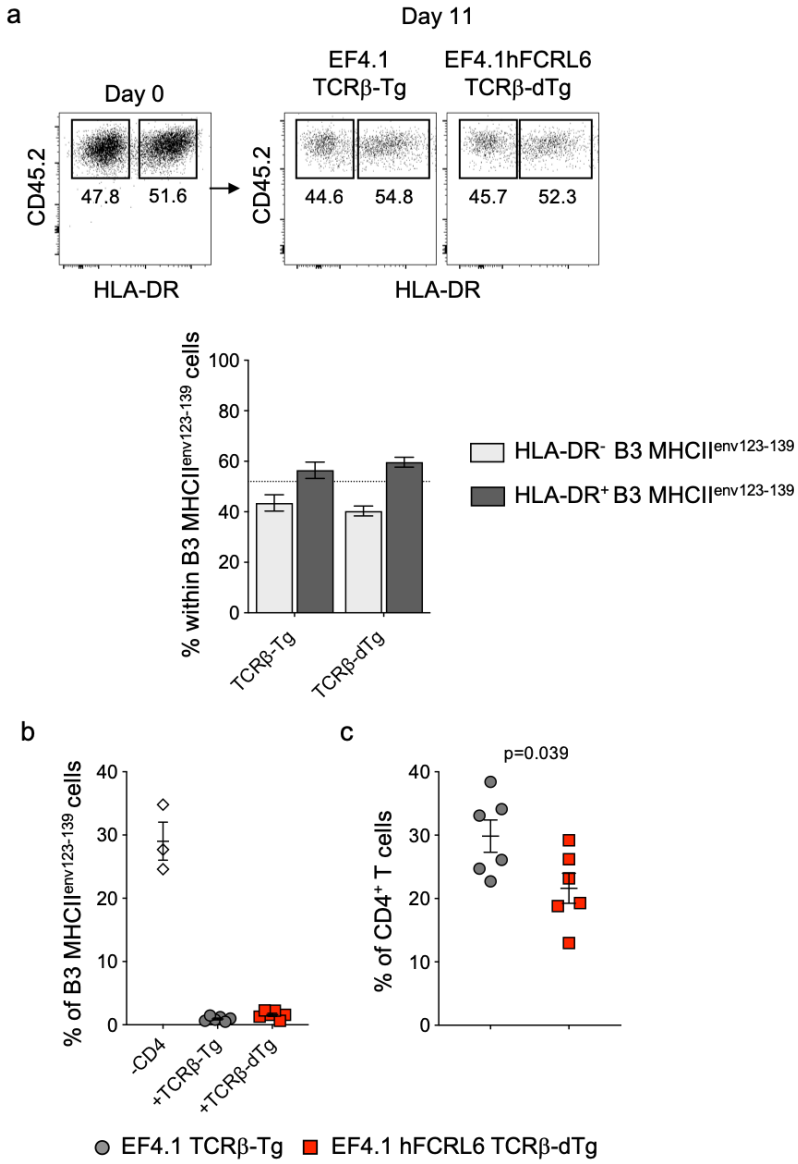

(a) Proportion of HLA-DR⁺ and HLA-DR⁻ B3 MHCII$^{env123-139}$ cells at day 7 following adoptive transfer of EF4.1 TCRβ-Tg or EF4.1 hFCRL6 TCRβ-dTg CD4⁺ T cells into B and T cell-deficient recipient mice. Dotted line indicates injected percentage of HLA-DR⁺ B3 MHCII$^{env123-139}$ cells. (b) Percentage of HLA-DR⁺ and HLA-DR⁻ B3 MHCII$^{env123-139}$ cells in the spleen of recipient mice at day 7 following transfer of EF4.1 TCRβ-Tg and EF4.1 hFCRL6 TCRβ-dTg CD4⁺ T cells. (c) Percentage of EF4.1 TCRβ-Tg and EF4.1 hFCRL6 TCRβ-dTg CD4⁺ T cells at day 7 following adoptive transfer into B and T cell-deficient recipient mice. Symbols represent mean ± SEM of 6

biological repeats per genotype. $CD4^+$ T cells were isolated as described in section 2.2.4 of materials and methods. $CD45.2^+$ HLA-DR^+ B3 $MHCII^{env123-139}$ cells were mixed with $CD45.2^+$ HLA-DR^- B3 $MHCII^{env123-139}$ cells (51.6% HLA-DR^+ B3 $MHCII^{env123-139}$ cells) and injected intravenously into recipient mice followed 4 days later by $1.0x10^6$ $CD45.2^+$ EF4.1 TCRβ-Tg or EF4.1 hFCRL6 TCRβ-dTg $CD4^+$ T cells. Killing was analysed 7 days following $CD4^+$ T cell transfer via flow cytometry. CD4+ T cells were gated as $CD45.2^+$ $TCR\beta^+$ $CD4^+$. B3 $MHCII^{env123-139}$ cells were gated as $CD45.2^+$ $TCR\beta^-$ $CD4^-$. TCRβ-Tg, EF4.1 TCRβ-Tg; TCRβ-dTg, EF4.1 hFCRL6 TCRβ-dTg.

6.4 Discussion

6.4.1 Mouse FCRL6

The expression of FCRL6 on human T cells is concentrated on those with a terminally differentiated phenotype (Schreeder *et al.* 2008; Wilson *et al.* 2007b). Contrastingly, we were unable to detect the expression of FCRL6 via qRT-PCR in mature $CD4^+$ or $CD8^+$ T cell subsets as well as developing T cell populations in the thymus. Publicly available data on ImmGen indicates the expression of *Fcrl6* in mTECs, thereby raising the possibility that the receptor despite a lack of expression in T-lineage cells may still affect T cell development due to the crucial role of mTECs in the establishment of central tolerance (Kyewski & Klein 2006). We did not observe differences in the relative proportion or number of thymocytes and mature $CD4^+$ and $CD8^+$ T cells as well as their subsets in the spleen *Fcrl6*$^{-/-}$ mice. Thus, we concluded following evaluation of developing and mature T cell populations in *Fcrl6*$^{-/-}$ mice, and also due to the lack of autoimmune phenotypes in these mice that deletion of FCRL6 does not affect T cell development and also likely does not affect their phenotype. As the reported expression of FCRL6 in mTECs relates to gene expression level, it is possible that the receptor is not expressed at the protein level in mature mTECs as it likely does not serve a purpose during T cell development. Thus, FCRL6 may be involved in other processes in mTECs such as their formation during homeostatic renewal of the population in the thymus. Future studies should aim to characterise the surface expression of FCRL6 on mTEC-lineage cells and examine the role of this receptor in these cells using mTEC conditional *Fcrl6*$^{-/-}$ mice.

6.4.2 Human FCRL6

In order to investigate the inhibitory potential of hFCRL6, we generated Tg mice expressing the canonical isoform of hFCRL6 using the hCD2-VA expression cassette. The use of this expression cassette allowed for robust expression of hFCRL6 on T-lineage cells from at least the double negative stage in the thymus, thereby raising the possibility of altered T cell development. However, we did not observe differences in the relative proportion or number of thymocytes and

mature splenic $CD4^+$ and $CD8^+$ T cells as well their subsets. Thus, we concluded that transgene expression of hFCRL6 does not affect T cell development.

Subsequently, we started investigating the effect of hFCRL6 expression on the activation of T cells. We did not detect differences in the activation or proliferation of polyclonal $hFCRL6^+$ $CD4^+$ and $CD8^+$ T cells in response to *in vitro* and *in vivo* stimulation. Next, we crossed $hFCRL6^+$ Tg mice with EF4.1 mice to generate a mouse that would serve as a source of antigen-specific $hFCRL6^+$ $CD4^+$ T cells and allow us to investigate the relationship between the level of T cell stimulation and the inhibitory potential of hFCRL6. We activated $hFCRL6^+$ $CD4^+$ T cells from these mice in an *in vitro* setting with a range of cognate peptide concentrations and did not detect differences in the activation or proliferation of these cells. We also did not detect a difference in the *in vivo* activation and expansion of $hFCRL6^+$ $CD4^+$ T cells to both high and low affinity antigens. We investigated the *in vivo* activation of $hFCRL6^+$ $CD4^+$ T cells in B and T cell deficient recipient mice in order to avoid rejection of adoptively transferred cells by the recipient immune system due to the expression of a human protein. In order to discount anomalies arising from the activation of $CD4^+$ T cells in immunodeficient recipient mice, we crossed $hFCRL6^+$ Tg mice with $CD45.1/2^+$ wild type mice to generate hFCRL6 tolerised recipient mice, thereby allowing analysis of the activation of $hFCRL6^+$ $CD4^+$ T cells in an immunocompetent setting. Similar to the results observed in immunodeficient mice, we did not observe a difference in the activation and expansion of $hFCRL6^+$ $CD4^+$ T cells in response to a high affinity antigen following their transfer into hFCRL6 tolerised wild type recipient mice. Collectively, our initial *in vitro* and *in vivo* results indicated that the expression of hFCRL6 did not affect the activation of mouse $CD4^+$ T cells. This could have occurred either due to 1) an absence of potential ligands that are capable of binding and activating hFCRL6 in mice, 2) an inability of hFCRL6 to initiate inhibitory signalling due to incompatibility with mouse intracellular signalling molecules or 3) an intrinsic lack of immunoregulatory ability of hFCRL6. To address this, we next analysed the activation of $hFCRL6^+$ $CD4^+$ T cells in the presence of a potential ligand of the receptor.

Despite the presence of HLA-DR, an MHC Class II receptor that so far is the only identified ligand of FCRL6 in humans (Schreeder *et al.* 2010), we did not observe a difference in the initial activation of hFCRL6$^+$ CD4$^+$ T cells following *in vitro* stimulation with a range of concentrations of the aforementioned cognate peptide. This suggested that events following initial TCR stimulation likely remained largely unaffected by the interaction of hFCRL6 with HLA-DR. However, later T cell proliferative events are significantly reduced in the presence of both hFCRL6 on CD4$^+$ T cells and HLA-DR on APCs. This could have occurred as a result of impaired proliferation or survival, or a combination of both. However, it is more likely that the potential signalling induced by hFCRL6 has a major effect on the survival of proliferating cells rather than impairing their proliferation altogether as we observed a remarkable difference in proliferation at day 6 compared to day 3 following activation. The impact of hFCRL6 on T cell survival during proliferation could be driven by attenuated production of γ-chain (γ_c) cytokines such as IL-2 which have been demonstrated to be essential for the survival rather than proliferation of CD4$^+$ T cells following *in vitro* activation (Shi *et al.* 2009). The tyrosine phosphatase Shp-1 has been shown to be recruited to the IL-2 receptor complex following IL-2 stimulation where it mediates the dephosphorylation of IL-2Rβ as well as associated Jak kinases, Jak1 and Jak3, thereby reducing signals initiated through the IL-2 receptor (Migone *et al.* 1998). The potential recruitment of Shp-1 by hFCRL6 may also allow downmodulation of IL-2 receptor signalling through this mechanism.

Next, we activated hFCRL6$^+$ CD4$^+$ T cells with a stronger stimulus in the form of a covalently linked MHCII peptide and detected reduced proliferation of hFCRL6$^+$ compared to wild type CD4$^+$ T cells in the presence of HLA-DR, thereby confirming the potential inhibitory role of the hFCRL6:HLA axis. However, the difference between the proliferation of hFCRL6$^+$ and wild type CD4$^+$ T cells was reduced in this scenario compared to the aforementioned *in vitro* setting, thereby suggesting that the inhibitory potential of human FCRL6 may be affected by the strength of TCR stimulation. Subsequently, we activated a mixed suspension of hFCRL6$^+$ and wild type CD4$^+$ T cells *in vivo* with the same covalently linked MHCII peptide in the presence of HLA-DR. However, we were not able to recapitulate the inhibitory effect of the hFCRL6:HLA axis in an *in vivo* setting. This could have occurred due to 1) compensation of potential deficits by cotransferred wild type

$CD4^+$ T cells, 2) a reduced requirement of γ_c cytokine function during *in vivo* $CD4^+$ T cell activation (Lantz *et al.* 2000), or 3) reduced ability of hFCRL6 to mediate an inhibitory effect in response to strong TCR stimulation as evidenced during *in vitro* activation, or a combination of all three. We detected a reduction in the expansion of total $CD4^+$ T cells in mice injected with B3 cells expressing HLA-DR. However, a lack of difference in the end ratio of $hFCRL6^+$ and wild type $CD4^+$ T cells compared to the initial ratio suggests that the reduced percentage of total $CD4^+$ T cells is most likely due to differences during priming caused by differing levels of peptide bound MHCII expression on $HLA\text{-}DR^+$ and $HLA\text{-}DR^-$ B3 cells. We also investigated the *in vivo* killing of $HLA\text{-}DR^+$ and $HLA\text{-}DR^-$ B3 cells expressing the aforementioned covalently bound MHCII peptide. We detected equal killing of cotransferred $HLA\text{-}DR^+$ and $HLA\text{-}DR^-$ B3 cells by $hFCRL6^+$ $CD4^+$ T cells. This could have occurred due to the inability of hFCRL6 to mediate an inhibitory effect following strong TCR stimulation. There was a slight reduction in the expansion of $hFCRL6^+$ compared to wild type $CD4^+$ T cells. However, previous data suggests this was more likely due to an inadvertent difference in the number of injected $CD4^+$ T cells rather than due to an inhibitory effect of hFCRL6.

Overall, these results hinted that hFCRL6 may possess inhibitory functionality as predicted by its signalling potential in previous studies (Kulemzin *et al.* 2011a; Schreeder *et al.* 2008; Wilson *et al.* 2007b). However, this potential inhibitory capacity of hFCRL6 appeared to be affected by the strength of TCR stimulation in our experimental system. It must be noted though that the inhibitory capacity of FCRL6 might be greater in human T cells and consequently may not be regulated by the strength of TCR stimulation due to 1) competition with the TCR for HLA-DR binding following potential colocalization with the TCR during priming of $CD4^+$ T cells, 2) disruption of TCR-peptide HLA-DR interaction by the binding of FCRL6 to HLA-DR, 3) downregulation of HLA-DR expression following FCRL6 engagement or increased availability of compatible signalling molecules in human T cells, 4) other unknown ligands that are able to induce more potent inhibitory signalling, or a combination of all these and other unknown factors.

6.4.3 Future work

We did not detect major differences in the initial *in vitro* activation or proliferation of hFCRL6$^+$ CD4$^+$ T cells in the presence of HLA-DR, a known ligand of hFCRL6. However, later proliferation of hFCRL6$^+$ CD4$^+$ T cells appeared to be significantly reduced in the presence of HLA-DR. This led us to speculate that hFCRL6$^+$ CD4$^+$ T cells may be unable to maintain their proliferation and ultimately undergo cell death. Thus, it would be of interest to future studies to quantify cell death as well as proliferation following *in vitro* activation of these cells. The cytokine production of hFCRL6$^+$ CD4$^+$ T cells should also be analysed at each time point to determine if deficits could be linked to differences in proliferation and potentially cell death. Additionally, the binding of hFCRL6 with HLA-DR should be confirmed in our experimental system to definitively confirm that the observed differences are due to an interaction between these two proteins. Whole transcriptome sequencing of hFCRL6$^+$ CD4$^+$ T cells following *in vitro* activation should also be considered in future studies to identify differentially regulated genes and potential pathways that could account for differences in the proliferation of these cells. One of the potential reasons underlying an absence of differences in the *in vivo* expansion of hFCRL6$^+$ CD4+ T cells is compensation by cotransferred wild type CD4$^+$ T cells. This could be investigated by analysing the *in vitro* activation and proliferation of a mixed suspension of hFCRL6$^+$ and wild type CD4$^+$ T cells. Our data suggested that the inhibitory effect of hFCRL6 at least in our experimental system may be dictated by the strength of TCR stimulation. This should be explored further via *in vitro* activation of hFCRL6$^+$ CD4$^+$ T cells in the presence of HLA-DR with variants of the $env_{122\text{-}141}$ peptide that activate CD4$^+$ T cells less potently than the cognate peptide. HLA-DR expressing peptide pulsed B3 cells should be used in future studies instead of B3 cells expressing a covalently linked MHCII peptide to reveal potential differences during *in vivo* activation of hFCRL6$^+$ CD4$^+$ T cells and also examine their *in vivo* cytotoxic capacity.

The effect of FCRL6 on human T cell effector function following its engagement by a known ligand of the receptor such as HLA-DR has not yet been formally investigated. Thus, this should be a priority for future studies in order to determine the validity of the findings obtained from our experimental model. Whole transcriptome sequencing of human T cells following HLA-DR

engagement should also be utilised to determine the molecular mechanisms driving the potential inhibitory effect of this receptor. Although it is established that MHCII$^+$ tumour cells can promote direct CD4$^+$ Th cell activation as well as cytotoxicity and prevent tumour growth (Axelrod *et al.* 2019; Haabeth *et al.* 2014; Thibodeau *et al.* 2012), tumour MHCII or specifically HLA-DR expression may also have a deleterious effect on the anti-tumour immune response due to the expression of FCRL6 by cytotoxic CD4$^+$ T cells. Thus, expression of FCRL6 on cytotoxic CD4$^+$ T cells from tumours with high HLA-DR expression as well as the functionality of FCRL6 expressing cytotoxic CD4$^+$ T cells should be examined in future studies to provide an indication as to if the receptor can cause T cell exhaustion. The survival of patients with both high HLA-DR tumour and FCRL6 expression on cytotoxic CD4$^+$ T cells may also be investigated to determine the immunoregulatory importance of this receptor in this setting. It should also be of interest to future studies to identify the affinity of hFCRL6 for HLA-DR, and examine if the receptor colocalizes with the TCR on human T cells following activation to determine if its potential immunoregulatory function could be reliant on out competition of the TCR for HLA-DR binding as well as through induction of inhibitory signalling. Additional ligands of FCRL6 should also be identified in humans to further understand the role of this receptor. Mice expressing HLA-DR as well as other potential ligands could be crossed with hFCRL6 expressing Tg mice in future studies to allow investigation of receptor function in T cells in an *in vivo* environment. Additionally, the expression of FCRL6 may be increased on tumour infiltrating cytotoxic CD4$^+$ and CD8$^+$ T cells from patients with resistance to currently available checkpoint inhibitors as a possible compensation mechanism. This could occur due to the ability of FCRL6 to bind HLA-DR or other unknown ligands and deliver potentially inhibitory signals that could terminate the effector function of these cytotoxic cells. Thus, the expression of FCRL6 on tumour infiltrating cytotoxic CD4$^+$ and CD8$^+$ T cells from such patients should be examined alongside the effect of its blockade in these circumstances to determine if the receptor could be involved in resistance to checkpoint inhibitor blockade.

Chapter 7. Discussion

The expression and signalling potential of human FCRL6 suggests a potential immunoregulatory role for this receptor. However, there is very limited data in the literature regarding its function. Therefore, this study aimed at investigating the function of FCRL6 using mice as model organisms. The expression profile of mouse FCRL6 had not been determined prior to the start of this study. We investigated the expression of FCRL6 via qRT-PCR and detected its presence in developing B cells and mature NK cells. In contrast to the expression of human FCRL6, we did not detect the expression of mouse FCRL6 in developing or mature T cells. We were also unable to observe the expression of mouse FCRL6 in T cells following their activation. Consequently, we initially focused on investigating the function of mouse FCRL6 in B and NK cells.

The expression of mouse FCRL6 in pro-B and pre-B cells implies a possible role of this receptor during B cell development. However, we did not observe altered B cell development during competition of wild type and *Fcrl6*$^{-/-}$ bone marrow in mixed bone marrow chimeras and in *Fcrl6*$^{-/-}$ mice. The ability of B cells to mount antibody responses to DNP-OVA and FV was also unaffected by the absence of FCRL6. Thus, we concluded that FCRL6 is dispensable for the development of B cells as well as antibody generation at least in response to T-dependent antigens. Although we did not observe differences in the bone marrow development of NK cells in *Fcrl6*$^{-/-}$ and NK conditional *Fcrl6*$^{-/-}$ mice, we detected a reduction in the number and percentage of mature NK cells in the spleen of NK conditional *Fcrl6*$^{-/-}$ but not *Fcrl6*$^{-/-}$ mice. This could likely be attributed to the emergence of compensatory mechanisms in *Fcrl6*$^{-/-}$ mice due to germline FCRL6 deletion in these mice compared to NK conditional *Fcrl6*$^{-/-}$ mice where FCRL6 is deleted at a later stage of NK cell development. Splenic NK cells primarily originate from the bone marrow and as NK cell bone marrow development remained unaffected by the absence of FCRL6, this suggested a possible role of the receptor in the migration of bone marrow derived NK cells. Additionally, despite normal development of NK cells in the bone marrow, we could not discount a role of this receptor in developing NK cells again possibly due to compensatory mechanisms in *Fcrl6*$^{-/-}$ mice and the later deletion of FCRL6 in NK conditional *Fcrl6*$^{-/-}$ mice. The expression of mouse FCRL6

in mature NK cells mirrored that of FCRL6 on human NK cells. However, we did not detect differences in the NK cell response following FV infection or inoculation of B16 melanoma cells in the absence of FCRL6. This result alongside an absence of FCRL6 expression in mouse T-linage cells during the steady state and following activation suggests that mouse FCRL6 does not likely possess the potential immunoregulatory functionality of its human counterpart. Further evidence for this is provided by the differences observed in the extracellular region of human and mouse FCRL6. It could be argued that these differences could have arisen due to the requirement of binding similar but structurally altered ligands in both species. However, differences in the expression profile as well as extracellular region of mouse FCRL6 alongside the absence of a consensus immunoregulatory motif in its cytoplasmic region suggests that it is more likely that evolution has led to the divergence of FCRL6 in mice to mediate non-immunoregulatory functions compared to its human counterpart. Thus, mouse FCRL6 may not represent an ideal model to study the function of human FCRL6. Consequently, in order to investigate the potential immunoregulatory functionality of FCRL6, we generated Tg mice that expressed hFCRL6 on $CD4^+$ and $CD8^+$ T cells.

We did not observe an immunoregulatory role of hFCRL6 in T cells following stimulation with both high and low affinity antigens in a range of *in vitro* and *in vivo* settings until the introduction of HLA-DR, a known ligand of the receptor in our experimental system. The presence of both hFCRL6 and HLA-DR appeared to have an inhibitory effect on *in vitro* $CD4^+$ T cell proliferation possibly due to signalling induced following their interaction. However, this potential inhibitory effect of hFCRL6 appeared to be dependent on the strength of TCR stimulation as stronger activation reduced or completely inhibited the functionality of the receptor. It must be considered though that this may not be the case in humans where increased functionality of FCRL6 may be evident due to possible reasons outlined in section 6.2.4 of the thesis. Overall, the data obtained in this study suggested that FCRL6 may possess inhibitory functionality at least in the context of T cells. Its role in humans may be especially evident in patients with HLA-DR expressing tumours and also those with resistance to immune checkpoint blockade due to induction of FCRL6 expression as a possible compensation mechanism. Further investigation detailed in section 6.2.4

of the thesis is required to definitively understand the function of the receptor. An increased understanding of its function may allow for the development of novel therapeutics that could be used in combination with current strategies to improve our immunotherapy-based arsenal against infectious disease, cancer and autoimmunity.

Reference List

Agresta, L., Hoebe, K. H. N., & Janssen, E. M. (2018). The Emerging Role of CD244 Signaling in Immune Cells of the Tumor Microenvironment. *Frontiers in Immunology*, **9**, 2809.

Ahmadzadeh, M., Johnson, L. A., Heemskerk, B., … Rosenberg, S. A. (2009). Tumor antigen–specific CD8 T cells infiltrating the tumor express high levels of PD-1 and are functionally impaired. *Blood*, **114**(8), 1537–1544.

Ahn, E., Araki, K., Hashimoto, M., … Ahmed, R. (2018). Role of PD-1 during effector CD8 T cell differentiation. *Proceedings of the National Academy of Sciences of the United States of America*, **115**(18), 4749–4754.

Alcover, A., & Alarcón, B. (2000). Internalization and intracellular fate of TCR-CD3 complexes. *Critical Reviews in Immunology*, **20**(4), 325–46.

Aldrich, M. F., & Kellems, R. E. (2001). *Lymphocyte Development: Cell Selection Events and Signals during Immune Ontogeny* . Shiv Pillai. *The Quarterly Review of Biology*, **76**(3), 349–349.

Allman, D., Lindsley, R. C., DeMuth, W., Rudd, K., Shinton, S. A., & Hardy, R. R. (2001). Resolution of Three Nonproliferative Immature Splenic B Cell Subsets Reveals Multiple Selection Points During Peripheral B Cell Maturation. *The Journal of Immunology*, **167**(12), 6834–6840.

Alsaab, H. O., Sau, S., Alzhrani, R., … Iyer, A. K. (2017). PD-1 and PD-L1 Checkpoint Signaling Inhibition for Cancer Immunotherapy: Mechanism, Combinations, and Clinical Outcome. *Frontiers in Pharmacology*, **8**, 561.

Amarante-Mendes, G. P., Adjemian, S., Branco, L. M., Zanetti, L. C., Weinlich, R., & Bortoluci, K. R. (2018). Pattern Recognition Receptors and the Host Cell Death Molecular Machinery. *Frontiers in Immunology*, **9**, 2379.

Antunes, I., Tolaini, M., Kissenpfennig, A., … Kassiotis, G. (2008). Retrovirus-specificity of regulatory T cells is neither present nor required in preventing retrovirus-induced bone marrow immune pathology. *Immunity*, **29**(5), 782–94.

Arnold, R., Brenner, D., Becker, M., Frey, C. R., & Krammer, P. H. (2006). How T lymphocytes switch between life and death. *European Journal of Immunology*, **36**(7), 1654–1658.

Avril, T., Floyd, H., Lopez, F., Vivier, E., & Crocker, P. R. (2004). The Membrane-Proximal Immunoreceptor Tyrosine-Based Inhibitory Motif Is Critical for the Inhibitory Signaling Mediated by Siglecs-7 and -9, CD33-Related Siglecs Expressed on Human Monocytes and NK Cells. *The Journal of Immunology*, **173**(11), 6841–6849.

Axelrod, M. L., Cook, R. S., Johnson, D. B., & Balko, J. M. (2019). Biological Consequences of MHC-II Expression by Tumor Cells in Cancer. *Clinical Cancer Research*, **25**(8), 2392–2402.

Barber, D. L., Wherry, E. J., Masopust, D., … Ahmed, R. (2006). Restoring function in exhausted CD8 T cells during chronic viral infection. *Nature*, **439**(7077), 682–687.

Basu, S., Ray, A., & Dittel, B. N. (2013). Differential Representation of B Cell Subsets in Mixed Bone Marrow Chimera Mice Due to Expression of Allelic Variants of CD45 (CD45.1/CD45.2). *Journal of Immunological Methods*, **396**(0). doi:10.1016/J.JIM.2013.07.008

Batista, F. D., & Harwood, N. E. (2009). The who, how and where of antigen presentation to B cells. *Nature Reviews Immunology*, **9**(1), 15–27.

Baumgarth, N. (2017). A Hard(y) Look at B-1 Cell Development and Function. *Journal of Immunology (Baltimore, Md. : 1950)*, **199**(10), 3387–3394.

Bell, J. K., Mullen, G. E. D., Leifer, C. A., Mazzoni, A., Davies, D. R., & Segal, D. M. (2003). Leucine-rich repeats and pathogen recognition in Toll-like receptors. *Trends in Immunology*, **24**(10), 528–533.

Bhoj, V. G., & Chen, Z. J. (2009). Ubiquitylation in innate and adaptive immunity. *Nature*, **458**(7237), 430–437.

Blackburn, S. D., Shin, H., Haining, W. N., … Wherry, E. J. (2009). Coregulation of CD8+ T cell exhaustion by multiple inhibitory receptors during chronic viral infection. *Nature Immunology*, **10**(1), 29–37.

Blom, N., Gammeltoft, S., & Brunak, S. (1999). Sequence and structure-based prediction of eukaryotic protein phosphorylation sites. *Journal of Molecular Biology*, **294**(5), 1351–62.

Bock, M., Bishop, K. N., Towers, G., & Stoye, J. P. (2000). Use of a transient assay for studying the genetic determinants of Fv1 restriction. *Journal of Virology*, **74**(16), 7422–30.

Boles, K. S., Stepp, S. E., Bennett, M., Kumar, V., & Mathew, P. A. (2001). 2B4 (CD244) and CS1: novel members of the CD2 subset of the immunoglobulin superfamily molecules expressed on natural killer cells and other leukocytes. *Immunological Reviews*, **181**(1), 234–249.

Bolland, S., & Ravetch, J. V. (2000). Spontaneous autoimmune disease in Fc(gamma)RIIB-deficient mice results from strain-specific epistasis. *Immunity*, **13**(2), 277–85.

Bonilla, F. A., & Oettgen, H. C. (2010). Adaptive immunity. *Journal of Allergy and Clinical Immunology*, **125**(2), S33–S40.

Boos, M. D., Yokota, Y., Eberl, G., & Kee, B. L. (2007). Mature natural killer cell and lymphoid tissue–inducing cell development requires Id2-mediated suppression of E protein activity. *The Journal of Experimental Medicine*, **204**(5), 1119–1130.

Boudreau, J. E., Hsu, K. C., Ca, J. B., Boudreau, (J E, Org, (K C, & Hsu,). (2018). Natural Killer Cell Education and the Response to Infection and Cancer Therapy: Stay Tuned. *Trends in Immunology*, **39**(3), 222–239.

Bour-Jordan, H., Esensten, J. H., Martinez-Llordella, M., Penaranda, C., Stumpf, M., & Bluestone, J. A. (2011). Intrinsic and extrinsic control of peripheral T-cell tolerance by costimulatory molecules of the CD28/B7 family. *Immunological Reviews*, **241**(1), 180–205.

Brodin, P., Kärre, K., & Höglund, P. (2009). NK cell education: not an on-off switch but a tunable rheostat. *Trends in Immunology*, **30**(4), 143–149.

Bryceson, Y. T., March, M. E., Ljunggren, H.-G., & Long, E. O. (2006). Synergy among receptors on resting NK cells for the activation of natural cytotoxicity and cytokine secretion. *Blood*, **107**(1), 159–166.

Buchanan, R. M., Arulanandam, B. P., & Metzger, D. W. (1998). IL-12 enhances antibody responses to T-independent polysaccharide vaccines in the absence of T and NK cells. *Journal of Immunology (Baltimore, Md. : 1950)*, **161**(10), 5525–33.

Cabaniols, J. P., Fazilleau, N., Casrouge, A., Kourilsky, P., & Kanellopoulos, J. M. (2001). Most alpha/beta T cell receptor diversity is due to terminal deoxynucleotidyl transferase. *The Journal of Experimental Medicine*, **194**(9), 1385–90.

Cai, Z., Kishimoto, H., Brunmark, A., Jackson, M. R., Peterson, P. A., & Sprent, J. (1997). Requirements for Peptide-induced T Cell Receptor Downregulation on Naive CD8 $^{+}$ T Cells. *The Journal of Experimental Medicine*, **185**(4), 641–652.

Cameron, F., Whiteside, G., & Perry, C. (2011). Ipilimumab. *Drugs*, **71**(8), 1093–1104.

Capone, M., Bryant, J. M., Sutkowski, N., & Haque, A. (2016). Fc Receptor-Like Proteins in Pathophysiology of B-cell Disorder. *Journal of Clinical & Cellular Immunology*, **7**(3). doi:10.4172/2155-9899.1000427

Carreno, B. M., Bennett, F., Chau, T. A., … Madrenas, J. (2000). CTLA-4 (CD152) can inhibit T cell activation by two different mechanisms depending on its level of cell surface expression. *Journal of Immunology (Baltimore, Md. : 1950)*, **165**(3), 1352–6.

Chambers, C. A., Kuhns, M. S., Egen, J. G., & Allison, J. P. (2001). C TLA -4-M EDIATED I NHIBITION IN R EGULATION OF T C ELL R ESPONSES : Mechanisms and Manipulation in Tumor Immunotherapy. *Annual Review of Immunology*, **19**(1), 565–594.

Chan, P. L., & Sinclair, N. R. (1971). Regulation of the immune response. V. An analysis of the function of the Fc portion of antibody in suppression of an immune response with respect to

interaction with components of the lymphoid system. *Immunology*, **21**(6), 967–81.

Chaplin, D. D. (2010). Overview of the immune response. *The Journal of Allergy and Clinical Immunology*, **125**(2 Suppl 2), S3-23.

Chaudhary, N., & Wesemann, D. R. (2018). Analyzing Immunoglobulin Repertoires. *Frontiers in Immunology*, **9**, 462.

Chemnitz, J. M., Parry, R. V., Nichols, K. E., June, C. H., & Riley, J. L. (2004). SHP-1 and SHP-2 Associate with Immunoreceptor Tyrosine-Based Switch Motif of Programmed Death 1 upon Primary Human T Cell Stimulation, but Only Receptor Ligation Prevents T Cell Activation. *The Journal of Immunology*, **173**(2), 945–954.

Chen, G., Tai, A. K., Lin, M., Chang, F., Terhorst, C., & Huber, B. T. (2007). Increased proliferation of CD8+ T cells in SAP-deficient mice is associated with impaired activation-induced cell death. *European Journal of Immunology*, **37**(3), 663–674.

Chen, L. (2004). Co-inhibitory molecules of the B7–CD28 family in the control of T-cell immunity. *Nature Reviews Immunology*, **4**(5), 336–347.

Chen, X., & Jensen, P. E. (2008). The role of B lymphocytes as antigen-presenting cells. *Archivum Immunologiae et Therapiae Experimentalis*, **56**(2), 77–83.

Chen, Y., Zander, R., Khatun, A., Schauder, D. M., & Cui, W. (2018). Transcriptional and Epigenetic Regulation of Effector and Memory CD8 T Cell Differentiation. *Frontiers in Immunology*, **9**, 2826.

Chibueze, C. E., Yoshimitsu, M., & Arima, N. (2014). CD160 expression defines a uniquely exhausted subset of T lymphocytes in HTLV-1 infection. *Biochemical and Biophysical Research Communications*, **453**(3), 379–384.

Chikaev, N. A., Bykova, E. A., Najakshin, A. M., … Taranin, A. V. (2005). Cloning and characterization of the human FCRL2 gene. *Genomics*, **85**(2), 264–72.

Chiossone, L., Chaix, J., Fuseri, N., Roth, C., Vivier, E., & Walzer, T. (2009a). Maturation of mouse NK cells is a 4-stage developmental program. *Blood*, **113**(22), 5488–96.

Chiossone, L., Chaix, J., Fuseri, N., Roth, C., Vivier, E., & Walzer, T. (2009b). Maturation of mouse NK cells is a 4-stage developmental program. *Blood*, **113**(22), 5488–5496.

Chisolm, D. A., Cheng, W., Colburn, S. A., … Weinmann, A. S. (2019). Defining Genetic Variation in Widely Used Congenic and Backcrossed Mouse Models Reveals Varied Regulation of Genes Important for Immune Responses. *Immunity*, **51**(1), 155-168.e5.

Choi, J.-M., Kim, S.-H., Shin, J.-H., … Lee, S.-K. (2008). Transduction of the cytoplasmic domain of CTLA-4 inhibits TcR-specific activation signals and prevents collagen-induced arthritis. *Proceedings of the National Academy of Sciences*, **105**(50), 19875–19880.

Chowdhury, D., & Sen, R. (2001). Stepwise activation of the immunoglobulin mu heavy chain gene locus. *The EMBO Journal*, **20**(22), 6394–403.

Chung, J. B., Silverman, M., & Monroe, J. G. (2003). Transitional B cells: step by step towards immune competence. *Trends in Immunology*, **24**(6), 342–348.

Clynes, R., Maizes, J. S., Guinamard, R., Ono, M., Takai, T., & Ravetch, J. V. (1999). Modulation of Immune Complex–induced Inflammation In Vivo by the Coordinate Expression of Activation and Inhibitory Fc Receptors. *The Journal of Experimental Medicine*, **189**(1), 179–186.

Cobaleda, C., Jochum, W., & Busslinger, M. (2007a). Conversion of mature B cells into T cells by dedifferentiation to uncommitted progenitors. *Nature*, **449**(7161), 473–477.

Cobaleda, C., Schebesta, A., Delogu, A., & Busslinger, M. (2007b). Pax5: the guardian of B cell identity and function. *Nature Immunology*, **8**(5), 463–470.

Collins, A. V., Brodie, D. W., Gilbert, R. J. C., … Davis, S. J. (2002). The Interaction Properties of Costimulatory Molecules Revisited. *Immunity*, **17**(2), 201–210.

Constantinides, M. G., Gudjonson, H., McDonald, B. D., … Bendelac, A. (2015). PLZF expression maps the early stages of ILC1 lineage development. *Proceedings of the National Academy*

of Sciences, **112**(16), 5123–5128.

Cooper, M. A., Fehniger, T. A., & Caligiuri, M. A. (2001). The biology of human natural killer-cell subsets. *Trends in Immunology*, **22**(11), 633–40.

Crotty, S. (2014). T follicular helper cell differentiation, function, and roles in disease. *Immunity*, **41**(4), 529–42.

Dam, J., Guan, R., Natarajan, K., … Mariuzza, R. A. (2003). Variable MHC class I engagement by Ly49 natural killer cell receptors demonstrated by the crystal structure of Ly49C bound to H-2Kb. *Nature Immunology*, **4**(12), 1213–1222.

Darvin, P., Toor, S. M., Sasidharan Nair, V., & Elkord, E. (2018). Immune checkpoint inhibitors: recent progress and potential biomarkers. *Experimental & Molecular Medicine*, **50**(12), 165.

Das, A., Hoare, M., Davies, N., … Maini, M. K. (2008). Functional skewing of the global CD8 T cell population in chronic hepatitis B virus infection. *The Journal of Experimental Medicine*, **205**(9), 2111–24.

Davis, M. M., & Bjorkman, P. J. (1988). T-cell antigen receptor genes and T-cell recognition. *Nature*, **334**(6181), 395–402.

Davis, R., Ehrhardt, G. ?A., Leu, C.-M., Hirano, M., & Cooper, M. (2005). An extended family of Fc receptor relatives. *European Journal of Immunology*, **35**(3), 674–680.

Davis, R. S. (2007). Fc Receptor-Like Molecules. *Annual Review of Immunology*, **25**(1), 525–560.

Davis, R. S., Dennis, G., Kubagawa, H., & Cooper, M. D. (2002a). Fc receptor homologs (FcRH1-5) extend the Fc receptor family. *Current Topics in Microbiology and Immunology*, **266**, 85–112.

Davis, R. S., Dennis, G., Odom, M. R., … Cooper, M. D. (2002b). Fc receptor homologs: newest members of a remarkably diverse Fc receptor gene family. *Immunological Reviews*, **190**, 123–36.

Davis, R. S., Li, H., Chen, C.-C., Wang, Y.-H., Cooper, M. D., & Burrows, P. D. (2002c). Definition of an Fc receptor-related gene (FcRX) expressed in human and mouse B cells. *International Immunology*, **14**(9), 1075–83.

Davis, R. S., Wang, Y. H., Kubagawa, H., & Cooper, M. D. (2001). Identification of a family of Fc receptor homologs with preferential B cell expression. *Proceedings of the National Academy of Sciences of the United States of America*, **98**(17), 9772–7.

Day, C. L., Kaufmann, D. E., Kiepiela, P., … Walker, B. D. (2006). PD-1 expression on HIV-specific T cells is associated with T-cell exhaustion and disease progression. *Nature*, **443**(7109), 350–354.

De Silva, N. S., & Klein, U. (2015). Dynamics of B cells in germinal centres. *Nature Reviews. Immunology*, **15**(3), 137–48.

Derbinski, J., Schulte, A., Kyewski, B., & Klein, L. (2001). Promiscuous gene expression in medullary thymic epithelial cells mirrors the peripheral self. *Nature Immunology*, **2**(11), 1032–1039.

Dias, S., Silva, H., Cumano, A., Vieira, P., & Vieira, P. (2005). Interleukin-7 is necessary to maintain the B cell potential in common lymphoid progenitors. *The Journal of Experimental Medicine*, **201**(6), 971–9.

Dietrich, J., Hou, X., Wegener, A. M., & Geisler, C. (1994). CD3 gamma contains a phosphoserine-dependent di-leucine motif involved in down-regulation of the T cell receptor. *The EMBO Journal*, **13**(9), 2156–66.

Dittmer, U., Brooks, D. M., & Hasenkrug, K. J. (1999). Requirement for multiple lymphocyte subsets in protection by a live attenuated vaccine against retroviral infection. *Nature Medicine*, **5**(2), 189–193.

Dittmer, U., Sutter, K., Kassiotis, G., … Hasenkrug, K. J. (2019). Friend retrovirus studies reveal complex interactions between intrinsic, innate and adaptive immunity. *FEMS Microbiology Reviews*. doi:10.1093/femsre/fuz012

Dokun, A. O., Kim, S., Smith, H. R. C., Kang, H.-S. P., Chu, D. T., & Yokoyama, W. M. (2001). Specific and nonspecific NK cell activation during virus infection. *Nature Immunology*, **2**(10), 951–956.

Du, X., Almeida, P. de, Manieri, N., … Chiang, E. Y. (2018). CD226 regulates natural killer cell antitumor responses via phosphorylation-mediated inactivation of transcription factor FOXO1. *Proceedings of the National Academy of Sciences*, **115**(50), E11731–E11740.

Dustin, M. L. (2002). The immunological synapse. *Arthritis Research*, **4**(Suppl 3), S119.

Ebihara, T., Song, C., Ryu, S. H., … Yokoyama, W. M. (2015). Runx3 specifies lineage commitment of innate lymphoid cells. *Nature Immunology*, **16**(11), 1124–1133.

Ehrhardt, G. R. A., Davis, R. S., Hsu, J. T., Leu, C.-M., Ehrhardt, A., & Cooper, M. D. (2003). The inhibitory potential of Fc receptor homolog 4 on memory B cells. *Proceedings of the National Academy of Sciences of the United States of America*, **100**(23), 13489–94.

El Firar, A., Voisin, T., Rouyer-Fessard, C., Ostuni, M. A., Couvineau, A., & Laburthe, M. (2009). Discovery of a functional immunoreceptor tyrosine-based switch motif in a 7-transmembrane-spanning receptor: role in the orexin receptor OX1R-driven apoptosis. *The FASEB Journal*, **23**(12), 4069–4080.

Esensten, J. H., Helou, Y. A., Chopra, G., Weiss, A., & Bluestone, J. A. (2016). CD28 Costimulation: From Mechanism to Therapy. *Immunity*. doi:10.1016/j.immuni.2016.04.020

Facchetti, F., Cella, M., Festa, S., Fremont, D. H., & Colonna, M. (2002). An unusual Fc receptor-related protein expressed in human centroblasts. *Proceedings of the National Academy of Sciences of the United States of America*, **99**(6), 3776–81.

Fan, M. Y., Low, J. S., Tanimine, N., … Turka, L. A. (2018). Differential Roles of IL-2 Signaling in Developing versus Mature Tregs. *Cell Reports*, **25**(5), 1204-1213.e4.

Feng, Y., Roy, A., Masson, E., Chen, T.-T., Humphrey, R., & Weber, J. S. (2013). Exposure-Response Relationships of the Efficacy and Safety of Ipilimumab in Patients with Advanced Melanoma. *Clinical Cancer Research*, **19**(14), 3977–3986.

Ferguson, S. S. (2001). Evolving concepts in G protein-coupled receptor endocytosis: the role in receptor desensitization and signaling. *Pharmacological Reviews*, **53**(1), 1–24.

Fife, B. T., & Pauken, K. E. (2011). The role of the PD-1 pathway in autoimmunity and peripheral tolerance. *Annals of the New York Academy of Sciences*, **1217**(1), 45–59.

Firth, M. A., Madera, S., Beaulieu, A. M., … Sun, J. C. (2013). Nfil3-independent lineage maintenance and antiviral response of natural killer cells. *The Journal of Experimental Medicine*, **210**(13), 2981–2990.

Fisher, A. G., Burdet, C., Bunce, C., Merkenschlager, M., & Ceredig, R. (1995). Lymphoproliferative disorders in IL-7 transgenic mice: expansion of immature B cells which retain macrophage potential. *International Immunology*, **7**(3), 415–423.

Flannagan, R. S., Heit, B., & Heinrichs, D. E. (2015). Antimicrobial Mechanisms of Macrophages and the Immune Evasion Strategies of Staphylococcus aureus. *Pathogens (Basel, Switzerland)*, **4**(4), 826–68.

Fleming, H. E., & Paige, C. J. (2001). Pre-B cell receptor signaling mediates selective response to IL-7 at the pro-B to pre-B cell transition via an ERK/MAP kinase-dependent pathway. *Immunity*, **15**(4), 521–31.

Fourcade, J., Sun, Z., Benallaoua, M., … Zarour, H. M. (2010). Upregulation of Tim-3 and PD-1 expression is associated with tumor antigen–specific CD8 $^{+}$ T cell dysfunction in melanoma patients. *The Journal of Experimental Medicine*, **207**(10), 2175–2186.

Fracchia, K. M., Pai, C. Y., & Walsh, C. M. (2013). Modulation of T Cell Metabolism and Function through Calcium Signaling. *Frontiers in Immunology*, **4**, 324.

Freeman, G. J., Long, A. J., Iwai, Y., … Honjo, T. (2000). Engagement of the PD-1 immunoinhibitory receptor by a novel B7 family member leads to negative regulation of lymphocyte activation. *The Journal of Experimental Medicine*, **192**(7), 1027–34.

Friend, C. (1957). Cell-free transmission in adult Swiss mice of a disease having the character of a leukemia. *The Journal of Experimental Medicine*, **105**(4), 307–18.

Fuertes Marraco, S. A., Neubert, N. J., Verdeil, G., & Speiser, D. E. (2015). Inhibitory Receptors Beyond T Cell Exhaustion. *Frontiers in Immunology*, **6**, 310.

Fuxa, M., & Busslinger, M. (2007). Reporter gene insertions reveal a strictly B lymphoid-specific expression pattern of *Pax5* in support of its B cell identity function. *The Journal of Immunology*, **178**(12), 8221.2-8221.

Gasser, S., & Raulet, D. H. (2006). Activation and self-tolerance of natural killer cells. *Immunological Reviews*, **214**(1), 130–142.

Geiger, T. L., & Sun, J. C. (2016). Development and maturation of natural killer cells. *Current Opinion in Immunology*, **39**, 82–9.

Germain, R. N. (2002). T-cell development and the CD4–CD8 lineage decision. *Nature Reviews Immunology*, **2**(5), 309–322.

Gilfillan, S., Dierich, A., Lemeur, M., Benoist, C., & Mathis, D. (1993). Mice lacking TdT: mature animals with an immature lymphocyte repertoire. *Science*, **261**(5125), 1175–1178.

Giraud, M., Yoshida, H., Abramson, J., … Benoist, C. (2012). Aire unleashes stalled RNA polymerase to induce ectopic gene expression in thymic epithelial cells. *Proceedings of the National Academy of Sciences*, **109**(2), 535–540.

Godfrey, D. I., Kennedy, J., Suda, T., & Zlotnik, A. (1993). A developmental pathway involving four phenotypically and functionally distinct subsets of CD3-CD4-CD8- triple-negative adult mouse thymocytes defined by CD44 and CD25 expression. *Journal of Immunology (Baltimore, Md. : 1950)*, **150**(10), 4244–52.

Golden-Mason, L., Palmer, B. E., Kassam, N., … Rosen, H. R. (2009). Negative Immune Regulator Tim-3 Is Overexpressed on T Cells in Hepatitis C Virus Infection and Its Blockade Rescues Dysfunctional CD4+ and CD8+ T Cells. *Journal of Virology*, **83**(18), 9122–9130.

Gordon, S. M., Chaix, J., Rupp, L. J., … Reiner, S. L. (2012). The Transcription Factors T-bet and Eomes Control Key Checkpoints of Natural Killer Cell Maturation. *Immunity*, **36**(1), 55–67.

Gorelik, E., Wiltrout, R. H., Okumura, K., Habu, S., & Herberman, R. B. (1982). Role of NK cells in the control of metastatic spread and growth of tumor cells in mice. *International Journal of Cancer*, **30**(1), 107–112.

Greenfeder, S. A., Nunes, P., Kwee, L., Labow, M., Chizzonite, R. A., & Ju, G. (1995). Molecular Cloning and Characterization of a Second Subunit of the Interleukin 1 Receptor Complex. *Journal of Biological Chemistry*, **270**(23), 13757–13765.

Greenwald, R. J., Freeman, G. J., & Sharpe, A. H. (2005). THE B7 FAMILY REVISITED. *Annual Review of Immunology*, **23**(1), 515–548.

Groom, J. R., & Luster, A. D. (2011). CXCR3 in T cell function. *Experimental Cell Research*, **317**(5), 620–31.

Grundy, M. A., Zhang, T., & Sentman, C. L. (2007). NK cells rapidly remove B16F10 tumor cells in a perforin and interferon-gamma independent manner in vivo. *Cancer Immunology, Immunotherapy*, **56**(8), 1153–1161.

Guo, C., Yoon, H. S., Franklin, A., … Alt, F. W. (2011). CTCF-binding elements mediate control of V(D)J recombination. *Nature*, **477**(7365), 424–430.

Guo, Y., Maillard, I., Chakraborti, S., Rothenberg, E. V., & Speck, N. A. (2008a). Core binding factors are necessary for natural killer cell development and cooperate with Notch signaling during T-cell specification. *Blood*, **112**(3), 480–492.

Guo, Y., Maillard, I., Chakraborti, S., Rothenberg, E. V, & Speck, N. A. (2008b). Core binding factors are necessary for natural killer cell development and cooperate with Notch signaling during T-cell specification. *Blood*, **112**(3), 480–92.

Guselnikov, S. V, Ershova, S. A., Mechetina, L. V, … Taranin, A. V. (2002). A family of highly diverse human and mouse genes structurally links leukocyte FcR, gp42 and PECAM-1.

Immunogenetics, **54**(2), 87–95.

Guselnikov, S. V, Ramanayake, T., Erilova, A. Y., … Taranin, A. V. (2008). The Xenopus FcR family demonstrates continually high diversification of paired receptors in vertebrate evolution. *BMC Evolutionary Biology*, **8**, 148.

Haabeth, O. A. W., Tveita, A. A., Fauskanger, M., … Bogen, B. (2014). How Do CD4+ T Cells Detect and Eliminate Tumor Cells That Either Lack or Express MHC Class II Molecules? *Frontiers in Immunology*, **5**, 174.

Haga, C. L., Ehrhardt, G. R. A., Boohaker, R. J., Davis, R. S., & Cooper, M. D. (2007). Fc receptor-like 5 inhibits B cell activation via SHP-1 tyrosine phosphatase recruitment. *Proceedings of the National Academy of Sciences of the United States of America*, **104**(23), 9770–5.

Haks, M. C., Lefebvre, J. M., Lauritsen, J. P. H., … Wiest, D. L. (2005). Attenuation of γδTCR Signaling Efficiently Diverts Thymocytes to the αβ Lineage. *Immunity*, **22**(5), 595–606.

Hanna, N. (1982). Role of natural killer cells in control of cancer metastasis. *Cancer Metastasis Reviews*, **1**(1), 45–64.

Hardy, R. R., Carmack, C. E., Shinton, S. A., Kemp, J. D., & Hayakawa, K. (1991). Resolution and characterization of pro-B and pre-pro-B cell stages in normal mouse bone marrow. *Journal of Experimental Medicine*, **173**(5), 1213–1225.

Hardy, R. R., & Hayakawa, K. (2001). B C ELL D EVELOPMENT P ATHWAYS. *Annual Review of Immunology*, **19**(1), 595–621.

Harty, J. T., Tvinnereim, A. R., & White, D. W. (2000). *CD8 T CELL EFFECTOR MECHANISMS IN RESISTANCE TO INFECTION*. *Annu. Rev. Immunol*, Vol. 18. Retrieved from www.annualreviews.org

Hasenkrug, K. J., Brooks, D. M., & Dittmer, U. (1998). Critical role for CD4(+) T cells in controlling retrovirus replication and spread in persistently infected mice. *Journal of Virology*, **72**(8), 6559–64.

Hasenkrug, K. J., & Chesebro, B. (1997). Immunity to retroviral infection: the Friend virus model. *Proceedings of the National Academy of Sciences of the United States of America*, **94**(15), 7811–6.

Hashimoto, M., Kamphorst, A. O., Im, S. J., … Ahmed, R. (2018). CD8 T Cell Exhaustion in Chronic Infection and Cancer: Opportunities for Interventions. *Annual Review of Medicine*, **69**(1), 301–318.

Hatzivassiliou, G., Miller, I., Takizawa, J., … Dalla-Favera, R. (2001a). IRTA1 and IRTA2, novel immunoglobulin superfamily receptors expressed in B cells and involved in chromosome 1q21 abnormalities in B cell malignancy. *Immunity*, **14**(3), 277–89.

Hatzivassiliou, G., Miller, I., Takizawa, J., … Dalla-Favera, R. (2001b). IRTA1 and IRTA2, Novel Immunoglobulin Superfamily Receptors Expressed in B Cells and Involved in Chromosome 1q21 Abnormalities in B Cell Malignancy. *Immunity*, **14**(3), 277–289.

He, L., Zhang, G., He, Y., Zhu, H., Zhang, H., & Feng, Z. (2005). Blockade of B7-H1 with sPD-1 improves immunity against murine hepatocarcinoma. *Anticancer Research*, **25**(5), 3309–13.

He, Y., & Tian, Z. (2017). NK cell education via nonclassical MHC and non-MHC ligands. *Cellular & Molecular Immunology*, **14**(4), 321–330.

Hedges, S. B., & Kumar, S. (1998). A molecular timescale for vertebrate evolution. *Nature*, **392**(6679), 917–920.

Hermiston, M. L., Xu, Z., & Weiss, A. (2003). CD45: A Critical Regulator of Signaling Thresholds in Immune Cells. *Annual Review of Immunology*, **21**(1), 107–137.

Hildeman, D. A., Zhu, Y., Mitchell, T. C., Kappler, J., & Marrack, P. (2002). Molecular mechanisms of activated T cell death in vivo. *Current Opinion in Immunology*, **14**(3), 354–359.

Hirano, M., Das, S., Guo, P., & Cooper, M. D. (2011). The Evolution of Adaptive Immunity in Vertebrates. In *Advances in immunology*, Vol. 109, pp. 125–157.

Hobeika, E., Thiemann, S., Storch, B., … Reth, M. (2006). Testing gene function early in the B

cell lineage in mb1-cre mice. *Proceedings of the National Academy of Sciences of the United States of America*, **103**(37), 13789–94.

Holmes, M. L., Huntington, N. D., Thong, R. P., … Nutt, S. L. (2014). Peripheral natural killer cell maturation depends on the transcription factor Aiolos. *The EMBO Journal*, **33**(22), 2721–2734.

Hoving, J. C., Wilson, G. J., & Brown, G. D. (2014). Signalling C-type lectin receptors, microbial recognition and immunity. *Cellular Microbiology*, **16**(2), 185–94.

Huard, B., Gaulard, P., Faure, F., Hercend, T., & Triebel, F. (1994). Cellular expression and tissue distribution of the human LAG-3-encoded protein, an MHC class II ligand. *Immunogenetics*, **39**(3). doi:10.1007/BF00241263

Humphrey, M. B., Lanier, L. L., & Nakamura, M. C. (2005). Role of ITAM-containing adapter proteins and their receptors in the immune system and bone. *Immunological Reviews*, **208**(1), 50–65.

Imboden, J. B., Eriksson, E. C., McCutcheon, M., Reynolds, C. W., & Seaman, W. E. (1989). Identification and characterization of a cell-surface molecule that is selectively induced on rat lymphokine-activated killer cells. *Journal of Immunology (Baltimore, Md. : 1950)*, **143**(9), 3100–3.

Intlekofer, A. M., Takemoto, N., Wherry, E. J., … Reiner, S. L. (2005). Effector and memory CD8+ T cell fate coupled by T-bet and eomesodermin. *Nature Immunology*, **6**(12), 1236–1244.

Ishida, M., Iwai, Y., Tanaka, Y., … Honjo, T. (2002). Differential expression of PD-L1 and PD-L2, ligands for an inhibitory receptor PD-1, in the cells of lymphohematopoietic tissues. *Immunology Letters*, **84**(1), 57–62.

Ishida, Y., Agata, Y., Shibahara, K., & Honjo, T. (1992). Induced expression of PD-1, a novel member of the immunoglobulin gene superfamily, upon programmed cell death. *The EMBO Journal*, **11**(11), 3887–3895.

Ito, M., Maruyama, T., Saito, N., Koganei, S., Yamamoto, K., & Matsumoto, N. (2006). Killer cell lectin-like receptor G1 binds three members of the classical cadherin family to inhibit NK cell cytotoxicity. *The Journal of Experimental Medicine*, **203**(2), 289–95.

Iwasaki, A., & Medzhitov, R. (2010). Regulation of adaptive immunity by the innate immune system. *Science (New York, N.Y.)*, **327**(5963), 291–5.

Iwashiro, M., Kondo, T., Shimizu, T., … Ishimoto, A. (1993). Multiplicity of virus-encoded helper T-cell epitopes expressed on FBL-3 tumor cells. *Journal of Virology*, **67**(8), 4533–42.

Jackson, T. A., Haga, C. L., Ehrhardt, G. R. A., Davis, R. S., & Cooper, M. D. (2010). FcR-like 2 Inhibition of B cell receptor-mediated activation of B cells. *Journal of Immunology (Baltimore, Md. : 1950)*, **185**(12), 7405–12.

Jamieson, A. M., Diefenbach, A., McMahon, C. W., Xiong, N., Carlyle, J. R., & Raulet, D. H. (2002). The role of the NKG2D immunoreceptor in immune cell activation and natural killing. *Immunity*, **17**(1), 19–29.

Janeway, C. (2001). *Immunobiology 5 : the immune system in health and disease*, Garland Pub.

Janssens, S., Burns, K., Tschopp, J., & Beyaert, R. (2002). Regulation of interleukin-1- and lipopolysaccharide-induced NF-kappaB activation by alternative splicing of MyD88. *Current Biology : CB*, **12**(6), 467–71.

Jenkins, N. A., Copeland, N. G., Taylor, B. A., & Lee, B. K. (1982). Organization, distribution, and stability of endogenous ecotropic murine leukemia virus DNA sequences in chromosomes of Mus musculus. *Journal of Virology*, **43**(1), 26–36.

Jenne, C. N., Enders, A., Rivera, R., … Chun, J. (2009). T-bet–dependent S1P $_5$ expression in NK cells promotes egress from lymph nodes and bone marrow. *The Journal of Experimental Medicine*, **206**(11), 2469–2481.

Jiang, Y., Li, Y., & Zhu, B. (2015). T-cell exhaustion in the tumor microenvironment. *Cell Death & Disease*, **6**(6), e1792–e1792.

Joedicke, J. J., Zelinskyy, G., Dittmer, U., & Hasenkrug, K. J. (2014). CD8+ T cells are essential for controlling acute friend retrovirus infection in C57BL/6 mice. *Journal of Virology*, **88**(9), 5200–1.

Johnson, D. B., Nixon, M. J., Wang, Y., … Balko, J. M. (2018a). Tumor-specific MHC-II expression drives a unique pattern of resistance to immunotherapy via LAG-3/FCRL6 engagement. *JCI Insight*, **3**(24). doi:10.1172/jci.insight.120360

Johnson, D. B., Nixon, M. J., Wang, Y., … Balko, J. M. (2018b). Tumor-specific MHC-II expression drives a unique pattern of resistance to immunotherapy via LAG-3/FCRL6 engagement. *JCI Insight*, **3**(24). doi:10.1172/JCI.INSIGHT.120360

Jones, R. B., Ndhlovu, L. C., Barbour, J. D., … Ostrowski, M. A. (2008). Tim-3 expression defines a novel population of dysfunctional T cells with highly elevated frequencies in progressive HIV-1 infection. *The Journal of Experimental Medicine*, **205**(12), 2763–79.

José, E. S., Borroto, A., Niedergang, F., Alcover, A., & Alarcón, B. (2000). Triggering the TCR Complex Causes the Downregulation of Nonengaged Receptors by a Signal Transduction-Dependent Mechanism. *Immunity*, **12**(2), 161–170.

Kaech, S. M., & Cui, W. (2012). Transcriptional control of effector and memory CD8+ T cell differentiation. *Nature Reviews. Immunology*, **12**(11), 749–61.

Kahan, S. M., Wherry, E. J., & Zajac, A. J. (2015). T cell exhaustion during persistent viral infections. *Virology*, **479**–**480**, 180–193.

Kamimura, Y., & Lanier, L. L. (2015). Homeostatic Control of Memory Cell Progenitors in the Natural Killer Cell Lineage. *Cell Reports*, **10**(2), 280–291.

Kane, B. A., Bryant, K. J., McNeil, H. P., & Tedla, N. T. (2014). Termination of immune activation: an essential component of healthy host immune responses. *Journal of Innate Immunity*, **6**(6), 727–38.

Kantor, A. B., & Herzenberg, L. A. (1993). Origin of Murine B Cell Lineages. *Annual Review of Immunology*, **11**(1), 501–538.

Kaplan, M. H., Hufford, M. M., & Olson, M. R. (2015). The development and in vivo function of T helper 9 cells. *Nature Reviews Immunology*, **15**(5), 295–307.

Kappes, D. J., He, X., & He, X. (2005). CD4-CD8 lineage commitment: an inside view. *Nature Immunology*, **6**(8), 761–766.

Karo, J. M., Schatz, D. G., & Sun, J. C. (2014). The RAG Recombinase Dictates Functional Heterogeneity and Cellular Fitness in Natural Killer Cells. *Cell*, **159**(1), 94–107.

Kawai, T., & Akira, S. (2006). TLR signaling. *Cell Death & Differentiation*, **13**(5), 816–825.

Kawai, T., & Akira, S. (2009). The roles of TLRs, RLRs and NLRs in pathogen recognition. *International Immunology*, **21**(4), 317–37.

Kawasaki, T., & Kawai, T. (2014). Toll-like receptor signaling pathways. *Frontiers in Immunology*, **5**, 461.

Kaye, J. (2008). CD160 and BTLA: LIGHTs out for CD4+ T cells. *Nature Immunology*, **9**(2), 122–124.

Kennedy, M. K., Glaccum, M., Brown, S. N., … Peschon, J. J. (2000). Reversible defects in natural killer and memory CD8 T cell lineages in interleukin 15-deficient mice. *The Journal of Experimental Medicine*, **191**(5), 771–80.

Keppel, M. P., Yang, L., & Cooper, M. A. (2013). Murine NK Cell Intrinsic Cytokine-Induced Memory-like Responses Are Maintained following Homeostatic Proliferation. *The Journal of Immunology*, **190**(9), 4754–4762.

Kienle, K., & Lämmermann, T. (2016). Neutrophil swarming: an essential process of the neutrophil tissue response. *Immunological Reviews*, **273**(1), 76–93.

Kim, S., Poursine-Laurent, J., Truscott, S. M., … Yokoyama, W. M. (2005). Licensing of natural killer cells by host major histocompatibility complex class I molecules. *Nature*, **436**(7051), 709–713.

King, S. R., Bersont, B. J., & Risser, R. (1988). Mechanism of interaction between endogenous ecotropic murine leukemia viruses in (BALB/c × C57BL/6) hybrid cells. *Virology*, **162**(1), 1–11.

Klein, L., Kyewski, B., Allen, P. M., & Hogquist, K. A. (2014). Positive and negative selection of the T cell repertoire: what thymocytes see (and don't see). *Nature Reviews Immunology*, **14**(6), 377–391.

Kobayashi, K., Hernandez, L. D., Galán, J. E., Janeway, C. A., Medzhitov, R., & Flavell, R. A. (2002). IRAK-M is a negative regulator of Toll-like receptor signaling. *Cell*, **110**(2), 191–202.

Kochi, Y., Myouzen, K., Yamada, R., … Yamamoto, K. (2009). FCRL3, an autoimmune susceptibility gene, has inhibitory potential on B-cell receptor-mediated signaling. *Journal of Immunology (Baltimore, Md. : 1950)*, **183**(9), 5502–10.

Kondo, M., Weissman, I. L., & Akashi, K. (1997). Identification of clonogenic common lymphoid progenitors in mouse bone marrow. *Cell*, **91**(5), 661–72.

Kozako, T., Yoshimitsu, M., Fujiwara, H., … Arima, N. (2009). PD-1/PD-L1 expression in human T-cell leukemia virus type 1 carriers and adult T-cell leukemia/lymphoma patients. *Leukemia*, **23**(2), 375–382.

Krangel, M. S. (2009). Mechanics of T cell receptor gene rearrangement. *Current Opinion in Immunology*, **21**(2), 133–139.

Krieg, C., Boyman, O., Fu, Y.-X., & Kaye, J. (2007). B and T lymphocyte attenuator regulates CD8+ T cell–intrinsic homeostasis and memory cell generation. *Nature Immunology*, **8**(2), 162–171.

Kruse, P. H., Matta, J., Ugolini, S., & Vivier, E. (2014). Natural cytotoxicity receptors and their ligands. *Immunology and Cell Biology*, **92**(3), 221–229.

Kulemzin, S. V., Zamoshnikova, A. Y., Yurchenko, M. Y., … Mechetina, L. V. (2011a). FCRL6 receptor: Expression and associated proteins. *Immunology Letters*, **134**(2), 174–182.

Kulemzin, S. V, Zamoshnikova, A. Y., Yurchenko, M. Y., … Mechetina, L. V. (2011b). FCRL6 receptor: expression and associated proteins. *Immunology Letters*, **134**(2), 174–82.

Kurosaki, T., Shinohara, H., & Baba, Y. (2010). B Cell Signaling and Fate Decision. *Annual Review of Immunology*, **28**(1), 21–55.

Kyewski, B., & Klein, L. (2006). A CENTRAL ROLE FOR CENTRAL TOLERANCE. *Annual Review of Immunology*, **24**(1), 571–606.

Lander, M. R., & Chattopadhyay, S. K. (1984). A Mus dunni cell line that lacks sequences closely related to endogenous murine leukemia viruses and can be infected by ectropic, amphotropic, xenotropic, and mink cell focus-forming viruses. *Journal of Virology*, **52**(2), 695–8.

Lantz, O., Grandjean, I., Matzinger, P., & Di Santo, J. P. (2000). γ chain required for naïve CD4+ T cell survival but not for antigen proliferation. *Nature Immunology*, **1**(1), 54–58.

Latchman, Y., Wood, C. R., Chernova, T., … Freeman, G. J. (2001). PD-L2 is a second ligand for PD-1 and inhibits T cell activation. *Nature Immunology*, **2**(3), 261–268.

Latour, S., & Veillette, A. (2001). Proximal protein tyrosine kinases in immunoreceptor signaling. *Current Opinion in Immunology*, **13**(3), 299–306.

Lee, M. S., & Kim, Y.-J. (2007). Signaling Pathways Downstream of Pattern-Recognition Receptors and Their Cross Talk. *Annual Review of Biochemistry*, **76**(1), 447–480.

Lee, P. P., Yee, C., Savage, P. A., … Davis, M. M. (1999). Characterization of circulating T cells specific for tumor-associated antigens in melanoma patients. *Nature Medicine*, **5**(6), 677–685.

León, B., López-Bravo, M., & Ardavín, C. (2007). Monocyte-Derived Dendritic Cells Formed at the Infection Site Control the Induction of Protective T Helper 1 Responses against Leishmania. *Immunity*, **26**(4), 519–531.

Leu, C.-M., Davis, R. S., Gartland, L. A., Fine, W. D., & Cooper, M. D. (2005). FcRH1: an

activation coreceptor on human B cells. *Blood*, **105**(3), 1121–6.

Levine, S. J. (2004). Mechanisms of Soluble Cytokine Receptor Generation. *The Journal of Immunology*, **173**(9), 5343–5348.

Li, C., Siemasko, K., Clark, M. R., & Song, W. (2002). Cooperative interaction of Ig(alpha) and Ig(beta) of the BCR regulates the kinetics and specificity of antigen targeting. *International Immunology*, **14**(10), 1179–91.

Li, F. J., Won, W. J., Becker, E. J., … Davis, R. S. (2014a). Emerging roles for the FCRL family members in lymphocyte biology and disease. *Current Topics in Microbiology and Immunology*, **382**, 29–50.

Li, F., Smith, P., & Ravetch, J. V. (2014b). Inhibitory Fcγ receptor is required for the maintenance of tolerance through distinct mechanisms. *Journal of Immunology (Baltimore, Md. : 1950)*, **192**(7), 3021–8.

Li, X., Gadzinsky, A., Gong, L., … Gu, H. (2018). Cbl Ubiquitin Ligases Control B Cell Exit from the Germinal-Center Reaction. *Immunity*, **48**(3), 530-541.e6.

Li, Y. S., Wasserman, R., Hayakawa, K., & Hardy, R. R. (1996). Identification of the earliest B lineage stage in mouse bone marrow. *Immunity*, **5**(6), 527–35.

Liew, F. Y., Xu, D., Brint, E. K., & O'Neill, L. A. J. (2005). Negative regulation of Toll-like receptor-mediated immune responses. *Nature Reviews Immunology*, **5**(6), 446–458.

Lin, J., Miller, M. J., & Shaw, A. S. (2005). The c-SMAC: Sorting it all out (or in). *Journal of Cell Biology*. doi:10.1083/jcb.200503032

Lindsley, R. C., Thomas, M., Srivastava, B., & Allman, D. (2007). Generation of peripheral B cells occurs via two spatially and temporally distinct pathways. *Blood*, **109**(6), 2521–2528.

Littwitz, E., Francois, S., Dittmer, U., & Gibbert, K. (2013). Distinct roles of NK cells in viral immunity during different phases of acute Friend retrovirus infection. *Retrovirology*, **10**, 127.

Liu, H., Schmidt-Supprian, M., Shi, Y., … Shi, Y. (2007). Yin Yang 1 is a critical regulator of B-cell development. *Genes & Development*, **21**(10), 1179–89.

Lohoff, M., Duncan, G. S., Ferrick, D., … Mak, T. W. (2000). Deficiency in the Transcription Factor Interferon Regulatory Factor (Irf)-2 Leads to Severely Compromised Development of Natural Killer and T Helper Type 1 Cells. *The Journal of Experimental Medicine*, **192**(3), 325–336.

Love, P. E., & Hayes, S. M. (2010). ITAM-mediated signaling by the T-cell antigen receptor. *Cold Spring Harbor Perspectives in Biology*, **2**(6), a002485.

Lund, F. E. (2008). Cytokine-producing B lymphocytes—key regulators of immunity. *Current Opinion in Immunology*, **20**(3), 332–338.

Magalhaes, A. C., Dunn, H., & Ferguson, S. S. (2012). Regulation of GPCR activity, trafficking and localization by GPCR-interacting proteins. *British Journal of Pharmacology*, **165**(6), 1717–1736.

Maillard, I., Fang, T., & Pear, W. S. (2005). REGULATION OF LYMPHOID DEVELOPMENT, DIFFERENTIATION, AND FUNCTION BY THE NOTCH PATHWAY. *Annual Review of Immunology*, **23**(1), 945–974.

Male, V., Nisoli, I., Kostrzewski, T., … Brady, H. J. M. (2014). The transcription factor E4bp4/Nfil3 controls commitment to the NK lineage and directly regulates Eomes and Id2 expression. *The Journal of Experimental Medicine*, **211**(4), 635–642.

Maloy, K. J., & Uhlig, H. H. (2013). ILC1 Populations Join the Border Patrol. *Immunity*, **38**(4), 630–632.

Maltais, L. J., Lovering, R. C., Taranin, A. V, … Davis, R. S. (2006). New nomenclature for Fc receptor–like molecules. *Nature Immunology*, **7**(5), 431–432.

Malynn, B. A., & Ma, A. (2010). Ubiquitin Makes Its Mark on Immune Regulation. *Immunity*, **33**(6), 843–852.

Mandl, J. N., Monteiro, J. P., Vrisekoop, N., & Germain, R. N. (2013). T Cell-Positive Selection

Uses Self-Ligand Binding Strength to Optimize Repertoire Recognition of Foreign Antigens. *Immunity*, **38**(2), 263–274.

Mansson, R., Zandi, S., Anderson, K., … Sigvardsson, M. (2008). B-lineage commitment prior to surface expression of B220 and CD19 on hematopoietic progenitor cells. *Blood*, **112**(4), 1048–1055.

Manzke, N., Akhmetzyanova, I., Hasenkrug, K. J., Trilling, M., Zelinskyy, G., & Dittmer, U. (2013). CD4+ T Cells Develop Antiretroviral Cytotoxic Activity in the Absence of Regulatory T Cells and CD8+ T Cells. *Journal of Virology*, **87**(11), 6306–6313.

Marçais, A., Cherfils-Vicini, J., Viant, C., … Walzer, T. (2014). The metabolic checkpoint kinase mTOR is essential for IL-15 signaling during the development and activation of NK cells. *Nature Immunology*, **15**(8), 749–757.

Marques, R., Antunes, I., Eksmond, U., Stoye, J., Hasenkrug, K., & Kassiotis, G. (2008). B lymphocyte activation by coinfection prevents immune control of friend virus infection. *Journal of Immunology (Baltimore, Md. : 1950)*, **181**(5), 3432–40.

Marrack, P., Scott-Browne, J. P., Dai, S., Gapin, L., & Kappler, J. W. (2008). Evolutionarily Conserved Amino Acids That Control TCR-MHC Interaction. *Annual Review of Immunology*, **26**(1), 171–203.

Martinez-Lostao, L., Anel, A., & Pardo, J. (2015). How Do Cytotoxic Lymphocytes Kill Cancer Cells? *Clinical Cancer Research*, **21**(22), 5047–5056.

Maruhashi, T., Okazaki, I., Sugiura, D., … Okazaki, T. (2018). LAG-3 inhibits the activation of CD4+ T cells that recognize stable pMHCII through its conformation-dependent recognition of pMHCII. *Nature Immunology*, **19**(12), 1415–1426.

Masteller, E. L., Chuang, E., Mullen, A. C., Reiner, S. L., & Thompson, C. B. (2000). Structural analysis of CTLA-4 function in vivo. *Journal of Immunology (Baltimore, Md. : 1950)*, **164**(10), 5319–27.

Masuda, K., Mori, H., Ohara, O., Nakayama, M., Wang, J.-Y., & Burrows, P. D. (2010). Defining the immunological phenotype of Fc receptor-like B (FCRLB) deficient mice: Confounding role of the inhibitory FcγRIIb. *Cellular Immunology*, **266**(1), 24–31.

Mauri, C., & Bosma, A. (2012). Immune Regulatory Function of B Cells. *Annual Review of Immunology*, **30**(1), 221–241.

Mazzucchelli, R., Hixon, J. A., Spolski, R., … Durum, S. K. (2008). Development of regulatory T cells requires IL-7Ralpha stimulation by IL-7 or TSLP. *Blood*, **112**(8), 3283–92.

McGuire, K. L., & Vitetta, E. S. (1981). kappa/lambda Shifts do not occur during maturation of murine B cells. *Journal of Immunology (Baltimore, Md. : 1950)*, **127**(4), 1670–73.

McLane, L. M., Abdel-Hakeem, M. S., & Wherry, E. J. (2019). CD8 T Cell Exhaustion During Chronic Viral Infection and Cancer. *Annual Review of Immunology*, **37**(1), 457–495.

McMahan, R. H., Golden-Mason, L., Nishimura, M. I., … Rosen, H. R. (2010). Tim-3 expression on PD-1+ HCV-specific human CTLs is associated with viral persistence, and its blockade restores hepatocyte-directed in vitro cytotoxicity. *Journal of Clinical Investigation*, **120**(12), 4546–4557.

Mebius, R. E., & Kraal, G. (2005). Structure and function of the spleen. *Nature Reviews Immunology*, **5**(8), 606–616.

Mechetina, L. V, Najakshin, A. M., Volkova, O. Y., … Taranin, A. V. (2002). FCRL, a novel member of the leukocyte Fc receptor family possesses unique structural features. *European Journal of Immunology*, **32**(1), 87–96.

Merkenschlager, J., Eksmond, U., Danelli, L., … Kassiotis, G. (2019). MHC class II cell-autonomously regulates self-renewal and differentiation of normal and malignant B cells. *Blood*, **133**(10), 1108–1118.

Merrell, K. T., Benschop, R. J., Gauld, S. B., … Cambier, J. C. (2006). Identification of Anergic B Cells within a Wild-Type Repertoire. *Immunity*, **25**(6), 953–962.

Messer, R. J., Dittmer, U., Peterson, K. E., & Hasenkrug, K. J. (2004). Essential role for virus-neutralizing antibodies in sterilizing immunity against Friend retrovirus infection. *Proceedings of the National Academy of Sciences*, **101**(33), 12260–12265.

Migone, T. S., Cacalano, N. A., Taylor, N., Yi, T., Waldmann, T. A., & Johnston, J. A. (1998). Recruitment of SH2-containing protein tyrosine phosphatase SHP-1 to the interleukin 2 receptor; loss of SHP-1 expression in human T-lymphotropic virus type I-transformed T cells. *Proceedings of the National Academy of Sciences of the United States of America*, **95**(7), 3845–50.

Miller, I., Hatzivassiliou, G., Cattoretti, G., Mendelsohn, C., & Dalla-Favera, R. (2002). IRTAs: a new family of immunoglobulinlike receptors differentially expressed in B cells. *Blood*, **99**(8), 2662–9.

Monjas, A., Alcover, A., & Alarcón, B. (2004). Engaged and Bystander T Cell Receptors Are Down-modulated by Different Endocytotic Pathways. *Journal of Biological Chemistry*, **279**(53), 55376–55384.

Montecino-Rodriguez, E., & Dorshkind, K. (2012). B-1 B Cell Development in the Fetus and Adult. *Immunity*, **36**(1), 13–21.

Moretta, L. (2010). Dissecting CD56dim human NK cells. *Blood*, **116**(19), 3689–91.

Mostoslavsky, R., Singh, N., Kirillov, A., … Bergman, Y. (1998). Kappa chain monoallelic demethylation and the establishment of allelic exclusion. *Genes & Development*, **12**(12), 1801–11.

Mottok, A., Woolcock, B., Chan, F. C., … Steidl, C. (2015). Genomic Alterations in CIITA Are Frequent in Primary Mediastinal Large B Cell Lymphoma and Are Associated with Diminished MHC Class II Expression. *Cell Reports*, **13**(7), 1418–1431.

Mueller, D. L. (2010). Mechanisms maintaining peripheral tolerance. *Nature Immunology*, **11**(1), 21–27.

Nagata, S., Ise, T., & Pastan, I. (2009). Fc receptor-like 3 protein expressed on IL-2 nonresponsive subset of human regulatory T cells. *Journal of Immunology (Baltimore, Md.: 1950)*, **182**(12), 7518–26.

Naito, T., & Taniuchi, I. (2010). The network of transcription factors that underlie the CD4 versus CD8 lineage decision. *International Immunology*, **22**(10), 791–796.

Nakae, S., Suto, H., Iikura, M., … Galli, S. J. (2006). Mast Cells Enhance T Cell Activation: Importance of Mast Cell Costimulatory Molecules and Secreted TNF. *The Journal of Immunology*, **176**(4), 2238–2248.

Nakayama, Y., Weissman, S. M., & Bothwell, A. L. (2001). BXMAS1 identifies a cluster of homologous genes differentially expressed in B cells. *Biochemical and Biophysical Research Communications*, **285**(3), 830–7.

Narni-Mancinelli, E., Chaix, J., Fenis, A., … Vivier, E. (2011). Fate mapping analysis of lymphoid cells expressing the NKp46 cell surface receptor. *Proceedings of the National Academy of Sciences of the United States of America*, **108**(45), 18324–9.

Norvell, A., Mandik, L., & Monroe, J. G. (1995). Engagement of the antigen-receptor on immature murine B lymphocytes results in death by apoptosis. *Journal of Immunology (Baltimore, Md. : 1950)*, **154**(9), 4404–13.

Nurieva, R. I., Liu, X., & Dong, C. (2011). Molecular mechanisms of T-cell tolerance. *Immunological Reviews*, **241**(1), 133–144.

Nutt, S. L., Heavey, B., Rolink, A. G., & Busslinger, M. (1999). Commitment to the B-lymphoid lineage depends on the transcription factor Pax5. *Nature*, **401**(6753), 556–562.

O'Keefe, T. L., Williams, G. T., Batista, F. D., & Neuberger, M. S. (1999). Deficiency in CD22, a B Cell–specific Inhibitory Receptor, Is Sufficient to Predispose to Development of High Affinity Autoantibodies. *Journal of Experimental Medicine*, **189**(8), 1307–1313.

O'Keefe, T. L., Williams, G. T., Davies, S. L., & Neuberger, M. S. (1996). Hyperresponsive B Cells

in CD22-Deficient Mice. *Science*, **274**(5288), 798–801.

O'Neill, L. A. J., Golenbock, D., & Bowie, A. G. (2013). The history of Toll-like receptors — redefining innate immunity. *Nature Reviews Immunology*, **13**(6), 453–460.

O'Riordan, M., & Grosschedl, R. (1999). Coordinate regulation of B cell differentiation by the transcription factors EBF and E2A. *Immunity*, **11**(1), 21–31.

Oettinger, M., Schatz, D., Gorka, C., & Baltimore, D. (1990). RAG-1 and RAG-2, adjacent genes that synergistically activate V(D)J recombination. *Science*, **248**(4962), 1517–1523.

Okazaki, T., & Honjo, T. (2006). The PD-1–PD-L pathway in immunological tolerance. *Trends in Immunology*, **27**(4), 195–201.

Okazaki, T., Maeda, A., Nishimura, H., Kurosaki, T., & Honjo, T. (2001). PD-1 immunoreceptor inhibits B cell receptor-mediated signaling by recruiting src homology 2-domain-containing tyrosine phosphatase 2 to phosphotyrosine. *Proceedings of the National Academy of Sciences of the United States of America*, **98**(24), 13866–71.

Orr, M. T., & Lanier, L. L. (2010). Natural killer cell education and tolerance. *Cell*, **142**(6), 847–56.

Overwijk, W. W., & Restifo, N. P. (2001). B16 as a mouse model for human melanoma. *Current Protocols in Immunology*, **Chapter 20**, Unit 20.1.

Pang, J., Taylor, G. R., Munroe, D. G., … Zhou, L. (1993). Characterization of the gene for the human high affinity IgE receptor (Fc epsilon RI) alpha-chain. *The Journal of Immunology*, **151**(11). Retrieved from http://www.jimmunol.org/content/151/11/6166

Papayannopoulos, V. (2018). Neutrophil extracellular traps in immunity and disease. *Nature Reviews Immunology*, **18**(2), 134–147.

Parkin, J., & Cohen, B. (2001). An overview of the immune system. *The Lancet*, **357**(9270), 1777–1789.

Pasquier, B., Launay, P., Kanamaru, Y., … Monteiro, R. C. (2005). Identification of FcαRI as an Inhibitory Receptor that Controls Inflammation. *Immunity*, **22**(1), 31–42.

Patra, A. K., Avots, A., Zahedi, R. P., … Serfling, E. (2013). An alternative NFAT-activation pathway mediated by IL-7 is critical for early thymocyte development. *Nature Immunology*, **14**(2), 127–135.

Patsoukis, N., Freeman, G. J., & Boussiotis, V. A. (2013). Distinct Roles Of PD-1 Itsm and ITIM In Regulating Interactions With SHP-2, ZAP-70 and Lck, and PD-1-Mediated Inhibitory Function. *Blood*, **122**(21). Retrieved from http://www.bloodjournal.org/content/122/21/191

Paul, S., & Lal, G. (2017). The Molecular Mechanism of Natural Killer Cells Function and Its Importance in Cancer Immunotherapy. *Frontiers in Immunology*, **8**, 1124.

Pegram, H. J., Andrews, D. M., Smyth, M. J., Darcy, P. K., & Kershaw, M. H. (2011). Activating and inhibitory receptors of natural killer cells. *Immunology and Cell Biology*, **89**(2), 216–224.

Pelanda, R., & Torres, R. M. (2012). Central B-cell tolerance: where selection begins. *Cold Spring Harbor Perspectives in Biology*, **4**(4), a007146.

Pennock, N. D., White, J. T., Cross, E. W., Cheney, E. E., Tamburini, B. A., & Kedl, R. M. (2013). T cell responses: naïve to memory and everything in between. *Advances in Physiology Education*, **37**(4), 273.

Pillai, S., & Cariappa, A. (2009). The follicular versus marginal zone B lymphocyte cell fate decision. *Nature Reviews Immunology*, **9**(11), 767–777.

Ploquin, M. J.-Y., Eksmond, U., & Kassiotis, G. (2011). B cells and TCR avidity determine distinct functions of CD4+ T cells in retroviral infection. *Journal of Immunology (Baltimore, Md.: 1950)*, **187**(6), 3321–30.

Poe, J. C., & Tedder, T. F. (2012). CD22 and Siglec-G in B cell function and tolerance. *Trends in Immunology*, **33**(8), 413–420.

Polson, A. G., Zheng, B., Elkins, K., … Ebens, A. (2006). Expression pattern of the human FcRH/IRTA receptors in normal tissue and in B-chronic lymphocytic leukemia. *International Immunology*, **18**(9), 1363–73.

Prinz, I., Sansoni, A., Kissenpfennig, A., Ardouin, L., Malissen, M., & Malissen, B. (2006). Visualization of the earliest steps of γδ T cell development in the adult thymus. *Nature Immunology*, **7**(9), 995–1003.

Prokopec, K. E., Georgoudaki, A.-M., Sohn, S., … Karlsson, M. C. I. (2016). Cutting Edge: Marginal Zone Macrophages Regulate Antigen Transport by B Cells to the Follicle in the Spleen via CD21. *Journal of Immunology (Baltimore, Md. : 1950)*, **197**(6), 2063–8.

Qiu, W. Q., de Bruin, D., Brownstein, B. H., Pearse, R., & Ravetch, J. V. (1990). Organization of the human and mouse low-affinity Fc gamma R genes: duplication and recombination. *Science (New York, N.Y.)*, **248**(4956), 732–5.

Qureshi, O. S., Zheng, Y., Nakamura, K., … Sansom, D. M. (2011). Trans-Endocytosis of CD80 and CD86: A Molecular Basis for the Cell-Extrinsic Function of CTLA-4. *Science*, **332**(6029), 600–603.

Radtke, F., Wilson, A., Stark, G., … Aguet, M. (1999). Deficient T cell fate specification in mice with an induced inactivation of Notch1. *Immunity*, **10**(5), 547–58.

Ravetch, J. V, & Lanier, L. L. (2000). Immune inhibitory receptors. *Science (New York, N.Y.)*, **290**(5489), 84–9.

Robey, E., & Fowlkes, B. J. (1994). Selective Events in T Cell Development. *Annual Review of Immunology*, **12**(1), 675–705.

Rose-John, S., Scheller, J., Elson, G., & Jones, S. A. (2006). Interleukin-6 biology is coordinated by membrane-bound and soluble receptors: role in inflammation and cancer. *Journal of Leukocyte Biology*, **80**(2), 227–236.

Roy, D. C., & Perreault, C. (2017). Major vs minor histocompatibility antigens. *Blood*, **129**(6), 664–666.

Rumfelt, L. L., Zhou, Y., Rowley, B. M., Shinton, S. A., & Hardy, R. R. (2006). Lineage specification and plasticity in CD19 $^{-}$ early B cell precursors. *The Journal of Experimental Medicine*, **203**(3), 675–687.

Sakuishi, K., Apetoh, L., Sullivan, J. M., Blazar, B. R., Kuchroo, V. K., & Anderson, A. C. (2010). Targeting Tim-3 and PD-1 pathways to reverse T cell exhaustion and restore anti-tumor immunity. *The Journal of Experimental Medicine*, **207**(10), 2187–2194.

Sallusto, F., & Lanzavecchia, A. (2002). The instructive role of dendritic cells on T-cell responses. *Arthritis Research*, **4 Suppl 3**(Suppl 3), S127-32.

Sandquist, I., & Kolls, J. (2018). Update on regulation and effector functions of Th17 cells. *F1000Research*, **7**, 205.

Saravia, J., Chapman, N. M., & Chi, H. (2019). Helper T cell differentiation. *Cellular & Molecular Immunology*, **16**(7), 634–643.

Schatz, D. G., Oettinger, M. A., & Baltimore, D. (1989). The V(D)J recombination activating gene, RAG-1. *Cell*, **59**(6), 1035–1048.

Schönrich, G., Kalinke, U., Momburg, F., … Arnold, B. (1991). Down-regulation of T cell receptors on self-reactive T cells as a novel mechanism for extrathymic tolerance induction. *Cell*, **65**(2), 293–304.

Schreeder, D. M., Cannon, J. P., Wu, J., Li, R., Shakhmatov, M. A., & Davis, R. S. (2010). Cutting edge: FcR-like 6 is an MHC class II receptor. *Journal of Immunology (Baltimore, Md. : 1950)*, **185**(1), 23–7.

Schreeder, D. M., Pan, J., Li, F. J., Vivier, E., & Davis, R. S. (2008). FCRL6 distinguishes mature cytotoxic lymphocytes and is upregulated in patients with B-cell chronic lymphocytic leukemia. *European Journal of Immunology*, **38**(11), 3159–3166.

Schultz, K., Klarnet, J., Gieni, R., HayGlass, K., & Greenberg, P. (1990). The role of B cells for in vivo T cell responses to a Friend virus-induced leukemia. *Science*, **249**(4971), 921–923.

Schweighoffer, E., Vanes, L., Mathiot, A., Nakamura, T., & Tybulewicz, V. L. J. (2003). Unexpected requirement for ZAP-70 in pre-B cell development and allelic exclusion.

Immunity, **18**(4), 523–33.

Sedy, J. R., Gavrieli, M., Potter, K. G., … Murphy, K. M. (2005). B and T lymphocyte attenuator regulates T cell activation through interaction with herpesvirus entry mediator. *Nature Immunology*, **6**(1), 90–98.

Segal, A. W. (2005). How neutrophils kill microbes. *Annual Review of Immunology*, **23**, 197–223.

Sharpe, A. H., Wherry, E. J., Ahmed, R., & Freeman, G. J. (2007). The function of programmed cell death 1 and its ligands in regulating autoimmunity and infection. *Nature Immunology*, **8**(3), 239–245.

Shi, M., Lin, T. H., Appell, K. C., Berg, L. J., & Shevach, E. M. (2009). Cell cycle progression following naive T cell activation is independent of Jak3/common gamma-chain cytokine signals. *Journal of Immunology (Baltimore, Md. : 1950)*, **183**(7), 4493–501.

Shimizu, T., Uenishi, H., Teramura, Y., … Yamagishi, H. (1994). Fine structure of a virus-encoded helper T-cell epitope expressed on FBL-3 tumor cells. *Journal of Virology*, **68**(12), 7704–8.

Shlapatska, L. M., Mikhalap, S. V., Berdova, A. G., … Sidorenko, S. P. (2001). CD150 Association with Either the SH2-Containing Inositol Phosphatase or the SH2-Containing Protein Tyrosine Phosphatase Is Regulated by the Adaptor Protein SH2D1A. *The Journal of Immunology*, **166**(9), 5480–5487.

Sims, J. E., & Smith, D. E. (2010). The IL-1 family: regulators of immunity. *Nature Reviews Immunology*, **10**(2), 89–102.

Singer, A., Adoro, S., & Park, J.-H. (2008). Lineage fate and intense debate: myths, models and mechanisms of CD4- versus CD8-lineage choice. *Nature Reviews. Immunology*, **8**(10), 788–801.

Sitnicka, E., Brakebusch, C., Martensson, I.-L., … Jacobsen, S. E. W. (2003). Complementary Signaling through flt3 and Interleukin-7 Receptor α Is Indispensable for Fetal and Adult B Cell Genesis. *The Journal of Experimental Medicine*, **198**(10), 1495–1506.

Sojka, D. K., Plougastel-Douglas, B., Yang, L., … Yokoyama, W. M. (2014). Tissue-resident natural killer (NK) cells are cell lineages distinct from thymic and conventional splenic NK cells. *ELife*, **3**. doi:10.7554/ELIFE.01659

SPÄT, A., & HUNYADY, L. (2004). Control of Aldosterone Secretion: A Model for Convergence in Cellular Signaling Pathways. *Physiological Reviews*, **84**(2), 489–539.

Steidl, C., Shah, S. P., Woolcock, B. W., … Gascoyne, R. D. (2011a). MHC class II transactivator CIITA is a recurrent gene fusion partner in lymphoid cancers. *Nature*, **471**(7338), 377–381.

Steidl, C., Woolcock, B., Rogic, S., … Gascoyne, R. D. (2011b). Inactivating Gene Alterations of MHC Class II Transactivator CIITA Are Recurrent in Primary Mediastinal B Cell Lymphoma and Hodgkin Lymphoma. *Blood*, **118**(21). Retrieved from http://www.bloodjournal.org/content/118/21/437.abstract?sso-checked=true

Steinman, R., Mordoh, J., Wainstok, R., Goldszmid, R. S., Idoyaga, J., & Bravo, A. I. (2003). B16 Melanoma T Cell Immunity against + and CD8 + CD4 Tumor Cells Induce Long-Lived Protective Dendritic Cells Charged with Apoptotic. *J Immunol References*, **171**, 5940–5947.

Strominger, J. (1989). Developmental biology of T cell receptors. *Science*, **244**(4907), 943–950.

Sugiura, D., Maruhashi, T., Okazaki, I.-M., … Okazaki, T. (2019). Restriction of PD-1 function by cis-PD-L1/CD80 interactions is required for optimal T cell responses. *Science (New York, N.Y.)*, **364**(6440), 558–566.

Sun, L., & Ye, R. D. (2012). Role of G protein-coupled receptors in inflammation. *Acta Pharmacologica Sinica*, **33**(3), 342–350.

Sun, S.-C. (2008). Deubiquitylation and regulation of the immune response. *Nature Reviews Immunology*, **8**(7), 501–511.

Surh, C. D., & Sprent, J. (1994). T-cell apoptosis detected in situ during positive and negative selection in the thymus. *Nature*, **372**(6501), 100–103.

Takada, A., Yoshida, S., Kajikawa, M., … Kasahara, M. (2008). Two Novel NKG2D Ligands of

the Mouse H60 Family with Differential Expression Patterns and Binding Affinities to NKG2D. *The Journal of Immunology*, **180**(3), 1678–1685.

Takamura, S., Tsuji-Kawahara, S., Yagita, H., … Miyazawa, M. (2010). Premature terminal exhaustion of Friend virus-specific effector CD8+ T cells by rapid induction of multiple inhibitory receptors. *Journal of Immunology (Baltimore, Md. : 1950)*, **184**(9), 4696–707.

Takeda, K., Hayakawa, Y., Smyth, M. J., … Okumura, K. (2001). Involvement of tumor necrosis factor-related apoptosis-inducing ligand in surveillance of tumor metastasis by liver natural killer cells. *Nature Medicine*, **7**(1), 94–100.

Takeda, K., Nakayama, M., Sakaki, M., … Smyth, M. J. (2011). IFN-γ production by lung NK cells is critical for the natural resistance to pulmonary metastasis of B16 melanoma in mice. *Journal of Leukocyte Biology*, **90**(4), 777–785.

Takeuchi, A., Badr, M. E. S. G., Miyauchi, K., … Saito, T. (2016). CRTAM determines the CD4+ cytotoxic T lymphocyte lineage. *The Journal of Experimental Medicine*, **213**(1), 123–38.

Takeuchi, O., & Akira, S. (2010). Pattern Recognition Receptors and Inflammation. *Cell*, **140**(6), 805–820.

Taki, S., Nakajima, S., Ichikawa, E., Saito, T., & Hida, S. (2005). IFN Regulatory Factor-2 Deficiency Revealed a Novel Checkpoint Critical for the Generation of Peripheral NK Cells. *The Journal of Immunology*, **174**(10), 6005–6012.

Tangye, S. G. (2013). To B1 or not to B1: that really is still the question! *Blood*, **121**(26), 5109–10.

Teague, B. N., Pan, Y., Mudd, P. A., … Farris, A. D. (2007). Cutting edge: Transitional T3 B cells do not give rise to mature B cells, have undergone selection, and are reduced in murine lupus. *Journal of Immunology (Baltimore, Md. : 1950)*, **178**(12), 7511–5.

Teigler, J. E., Zelinskyy, G., Eller, M. A., … Streeck, H. (2017). Differential Inhibitory Receptor Expression on T Cells Delineates Functional Capacities in Chronic Viral Infection. *Journal of Virology*, **91**(23). doi:10.1128/JVI.01263-17

ten Boekel, E., Melchers, F., & Rolink, A. G. (1998). Precursor B cells showing H chain allelic inclusion display allelic exclusion at the level of pre-B cell receptor surface expression. *Immunity*, **8**(2), 199–207.

Thibodeau, J., Bourgeois-Daigneault, M.-C., & Lapointe, R. (2012). Targeting the MHC Class II antigen presentation pathway in cancer immunotherapy. *Oncoimmunology*, **1**(6), 908–916.

Tischner, D., Gaggl, I., Peschel, I., … Jan Wiegers, G. (2012). Defective cell death signalling along the Bcl-2 regulated apoptosis pathway compromises Treg cell development and limits their functionality in mice. *Journal of Autoimmunity*, **38**(1), 59–69.

Tourdot, B. E., Brenner, M. K., Keough, K. C., Holyst, T., Newman, P. J., & Newman, D. K. (2013). Immunoreceptor tyrosine-based inhibitory motif (ITIM)-mediated inhibitory signaling is regulated by sequential phosphorylation mediated by distinct nonreceptor tyrosine kinases: a case study involving PECAM-1. *Biochemistry*, **52**(15), 2597–608.

Trautmann, L., Janbazian, L., Chomont, N., … Sekaly, R.-P. (2006). Upregulation of PD-1 expression on HIV-specific CD8+ T cells leads to reversible immune dysfunction. *Nature Medicine*, **12**(10), 1198–1202.

Urbani, S., Amadei, B., Tola, D., … Ferrari, C. (2006). PD-1 expression in acute hepatitis C virus (HCV) infection is associated with HCV-specific CD8 exhaustion. *Journal of Virology*, **80**(22), 11398–403.

Valitutti, S., Müller, S., Dessing, M., & Lanzavecchia, A. (1996). Signal extinction and T cell repolarization in T helper cell-antigen-presenting cell conjugates. *European Journal of Immunology*, **26**(9), 2012–2016.

van de Winkel, J. G., Ernst, L. K., Anderson, C. L., & Chiu, I. M. (1991). Gene organization of the human high affinity receptor for IgG, Fc gamma RI (CD64). Characterization and evidence for a second gene. *The Journal of Biological Chemistry*, **266**(20), 13449–55.

van de Winkel, J. G. J., & Capel, P. J. A. (1993). Human IgG Fc receptor heterogeneity: molecular aspects and clinical implications. *Immunology Today*, **14**(5), 215–221.

van den Broek, M. F., Kägi, D., Zinkernagel, R. M., & Hengartner, H. (1995). Perforin dependence of natural killer cell-mediated tumor controlin vivo. *European Journal of Immunology*, **25**(12), 3514–3516.

van Egmond, M., Damen, C. A., van Spriel, A. B., Vidarsson, G., van Garderen, E., & van de Winkel, J. G. (2001). IgA and the IgA Fc receptor. *Trends in Immunology*, **22**(4), 205–11.

van Gent, D. C., Ramsden, D. A., & Gellert, M. (1996). The RAG1 and RAG2 proteins establish the 12/23 rule in V(D)J recombination. *Cell*, **85**(1), 107–13.

Vance, R. E., Kraft, J. R., Altman, J. D., Jensen, P. E., & Raulet, D. H. (1998). Mouse CD94/NKG2A is a natural killer cell receptor for the nonclassical major histocompatibility complex (MHC) class I molecule Qa-1(b). *The Journal of Experimental Medicine*, **188**(10), 1841–8.

Varol, C., Mildner, A., & Jung, S. (2015). Macrophages: Development and Tissue Specialization. *Annual Review of Immunology*, **33**(1), 643–675.

Velu, V., Titanji, K., Zhu, B., … Amara, R. R. (2009). Enhancing SIV-specific immunity in vivo by PD-1 blockade. *Nature*, **458**(7235), 206–210.

Viganò, S., Perreau, M., Pantaleo, G., & Harari, A. (2012). Positive and Negative Regulation of Cellular Immune Responses in Physiologic Conditions and Diseases. *Clinical and Developmental Immunology*, **2012**, 1–11.

Vinuesa, C. G., & Chang, P.-P. (2013). Innate B cell helpers reveal novel types of antibody responses. *Nature Immunology*, **14**(2), 119–126.

Vivier, E., Tomasello, E., Baratin, M., Walzer, T., & Ugolini, S. (2008). Functions of natural killer cells. *Nature Immunology*, **9**(5), 503–510.

von Boehmer, H., & Fehling, H. J. (1997). STRUCTURE AND FUNCTION OF THE PRE-T CELL RECEPTOR. *Annual Review of Immunology*, **15**(1), 433–452.

Voskoboinik, I., Smyth, M. J., & Trapani, J. A. (2006). Perforin-mediated target-cell death and immune homeostasis. *Nature Reviews Immunology*, **6**(12), 940–952.

Walker, J. A., & McKenzie, A. N. J. (2018). TH2 cell development and function. *Nature Reviews Immunology*, **18**(2), 121–133.

Walker, L. S. K., & Sansom, D. M. (2015). Confusing signals: Recent progress in CTLA-4 biology. *Trends in Immunology*, **36**(2), 63–70.

Wang, J., Knaut, H., He, X., … Pleasure, S. J. (2014). Chemokine signaling in development and disease. *Development (Cambridge, England)*, **141**(22), 4199–205.

Wang, Y., Shi, J., Yan, J., … Qi, H. (2017). Germinal-center development of memory B cells driven by IL-9 from follicular helper T cells. *Nature Immunology*, **18**(8), 921–930.

Weisel, F. J., Zuccarino-Catania, G. V., Chikina, M., & Shlomchik, M. J. (2016). A Temporal Switch in the Germinal Center Determines Differential Output of Memory B and Plasma Cells. *Immunity*, **44**(1), 116–130.

Wherry, E. J., & Ahmed, R. (2004). Memory CD8 T-Cell Differentiation during Viral Infection. *Journal of Virology*, **78**(11), 5535–5545.

Wherry, E. J., Blattman, J. N., Murali-Krishna, K., van der Most, R., & Ahmed, R. (2003). Viral persistence alters CD8 T-cell immunodominance and tissue distribution and results in distinct stages of functional impairment. *Journal of Virology*, **77**(8), 4911–27.

Wherry, E. J., Ha, S.-J., Kaech, S. M., … Ahmed, R. (2007). Molecular Signature of CD8+ T Cell Exhaustion during Chronic Viral Infection. *Immunity*, **27**(4), 670–684.

Wilson, T. J., & Colonna, M. (2005). A new Fc receptor homolog, FREB2, found in germinal center B cells. *Genes and Immunity*, **6**(4), 341–6.

Wilson, T. J., Fuchs, A., & Colonna, M. (2012). Cutting edge: human FcRL4 and FcRL5 are receptors for IgA and IgG. *Journal of Immunology (Baltimore, Md.: 1950)*, **188**(10), 4741–

5.
Wilson, T. J., Presti, R. M., Tassi, I., Overton, E. T., Cella, M., & Colonna, M. (2007a). FcRL6, a new ITIM-bearing receptor on cytolytic cells, is broadly expressed by lymphocytes following HIV-1 infection. *Blood*, **109**(9), 3786–3793.
Wilson, T. J., Presti, R. M., Tassi, I., Overton, E. T., Cella, M., & Colonna, M. (2007b). FcRL6, a new ITIM-bearing receptor on cytolytic cells, is broadly expressed by lymphocytes following HIV-1 infection. *Blood*, **109**(9), 3786–3793.
Wiltrout, R. H., Herberman, R. B., Zhang, S. R., … Talmadge, J. E. (1985). Role of organ-associated NK cells in decreased formation of experimental metastases in lung and liver. *Journal of Immunology (Baltimore, Md. : 1950)*, **134**(6), 4267–75.
Wong, S., Freeman, J. D., Kelleher, C., Mager, D., & Takei, F. (1991). Ly-49 multigene family. New members of a superfamily of type II membrane proteins with lectin-like domains. *Journal of Immunology (Baltimore, Md. : 1950)*, **147**(4), 1417–23.
Xu, C.-R., Schaffer, L., Head, S. R., & Feeney, A. J. (2008). Reciprocal patterns of methylation of H3K36 and H3K27 on proximal vs. distal IgVH genes are modulated by IL-7 and Pax5. *Proceedings of the National Academy of Sciences*, **105**(25), 8685–8690.
Xu, M. J., Zhao, R., & Zhao, Z. J. (2001). Molecular cloning and characterization of SPAP1, an inhibitory receptor. *Biochemical and Biophysical Research Communications*, **280**(3), 768–75.
Yang, J., Zhang, L., Yu, C., Yang, X.-F., & Wang, H. (2014). Monocyte and macrophage differentiation: circulation inflammatory monocyte as biomarker for inflammatory diseases. *Biomarker Research*, **2**(1), 1.
Yang, M., Li, D., Chang, Z., Yang, Z., Tian, Z., & Dong, Z. (2015a). PDK1 orchestrates early NK cell development through induction of E4BP4 expression and maintenance of IL-15 responsiveness. *The Journal of Experimental Medicine*, **212**(2), 253–265.
Yang, Q., Li, F., Harly, C., … Bhandoola, A. (2015b). TCF-1 upregulation identifies early innate lymphoid progenitors in the bone marrow. *Nature Immunology*, **16**(10), 1044–1050.
Yasutomo, K., Lucas, B., & Germain, R. N. (2000). TCR signaling for initiation and completion of thymocyte positive selection has distinct requirements for ligand quality and presenting cell type. *Journal of Immunology (Baltimore, Md. : 1950)*, **165**(6), 3015–22.
Yokosuka, T., Takamatsu, M., Kobayashi-Imanishi, W., Hashimoto-Tane, A., Azuma, M., & Saito, T. (2012). Programmed cell death 1 forms negative costimulatory microclusters that directly inhibit T cell receptor signaling by recruiting phosphatase SHP2. *The Journal of Experimental Medicine*, **209**(6), 1201–17.
Yokota, Y., Mansouri, A., Mori, S., … Gruss, P. (1999). Development of peripheral lymphoid organs and natural killer cells depends on the helix–loop–helix inhibitor Id2. *Nature*, **397**(6721), 702–706.
Young, G. R., Ploquin, M. J.-Y., Eksmond, U., Wadwa, M., Stoye, J. P., & Kassiotis, G. (2012). Negative Selection by an Endogenous Retrovirus Promotes a Higher-Avidity CD4+ T Cell Response to Retroviral Infection. *PLoS Pathogens*, **8**(5), e1002709.
Yu, J., Freud, A. G., & Caligiuri, M. A. (2013). Location and cellular stages of natural killer cell development. *Trends in Immunology*, **34**(12), 573–82.
Yusa, S., Catina, T. L., & Campbell, K. S. (2004). KIR2DL5 Can Inhibit Human NK Cell Activation Via Recruitment of Src Homology Region 2-Containing Protein Tyrosine Phosphatase-2 (SHP-2). *The Journal of Immunology*, **172**(12), 7385–7392.
Zajac, A. J., Blattman, J. N., Murali-Krishna, K., … Ahmed, R. (1998). Viral immune evasion due to persistence of activated T cells without effector function. *The Journal of Experimental Medicine*, **188**(12), 2205–13.
Zanders, E. D., Lamb, J. R., Feldmann, M., Green, N., & Beverley, P. C. L. (1983). Tolerance of T-cell clones is associated with membrane antigen changes. *Nature*, **303**(5918), 625–627.

Zandi, S., Mansson, R., Tsapogas, P., Zetterblad, J., Bryder, D., & Sigvardsson, M. (2008). EBF1 Is Essential for B-Lineage Priming and Establishment of a Transcription Factor Network in Common Lymphoid Progenitors. *The Journal of Immunology*, **181**(5), 3364–3372.

Zandvoort, A., & Timens, W. (2002). The dual function of the splenic marginal zone: essential for initiation of anti-TI-2 responses but also vital in the general first-line defense against blood-borne antigens. *Clinical and Experimental Immunology*, **130**(1), 4–11.

Zelinskyy, G., Dietze, K. K., Hüsecken, Y. P., … Dittmer, U. (2009). The regulatory T-cell response during acute retroviral infection is locally defined and controls the magnitude and duration of the virus-specific cytotoxic T-cell response. *Blood*, **114**(15), 3199–207.

Zhang, J. (2004). Ubiquitin ligases in T cell activation and autoimmunity. *Clinical Immunology*, **111**(3), 234–240.

Zhang, Y., Zhang, Y., Gu, W., He, L., & Sun, B. (2014). Th1/Th2 Cell's Function in Immune System, Springer, Dordrecht, pp. 45–65.

Zhu, C., Anderson, A. C., & Kuchroo, V. K. (2010). TIM-3 and Its Regulatory Role in Immune Responses, Springer, Berlin, Heidelberg, pp. 1–15.

Zhu, X., & Lang, J. (2017). Soluble PD-1 and PD-L1: predictive and prognostic significance in cancer. *Oncotarget*, **8**(57), 97671–97682.

Zhumabekov, T., Corbella, P., Tolaini, M., & Kioussis, D. (1995). Improved version of a human CD2 minigene based vector for T cell-specific expression in transgenic mice. *Journal of Immunological Methods*, **185**(1), 133–140.

Ziegler, S. F., & Buckner, J. H. (2009). FOXP3 and the regulation of Treg/Th17 differentiation. *Microbes and Infection*, **11**(5), 594–8.

Zúñiga-Pflücker, J. C. (2004). T-cell development made simple. *Nature Reviews Immunology*, **4**(1), 67–72.